Catalytic Methods for the Synthesis of 1,3-Disubstituted Bicyclo[1.1.1]pentanes

Bethany R. Shire

Lady Margaret Hall

University of Oxford

A thesis submitted to the Board of the Faculty of Physical Sciences in partial fulfilment of the requirements for the degree of

Doctor of Philosophy

Trinity Term 2022

Catalytic Methods for the Synthesis of 1-3-Disubstituted Bicyclo[1.1.1]pentanes

Bethany R. Shire

Lady Margaret Hall, University of Oxford | *Doctor of Philosophy* | Trinity Term 2022

Bicyclo[1.1.1]pentanes (BCPs) have emerged as useful bioisosteres for arenes in medicinal chemistry, demonstrating improved pharmacokinetic properties compared to the parent drugs. However, many syntheses still require the use of harsh conditions that are unsuitable for industrial applications. This thesis describes the development of new catalytic methodologies for the synthesis of 1,3-disubstituted BCPs, under mild conditions. Chapter 2 describes a photoredox-catalysed atom transfer radical addition between (hetero)aryl iodides and tricyclo[1.1.1.$0^{1,3}$]pentane (TCP), accessing 1-iodo-3-aryl-BCPs in a mild and efficient manner, and representing the first photoredox catalysed functionalisation of C–C σ bonds. Chapter 3 describes the iron-catalysed Kumada cross-coupling between (hetero)aryl Grignard reagents and 1-iodo-3-substituted BCPs. This established the first general cross-coupling in which BCPs act as the electrophilic cross-coupling component, as well as the first example of a Kumada cross-coupling of tertiary iodides. Chapter 4 describes the investigation of a copper-catalysed borylation of 1-iodo-3-substituted BCPs and their subsequent oxidation to access BCP alcohols, representing the first conversion of BCP iodides to BCP alcohols without the need for *tert*-butyl lithium.

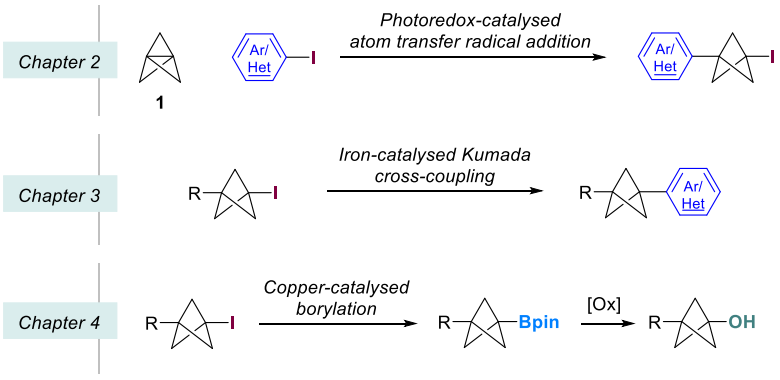

Declaration

The work presented in this thesis was conducted at the Department of Chemistry, University of Oxford. The thesis is a product of my own work and includes no results through collaboration, except where specifically indicated in the text. The work presented has not been submitted, either partially or in full, for any qualification at this or any other institution.

Bethany R. Shire

April 2022

Acknowledgements

Firstly, I would like to thank Prof. Edward Anderson for his support and guidance over my 6 years in the group, from the beginning of my Part II in 2016 to the present. I greatly appreciate the opportunity to work in his group and on such an interesting project. I would also like to thank him greatly for the support and understanding he has shown over the course of the ongoing pandemic which made completing this DPhil even more challenging than expected!

I would also like to thank all my industrial supervisors who have helped and collaborated on these projects: James Mousseau, Ian Holsby, Sean Ng, Mike Ardolino and Yang Cao. Thank you for all of the discussions had, problems troubleshooted and chemicals supplied!

To Jieyan, Yongchen, Philip, Ryan, Ana, Zixuan, Guoduan, Kenny, Hannah, Pavle, Yasmine, Priyansh, Carlos, Felix, Christian, Claire, Kai, Mujji, Venky, Pauline, Yao and all of the EAA group, past and present, it has been a pleasure and a privilege to work with so many incredible people who have and made the lab such an enjoyable place to be.

To Team BCP (and BCH and BCB), thank you for being such an excellent group to work with – Jeremy, Helena, Ali, Marie, Nils, thank you for being the Best Chemistry Pals I could ask for. Special thanks go to Jeremy, who I learnt an enormous amount from and who gave me so much help and support through the whole of my DPhil. To Helena, we have quite literally been side-by-side for our entire DPhils, thank you for being a wonderful house mate, lab mate and friend.

I would also like to give special mention to Dimitri and Steve for helping me so much during my Part II and the start of my DPhil, I learnt so much from both of you and have greatly appreciated your friendship. Eddie, thank you for being such an excellent desk

buddy, and to Marius and Halli thank you for your guidance, I aspire to be as kind and patient as you both.

I am incredibly grateful to the friends I've made during my time at Oxford. Xinlan and Kayleigh, thank you for all the fun times and for those walks during lockdown that kept us sane! Flo and Tony, thank you for the study sessions, the snacks, and the support, and to all of the Pembroke group, I am lucky to have such a kind and supportive group of friends, I appreciate you all immensely.

To Sidney, 9 years ago you helped me with my toga on the first night of undergraduate, and you have been my best friend ever since. I would not have got where I am without your support and friendship, thank you for always being there from day one. To Matt, thank you for all the cups of tea and biscuits in first year and for everything since. I miss you both very much and I hope we can all celebrate together soon.

Richard, we've been together every step of the way, thank you for all of your support and for always believing in me, I wouldn't have made it here without you.

Finally, this thesis is dedicated to my sister Katy, who is the best person I know, and to my amazing parents, thank you so much for all of your love and support throughout everything, I can't ever thank you enough for everything you've done for me.

Abbreviations

1,3,5-TCH	1,3,5-trimethyl-1,3,5-triazinane
A	Amps
Å	Ångström
Ac	Acetyl
acac	Acetylacetonate
ACNH	1,1'-azobis(cyclohexanecarbonitrile)
Acr	Acridinium
Ad	Adamantyl
AMP	Artificial membrane permeability
amphos	Di-tert-butyl(4-dimethylaminophenyl)phosphine
app	Apparent
aq.	Aqueous
Ar	Aryl
ATRA	Atom transfer radical addition
ATRC	Atom transfer radical cyclisation
$A\beta_{42}$	β-Amyloid peptide chain of 42 amino acids
BCO	bicyclo[2.2.2]octane
BCP	bicyclo[1.1.1]pentane
BenzP*	(*R*,*R*)-(+)-1,2-Bis(tert-butylmethylphosphino)benzene
BHT	Butylated hydroxytoluene
Binap	2,2'-Bis(diphenylphosphino)-1,1'-binapthyl
Bn	benzyl
BNAH	1-Benzyl-1,4-dihydronicotinamide
Boc	*tert*-Butyloxycarbonyl
Bpin	Pinacol boronic ester
bpy	2,2'-Bipyridine
bpz	2,2'-Bipyrazine
br.	Broad
Bu	Butyl
c	Speed of light
cat	catechol
CataxiumA Pd G2	Chloro[(di(1-adamantyl)-*N*-butylphosphine)-2-(2-aminobiphenyl)]palladium(II)
Cbz	Benzyloxycarbonyl
$ChromLogD_{7.4}$	Chromatographic hydrophobicity index
CLND	Chemiluminescent nitrogen detection
clogP	Calculated partition coefficient for *n*-octanol/water
cod	1,5-Cyclooctadiene
Conc.	Concentration
COSY	Correlation Spectroscopy
CPG	Carboxyphenylglycine
CPME	Cyclopentyl methyl ether
Cy	Cyclohexyl
d	Doublet

d.r.	Diastereomeric ratio
DABCO	1,4-Diazabicyclo[2.2.2]octane
dap	Diammonium phosphate
DCM	Dichloromethane
dcypt	3,4-Bis(dicyclohexylphosphino)thiophene
DIPEA	N,N-Diisopropylethylamine
dmb	2,4-dimethoxybenzyl
DME	Dimethoxyethane
DMEDA	1,2-Dimethylethylenediamine
DMF	Dimethylformamide
DMP	Dess-Martin periodinane
DMSO	Dimethyl sulfoxide
dppbz	1,2-Bis(diphenylphosphino)benzene
dppe	1,2-Bis(diphenylphosphino)ethane
dppf	1,1'-Bis(diphenylphosphino)ferrocene
dtbpy	4,4'-Di-tert-butyl-2,2'-bipyridine
$E_{0,0}$	Zero-zero excitation energy
$E_{1/2}$	Half-peak potential
EDCI	1-Ethyl-3-(3-dimethylaminopropyl)carbodiimide
ee	Enantiomeric excess
EPR	Electron paramagnetic resonance
equiv.	Equivalents
E_{red}	Reduction potential
E^S	Reduction potential of singlet state
ESI	Electrospray ionisation
Et	Ethyl
et al.	Et alia (and others)
fac	Facial
FaSSIF	Fasted state simulated intestinal fluid
FG	Functional group
Fmoc	Fluorenylmethyloxycarbonyl
g	Grams
GC	Gas chromatography
h	Hours
HAT	Hydrogen atom transfer
HATU	1-[Bis(dimethylamino)methylene]-1*H*-1,2,3-triazolo[4,5-*b*]pyridinium 3-oxid hexafluorophosphate
Het	Heteroaryl
hex	Hexyl
HMBC	Heteronuclear multiple bond correlation
HMPA	Hexamethylphosphoramide
HMTA	Hexamethylenetetramine
HOBt	Hydroxybenzotriazole
HSQC	Heteronuclear single quantum conherence spectroscopy
hν	Photons
IC_{50}	Half maximal inhibitory concentration
i-	*iso*-

IR	Infrared
kcal	Kilocalories
LDA	Lithium diisopropylamide
LED	Light emitting diode
LiDBB	Lithium 4,4’-ditert-butylbiphenylide
LiHMDS	Lithium bis(trimethylsilyl)amide
$LpPLA_2$	Lipoprotein-associated phospholipase A2
M	Molar
m	meta
m.p.	Melting point
m-CPBA	meta-Chloroperoxybenzoic acide
Me	Methyl
Meppy	2-(*p*-Methylphenyl)-pyridine
mer	Meridional
mes	Mesityl
mGluR1	Metabotropic glutamate receptor 1
MHz	Megahertz
min	Minutes
mL	Mililitres
MLCT	Metal to ligand charge transfer
mol	Moles
MOM	Methoxy methyl
MTBE	Methyl tert-butyl ether
n	Normal
NaHMDS	Sodium bis(trimethylsilyl)amide
NCS	*N*-Chlorosuccinimide
NHC	*N*-Heterocyclic carbene
NMP	*N*-Methyl-2-pyrrolidone
NMR	Nuclear magnetic resonance
o	Ortho
oct	Octyl
p	Para
P_{app}	Passive absorptive permeability
PC	Photocatalyst
PFI	Property forecast index
PG	Protecting group
Ph	Phenyl
pH	Potential of hydrogen
pin	Pinacol
PMDTA	*N,N,N’N”,N”*-Pentamethyldiethylenetriamine
ppm	Parts per million
ppy	2-Phenylpyridine
Pr	Propyl
pz	Pyrazolyl
q	Quartet
quin.	Quintet
quant.	Quantitative

R_f	Retention factor
RRCK	Ralph Russ Canine Kidney
rt	Room temperature
s	Seconds
s	Singlet
SCE	Saturated calomel electrode
SciOPP	1,2-Bis[bis[3,5-di(tert-butyl)phenyl]phosphino]benzene
SC-XRD	Single crystal X-ray diffraction
SDS	Sodium dodecyl sulfate
SIMes	1,3-Bis(2,4,6-trimethylphenyl)-4,5-dihydroimidazol-2-ylidene
Sphos	2-Dicyclohexylphosphino-2',6'-dimethoxybiphenyl
t	Triplet
t-	Tertiary
TBAF	Tetra-*n*-butylammonium fluoride
TCP	Tricyclo[1.1.1.$0^{1,3}$]pentane
TEEDA	*N,N,N'N'*-Tetraethylethylenediamine
Tf	Trifluoromethanesulfonyl
TFE	2,2,2,-Trifluoroethanol
THF	Tetrahydrofuran
TMEDA	*N,N,N'N'*-Tetramethylethylenediamine
TMS	Trimethylsilyl
tol	Tolyl
Ts	*para*-Toluenesulfonyl
TTMSS	Tris(trimethylsilyl)silane
UHP	Urea hydrogen peroxide
UV	Ultraviolet
V	Volts
vs	Versus
W	Watts
X	Generic group/atom
Xantphos	4,5-Bis(diphenylphosphino)-9,9-dimethylxanthene
°C	Degrees Celsius
λ_{em}	Maximum emission
μ	Micro
Φ	Quantum yield

Photocatalysts

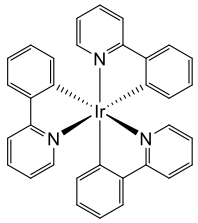

fac-Ir(ppy)$_3$

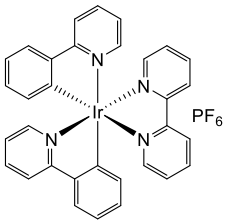

[Ir(ppy)$_2$(bpy)]PF$_6$

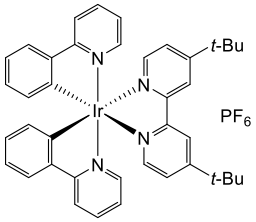

[Ir(dtbbpy)(ppy)$_2$]PF$_6$

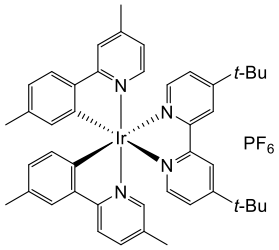

[Ir(3,4'-dMeppy)$_2$(dtbbpy)]PF$_6$

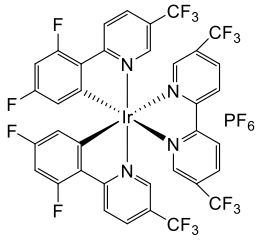

[Ir[dF(CF$_3$)ppy]$_2$(d(CF$_3$)bpy)]PF$_6$

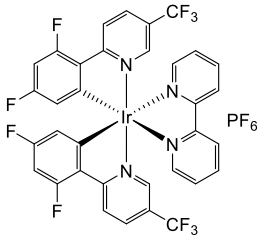

(Ir[dF(CF$_3$)ppy]$_2$(bpy))PF$_6$

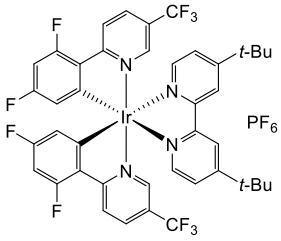

(Ir[dF(CF$_3$)ppy]$_2$(dtbpy))PF$_6$

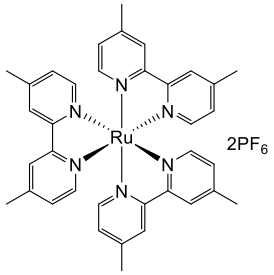

Ru(d(Me)bpy)$_3$(PF$_6$)$_2$

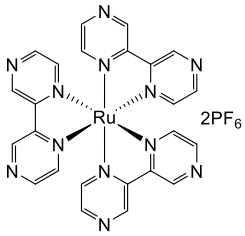

[Ru(bpz)$_3$](PF$_6$)$_2$

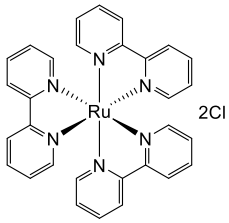

Ru(bpy)$_3$Cl$_2$

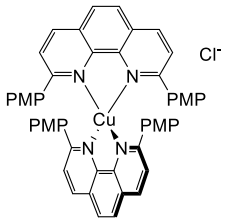

Cu(dap)$_2$Cl

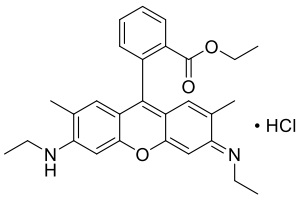

Rhodamine 6G

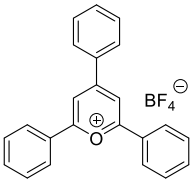

2,4,6-Triphenylpyrylium tetrafluoroborate

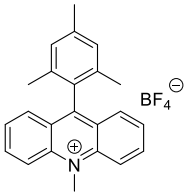

9-mesityl-10-methylacridinium tetrafluoroborate

Table of Contents

1

Introduction

1.1 Bioisosterism

The concept of isosterism was first described by Langmuir in 1919,[1] who expanded upon his 'octet theory'[2] to note that the number and arrangement of electrons in the nitrogen molecule and carbon monoxide molecule were the same, and these compounds possessed very similar physical properties. He theorised that other isoelectronic compounds should also have similar properties, and applied this idea to nitrous oxide and carbon dioxide; analysis of published data on their physical properties showed that they did indeed conform to his theory. He therefore classified compounds or groups of atoms with a relationship such as these as 'isosteres' (**Table 1.1**).

Type	Isosteres
1	H^-, He, Li^+
2	O^{2-}, F^-, Ne, Na^+, Mg^{2+}, Al^{3+}
3	S^{2-}, Cl^-, Ar, K^+, Ca^{2+}
4	Cu^+, Zn^{2+}
5	Br^-, Kr, Rb^+, Sr^{2+}
6	Ag^+, Cd^{2+}
7	I^-, Xe, Cs^+, Ba^{2+}
8	N_2, CO, CN^-
9	CH_4, NH_4^+
10	CO_2, N_2O, N_3^-, CNO^-

Table 1.1 *– Some groups of isosteres identified by Langmuir.*

In 1925 Grimm expanded on the concept of isosterism with the Hydride Displacement Law.[3] This law states "Atoms anywhere up to four places in the periodic system before an inert gas change their properties by uniting with one to four hydrogen atoms, in such a manner that the resulting combinations behave like pseudoatoms, which are similar to elements in the groups one to four places respectively to their right". In other words an atom bonded to a hydrogen atom will have similar properties to the atom with an atomic mass greater by one, and these are called 'pseudoatoms'(**Table 1.2**)

C	N	O	F	Ne	Na
	CH	NH	OH	FH	-
		CH_2	NH_2	OH_2	FH_2^+
			CH_3	NH_3	OH_3^+
				CH_4	NH_4^+

***Table 1.2** - Group of 'pseudoatoms' according to Grimm's Hydride Replacement Law.*

Erlenmeyer built upon Grimm's definition in 1932 to state "Atoms, ions, or molecules in which the peripheral layers of electrons can be considered to be identical are termed isosteres".[4] This greatly expanded what atoms or groups could be considered isosteric as, by this definition, all elements in the same periodic group are isosteres, as well as sulphur and HC=CH within an aromatic ring (**Table 1.3**).[5]

Number of Peripheral Electrons				
4	5	6	7	8
N^+	P	S	Cl	ClH
P^+	As	Se	Br	BrH
S^+	Sb	Te	I	IH
As^+		PH	SH	SH_2
Sb^+			PH_2	PH_3

***Table 1.3** - Isosteres according to Erlenmeyer based on the number of peripheral electrons.*

1. Introduction

In 1933 Erlenmeyer was the first to investigate isosterism in a biological setting, synthesising a series of isosteric antigens which all had similar antigenic properties.[6] Building on his hypothesis that S and HC=CH would be isosteric in an aromatic ring, he substituted a benzene ring in antigen **2** for a thiophene group (**3**) and reported that it was not possible to differentiate between the two compounds (**Figure 1.1**). He also showed that the thiophene isosteres of cocaine, eucaine A and novocaine also showed little change in activity.

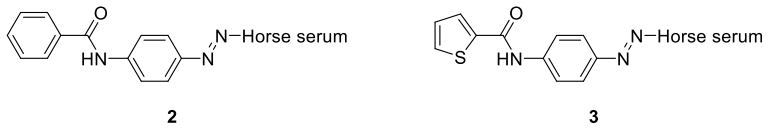

Figure 1.1 *- Thiophene antigen isostere shown by Erlenmeyer to have very similar antigenic properties.*

The term 'bioisostere' was first used by Friedman in 1951 when reviewing the various definitions of isosterism, who termed compounds "bio-isosteric" if they "fit the broadest definition for isosteres and have the same type of biological activity".[7] He noted that for two compounds to be bioisosteric they needed to act on the same biological target via the same mechanism. The definition was further adapted and redefined over the following 40 years; Thornber generalised the concept further, stating that "bioisosteres are groups or molecules which have chemical and physical similarities producing broadly similar biological properties".[8] Thornber elaborated on this definition to list properties of a lead compound that could be affected when making a bioisosteric substitution, namely size, shape, electronic distribution, lipid solubility, water solubility, pKa, chemical reactivity and hydrogen bonding capacity.

In 1991, Burger further expanded this definition, stating "bioisosteres are compounds or groups that possess near-equal molecular shapes and volumes, approximately the same distribution of electrons, and which exhibit similar physical properties such as

hydrophobicity. Bioisosteric compounds affect the same biochemical systems as agonists or antagonists and thereby produce biological properties that are related to each other".[9] This broad definition is the most useful for describing the wide range of bioisosteres that exist, and so is the one that is most appropriate for the context of this thesis.

Bioisosteres can be classified into two groups: classical and non-classical. Classical bioisosteres are described by Langmuir's definition, Grimm's hydride replacement rule or Erlenmeyer's isosteres, and can generally be classified into five groups: monovalent, divalent, trivalent, tetravalent and ring substitutes (**Figure 1.2**).

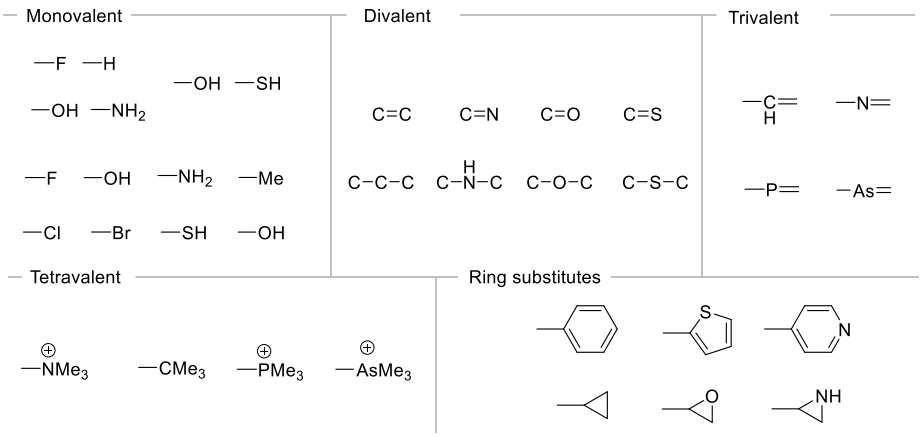

Figure 1.2 *- Classes of classical bioisosteres.*

Non-classical bioisosteres cover a broader range of compounds that do not fit into the steric or electronic criteria of a classical bioisostere, but still maintain the electronic and steric properties necessary for the retention of biological activity. Non-classical bioisosteres can be divided into two categories: cyclic vs acyclic structures, and exchangeable groups.[10–12] The former involve the replacement of cyclic groups with acyclic groups that have similar electronic or steric properties, while the latter involve bioisosteres that are replacements for functional groups that can have different structure and electronic properties. Examples of non-classical bioisosteres are shown in **Figure 1.3**.[11,13–18]

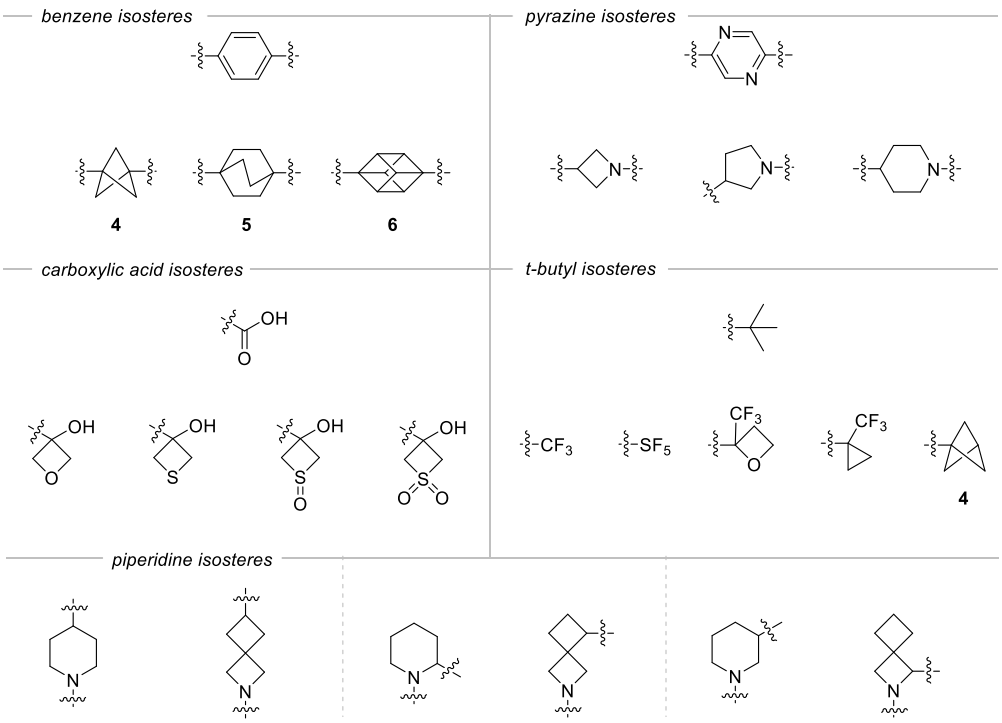

Figure 1.3 *– Some examples of non-classical bioisosteres.*

Of these many examples of non-classical bioisosteres, one of the most explored classes is that of *p*-disubstituted benzene isosteres, which can be substituted with bicyclo[1.1.1]pentanes (BCPs, **4**), bicyclo[2.2.2]octanes (BCOs, **5**) or cubanes (**6**). The presence of aromatic rings in drug candidates has been shown to generally limit developability, with more than three aromatic rings markedly increasing risk of compound attrition.[19] A more general trend has been shown for increasingly saturated compounds, which are more likely to have higher solubility, lower melting points, and to successfully transition from clinical trials to drugs.[20] Therefore making bioisosteric replacements of flat, unsaturated benzene rings with saturated, three dimensional units such as BCPs, BCOs and cubanes could improve the pharmacokinetic properties of a drug or drug candidate, a hypothesis that has been validated in many circumstances.[15,17]

Arguably the most useful of these bioisosteres is bicyclo[1.1.1]pentane (BCP) (**4**), which is discussed in more detail in the following section.

1.2 Bicyclo[1.1.1]pentane as a Bioisostere

Bicyclo[1.1.1]pentanes have been employed as bioisosteres for multiple functional groups: for example, as a *tert*-butyl group in BCP-bosentan **7**; an alkynyl group in BCP-tazarotene **8,** and as a 1,4-substituted arene in BCP-darapladib **9** (**Figure 1.4a**). Of these, its use as a 1,4-substituted arene is of most interest, as it maintains a substituent geometry of 180°, albeit with a slightly shorter unit length (**Figure 1.4b**). As noted above, the presence of benzene rings in drug candidates can be a major reason for attrition during development,[19] and therefore replacement with an alicyclic group such as a BCP can offer benefit during the drug discovery process.

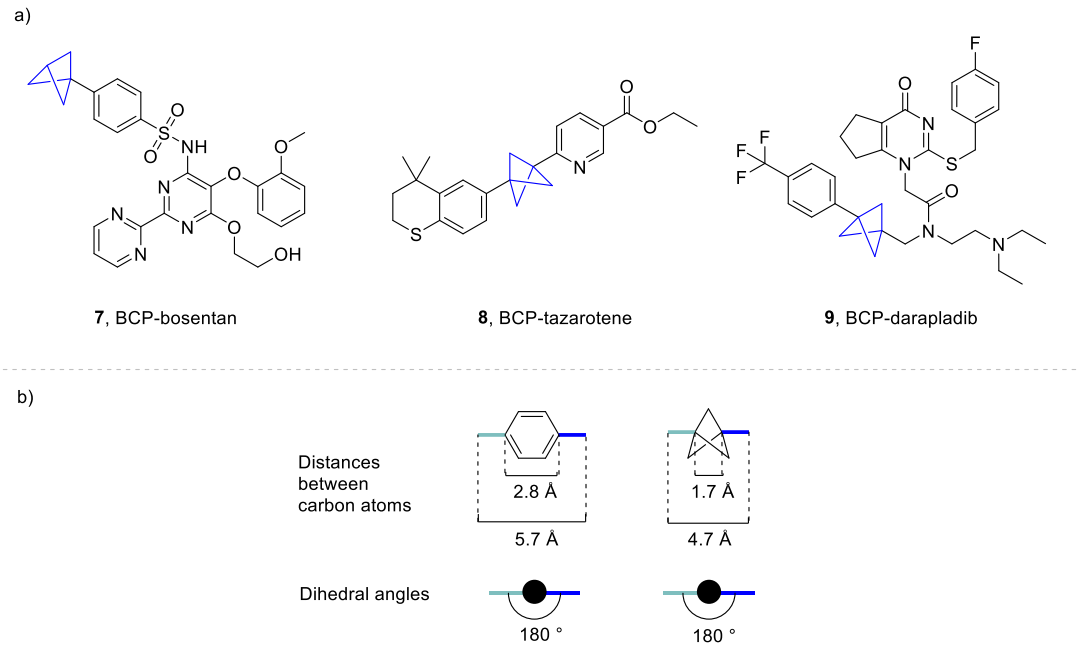

Figure 1.4 *– a) Examples of BCPs used as bioisosteres for t-Bu groups (BCP-bosentan), alkynyl groups (BCP-tazarotene) and 1,4-disubstituted arenes (BCP-darapladib). b) – Comparison of functional group size and dihedral angles in 1,4-disubstituted arenes and 1,3-disubstituted BCPs.*

The first example of the use of a BCP as a 1,4-arene bioisostere was reported by Pellicciari *et al.* in 1996, who synthesised **11** as a BCP analogue of (carboxyphenyl)glycine derivative **10** which is an antagonist for mGluR1 – a metabotropic glutamate receptor involved in important central nervous system functions (**Figure 1.5**).[21] They noted that while the coplanarity of the substituents either side of the arene in this class of compounds was generally accepted to be crucial for activity, no investigations had been performed into whether the aromaticity of the benzene ring was itself important. The BCP analogue **11** maintains the linearity of its substituents, and was found to maintain good potency as an mGluR1 antagonist. This suggested that the 1,4-arene in **10** acts as a spacer unit rather than contributing to the biological activity through other effects.

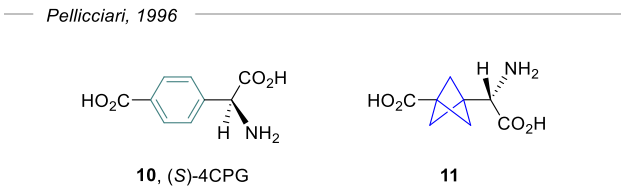

Figure 1.5 *– The mGluR1 antagonist (S)-4CPG and its BCP analogue.*

Since then there have been many examples of the use of BCPs as bioisosteres in drug discovery: perhaps the most notable is the use of a BCP as a fluorophenyl replacement in the γ-secretase inhibitor Avagacestat, demonstrated by Stepan *et al.* in 2012 (**Table 1.4**).[22] The BCP containing analogue **13** was found to maintain a similar level of γ-secretase inhibition, indicating that the fluorophenyl group was once again largely functioning as a spacer unit and may not be involved in specific interactions with the enzyme. As well as maintaining linearity of the oxadiazole and sulfonamide substituents, **13** exhibited improved aqueous solubility and passive permeability compared to **12**, resulting in a significantly higher level of oral absorption. This was attributed to the BCP

disrupting the planarity of the compound and the π stacking of the aromatic rings between molecules.

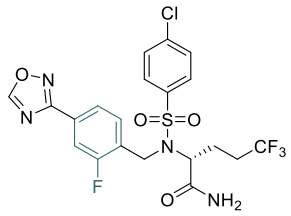

12, γ secretase inhibitor

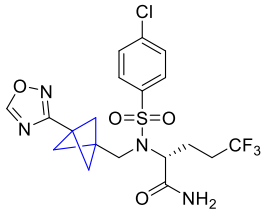

13, BCP analogue

	12	BCP-**13**
IC_{50} ($A\beta_{42}$, nM)	0.225	0.178
Kinetic solubility (pH 6.5, μM)	0.60	216
Thermodynamic solubility (pH 6.5, μM)	1.70	19.7
RRCK P_{app} (A to B) (10^{-6} cm/ s)	5.52	19.3

Table 1.4 *– comparison of pharmacokinetic data between γ-secretase inhibitor* ***12*** *and its BCP analogue* ***13****.*

Subsequently, Measom *et al.* found similar benefits arose from substitution of an aromatic ring in darapladib with a bicyclo[1.1.1]pentane (**Table 1.5**).[23] Darapladib (**14**) is a known $LpPLA_2$ inhibitor which shows excellent potency, however it suffers from low aqueous solubility and high lipophilicity. Measom *et al.* synthesised BCP analogue **15** and found that, when compared to the parent drug, high potency was maintained with kinetic solubility increasing 9-fold, and permeability also improving. While the substitution of an aromatic ring for a BCP did not improve all desired physiochemical properties in this instance, an overall improvement was still exhibited compared to the original compound.

BCPs have been implemented in a range of pharmaceutically active compounds as bioisosteres for 1,4-substituted arenes. Maintaining the 180° angle between substituents but with a slightly shorter unit length has made them suitable for bioisosteric replacements of arenes in many circumstances. However, care must be taken if the arene ring being

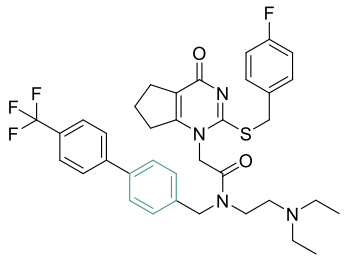

14, darapladib

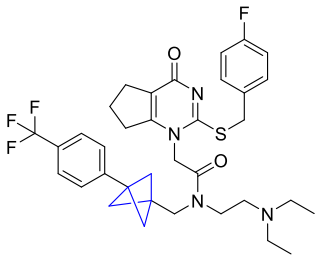

15, BCP-darapladib

	14	BCP-**15**
pIC_{50}	10.2	9.4
CLND (µM)	8	74
FaSSIF (µg/ mL)	399	>1000
AMP (nm/ s)	230	705
$ChromLogD_{7.4}$	6.3	7.0
PFI	10.3	10.0

Table 1.5 *– Comparison of pharmacokinetic properties between darapladib and BCP-darapladib.*

replaced is involved in important interactions between the drug molecule and its target protein.

Stepan and co-workers investigated the effect of various sp^3 bioisosteric replacements of a 1,4-substituted benzene ring in the leukaemia drug imatinib (**Figure 1.6**).[24] Imatinib (**16**) has a very low aqueous solubility of 0.01 mg/ mL and relatively high lipophilicity (clog P – 4.53).

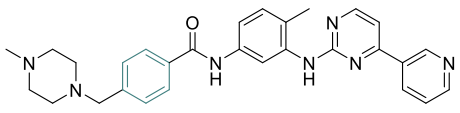

16, imatinib

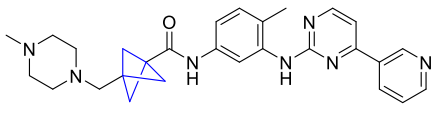

17, BCP-imatinib

Figure 1.6 *– Imatininb and its BCP analogue.*

As previous studies had shown that bioisosteric replacements with BCPs could improve the aqueous solubility of a drug compared to the parent compound,[22] BCP analogue **17** was synthesised. Although the BCP analogue **17** showed a greater than 80 × improvement in aqueous solubility, and decreased the lipophilicity to a clogP of 1.93, no significant improvement in metabolic stability was observed. Furthermore, the inhibitory potency against ABL1 kinase (the target of imatinib) *decreased* from an IC_{50} of 371 nM for the parent compound, to an IC_{50} of > 30 μM. This large loss in binding affinity was attributed to the disruption of key hydrogen-bonding interactions between the drug and residues in the protein active site as a result of the shorter unit length of a BCP compared to an arene, as well as the loss of hydrophobic interactions between the phenyl ring of the parent compound and the protein.

Despite these and other examples of BCPs being successful bioisosteric replacements for arenes, there is currently no consensus on exactly how the properties of a drug molecule will change upon substitution, or when a BCP is suitable. While BCPs appear to be fairly reliable in improving the solubility of a drug compared to the parent compound, other properties such as the metabolic stability and potency of the compound have been shown to either increase or decrease depending on the specific example.[22–24] In general, it appears that if the arene unit replaced is not involved in key interactions in the active site, the BCP unit is less likely to decrease potency. Overall, bioisosteric replacement is currently still a case of trial and error, but despite this, the BCP motif has been validated as a useful replacement to explore during the drug discovery process and has become a popular target.

1.3 Synthesis and structure of bicyclo[1.1.1]pentane

Bicyclo[1.1.1]pentane itself (BCP, **18**) was first synthesised in 1964 by Wiberg[25] in 4 steps from *exo*-methylene cyclobutane **19** (**Scheme 1.1a**). Addition of HBr to the alkene of **19**, followed by hydrolysis of the methyl ester formed carboxylic acid **21**. Hunsdiecker reaction of **21** gave dibromide **22**, which on reaction with Na in a Wurtz coupling reaction formed BCP **18,** albeit in only 1% yield. Over the next few years Wiberg reported two more syntheses of BCP: a similar Wurtz coupling of **22** using $Li(Hg)_x$ instead of Na gave BCP **18** in a slightly higher 6% yield (**Scheme 1.1b**),[26] and a carbene addition into the central bond of bicyclo[1.1.0]butane **23** using diazomethane (**Scheme 1.1c**) gave BCP in ~1% yield.[27]

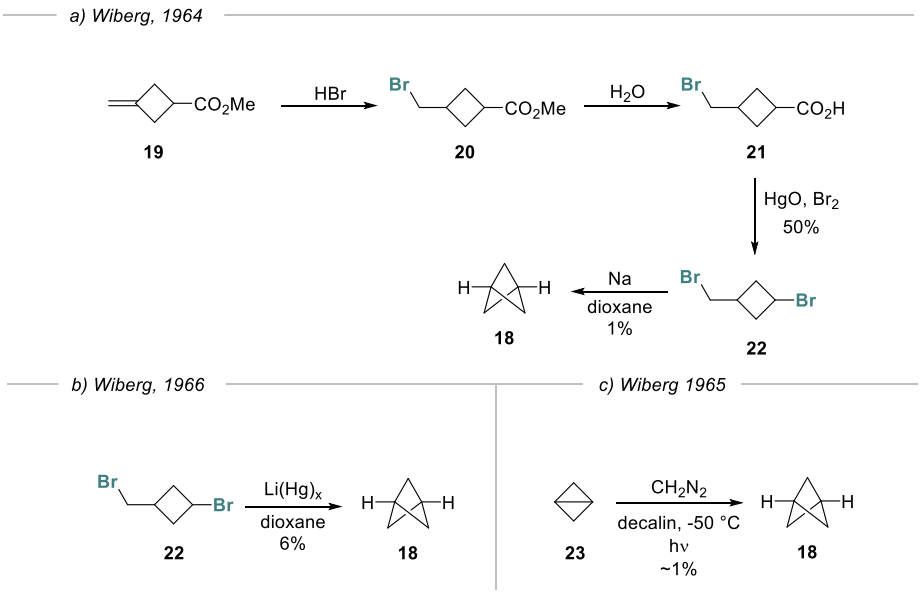

Scheme 1.1 *– a) The first synthesis of bicyclo[1.1.1]pentane by Wiberg from dibromide* ***22*** *and Na. b) Wiberg's synthesis of BCP from* ***22*** with $Li(Hg)_x$ *c) Wiberg's synthesis of BCP from bicyclo[1.1.0]butane with diazomethane.*

Following Wiberg's initial report, a number of other syntheses of BCP were also published including the mercury photosensitized internal cycloaddition of 1,4-pentadiene

24 (**Scheme 1.2a**) by Srinivasan[28], the mercury photosensitized ring contraction of ketone-bearing bicyclo[2.1.1]hexane **25** by Dimmel (**Scheme 1.2b**),[29] and the electrochemical Wurtz coupling of dibromide **26** by Rifi (**Scheme 1.2c**).[30]

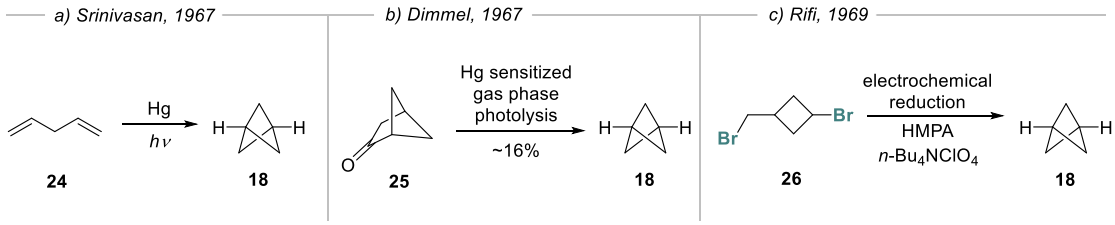

Scheme 1.2 *– Early syntheses of BCP using a) photosensitized internal cycloaddition. b) Hg sensitised ring contraction. c) electrochemical reduction/cyclisation.*

Since these early reports of the synthesis of BCP, many reactions have been developed for the synthesis of mono- and disubstituted BCPs,[31] as well as bridge substituted-BCPs.[32] While a number of approaches have been used, by far the most common method of synthesising BCPs is from reactions with tricyclo[1.1.1.$0^{1,3}$]pentane (TCP), also known as [1.1.1]propellane.

1.4 Reactivity of Tricyclo[1.1.1.$0^{1,3}$]pentane

Tricyclo[1.1.1.$0^{1,3}$]pentane (TCP, **1**) belongs to a class of molecules called propellanes, which consist of a central single bond with three 'bridges' of one or more carbon or heteroatoms bonded to the 'bridgehead' atoms either side of the central bond (**Figure 1.7a**). The nomenclature of propellanes was coined by Ginsburg in 1966:[33] any given propellane is given the name [x.y.z]propellane where x, y and z represent the number of atoms in each of the bridges respectively (and are greater than zero). TCP, which only has one carbon in each of its bridges, is also called [1.1.1]propellane, and is the smallest of the propellanes. Small ring propellanes inevitably contain an unusual

'inverted' tetrahedral geometry around the bridgehead atoms, which leads to unusual reactivities.

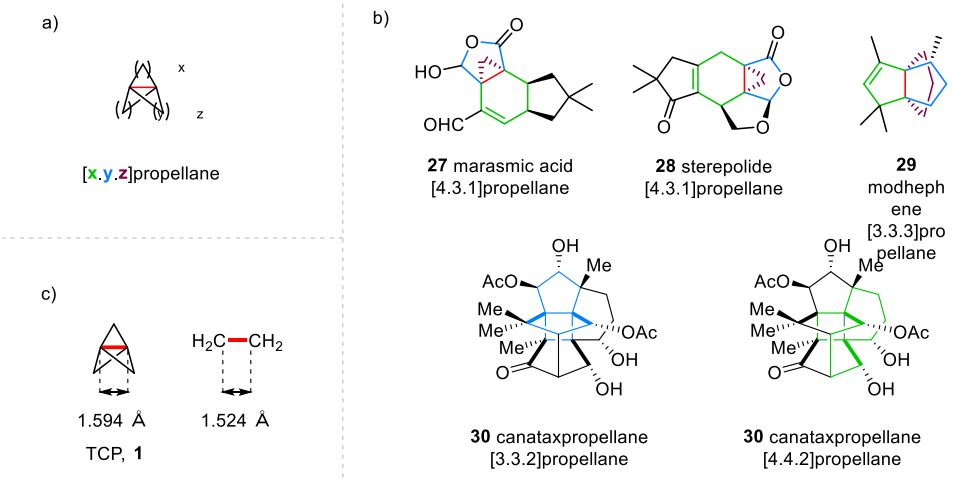

Figure 1.7 *– a) The general structure and nomenclature for [x.y.z.]propellanes. b) A selection of natural products containing propellanes. c) The comparison of bond lengths between the central bond of TCP and the C–C bond in ethane.*

While smaller propellanes (x/y/z < 3) are often reactive and unstable, the larger ring propellanes are often inert. The larger bridging ring lengths allow the bridgehead atoms to possess a more favourable geometry compared to their smaller ring counterparts. There are several instances of natural products containing larger propellanes.[34] The [4.3.1]propellane motif can be found in marasmic acid **27** and sterepolide **28**, and the [3.3.3]propellane motif can be found in modhephene **29**, while canataxpropellane **30** remarkably contains both a [3.3.2]propellane and a [4.4.2]propellane (**Figure 1.7b**).[35,36] While naturally occurring,[37] the larger bridging ring lengths of these higher propellanes do not confer the same interesting structural properties and reactivity that results from the 'strained' central bond of TCP. The central bond and structure of [1.1.1]propellane (TCP) has been the subject of much investigation. Its structure has been studied by both low-temperature X-ray diffraction[38] and gas phase electron diffraction,[39] and from this, the distance between the bridgehead atoms is found to be 1.594 Å – similar to the length of

the C–C bond in ethane (1.524 Å)[40] (**Figure 1.7c**). This distance is short enough to suggest the presence of a bond between the two bridgehead atoms, and many studies have been published investigating its exact nature.

In 1982, Wiberg calculated the bond energies of various small ring propellanes:[41] [1.1.1]propellane was calculated to have a bond energy of ~65 kcal mol^{-1}, whereas [2.1.1]propellane and [2.2.1]propellane had bond energies of ~30 and ~5 kcal mol^{-1} respectively. It was therefore predicted that the central bond of [1.1.1]propellane was significantly more stable than those of other small ring propellanes. However the bond was shown to be non-bonding,[42] with electron density depletion in between the two bridgehead atoms at the critical point.[43] The central bond was therefore described as a charge shift bond where stabilisation occurs through resonance between repulsive covalent and attractive ionic structures (**Figure 1.8a**).[44]

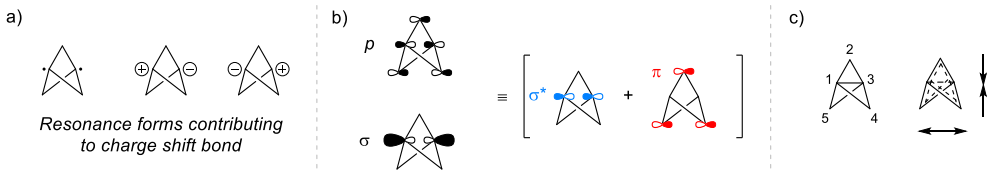

Figure 1.8 *- a) The central bond of TCP as a charge shift bond consisting of covalent and ionic contributions. b) Delocalisation of electrons from the bridgehead σ* orbital into the π-system of the bridging carbons. c) TCP undergoes lateral compression in order to maximise overlap of these orbitals.*

Recently, Sterling, Duarte and Anderson used further *in silico* experiments to show that electron density from the centre of the 'cage' can be delocalised onto the bridge carbon atoms (**Figure 1.8b**): electrons from the central bond σ orbital partially populate the σ* orbital, which is able to overlap with the π system of the bridging carbon atoms.[45] In order to maximise this overlap, the propellane cage is compressed laterally, lengthening the C1–C3 central bond and shortening the distance from C2 to C4 (**Figure 1.8c**). The overall effect of this is a decrease in Pauli repulsion between the electrons in the central

bond and the bridging bonds, as well as stabilising the propellane against fragmentation along the bridging (C1–C2) bonds.

The unusual electronic structure and stabilisation of TCP leads to interesting reactivities. TCP is omniphilic: it is able to react with radicals, anions and cations.[46] While neat [1.1.1]propellane (TCP) polymerises spontaneously in the liquid phase above 0 °C, and is only stable for a few minutes in the gas phase 110 °C,[41] it is possible to store TCP as a solid in liquid nitrogen,[47] or, more conveniently, as a solution in various solvents (usually ethers). In the latter, negligible decomposition is observed when stored at −20 °C for several months. This is in contrast to [2.1.1]propellane and [2.2.1]propellane, which are unstable above −223 °C and must be isolated in a N_2 matrix.

1.4.1 Synthesis of tricyclo[1.1.1.0^{1,3}]pentane

TCP was first synthesised by Wiberg in 1982 by reacting dibromo-BCP **31** with *t*-BuLi (**Scheme 1.3a**). [41] However, it was not isolated, they instead analysed the solution of TCP and *t*-butyl bromide formed on reaction in the reaction solvent. In 1985, Szeimies reported a very efficient route to TCP starting from cyclopropane **32** (**Scheme 1.3b**).[48] On addition of 2.2 equivalents of *n*-BuLi, **32** underwent two sequential cyclisations following lithium/halogen exchange with the bromide substituents, and the resultant mixture was distilled to give a solution of TCP in pentane/ether as the distillate. While only a modest yield of ~34% was obtained, this reaction has since been optimised, most recently by Baran, to give much higher yields.[49] This methodology is now suitable for relatively large (multi-100 g) scale syntheses of TCP (**Scheme 1.3c**), and several groups have demonstrated its use as a method of synthesis for some bridge-substituted analogues (**Scheme 1.3d**) which had also been shown earlier by Szeimies.[50–52]

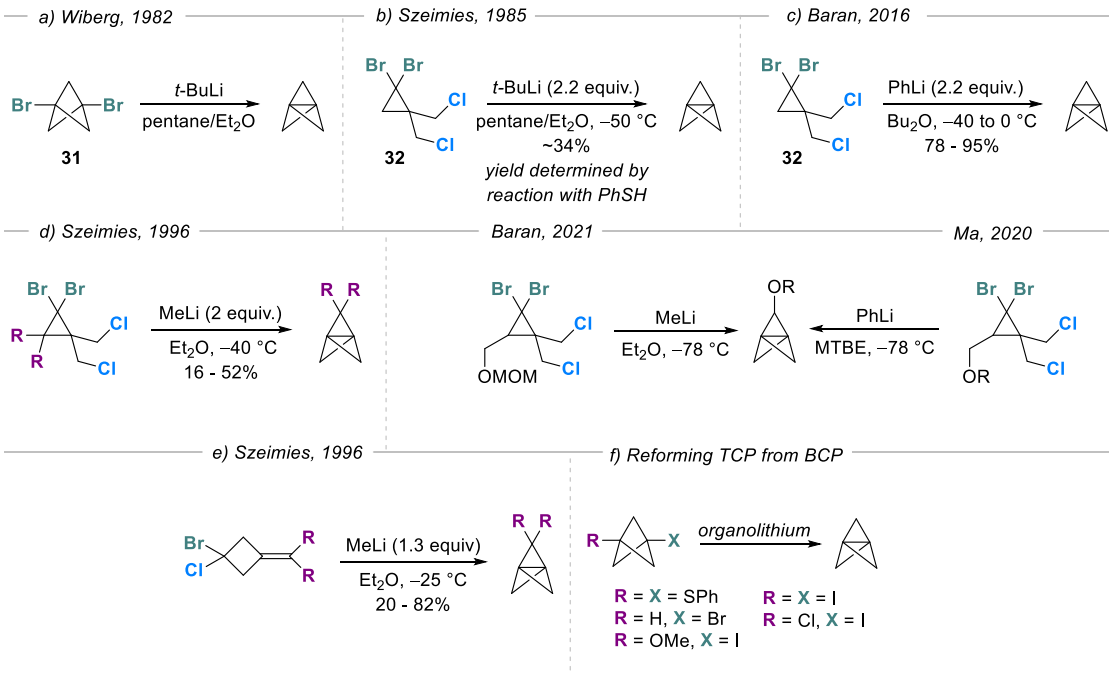

Scheme 1.3 *– Methods for the synthesis of tricyclo[1.1.1.0^{1,3}]pentane*

Other methods of TCP synthesis have since been developed involving intramolecular carbene addition to *exo*-methylene cyclobutanes[53] (**Scheme 1.3e**), and analogues of Wiberg's original synthesis of TCP work, reforming TCP from 1,3-disubstituted BCPs (**Scheme 1.3f**).[54–57]

1.4.2 Reactions of TCP with Cations

The reaction of TCP with cations has not been explored as thoroughly as its anionic and radical reactions. This is largely due to its propensity to spontaneously fragment upon formation of a partial positive charge at the bridgehead carbon atoms to give an exo-methylene cyclobutane cation **33** (**Scheme 1.4**).[45,58] The most common mechanism for this to occur is through charge transfer from TCP to a cation. This process is barrierless, and withdraws electron density from the 'cage' of TCP,[45] causing a loss of the stabilising

σ–π-delocalisation due to a reduction of Pauli repulsion, resulting in the TCP cation undergoing fragmentation.

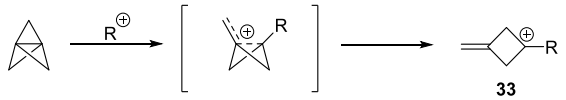

Scheme 1.4 *– Spontaneous fragmentation of the TCP cage on reaction with a cation to give the methylene cyclobutane cation.*

This fragmentation is demonstrated experimentally in the reaction of TCP with acetic acid to form methylene cyclobutane acetate **34** (**Scheme 1.5a**).[59] Fragmentation is also observed in the copper-catalysed synthesis of exocyclic allenic cyclobutanes on reaction with terminal alkynes,[60] and the nickel-catalysed cyclopropanation of TCP to form spiro-compounds [61] (**Schemes 1.5b** and **1.5c**, respectively).

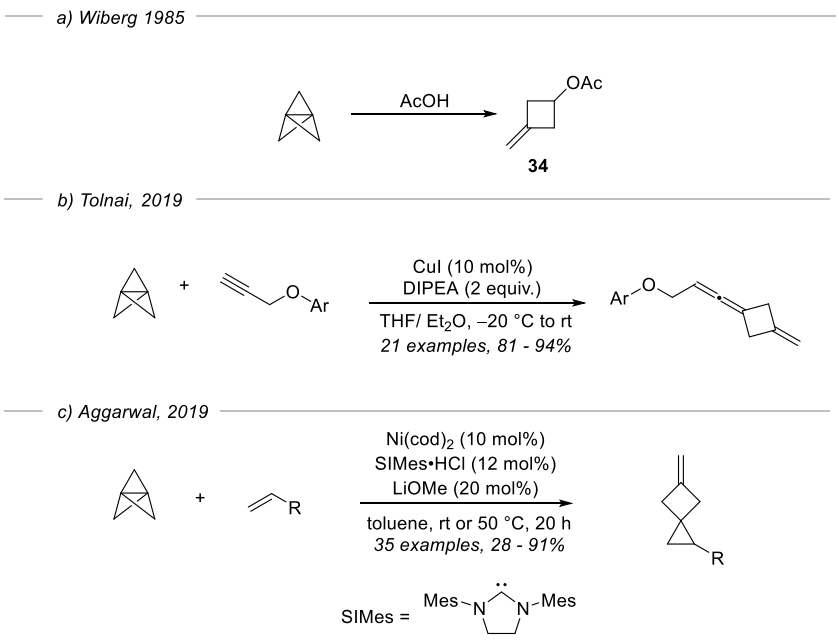

Scheme 1.5 *–Reactions of TCP with cationic species.*

1.4.3 Reactions of TCP with Anions

The reactivity of TCP with anions has been explored to a greater extent than that of cations, as it offers a useful route to substituted bicyclo[1.1.1]pentanes without competing fragmentation.[31,46] However, these reactions often require high temperatures and long reaction times in spite of the beneficial thermodynamic 'strain-release' associated with breaking the central bond of TCP on addition of an anion.

The use of anionic reactions with TCP has been shown to form a diverse range of unsymmetrical 1,3-disubstituted BCPs. Based on early reports of the addition of Grignard reagents across the central bond of TCP by Szeimies,[62,63] de Meijere demonstrated the addition of aryl Grignard reagents across TCP over several days at 35 °C to give the BCP Grignard reagents **35**, which were subsequently cross-coupled under both nickel and palladium catalysed conditions in moderate yields (**Scheme 1.6a**).[64]

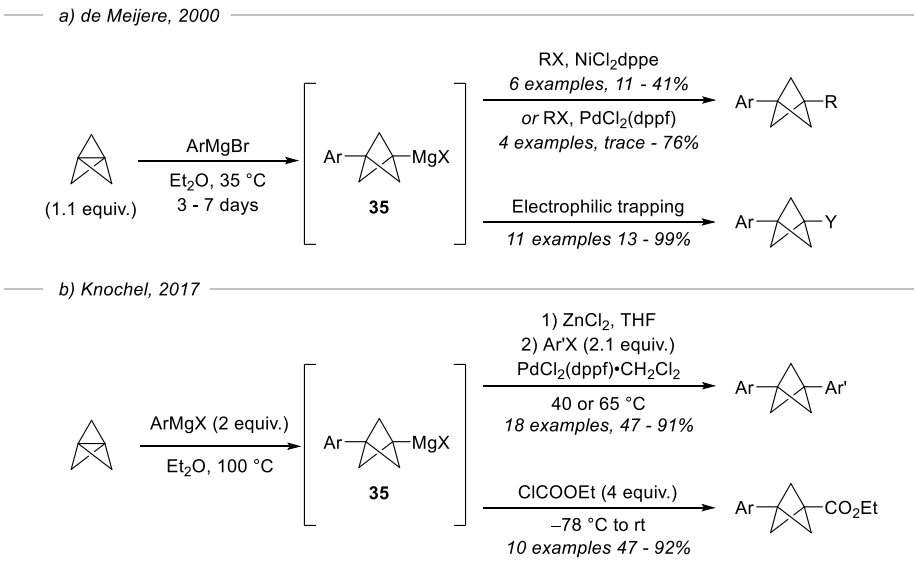

Scheme 1.6 *– Reactions of TCP with organomagnesium species.*

Knochel later expanded this work, forming BCP-Grignard intermediates **35** after treating TCP with aryl Grignard reagents at high temperatures, which significantly reduced the time needed for the reaction (**Scheme 1.6b**).[65] These intermediates can then be used to either trap electrophiles such as $ClCO_2Et$ or alternatively can be transmetallated to form a BCP-zincate species which can subsequently be subjected to Negishi cross-coupling with aryl halides to form 1,3-diaryl BCPs.

Similarly, Knochel has reported the addition of both allylic zinc halides and zinc enolates across TCP to directly form BCP-organozincs **36** and **37** (**Scheme 1.7**); these can undergo a variety of transformations including cross-coupling or electrophilic trapping.[66]

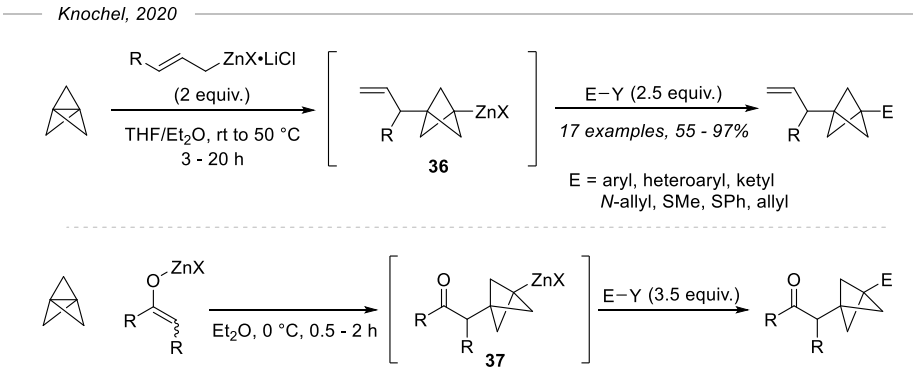

Scheme 1.7 *– Reactions of TCP with organozinc species.*

Nitrogen anions have also been demonstrated to add to TCP. Baran demonstrated an efficient synthesis of terminal amino-BCPs by reacting TCP with turbo-amides at high temperatures (**Scheme 1.8a**).[67] While the conditions used are not particularly mild, it demonstrated the first general, scalable synthesis of these compounds. Gleason has recently expanded upon this work, where the BCP magnesiate intermediates were formed on addition of turbo amides across TCP. They hypothesised that the BCP Grignard reagents had limited stability at high temperatures over extended periods of time, and indeed found an improvement in yield upon lowering the temperature used, with room temperature proving optimal. The BCP Grignard intermediates were then subjected to a

copper-catalysed alkylation with a range of alkyl halides to give 3-alkyl BCP amine substrates in a one-pot procedure (**Scheme 1.8b**).[68]

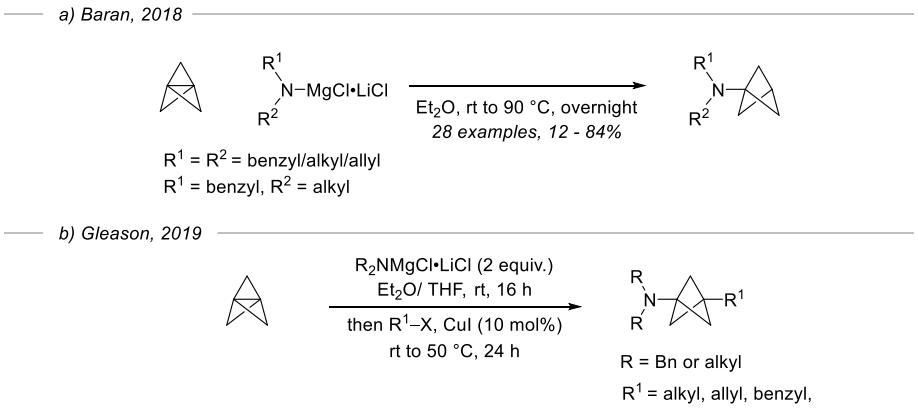

Scheme 1.8 *– Addition of turbo-amides across TCP.*

Walsh and co-workers demonstrated the addition of 2-azaallyl anions to an excess of TCP, using LiHMDS to form BCP benzyl amines (**Scheme 1.9a**),[69] with the view to their potential use as bioisosteres for diaryl methanamines. Walsh later reported the addition of 2-aryl-1,3-dithianes to TCP using NaHMDS (**Scheme 1.9b**), accessing bicyclopentylated dithianes **38** in high yields which could subsequently undergo further transformations, including deprotection to the BCP ketone derivatives **39**.[70]

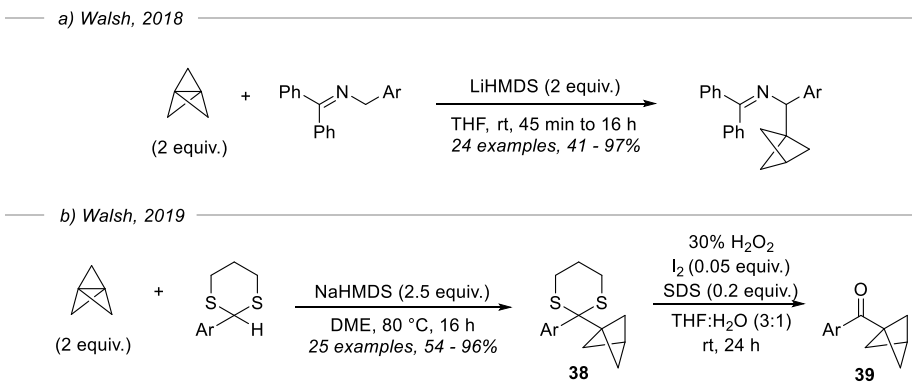

Scheme 1.9 *– Addition of anions adjacent to heteroatoms, to TCP.*

1.4.4 Reactions of TCP with Radicals

The addition of radicals across TCP has been explored more thoroughly than its reactions with electrophiles or nucleophiles, and has been used to synthesise many highly-substituted BCPs. Some of the first radical additions across TCP were discovered by Wiberg in 1986 (**Scheme 1.10**).[71] A variety of halides, aldehydes, disulfides and diselenides reacted with the central bond of TCP, with some requiring the addition of benzoyl peroxide as a radical initiator. While no yields were reported for these reactions, they demonstrated the ability of TCP to react readily with radicals. Wiberg later reported additional radical bicyclopentylations of ketones, ethers and amines,[72] although the products were often isolated as mixtures with the associated [n]staffanes, where [n] number of additional TCP molecules are trapped by the initially-formed BCP radical intermediate before the reaction terminates / propagates.

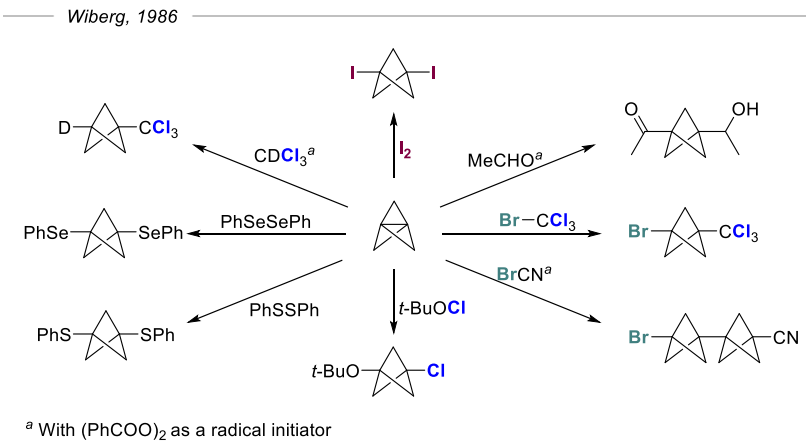

Scheme 1.10 *– Early additions of radicals to the central bond of TCP, discovered by Wiberg.*

Michl showed that diacetyl reacts with TCP under UV irradiation with a mercury lamp to give 1,3-diketo-BCP **40** (**Scheme 1.11a**); this product can be further transformed to the diacid **41** on reaction with NaOBr.[73] Diacid **41** has since proved to be a very valuable

building block for the synthesis of more complex BCP compounds,[74] and is one of the few commercially available BCPs. Recently, the addition of diacetyl to TCP has been optimised in a flow set-up, where large quantities of **40** could be prepared on a short timescale **(Scheme 1.11b)**.[75]

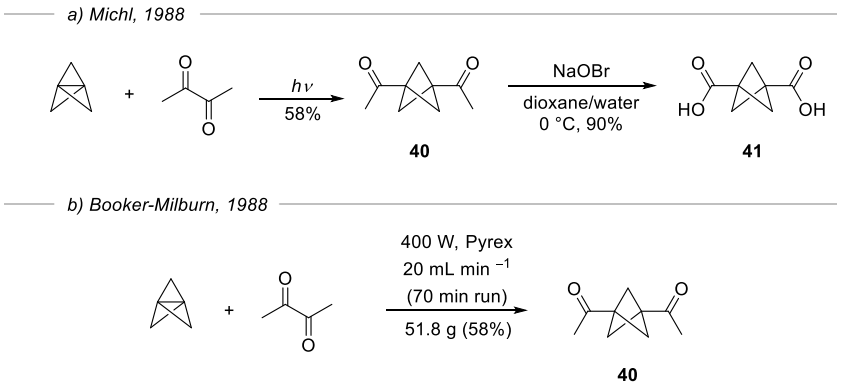

Scheme 1.11 *– Reactions of TCP with diacetyl to form di-carbonyl BCPs.*

Under irradiation, alkyl halides were shown to undergo radical addition to TCP by Michl and co-workers to give 1-halo-3-substituted-BCPs (**Scheme 1.12a**), which were subsequently activated with Bu_3SnH and added to a variety of alkenes, ketones and diacetyl traps in moderate yields.[76]

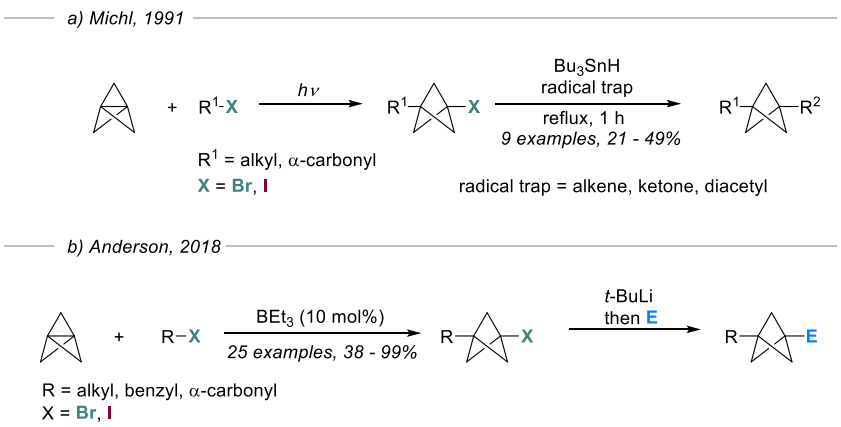

Scheme 1.12 *– Addition of alkyl halides across TCP using a) irradiation, and b) triethylborane initiation.*

More recently Anderson and co-workers reported a mild triethylborane-initiated addition of a variety of halides to TCP in good yield (**Scheme 1.12b**).[77] These 1-iodo-3-substituted BCPs (BCP iodides) were also shown to undergo further transformations with *t*-BuLi followed by electrophilic trapping or cross-coupling.

Since the early demonstrations of heteroatom radical additions to TCP by Wiberg (see **Scheme 1.10**), there have been many more reports of heteroatoms undergoing radical additions to the central bond of TCP. In 1985, Szeimies first reported the addition of thiophenol to TCP;[48] this reaction occurs spontaneously and in almost quantitative yields, and indeed is so reliable that it has be used to determine the concentration of TCP solutions (**Scheme 1.13a**).[72] More recently Bräse expanded this reaction and successfully added a range of alkyl and aryl thiols across TCP (**Scheme 1.13b**).[78]

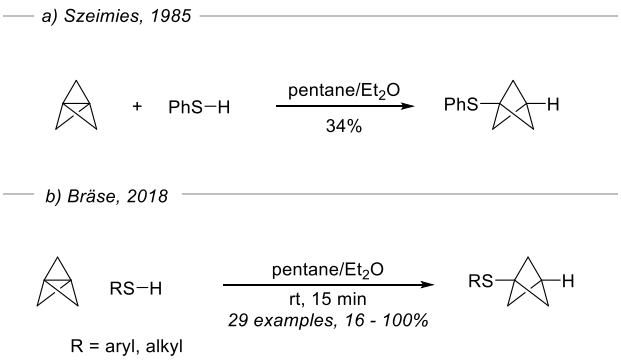

Scheme 1.13 *– Radical addition of thiols to TCP.*

1.5 Synthesis of aryl-bicyclo[1.1.1]pentanes

Despite many reported reactions of TCP with electrophiles, nucleophiles, and radicals over the past 40 years, few methods exist for the synthesis of aryl substituted BCPs. Formation of BCP-aryl species has involved high temperatures and organometallic reagents, such as Knochel's addition of aryl Grignard reagents across the central bond of

TCP (which requires heating an ethereal solution to 100 °C),[65] or the addition of organozinc complexes to TCP followed by subsequent cross-coupling with aryl halides[66] (**Scheme 1.14a**, see **Chapter 3.2.1** for further discussion). These harsh conditions make these approaches poorly suited to late stage functionalisations or industrial applications.

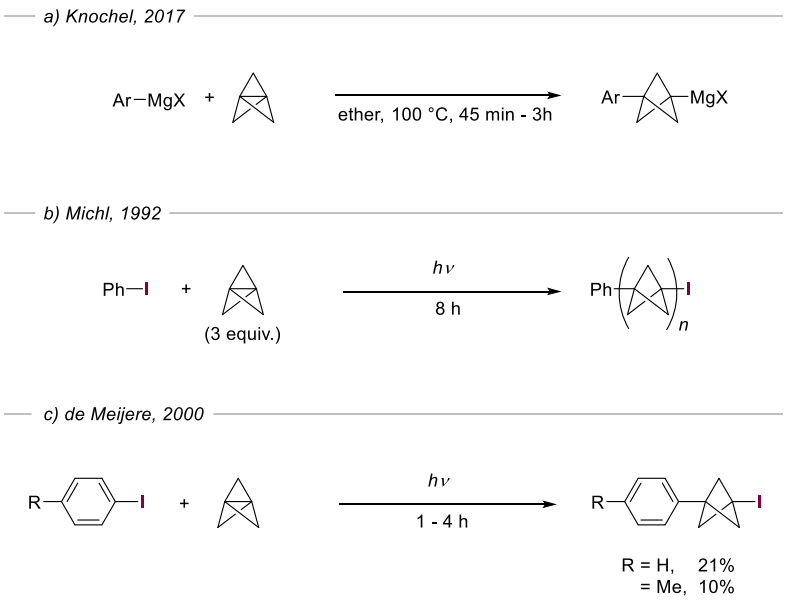

Scheme 1.14 *– Formation of aryl-substituted BCPs through a) addition of Grignard reagents, b) c) irradiation with a mercury lamp.*

Aryl-BCPs have also been accessed through the irradiation of iodobenzene with a mercury lamp. In 1992 Michl reported the formation of 1-iodo-3-phenyl-BCP in low yields along with a mixture of [n]staffanes which were difficult to separate and had to be used in subsequent steps as the crude mixture (**Scheme 1.14b**).[79] In 2000, de Meijere reported a similar approach and was able to isolate very low yields of two 1-iodo-3-aryl BCPs (**Scheme 1.14c**), however they noted that they saw a considerable decrease in yield on scaling up the reaction.[64]

1.6 Project overview

As discussed above, few methods exist for the synthesis of aryl-substituted BCPs. Of these, none is applicable for industrial use as they require harsh / unscalable reaction conditions. To further explore the bioisosteric replacement of 1,4-disubstituted arenes with 1,3-disubstituted BCPs in a pharmaceutical context, new, mild and scalable methodology for the synthesis of diverse BCPs is required.

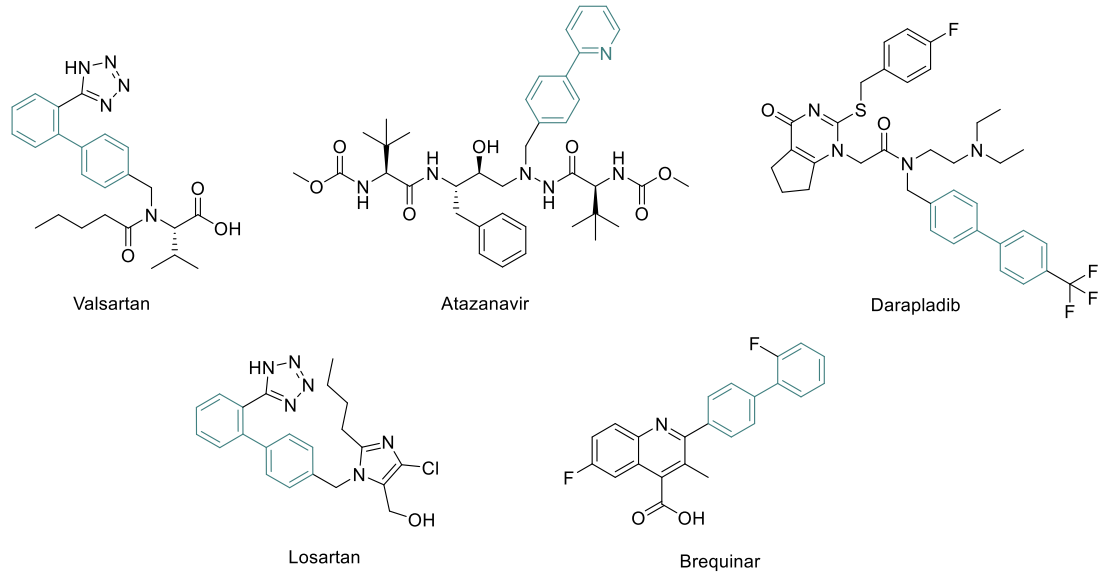

Figure 1.9 *– Drug compounds containing biaryl groups.*

This thesis details the development of new, catalytic and 'industry-friendly' methods for the synthesis of aryl-substituted BCPs, with a particular focus on the synthesis and applications of 1-iodo-3-carbo-BCPs (**Figure 1.10**). One key area we sought to further develop was the use of the iodide functionality of these compounds in further transformations.

Chapter 2 describes the use of photoredox catalysis to add (hetero)aryl iodides to the central bond of TCP to form 1-iodo-3-(hetero)aryl BCPs. The work presented in this chapter constitutes the first use of this mode of catalysis to functionalise C-C σ bonds.

Chapter 3 discusses the development of the iron-catalysed Kumada cross-coupling of 1-iodo-3-substituted BCPs with (hetero)aryl Grignard reagents. This represents the first general cross-coupling of BCPs where the BCP is the electrophilic component, as well as the first Kumada cross-coupling of tertiary alkyl iodides. **Chapter 4** reports the use of copper catalysis for the borylation of 1-iodo-3-substituted BCPs to form BCP boronate esters, and their subsequent oxidation to form the corresponding BCP alcohols. This work represents the first general conversion of BCP iodides to BCP boronates without the need for *tert*-butyllithium.

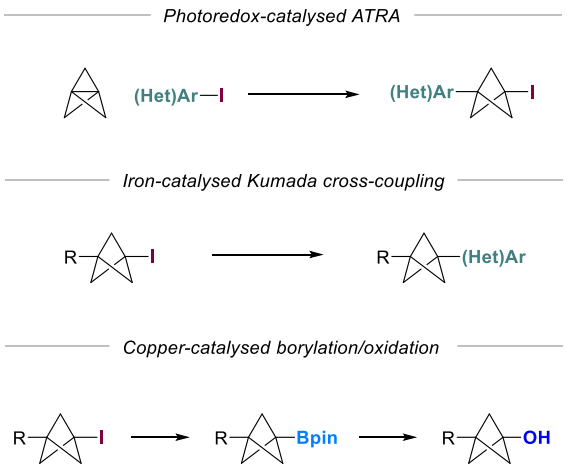

Figure 1.10 *– Methodologies developed and detailed in this thesis.*

2

Photoredox-catalysed atom transfer radical addition

2.1 Photoredox catalysis

Interest in photoredox catalysis has increased dramatically over the past decade as it offers mild and selective means to perform a wide range of chemical transformations in a more environmentally friendly and functional group tolerant way than previous alternative methods. The use of transition metal photoredox catalysts – activated by visible light – is particularly attractive, given the ability to finely tune the combination of metal and ligands to adjust the redox potential of the catalyst.

One of the earliest examples of visible light photoredox catalysis was demonstrated by Kellogg and co-workers in 1978, using the photocatalyst $[Ru(bpy)_3]Cl_2$ to accelerate the reduction of sulfonium ions by *N*-substituted 1,4-dihydropyridines (**Scheme 2.1a**).[80] In 1981, Pac and co-workers demonstrated the use of the same ruthenium photocatalyst and the reductant BNAH to reduce electron-poor alkenes (**Scheme 2.1b**), demonstrating the ability of photoredox catalysts to perform reactions under mild conditions.[81] In 1990 Fukuzumi demonstrated one of the first examples of a reductive halogenation of α-

bromocarbonyl compounds, also using $Ru(bpy)_3Cl_2$ as a photoredox catalyst for the activation of halides (**Scheme 2.1c**), and obtaining the reduced products in excellent yields.[82]

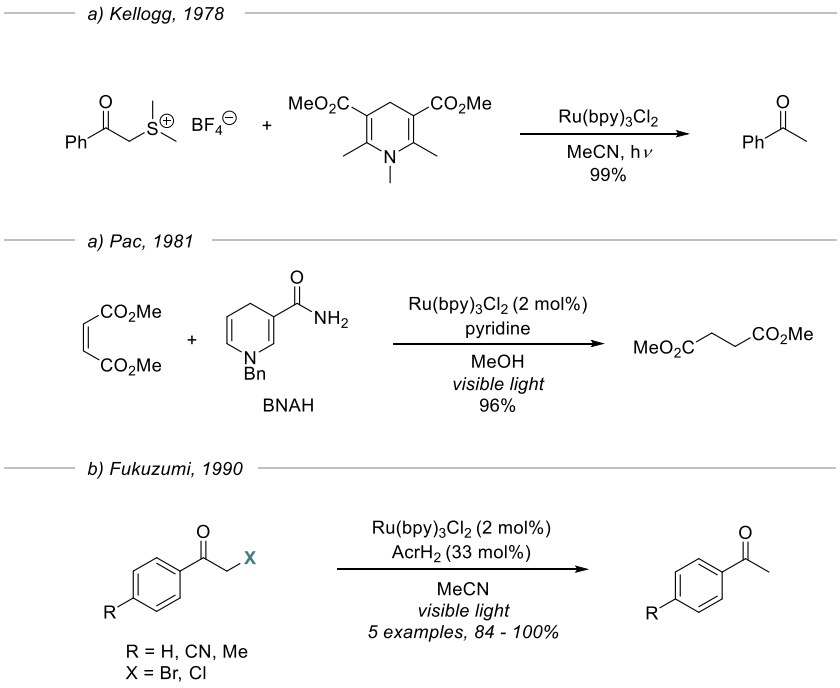

Scheme 2.1 *– Early examples of photoredox catalysis involving a) the reduction of electron poor alkenes and b) the reduction of α-bromocarbonyls.*

The interest in photoredox catalysis increased dramatically after 2008, upon the development of a number of key reactions that demonstrated powerful chemical transformations which greatly expanded the scope of what was possible using photoredox catalysis. Firstly, in 2008 Macmillan and co-workers published the asymmetric alkylation reaction of aldehydes with electron deficient halides – a reaction which had previously been elusive – using dual enamine catalysis and photoredox catalysis under visible light, forming products in both high yield and high e.e. (**Scheme 2.2a**).[83] Around the same time Yoon and co-workers demonstrated the ability of photoredox catalysis to facilitate the [2+2] cyclisation of dienones under mild conditions, forming cyclised products in

excellent yields and good d.r. (**Scheme 2.2b**).[84] The following year, Stephenson used photoredox catalysis to reductively cleave aliphatic halides without the need for toxic tin

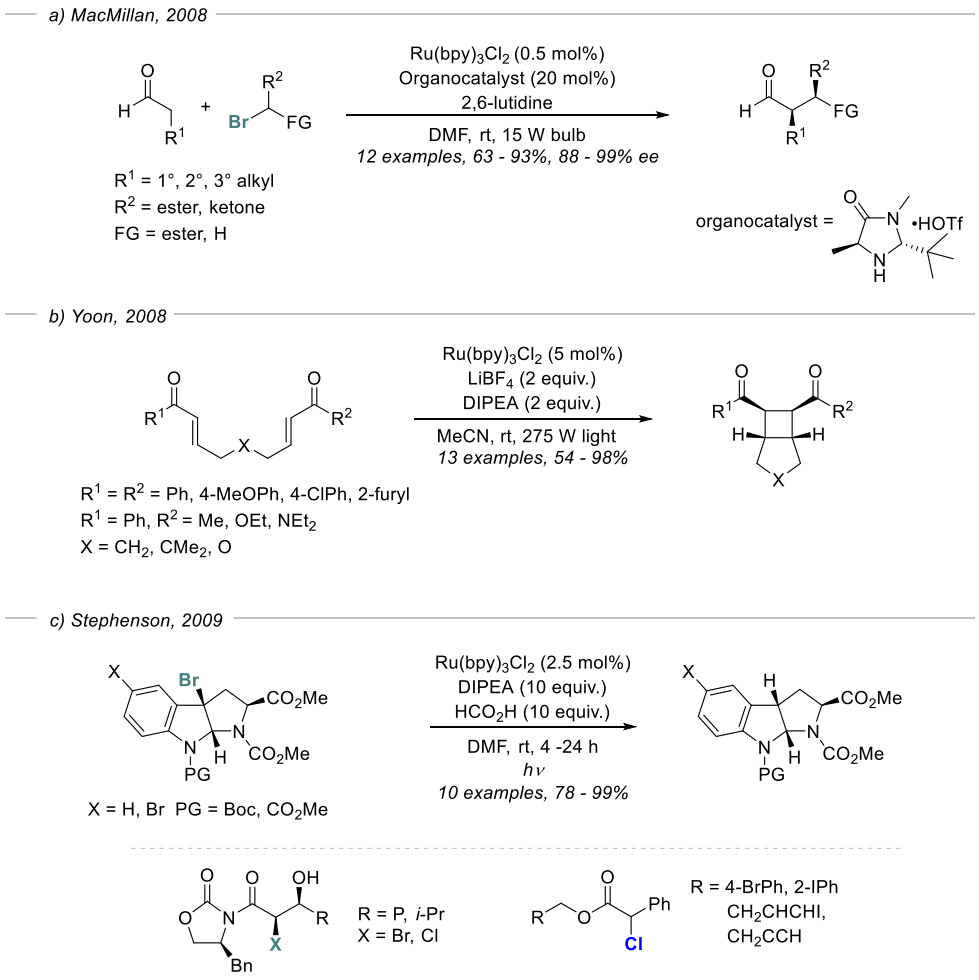

Scheme 2.2 *– Seminal publications on the use of photoredox catalysts for organic transformations involving a) Asymmetric alkylation of α-aldehydes using dual organo/photoredox catalysis. b) Photoredox catalysis [2+2] cyclisations. c) Reduction of aliphatic halides.*

reagents which had commonly been used for such transformations.[85] The reaction showed excellent functional group tolerance and gave high yields of the reduced products (**Scheme 2.2c**). Following these seminal studies, interest in photoredox catalysis increased rapidly and a large number of papers have been published on the topic spanning a wide range of transformations.[86–90]

2. Photoredox-catalysed atom transfer radical addition

Photoredox catalysts interact with a substrate via one of two pathways: oxidative or reductive quenching. The ground state catalyst is first excited by the wavelength of visible light necessary to initiate a metal-to-ligand charge transfer (MLCT) to a singlet-excited state S_1 (**Figure 2.1**).

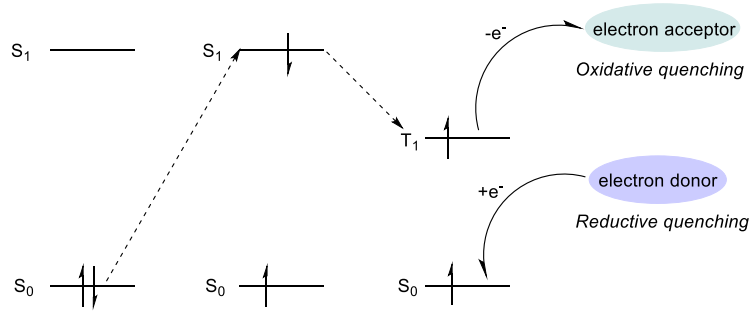

Figure 2.1 *– Excitation of ground state photocatalyst followed by intersystem crossing and then oxidative or reductive quenching, by the donation or accepting of an electron, respectively.*

This then undergoes intersystem crossing to the lowest energy triplet-excited state (T_1) which is sufficiently long-lived to be able to undergo electron transfer processes. This excited state photocatalyst can then either donate or accept an electron and is quenched in the process.

In oxidative quenching (**Figure 2.2a**) the excited catalyst donates an electron to a molecule of starting material or an oxidant present in the reaction mixture (**A_1**) and is itself oxidised to PC^{+1}. This oxidised catalyst can then accept an electron from a neutral radical species, or a reductant present in the reaction (**D_1**) to reform the initial ground state catalyst species. In reductive quenching (**Figure 2.2b**) the excited state catalyst can accept an electron from a molecule of starting material or a reductant (**D_2**) and is itself reduced to PC^{-1}. This can subsequently donate an electron to a radical species or to an oxidant (**A_2**) in order to return the starting catalyst. A redox potential is associated with each step in the catalytic cycle, indicating the ease of oxidising or reducing each species. The

pathway involving the most favourable redox potentials is likely to dominate the quenching pathway employed by the catalyst.

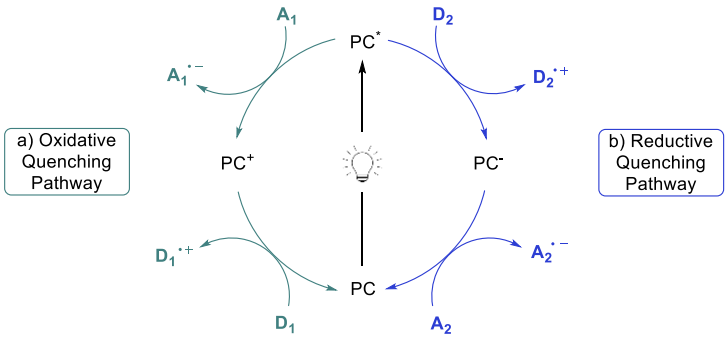

Figure 2.2 *– General mechanism of photoredox catalysis via a) oxidative quenching or b) reductive quenching.*

Iridium- and ruthenium-centred catalysts are commonly used in photoredox reactions (**Figure 2.3**) as the ligands surrounding these metals can be subtly tuned to increase or decrease the reductive and oxidative capabilities of the catalyst. Ir^{3+} and Ru^{2+} centred catalysts are generally considered to act via oxidation of the metal or reduction of the ligands.

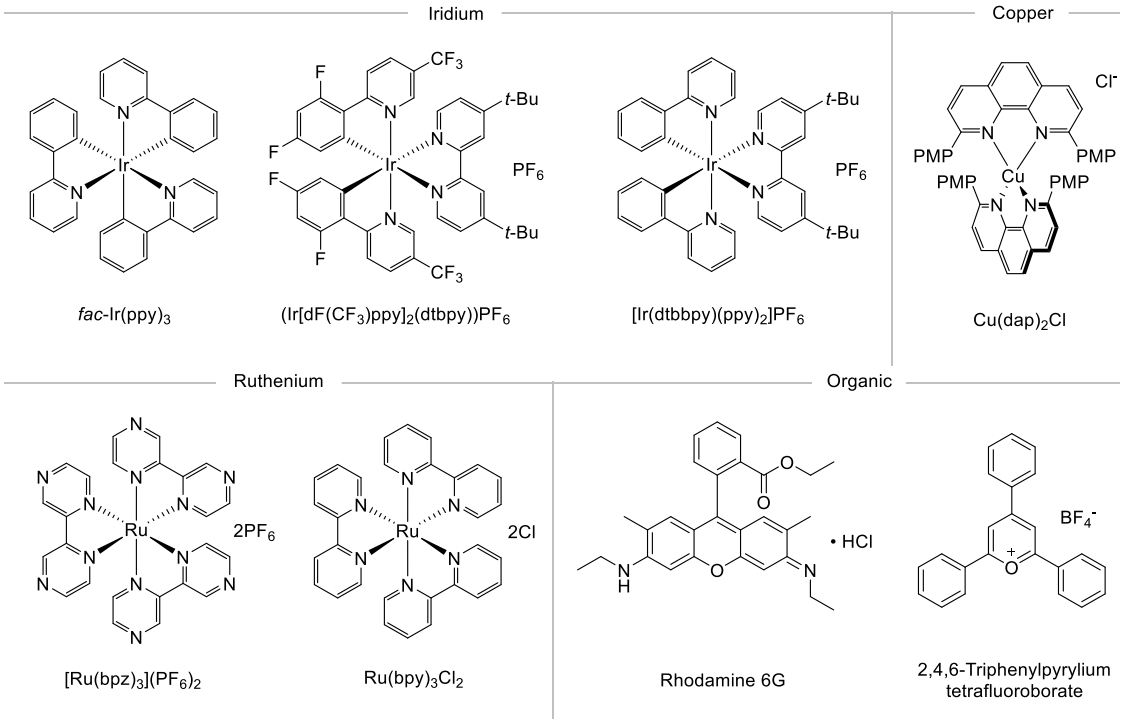

Figure 2.3 *– A range of commonly used iridium, copper, ruthenium and organic photocatalysts.*

The E_{red} half-reactions describing the reduction potential for these complexes reflect these effects: the more electron-donating the ligands, the more electron-rich the metal centre in the complex, and the more easily it is oxidised. This results in greater reducing power for the complex, or in other words, $E_{red}[M^{3+}/M^{2+}]$ is less positive (**Figure 2.4a**). In addition, the more electron dense the ligands in the complex, the easier they are to oxidise, and therefore the greater the reducing power of the complex, or $E_{red}[M^{2+}/M^{+}]$ is more negative (**Figure 2.4b**).

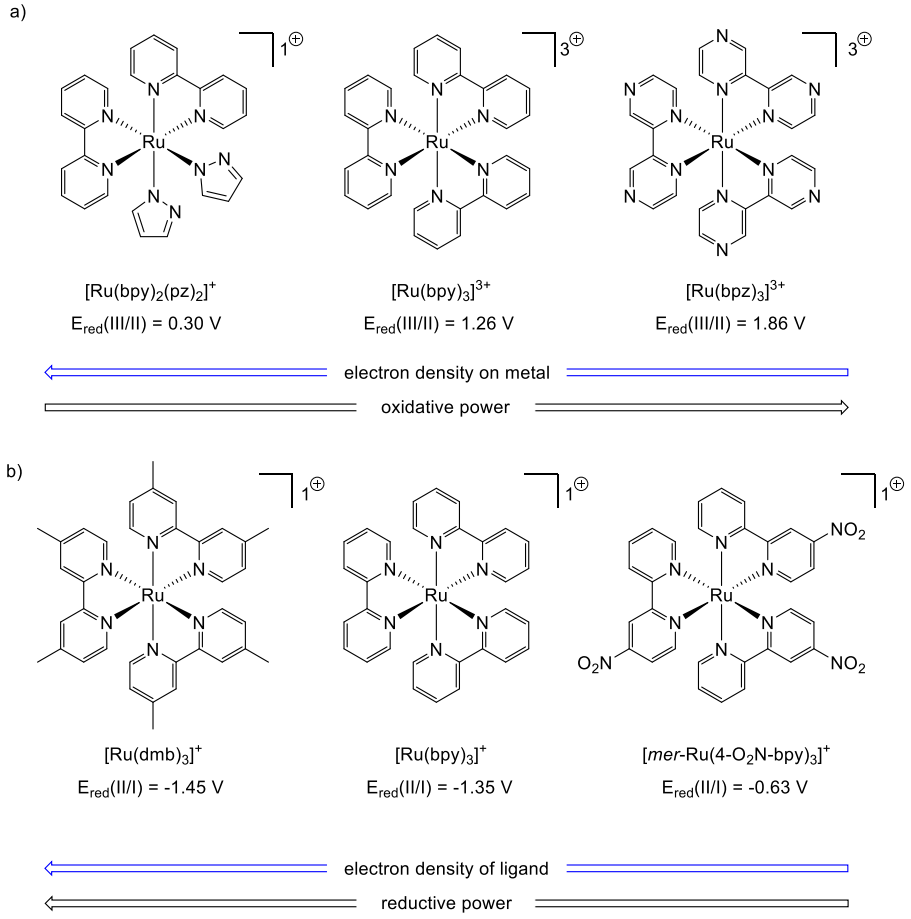

Figure 2.4 *– The effects of electron density of a) the metal centre and b) the ligand on the oxidative or reductive powers of Ru^{3+} photocatalysts. Reduction potentials given are vs SCE. Figure adapted from J. w. Tucker and C. R. J. Stephenson, J. Org. Chem.* ***2012****, 77, 1617 – 1622.*

Therefore, by adjusting the combination of metal centre and surrounding ligands, the redox potentials of photocatalysts can be tuned. In photoredox catalysis, the reduction

potentials of the excited states of the catalyst must also be considered, as these are the species undergoing oxidative or reductive quenching. These cannot be measured directly however, and instead are estimated by adding the ground state potential to the zero-zero excitation energy ($E_{0,0}$), which is defined as the energy difference between the T_1 state of the excited photocatalyst and the S_0 ground state of the photocatalyst. The zero-zero excitation energy can be estimated by $E_{0,0} = h(c/\lambda_{em})$ where λ_{em} is the maximum emission of the catalyst and can be measured by emission spectroscopy. These estimated reduction potentials of excited state photocatalysts can be matched to the desired chemical reaction by comparing with the reduction potential of the reactant bond in question.

2.2 Atom transfer radical additions

Atom transfer radical additions (ATRA) are a class of reactions where a molecule R–X is added across double or triple carbon–carbon bonds, either through a radical chain pathway, or under photoredox catalysis. ATRAs allow for highly efficient difunctionalisations, and when X is a halide, install a synthetic handle for further functionalisations. ATRA reactions are sometimes referred to as Kharasch reactions due to his seminal work on this reaction type in 1945 on the reaction of carbon tetrachloride with various alkenes when heated in the presence of a small amount of diacetyl or dibenzoyl peroxide as a radical initiator (**Scheme 2.3a**).[91] However, it was not until 1994 that the Barton group published the first example of a photoredox method of a group transfer radical addition reaction (**Scheme 2.3b**).[92] The group used catalytic $Ru(bpy)_3Cl_2$ under irradiation to initiate a chain reaction beginning with reducing the weak Se–S bond in Ts–SePh, in an oxidative quenching process.

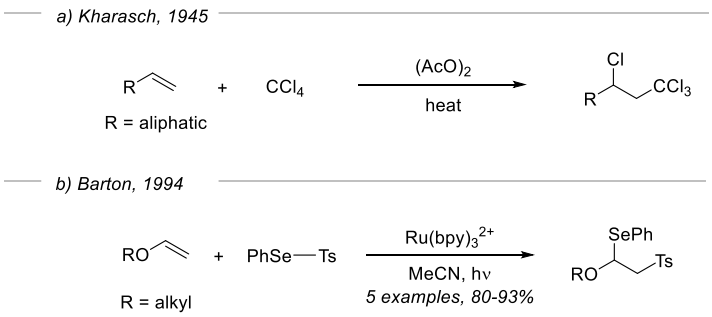

Scheme 2.3 *– Early examples of ATRA reactions. a) The first report of ATRA reaction. b) The first photoredox catalysed group transfer radical addition*

Despite photoredox catalysis gaining popularity and the number of publications in this area increasing dramatically, the first general photoredox catalysed ATRA of halides across alkenes was not published until 2011 by Stephenson *et al.* Opting for iridium rather than ruthenium, they used $Ir[(dF(CF_3)ppy)_2(dtbbpy)]PF_6$ with two equivalents of both an activated alkyl bromide and LiBr to add across various alkenes (**Scheme 2.4a**).[93] LiBr had previously been employed by Yoon and co-workers in the photocatalytic reduction of enones,[84] who suggested that the lithium cation can function as a Lewis acid to activate the enone through coordination to the carbonyl groups. In this case, the LiBr likely similarly activated the carbonyl groups on the alkyl halides, promoting the reduction of the carbon–halogen bond. The reaction also tolerated α-halocarbonyls and alkyl halides as well as CF_3I, and proceeded in good yields. The authors suggested a radical mechanism that proceeds via oxidative quenching of the excited catalyst with the alkyl halide, however they could not definitively determine whether the reaction then progressed as a chain reaction or a radical–polar crossover reaction. Stephenson continued work in this area to introduce several slightly altered reaction conditions, varying catalyst/additive combinations to widen the substrate scope to include chlorides, perfluoroalkyl iodides and more hindered alkenes as well as alkynes (**Scheme 2.4b**),[94] and demonstrating that the reaction was possible in flow.[95] The same year, Reiser et al.

developed a copper-catalysed photoredox ATRA reaction using green light irradiation to perform additions of a limited range of activated alkyl bromides across various alkenes (**Scheme 2.4c**).[96] However he also improved on this the next year to extend the scope to benzyl bromides,[89] and perform the reaction in a flow set-up in 2015.[97]

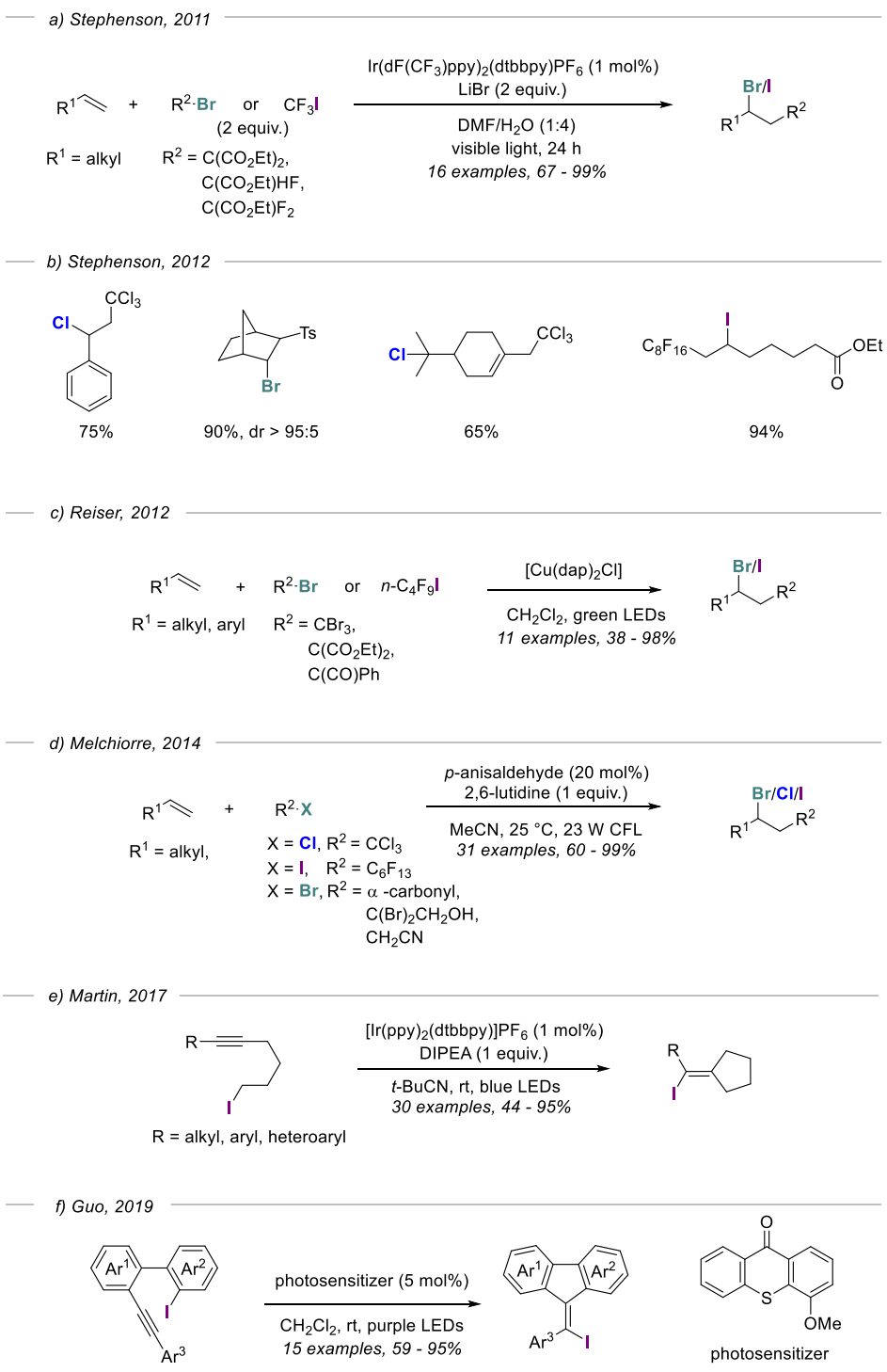

Scheme 2.4 *– Atom transfer radical additions of alkyl and aryl halides across unsaturated bonds.*

While transition metal catalysts are common for performing these reactions, organocatalysts can also be employed. In 2014, Melchiorre et al. developed an elegant metal-free ATRA reaction using catalytic *p*-anisaldehyde in combination with stoichiometric 2,6-lutidine, under irradiation by a compact fluorescent lamp, to efficiently add electron-poor alkyl halides to a range of alkenes (**Scheme 2.4d**).[98]

The aforementioned procedures were largely limited to activated alkyl bromides and a few iodides. However, in 2017 Martin and co-workers reported an iridium-catalysed photoredox atom transfer radical cyclisation (ATRC) reaction of unactivated alkyl iodides, with stoichiometric DIPEA present as a sacrificial reductant (**Scheme 2.4e**).[99] Cyclisations onto both alkenes and alkynes were demonstrated as well as a double cyclisation. In 2019, Guo and co-workers demonstrated the first example of an ATRC of aryl iodides across alkynes using an organic photosensitizer and purple light to form vinyl iodides in high yields (**Scheme 2.4f**).

As noted, the ATRA reactions discussed above largely focused on bromides, often next to electron withdrawing groups such as carbonyls. Meanwhile the reaction of iodides remained largely underdeveloped, only predominantly fluoroalkyl iodides. While addition across double and triple bonds were demonstrated by multiple authors, the functionalisation of single bonds remained elusive until the ATRA reaction of iodides with tricyclo[1.1.1.$0^{1,3}$]pentane (TCP, or [1.1.1]propellane) was reported by our group.

2.2.1 Atom transfer radical additions with [1.1.1]propellane

Previously, the Anderson group developed an efficient ATRA reaction of alkyl iodides and activated alkyl bromides across TCP to give 1-iodo, 3-substituted

bicyclo[1.1.1]pentanes (**Scheme 2.5**).[77] The reaction is metal free, conducted at room temperature (or below) under air, and reactions were generally complete in as little as 15 min, in high yields. A wide range of alkyl iodides including benzylic and α-carbonyl iodides were successfully transformed in the presence of aldehydes, chlorides, free alcohols, amides and sulfonyl groups. While this was effective for the synthesis of many BCPs, the use of the pyrophoric triethylborane as a radical initiator is somewhat hazardous, and the reaction displayed a number of substrate limitations. For example, benzyl iodide itself, and molecules containing free amines were unsuccessful in the reaction; and no aryl or heteroaryl iodides could be used, as the ethyl radical generated by triethylborane in the presence of oxygen is unable to break aryl iodide bonds in order to initiate the reaction,[100] due to the stronger sp^2 hybridised C–I bond strengths compared to sp^3 C–I bonds.[101]

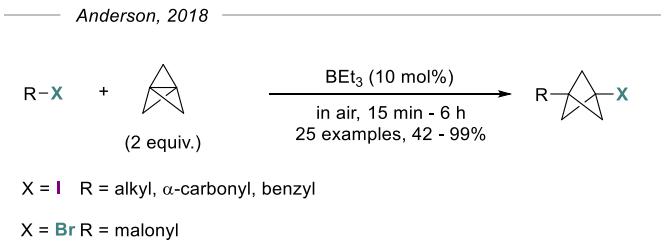

Scheme 2.5 *– Triethylborane initiated ATRA of iodides and bromides across TCP.*

While radical species are generally able to add efficiently to TCP,[102,103] the addition of aryl or heteroaryl iodides requires a different method of generating the requisite carbon-centred radical. Photoredox catalysts are able to reach (high) redox potentials that could be strong enough to reduce the C–I bond in these substrates and in doing so, generate the aryl radicals necessary to perform these ATRA reactions. While photoredox catalysts have been utilised to add a plethora of different radical species to double and triple carbon–carbon bonds, photoredox-catalysed addition of radicals to σ bonds had not been

demonstrated at this point. However, given the success of the triethylborane-initiated ATRA methodology, there was good reason to hypothesise that photoredox catalysis could be employed successfully in ATRA reactions of (hetero)aryl iodides with TCP. Moreover, as photoredox catalysis has been shown to activate aryl halides,[88,104,105] the synthesis of 1-iodo-3-arylbicyclo[1.1.1]pentanes could be possible (**Scheme 2.6**).

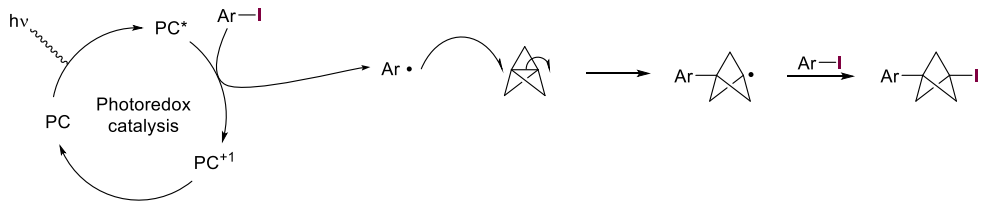

Scheme 2.6 *– Proposed photoredox catalysed pathway for ATRA of aryl iodides across TCP*

2.3 Optimisation of photoredox catalysed atom transfer radical addition of (hetero)aryl iodides with TCP

Optimisation began with 4-iodobenzonitrile **42** as a representative aryl iodide that was unreactive under the triethylborane-initiated conditions (**Table 2.1**). A range of photoredox catalysts were screened in the reaction, stirring under blue LED irradiation for 24 h. Two equivalents of TCP were used, and the reaction was run in *t*-BuCN as a solvent as this had been shown to be a suitable solvent in the Martin group's work on ATRA reaction of alkyl iodides and alkenes or alkynes, using an iridium photocatalyst.[99]

Pleasingly, a number of iridium, ruthenium and organic catalysts proved successful under these conditions, giving moderate amounts of the desired BCP iodide **43** (21-51%). The iridium catalyst *fac*-Ir(ppy)$_3$ performed best in the reaction, giving 51% of **43** (entry 1), it also has the highest reduction potential of the catalysts screened when undergoing oxidative quenching of −1.73 V (vs SCE), and therefore was able to reduce the starting material **42** most easily. A general trend was observed that the yield of **43** decreased as

the reduction potential of the catalysts used decreased, with the weakest catalyst $[Ru(bpy)_3](PF_6)_2$ with a reduction potential of −0.81 V (vs SCE) only forming 17% yield of **43** (entry 6).

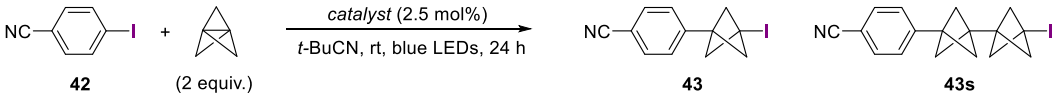

42 **43** **43s**

Entry	Catalyst	$E_{1/2}$ (M^{+1}/M^*)	Yield/[a] %	**43**:**43s**
1	*fac*-Ir(ppy)$_3$	−1.73 V	51	1:0.17
2	[Ir{dF(CF$_3$)ppy}$_2$](bpy)PF$_6$	−1.00 V	30	1:0.21
3	[Ir(dtbbpy)(ppy)$_2$]PF$_6$	−0.96 V	21	1:0.18
4	Rhodamine 6G	−0.95 V	16	1:0.02
5	[Ir{dF(CF$_3$)ppy}$_2$](dtbpy)PF$_6$	−0.89 V	35	1:0.15
6	[Ru(bpy)$_3$](PF$_6$)$_2$	−0.81 V	17	1:0.17

Table 2.1 *– Optimisation of the identity of the catalyst used in the ATRA reaction between aryl iodides and TCP. [a] Yields calculated by ^{1}H NMR spectroscopy using mesitylene as an internal standard.*

Interestingly, [Ir{dF(CF$_3$)ppy}$_2$](dtbpy)PF$_6$ was an exception to this trend; it has a reduction potential of only −0.81 V (vs SCE) however gave 35% yield of **43**. The organic catalyst Rhodamine 6G gave the lowest yield of the catalysts screened in the reaction, giving only 16% yield of **43** despite not having the lowest reduction potential (entry 4). The undesired staffane byproduct **43s** was also formed in all cases, where the BCP radical adds across another molecule of TCP before it is able to react with 4-iodobenzonitrile in order to propagate the reaction. The ratio of desired product **43** to staffane **43s** varied with the catalyst; the organometallic photocatalysts gave staffane in a ratio of between 1:0.15 to 1:0.21, whereas the organic catalyst gave a ratio of 1:0.02, albeit with a poor yield of desired product. There did not appear to be any clear reason for the varying amounts of staffane formation between catalysts.

As it was unknown whether this reaction was proceeding via an oxidative or reductive quenching pathway, these six catalysts were then screened in combination with one

equivalent of *N*,*N*-diisopropylethyl amine (DIPEA) in order to promote reductive quenching of the catalyst (**Table 2.2**).

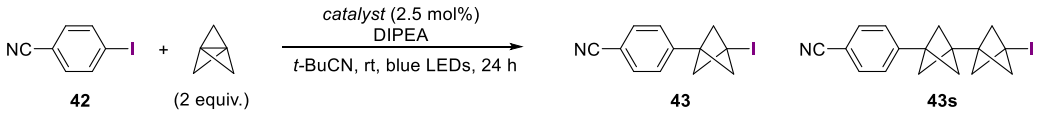

Entry	Catalyst	$E_{1/2}$ (M^*/M^{-1})	Yield/[a] %	**43**:**43s**
1	$[Ir\{dF(CF_3)ppy\}_2](bpy)PF_6$	1.68	42	1:0.19
2	$[Ir\{dF(CF_3)ppy\}_2](dtbpy)PF_6$	1.21	48	1:0.18
3	$[Ru(bpy)_3](PF_6)_2$	0.77	3	-
4	$[Ir(dtbbpy)(ppy)_2]PF_6$	0.66	49	1:0.29
5	*fac*-$Ir(ppy)_3$	0.31	40	1:0.19
6	Rhodamine 6G	-[b]	10	1:0.02

Table 2.2 *– Investigations into the effect of a tertiary amine additive on the ATRA reaction.* [a] *Yields calculated by* ^1H *NMR spectroscopy using mesitylene as an internal standard.* [b] *Reduction potential unknown.*

A different set of reduction potentials are associated with the reductive quenching pathway of the catalysts, with the most strongly reducing catalyst now being $[Ir[dF(CF_3)ppy\}_2](bpy)PF_6$ with $E_{1/2}$ (Ir(III)*/Ir(II) = 1.68 V (vs SCE), which gave 42% yield of BCP **43** (entry 1). This demonstrated an improvement in yield compared to the use of the catalyst without DIPEA present. There did not appear to be a correlation between the reduction potential of the catalyst and the observed yield of **43** when DIPEA was used however; $[Ir\{dF(CF_3)ppy\}_2](dtbpy)PF_6$ and $[Ir(dtbbpy)(ppy)_2]PF_6$ gave the highest yields of 48% and 49% of **43**, respectively (entries 2 and 4, respectively) despite having significantly lower reduction potentials. Although they gave very similar yields of **43**, $[Ir\{dF(CF_3)ppy\}_2](dtbpy)PF_6$ produced a significantly lower proportion of staffane (1:0.18 vs 1:0.29) and therefore was the most successful catalyst in the presence of DIPEA.

Whether the presence of a tertiary amine was beneficial was still unclear, therefore further investigations were performed into the nature of the tertiary amine in the reaction with the two catalysts that produced the highest yields – $Ir(ppy)_3$ and $[Ir\{dF(CF_3)ppy\}_2(dtbpy)]PF_6$. Both catalysts were submitted to the reaction in the presence of DIPEA, Triethylamine (Et_3N) or tributylamine (Bu_3N), however no improvement in yield was seen in any case, although DIPEA performed better than Et_3N or Bu_3N (**Table 2.3**, entries, 1-6). The equivalents of amine in the reaction were also explored. Photoredox activation of aryl halides can require several equivalents of amine for efficient reaction, however these are usually overall reductive processes to give the C–H bond, rather than redox neutral.[106] Reducing the equivalents to 0.5 (entry 7) resulted in a drop in yield from 40% to 34%, however, increasing the equivalents to 2.5 or 5 (entries 8 and 9, respectively) also resulted in significant decreases in yield. Overall, the use of $Ir(ppy)_3$ gave the highest yield and addition of amine appeared to offer no benefit, suggesting an

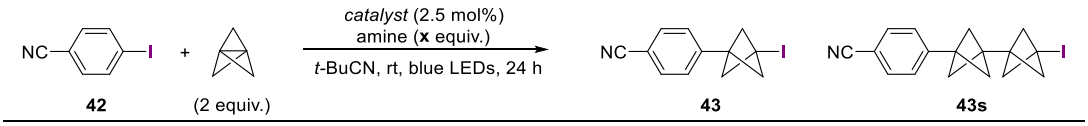

42 (2 equiv.) **43** **43s**

Entry	Catalyst	Amine	**x**	Yield/[a] %	**43**:**43s**
1	$Ir(ppy)_3$	DIPEA	1	40	1:0.19
2		Et_3N	1	35	1:0.16
3		Bu_3N	1	38	1:0.17
4	$[Ir\{dF(CF_3)ppy\}_2](dtbpy)PF_6$	DIPEA	1	48	1:0.18
5		Et_3N	1	46	1:0.13
6		Bu_3N	1	46	1:0.19
7	$Ir(ppy)_3$	DIPEA	0.5	34	1:0.13
8		DIPEA	2.5	29	1:0.13
9		DIPEA	5	26	1:0.14

*Table **2.3** – Optimisation of amine additive for ATRA reaction of 4-iodobenzonitrile with TCP.* [a] *Yields calculated by ^1H NMR spectroscopy using mesitylene as an internal standard.*

oxidative quenching mechanism is present. However, for catalysts such as [Ir{dF(CF_3)ppy}$_2$](dtbpy)PF_6, where an improvement in yield is observed on addition of amine, it is not possible to rule out that an alternative mechanism is in action in which reductive quenching does occur.

While Ir(ppy)$_3$ was identified as the best catalyst for this reaction, incomplete conversion and the formation of staffane **43s** continued to present a problem. Therefore, an investigation into the effects of reaction concentration and equivalents of TCP was performed. To attempt to limit staffane formation, the reaction concentration was reduced from 0.1 M to 0.075 M (**Table 2.4**, entry 1); however the yield of the reaction decreased from 51% to 44% and no reduction in staffane production was observed.

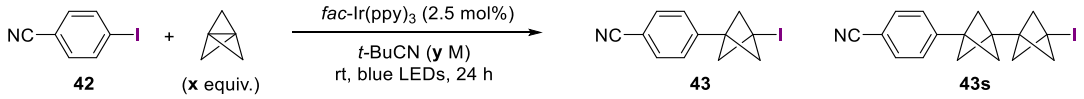

Entry	Concentration **y**/ M	TCP equiv.	Yield/[a] %	**43**:**43s**
1	0.075	2	44	1:0.17
2	0.15	2	54	1:0.18
3	0.2	2	54	1:0.22
4	0.3	2	55	1:0.22
5	0.1	1	44	1:0.02
6	0.1	1.5	49	1:0.15
7	0.1	3	45	1:0.36
8	0.15	1.5	38	1:0.11
9	0.15	1	37	1:0.04

Table 2.4 *– Optimisation of reaction concentration and TCP equivalents for ATRA reaction of 4-iodobenzonitrile with TCP.* [a] *Yields calculated by* ^{1}*H NMR spectroscopy using mesitylene as an internal standard.*

Conversely, increasing the reaction concentration increased the yield (entries 2-4): at 0.15 M the yield increased to 54% with a minimal increase in staffane formation. Increasing the concentration further did not increase the yield of the reaction however the proportion

of staffane did increase. Using fewer equivalents of TCP reduced the amount of staffane produced, however these reactions also suffered from a reduction in yield (entries 5 and 6). Increasing the equivalents of TCP from 2 to 3 did not improve yield but led to a large increase in staffane formation (entry 7). To attempt to balance increasing the yield without increasing staffane formation the reaction was run with 1.5 equivalents of TCP at 0.15 M; while lower staffane formation was observed in a ratio of 1:0.11, there was also a significant drop in yield to 37%. Finally, as starting material remained in all cases, the equivalents of the iodide and TCP were inverted to make TCP the limiting reagent (entry 9). While staffane formation was now very low, the reaction yield was also reduced to 37%.

The range of photocatalysts tested for this reaction was subsequently re-examined using the optimised concentration and stoichiometries of reagents (**Table 2.5**).

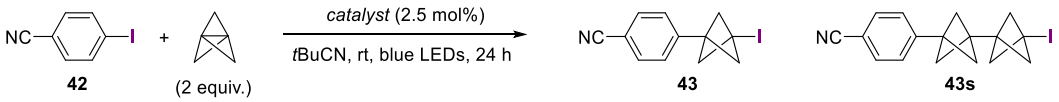

Entry	Catalyst	$E_{1/2}$ (M^{+1*}/M)	Yield/[a] %	**43**:**43s**
1	$[Ir(ppy)_2(bpy)]PF_6$	-[b]	44	1:0.16
2	$Ir(4'\text{-}CF_3ppy)_3$	−1.70 V	41	1:0.15
3	$Ru(d(Me)bpy)_3(PF_6)_2$	−1.43 V	10	1:0.14
4	$Ir[(3,4'\text{-}dMeppy)_2(dtbbpy)]\ PF_6$	−0.87 V	18	1:0.11
5	$Ir[(dF(CF_3)ppy)_2(d(CF_3)bpy)]\ PF_6$	−0.69 V	35	1:0.14
6	2,4,6-triphenylpyrylium tetrafluoroborate	2.55 V[c]	0	-
7	9-mesityl-10-methylacridinium tetrafluoroborate	2.08 V[c]	0	-

Table 2.5 *– Further screening of catalysts in the ATRA reaction.* [a] *Yields calculated by* ^1H *NMR spectroscopy using mesitylene as an internal standard.* [b] *Reduction potential unknown.* [c] *Value reported is for* E^S $(S^*/S^{\bullet-})$.

Of these, $[Ir(ppy)_2(bpy)]PF_6$ gave the highest yield of 44% of **43**, however its reduction potential is unknown (entry 1). The highest known reduction potentials of the transition

metal catalysts was Ir(4'-CF_3ppy)$_3$ with $E_{1/2}$ = 1.7 V (vs SCE), which gave BCP **43** in the next highest yield of 41% yield (entry 2). Interestingly, the two organic catalysts screened showed no reaction under these conditions, despite having high redox potentials (entries 6 and 7). Overall, *fac*-Ir(ppy)$_3$ still remained optimal for this reaction.

Following this, the effect of solvent on the reaction was explored. Solubility of the catalysts in *t*-BuCN appeared somewhat limited which could be hindering the reaction by preventing penetration of light. Therefore, more polar solvents such as DMSO, DMF and MeOH were screened (**Table 2.6**). While improved solubility was observed in the cases of DMSO and DMF, the yield of the reaction significantly decreased in all three cases. MeCN was also screened and a slight increase in yield to 56% was observed. However, the ratio of staffane also increased significantly to 1:0.27, and therefore *t*-BuCN was judged to be the optimal solvent.

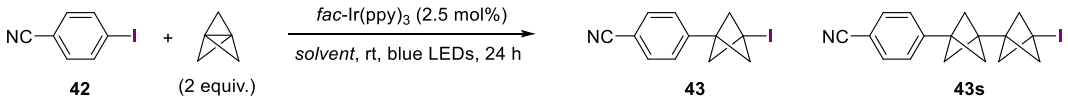

42 **43** **43s**

Entry	Solvent	Yield/[a] %	**43**:**43s**
1	*t*-BuCN	54	1:0.22
2	DMSO	35	-
3	DMF	24	-
4	MeOH	10	-
5	MeCN	56	1:0.27

Table 2.6 *– Optimisation of solvent in the ATRA reaction.* [a] *Yields calculated by* ^{1}*H NMR spectroscopy using mesitylene as an internal standard.*

To investigate the necessity of the light in the reaction (i.e., to determine whether the light/catalyst combination acted solely as an initiator or as a genuine catalyst), a light 'on/off' experiment was performed in which the blue LEDs were turned on and off at regular intervals over 6 h, and the yield of BCP product measured at each point (**Figure**

2.5). While the LED was turned on, an increase in yield was observed, while no such increase was seen when the light was turned off. This suggests light is necessary for the reaction to proceed – presumably through excitation of the photoredox catalyst. Although there is a very slight increase between 3 and 3.5 h from 41% to 42%, this could be due to a chain propagation after the light was turned off, or due to error in the NMR integration. However, it is clear that light is still required and beneficial for efficient progress of the reaction. The rate of reaction also appears somewhat inconsistent throughout the reaction: in the first hour, the reaction rate is relatively slow, only giving 8% yield in this time, then increasing between 1.5 and 3 hours. Following this, the reaction rate progressively decreases between 3.5 and 4.5 hours and then 5 and 6 hours, only increasing by 4% in the last hour. This could be a result of the TCP degradation over the course of the reaction.

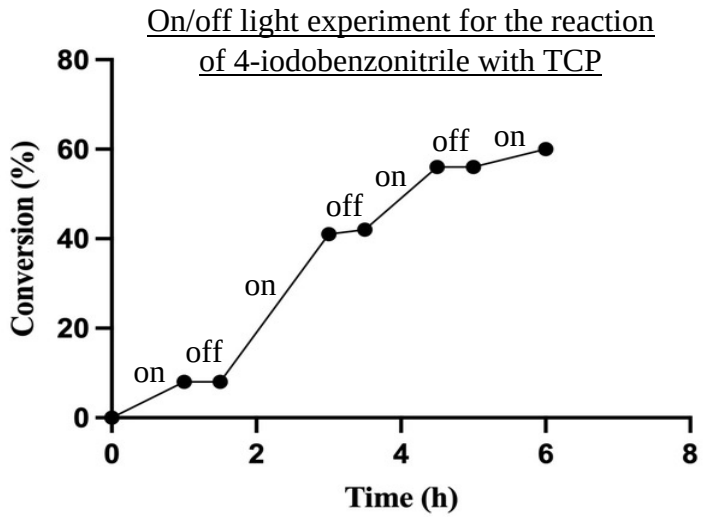

Figure 2.5 *– Light on/off experiment for the reaction of 4-iodobenzonitrile over 6 hours. Conversion measured by ^{1}H NMR spectrosopy in comparison to an internal standard.*

In all reaction conditions screened thus far, starting material remained. Given the potential instability of TCP at room temperature, it was considered whether the degradation of TCP over the course of the reaction was leading to incomplete reaction, and moreover it was

questioned whether $Ir(ppy)_3$ was facilitating this degradation. Therefore, TCP was stirred in *t*-BuCN in the presence of blue LEDs both with and without $Ir(ppy)_3$, and the concentration of TCP in the mixture measured at several time points over 24 h (**Figure 2.6**).

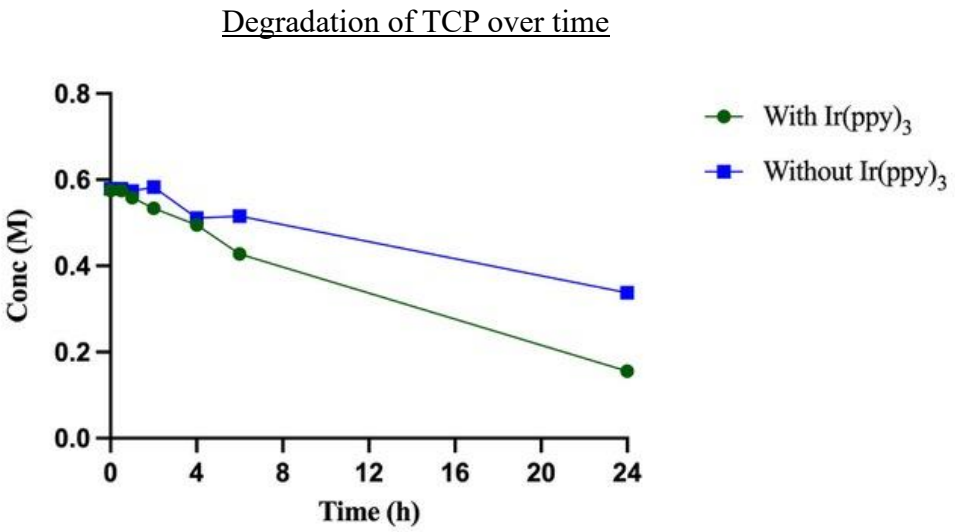

Figure 2.6 *– Degradation of TCP over time measured by the decrease of concentration of TCP in a solution of t-BuCN, stirred under blue LED lights both with and without $Ir(ppy)_3$ present. Concentration measured by ^1H NMR spectroscopy in comparison to an internal standard.*

In both cases, the concentration of TCP decreased over the 24 h, although the degradation was accelerated in the presence of the catalyst. The concentration of TCP reduced from 0.58 M to 0.34 M after 24 h with no catalyst but reduced to 0.16 M in the presence of the catalyst. This would account for the reaction slowing significantly with time.

Control reactions were conducted to confirm whether irradiation or photocatalyst was necessary in the reaction (**Scheme 2.7**). In the absence of catalyst, a 27% yield of **43** was observed which appears consistent with light on/off experiment. This suggests that another mechanism is possible that does not require excitation of the photocatalyst / reduction of the C–I bond for initiation. The blue light may be of sufficiently high energy

to cause some homolytic fission of the C–I bond, or alternatively the central C–C bond of TCP may be able to homolytically break on excitation with light and initiate the reaction by abstracting iodine from a molecule of the starting aryl iodide. In the absence of light, a very small amount of product formation was observed. This could be due to the small amount of light exposure that occurs between completion of the experiment and acquiring the NMR spectrum, as although care was taken to keep the sample away from light during this time, it was not possible to entirely eliminate it.

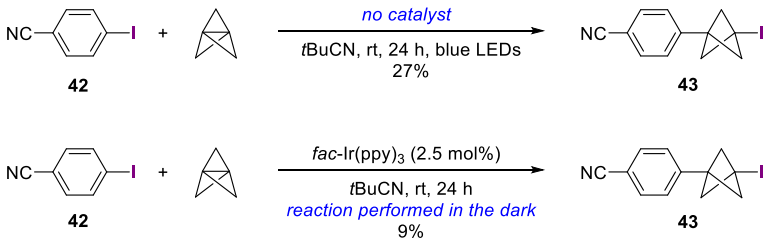

Scheme 2.7 *– Control reactions performed for the ATRA reaction of 4-iodobenzonitrile with TCP.*

2.4 Reaction scope

With optimised conditions now in hand – using 2.5 mol% of *fac*-Ir(ppy)$_3$ with two equivalents of TCP in *t*-BuCN, under irradiation by blue LED light for 24 h – the scope of the reaction was explored (**Figure 2.7**). Aryl iodides possessing electron-withdrawing groups were most successful under the reaction conditions, giving moderate to good yields of product (**43** – **47**, 40 – 60%). More electron-deficient aryl iodides gave higher yields of the desired BCP iodide, presumably due to the lower redox potentials of these C–I bonds as the more electron-deficient system is easier to reduce. 2-Iodopyridine reacted very efficiently to give BCP **48** in 84% yield, and both electron donating and

withdrawing groups were tolerated well on the pyridine giving Me-substituted pyridine **49** and CF_3-substituted pyridine **50** in 87% and 81% yield respectively. The greater success of the pyridines is potentially due to stabilisation of the radical formed on reduction of the starting material by electron-donation from the adjacent pyridyl nitrogen.[107] Also successful in the reaction were 3- and 4-iodopyridines, albeit in reduced yields of 40 and 49% of **51** and **52** respectively.

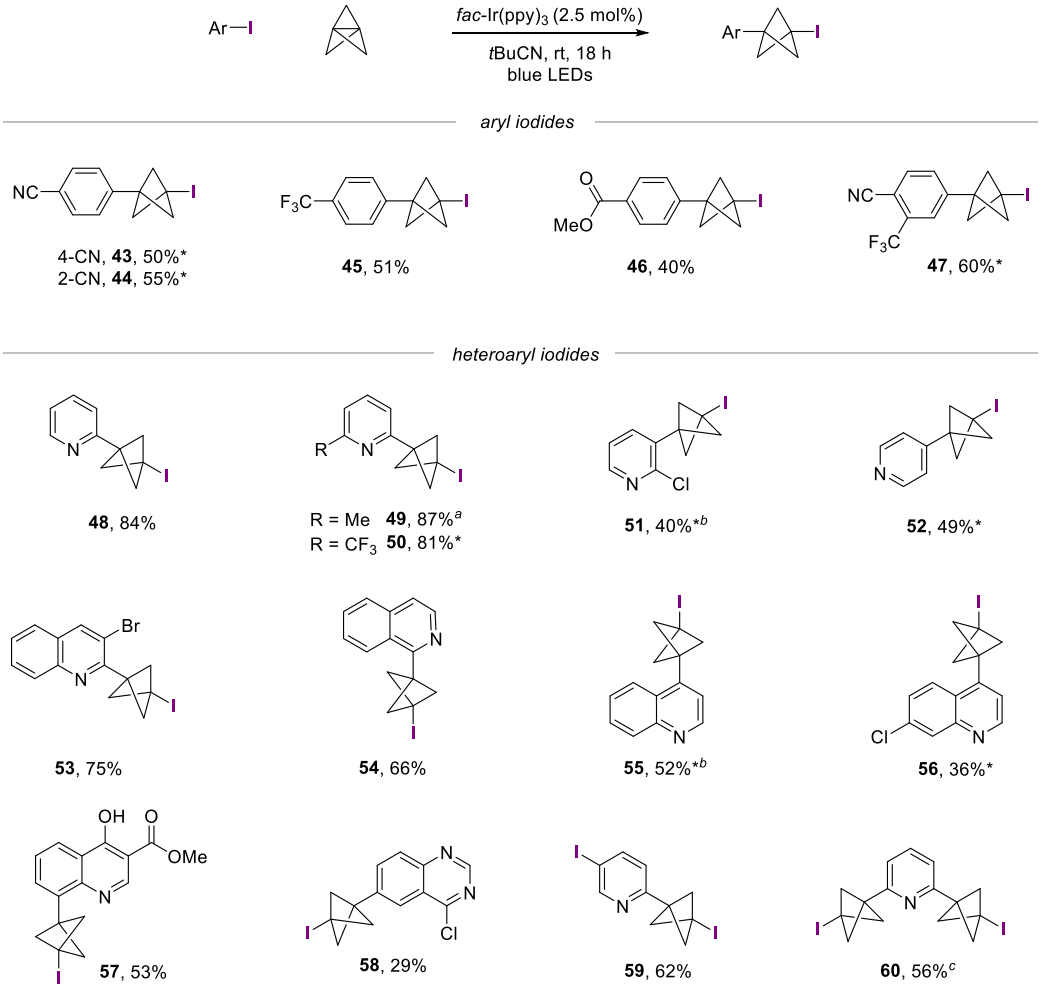

Figure 2.7 *– Scope of aryl and heteroaryl iodides in the Ir(ppy)$_3$ photoredox catalysed ATRA reaction with TCP. Yields reported are for BCP product; in examples were staffane was produced and inseparable, this has been taken into account in the reported yields. * Isolated as a mixture of product and staffane, for full staffane data, see experimental* ***section 7.3.3****.* [a] *Reaction performed by Dr Jeremy Nugent.* [b] *Reaction performed by Dr James Mousseau.* [c] *4 equivalents TCP used.*

Quinoline and isoquinoline iodide substrates showed a similar preference for the 2-position. 2-Iodoquinoline produced **53** in 75% yield, while 4-iodoquinolines gave **55** and **56** in 52% and 36% yield respectively, and an 8-iodoquinoline bearing ester and hydroxyl groups gave **57** in 53% yield. This preference in reactivity for the 2-position over others could also be exploited in the mono-bicyclopentylation of 2,5-diiodopyridine to give **59** in 62% yield, and the bis-bicyclopentylation of 2,6-diiodopyridine to give **60** in 56% yield. For the bis-bicyclopentylated product **60**, a mixture of the bis and mono reacted products was formed in a 4.5:1 ratio when 2.5 equivalents of TCP were used, but when 4 equivalents of TCP were used this ratio increased to 9:1. Quinazole **58** could also be isolated in a modest 29% yield.

Bromide-bearing quinoline **53** and chloride-bearing pyridine **51**, quinoline **56** and quinazole **58** were formed showing only activation of the C–I bond in the respective starting materials, with the other halides present remaining inert under reaction conditions.

A number of aryl and heteroaryl iodides reacted poorly in the reaction, with low conversion and/or producing complex inseparable mixtures (**Figure 2.8**). 1-Fluoro-4-iodobenzene was not sufficiently electron poor to enable efficient reduction of the C–I bond, forming **61** in only 27% yield.

While NO_2 is significantly more electron withdrawing, only 5% of **62** was formed, with the remainder being returned starting material. Photoredox catalysts have been used to reduce aryl-nitro groups to amines in the presence of proton sources;[108–111] it is possible that the nitro group in this instance is also able to quench the photocatalyst before it can reduce the C-I bond. Aryl iodides bearing electron donating or neutral groups generally gave very poor conversion and produced messy, inseparable mixtures (**63** to **66**), although

unsubstituted **63** formed in 45% yield but could not be separated from byproducts. Heteroaryl groups that featured 5-membered rings also gave no or poor reaction under the standard conditions (**67** to **70**).

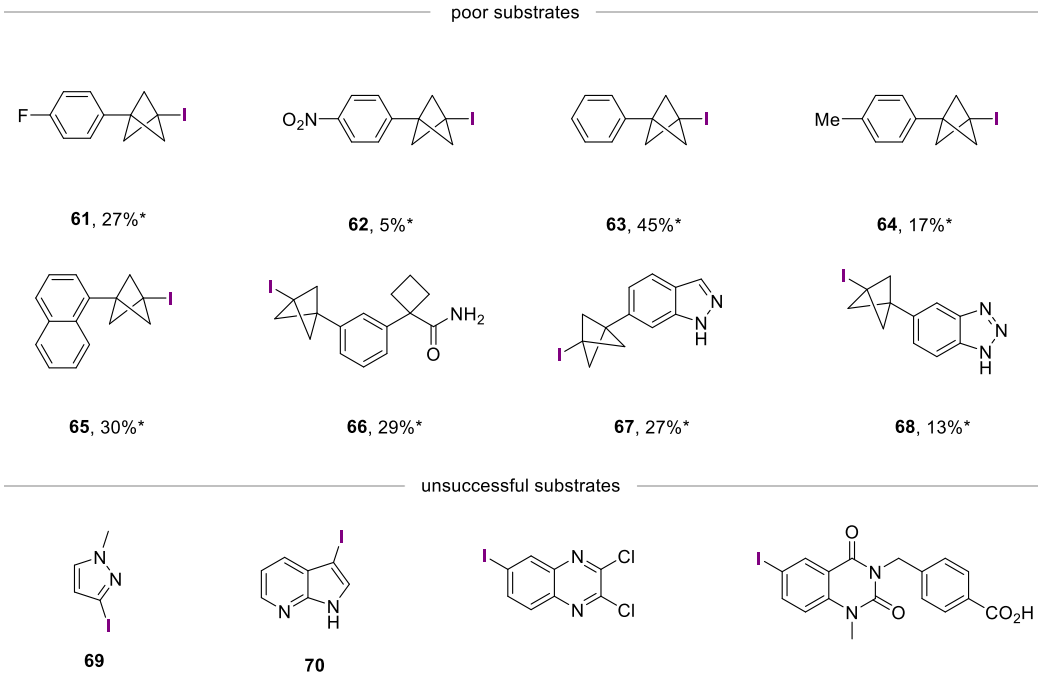

Figure 2.8 *– Poor and unsuccessful substrates in the fac-Ir(ppy)$_3$ photoredox catalysed ATRA reaction with TCP. *Yields calculated by ^{1}H NMR spectroscopy using mesitylene as an internal standard.*

2.5 Mechanism

While exploring the scope of aryl and heteroaryl iodides, it was clear that the catalyst was beneficial for the reaction, but not how it might be turned over. However, when 4-iodopyridine was submitted to the reaction conditions, a methylene cyclobutene byproduct **71** (**Scheme 2.8**) was also isolated alongside the desired product. The presence of this ring-opened product gives insight into the mechanism of the reaction, both in terms of a potential catalyst turnover step, and in affording evidence for the oxidative quenching mechanism. We propose that the Ir(III) is initially excited to Ir(III)* by the blue LED light, and subsequently this excited state photocatalyst can donate an electron to the C–I

σ* orbital of a molecule of the starting iodide **72**, in doing so reducing the C–I bond to give the aryl radical and an iodide ion. The aryl radical can then be trapped by a molecule of TCP to give the Ar–BCP• radical **73**. The BCP radical can then propagate the reaction by abstracting iodine from another molecule of starting material to give a molecule of the BCP iodide product and another molecule of aryl radical. This can then continue to propagate the reaction via a standard chain mechanism, or could reduce the catalyst back from Ir(IV) to Ir(III), and in doing so be oxidised to the BCP cation **74**.*

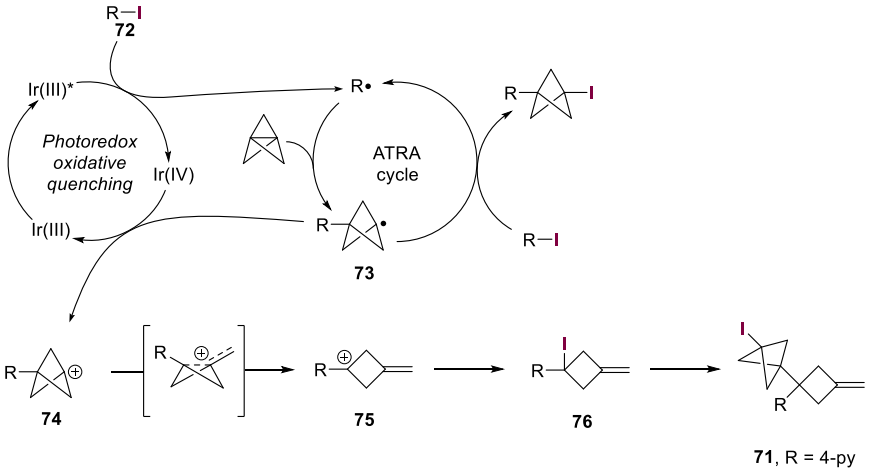

Scheme 2.8 *– Proposed mechanism for the ATRA reaction with isolated methylene cyclobutane byproduct **71**.*

Computational work by Alistair Sterling showed that if the BCP cation is formed, its fragmentation to give the methylene cyclobutene tertiary cation **75** is barrierless.[112] This cation can then be trapped by I^- to give the tertiary iodide **76**, which can then undergo a further ATRA reaction with TCP to give the observed quaternary BCP **71**. This compound was isolated in 4-6% yield.

As part of a wider project, the reaction conditions had also been applied to a range of alkyl iodides by Dr Jeremy Nugent, Dr Carlos Arroniz, Marie Wong, Dimitri Caputo, Helena Pickford and Benjamin Owen.[112] Quantum yield experiments were performed by Dr Jeremy Nugent and Alistair Sterling in order to investigate the extent of photoredox

* It is also possible that the iodide ion could turn over the catalyst by being oxidised to the iodine radical. Small amounts of I_2 could therefore be formed in the reaction which could be the source of iodine picked up by BCP radical **73**. This process would give an outcome equivalent to an ATRA.

catalysis vs radical chain reaction involved in the mechanism. At least some chain process was suspected, as the Ir(IV) oxidation of the BCP radical alone would preclude the formation of any BCP iodide product. The quantum yield was therefore measured for a range of iodides (**Table 2.7**).

Iodide	t/ s	Conversion	Φ
Ethyl iodoacetate	10	64%	682
2-Iodopyridine	900	56%	7.4
4-CF_3 Benzyl iodide	600	42%	7.4
Benzyl iodide	1200	13%	1.4

Table 2.7 *– Quantum yield experiments for various iodides. Experiments performed by Alistair Sterling and Dr Jeremy Nugent.*

For ethyl iodoacetate, a quantum yield of 682 indicates a very efficient chain process, and so the photocatalyst appears to act predominantly as an initiator in this instance. This reaction is also rapid, giving a 64% yield of product in just 10 s. Both 2-iodopyridine and 4-CF_3 benzyl iodide had quantum yields of 7.4, indicating the presence of some chain process, but with far less efficient propagation than ethyl iodoacetate; this implies that some level of catalysis is also necessary. This less efficient reaction is also demonstrated through the lower conversions of these two iodides even with significantly longer reaction times of 900 and 600 s. Benzyl iodide exhibited a quantum yield of 1.4 indicating a poor chain process, with inefficient propagation. Here, catalysis is important for efficient reaction progression. The poor propagation of benzyl iodide is also reflected in the low conversion of only 13% in 1200 s which could also indicate why this substrate is not successful under triethylborane-initiated conditions.

2.6 Applications

Having developed an efficient and mild route to aryl and heteroaryl BCPs, the utility of this reaction was demonstrated in the formal synthesis of BCP-darapladib. In 2017, Measom *et al.* at GSK published a synthesis of BCP-darapladib in order to evaluate its pharmacokinetic properties in comparison to the parent compound.[23] They synthesised this analogue in 10 steps, longest linear sequence, from commercial cyclobutanone **77** (**Scheme 2.9**).

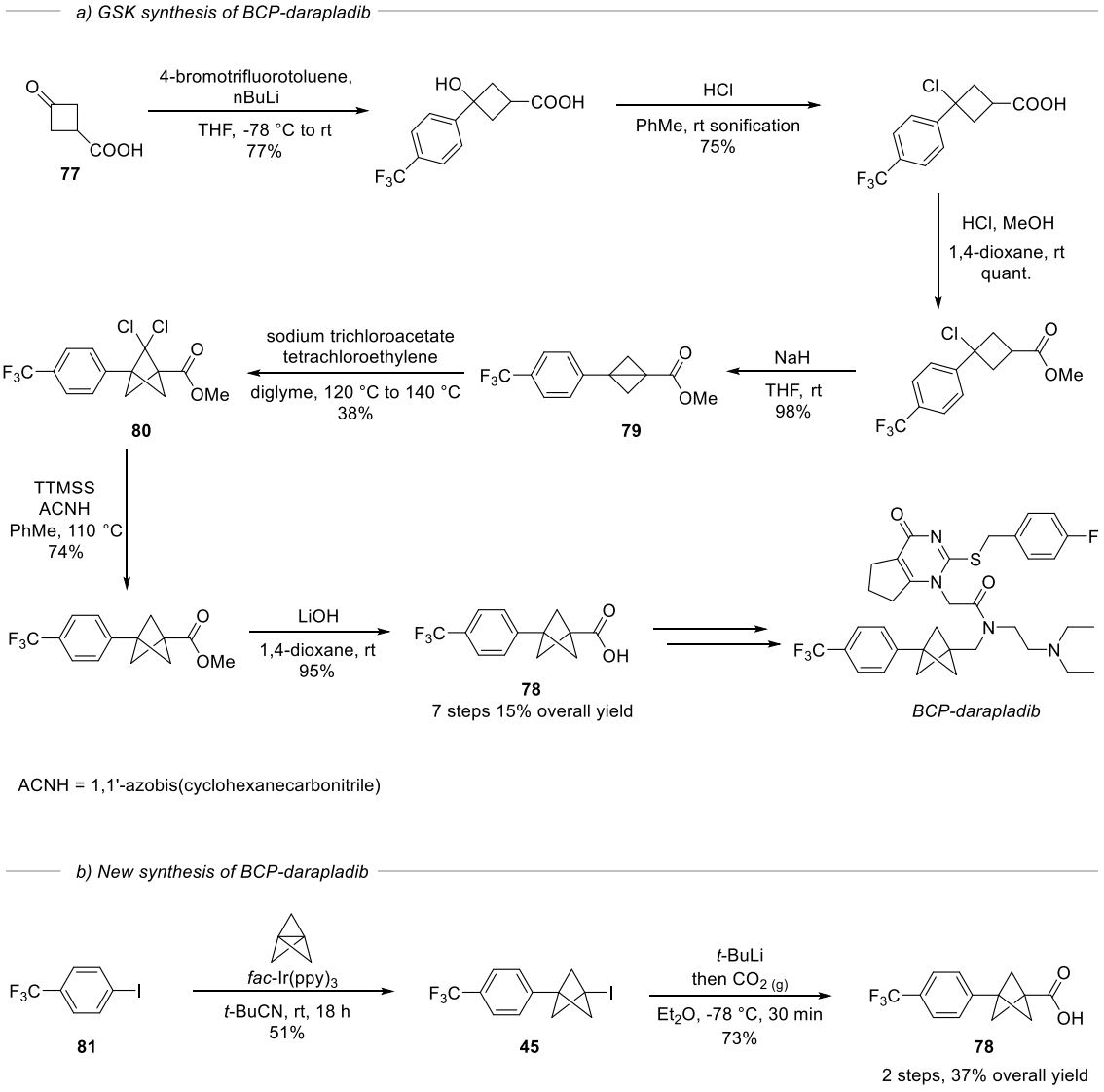

Scheme 2.9 *– a) Synthetic route to BCP-darpladib by GSK. Intermediate **78** synthesized in 7 steps. b) formal synthesis of BCP-darapladib via synthesis of intermediate **78** in two steps.*

They synthesised key intermediate BCP carboxylic acid **78** in seven steps, including a low yielding dichlorocarbene insertion to bicyclo[1.1.0]butane **79** to give the dichloro bridge-substituted BCP **80**, which then necessitated radical-mediated reduction of the dichloro functionality. Overall, intermediate **78** was synthesised in 15% yield over these seven steps. From there, three further steps were required to give BCP-darapladib in 5% yield over ten steps. However, by using the photoredox methodology developed here, the same intermediate **78** could be synthesised in just two steps from 4-CF_3-iodobenzene **81** (**Scheme 2.9b**). Under the photoredox reaction conditions, BCP iodide **45** was accessed in 51% yield; from here, simple lithiation with *t*-BuLi, followed by trapping with $CO_{2(g)}$ (from dry ice) gave the desired intermediate **78** in 73% yield, or 37% yield over two steps. This reduces the length of the synthesis of **78** by five steps and halves the number of steps in the overall synthesis, while more than doubling the overall yield to 12% over five steps.

2.7 Investigations towards ATRA of aryl bromides across TCP.

Given the success of adding aryl and heteroaryl iodides across TCP, investigations began into the possibility of an ATRA reaction of aryl bromides with TCP. Alkyl bromides can undergo photoredox catalysed ATRA under a variety of conditions, and this includes reactions with TCP.[112] Activation of aryl bromides using photoredox catalysis is also well known, although largely for reduction of the bromide in the presence of an H atom source such as a tertiary amine (**Scheme 2.10a**).[105,106] Aryl and heteroaryl bromides have also been shown to add to double bonds in an overall reductive process, both intra-[113] and intermolecularly[114] (**Schemes 2.10b** and **2.10c**, respectively), but no ATRA of aryl bromides using photoredox catalysis has been demonstrated.

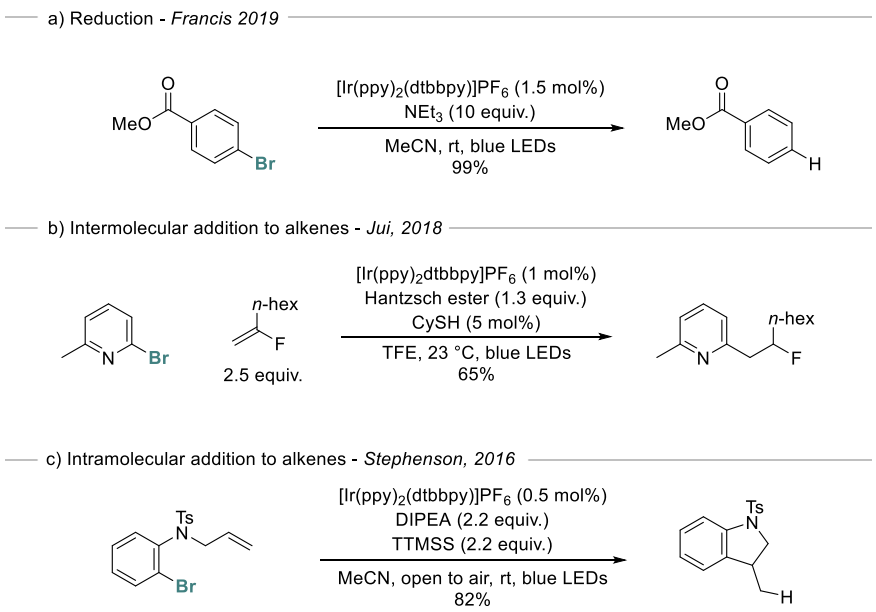

Scheme 2.10 *– Examples of photoredox activation of (hetero)aryl bromides to perform a) reductions, b) intermolecular addition to alkenes and c) intramolecular addition to alkenes.*

Stephenson and co-workers utilised 2 equivalents of DIPEA with 2 equivalents of TTMSS as a hydrogen atom source with the reaction performed under air.[113] Meanwhile Francis and co-workers did not include TTMSS and instead used 10 equivalents of NEt_3 as their hydrogen atom source, performing the reaction under nitrogen.[106] The combination of $[Ir(ppy)_2(dtbbpy)]PF_6$ with a tertiary amine in acetonitrile was common to both of these high yielding reactions, and so this served as a good starting place for investigating the possibility of an ATRA or HAT reaction of aryl bromides with TCP.

Our exploration of the addition of C–Br bonds to TCP commenced with the exact conditions of Stephenson's work (**Table 2.8**, entry 1). Activation of the bromide **82** was efficient with no starting material remaining after 18 h, however the major product was the direct reduction of the bromide to give 43% of acetophenone **83**. A small amount of addition to TCP with overall reduction to give 14% of the terminal BCP **84** occurred, along with 4% of the reduced staffane **84s**; none of the expected ATRA product was

observed. Given TCP is volatile, and only a small amount of bicyclopentylated products were observed, the reaction was then set up under air, but sealed before stirring for 18 h (entry 2), however this resulted in a reduction of all product formation. The same reaction was then performed under nitrogen, and interestingly a very similar yield and distribution of products was observed (entry 3). The equivalents of TCP used were then increased from 2 equivalents to 5 and the reaction performed both under air (entry 4) and under nitrogen (entry 5).

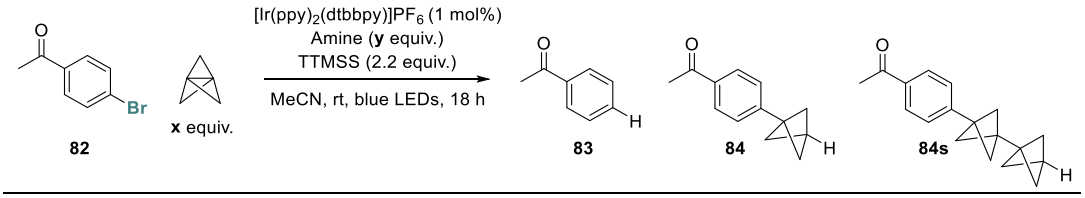

Entry	**x** (equiv.)	Amine	**y** (equiv.)	TTMSS?	Air/N_2	Yield/[a] %			
						82	**83**	**84**	**84s**
1	2	DIPEA	2.2	Yes	Air	0	43	14	4
2[b]	2	DIPEA	2.2	Yes	Air	0	15	5	2
3	2	DIPEA	2.2	Yes	N_2	0	45	17	1
4	5	DIPEA	2.2	Yes	Air	0	24	34	8
5	5	DIPEA	2.2	Yes	N_2	4	37	31	13
6[c]	2	DIPEA	2.2	Yes	Air	7	26	12	2
7	2	DIPEA	2.2	No	Air	0	5	18	6
8	2	DIPEA	2.2	No	N_2	0	21	17	5
9	5	DIPEA	2.2	No	Air	30	15	18	2
10	5	DIPEA	2.2	No	N_2	16	22	22	10
11[d]	2	DIPEA	2.2	Yes	Air	0	52	14	2
12	2	NEt_3	2.2	Yes	Air	0	5	3	0
13	2	NEt_3	10	No	N_2	0	36	18	7
14	2	DIPEA	10	No	N_2	0	14	8	2
15[e]	5	DIPEA	2.2	Yes	Air	60	10	12	10

Table 2.8 *– Investigations towards the ATRA reaction of aryl bromides with TCP* [a] *Yields calculated by* ^{1}*H NMR spectroscopy using mesitylene as an internal standard.* [b] Reaction vial was sealed after set up. [c] Reaction performed at a higher concentration. [d] 1.1 equiv. TTMSS used. [e] *fac*-Ir(ppy)$_3$ was used instead.

In both cases, a significant increase in the amount of BCP **84** formation was observed (34% and 31% respectively), along with an increase in staffane formation (8% and 13%, respectively). However in both cases a significant amount of the premature reduction of the aryl bromide to acetophenone was also observed. As TTMSS is an efficient H atom donor in these reactions and early reduction of the aryl bromide is problematic, the stoichiometry of TTMSS was halved to 1.1 equiv. (entry 6); while a decrease in acetophenone formation was observed, some starting material remained and only 12% of the BCP was formed. Removing TTMSS entirely caused a large decrease in acetophenone yield under air (entry 7) and a smaller reduction to 21% under nitrogen (entry 8). The reaction was therefore performed with 5 equivalents of TCP without TTMSS, both in air and in nitrogen (entries 9 & 10) in order to promote bicyclopentylation while limiting premature reduction of the aryl bromide. However in both instances, a significant amount of starting material was unreacted, and only 18% and 22% of BCP **84** was formed respectively. To promote aryl radical capture by TCP the reaction was run at a higher concentration (entry 11), however this also preferentially promoted radical capture by TTMSS, producing 52% of acetophenone. Switching the tertiary amine used from DIPEA to NEt_3 gave very poor yield of any products under the conditions from Stephenson (entry 12), however on employing the conditions from Francis with 10 equivalents of amine under nitrogen with no TTMSS (entry 13) increased the overall conversion, however only 18% of BCP **84**, and 36% of acetophenone **83**. Using DIPEA instead of NEt_3 decreased the yield (entry 14). Finally, *fac*-$Ir(ppy)_3$ was employed as this had been successful for aryl iodides and some alkyl bromides, however this largely returned unreacted starting material with only small amounts of **83**, **84** and **84s** present.

After these investigations, no ATRA product was ever observed and acetophenone proved to be the major product. Small amounts of the terminal BCP could be formed with a

maximum of 31% yield, but in combination with inseparable staffane. Given terminal aryl BCPs can be accessed in a variety of other ways in high yields, including forming the aryl iodide followed by reduction[77], as well as addition of Grignards to TCP,[65] this method appeared to be an inefficient way to access the BCP-H product, and investigations ceased.

2.8 Conclusions

A mild and efficient method was developed for the synthesis of 1-iodo, 3-aryl bicyclo[1.1.1]pentanes through photoredox-catalysed atom transfer radical addition reactions (**Scheme 2.11a**). Both electron-deficient aryl iodides and a wide range of heteroaryl iodides were suitable for the reaction with tricyclo[1.1.1.$0^{1,3}$]pentane, which proceeded selectively in the presence of other halides to form products that had previously been inaccessible through the triethylborane methodology. In collaboration with co-workers, this reaction was extended to a large number of alkyl iodides and activated bromides including more complex drug and agrochemical analogues, demonstrating the reaction's high functional group tolerance and suitability for late-stage functionalisations (**Scheme 2.11b**). The application of this methodology to the formal synthesis of BCP-darapladib in significantly higher yield and fewer steps than the previous published approach further demonstrates the utility of this reaction for bioisosteric replacements in pharmaceuticals. Importantly, by exploiting the high reactivity of TCP towards radicals, this reaction demonstrated the first photoredox-catalysed activation of a C–C σ-bond. The work presented in this chapter was published in *ACS Catalysis* in 2019.[112]

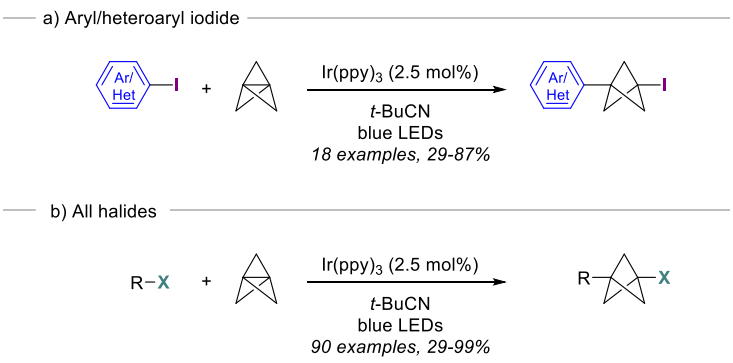

Scheme 2.11 *– a) Photoredox catalysed ATRA of aryl/heteroaryl iodides with TCP. b) Photoredox catalysed ATRA or iodides and bromides with TCP.*

3

Iron catalysed C–C Kumada cross-coupling

The use of iron salts to perform chemical transformations has become increasingly popular as a "greener", more sustainable alternative to reactions classically performed by noble metals such as palladium.[115] Many iron salts are typically readily available and cheap as well as significantly less toxic than their heavier counterparts: drug substances can tolerate up to 1,300 ppm of residual iron compared with ≤10 ppm for most transition metals.[116] Iron is a versatile transition metal with formal oxidation states spanning −II to +VI, allowing it to perform both one and two electron transfers in reductive and oxidative processes, and to act as a Lewis acid in transformations such as the Friedel-Crafts reaction.[117] As a result, iron salts have been used to accomplish an extremely wide range of reactions that have been well documented and utilised. One of the most widely explored uses of iron salts is in cross-coupling reactions, for which a number of catalytic systems have been developed.[117–119]

The first example of an iron-catalysed C–C cross-coupling was reported by Kochi and co-workers in 1971.[120] They found that reaction of *n*-hexylmagnesium bromide and vinyl bromide in the presence of $FeCl_3$ gave the cross-coupled product **85** (**Scheme 3.1**), although this catalyst failed to catalyse the cross-coupling of alkyl Grignard reagents with alkyl halides.

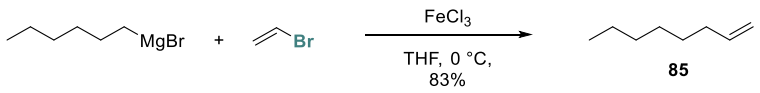

Scheme 3.1 *– First example of an iron catalysed C–C cross-coupling by Kochi*

Since this seminal discovery, there has been much work performed to develop cross-couplings using iron, one of the most useful of which is the iron-catalysed Kumada cross-coupling using Grignard reagents.

3.1 Iron-catalysed cross-couplings of alkyl halides with aryl Grignard Reagents

The first example of an iron-catalysed cross-coupling between alkyl halides and aryl Grignard reagents was reported in 2004 by Nakamura and co-workers.[121] They used catalytic amounts of $FeCl_3$ and a stoichiometric amount of an additive in THF to cross-couple various secondary alkyl chlorides, bromides and iodides with aryl Grignard reagents. While optimising the reaction between bromocycloheptane **86** and PhMgBr, they investigated a number of amine and phosphine additives, and found that the identity of this additive had a large influence on reaction conversion as well as the distribution of products (**Table 3.1**). Both tertiary monoamines and monophosphines gave large amounts of elimination product **88** (entries 2, 3 and 8) and very low yields of the desired product **87**. The use of DABCO (entry 4), NMP (entry 7) or dppe (entry 9) almost entirely prevented formation of the elimination product; however, formation of **87** was also low. When the diamine TMEDA was used, **87** was produced in 71% yield with 19% of the elimination product obtained (entry 5); however the use of the structurally similar TEEDA gave a poor yield (entry 6). Various other iron catalysts gave very variable results (0-32%), with the use of $FeCl_3$ generally giving the best yield by a considerable amount

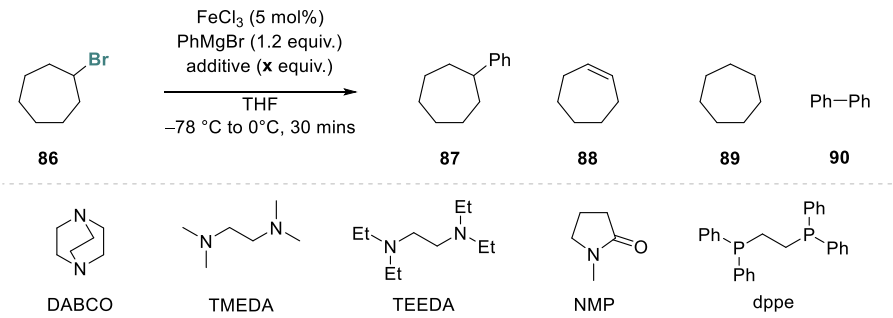

Entry	Additive	Additive equiv.	Yield[a]/ %				
			87	**88**	**89**	**86**	Ph–Ph
1	-	-	5	79	0	4	6
2	Et_3N	1.2	3	78	0	11	5
3	N-methyl morpholine	1.2	8	72	0	4	5
4	DABCO	1.2	20	2	0	75	3
5	TMEDA	1.2	71	19	3	Trace	10
6	TEEDA	1.2	23	48	1	11	9
7	NMP	1.2	15	3	Trace	79	4
8	PPh_3	0.1	6	70	Trace	6	7
9	dppe	0.05	4	8	0	81	8

Table 3.1 - [a] Yield determined by GC with decane as internal standard.

(71%). In all cases some homo-coupling of the Grignard reagent was observed, although typically in less than 10% yield. A significant increase in yield was observed when the Grignard reagent was added slowly (~1.4 mL/ min); this mode of addition limits the amount of homo-coupling of the Grignard reagent by keeping its concentration relatively low. Using the optimised conditions of entry 5, a range of alkyl halides were cross-coupled with aryl Grignard reagents in high yields (**Scheme 3.2a**). Secondary alkyl chlorides, bromides and iodides were all successfully used in the reaction, with iodides giving the best yield (87-99%). Electron-rich and neutral aryl Grignard reagents reacted much faster than those bearing electron-withdrawing groups, which gave a considerably lower yield. While the use of primary alkyl iodides and secondary alkyl halides was

reported, there are no instances of tertiary halides being subjected to cross-coupling under these reaction conditions.

Later the same year, several other papers were published on iron-catalysed Kumada cross-coupling between aryl Grignard reagents and akyl halides. Hayashi reported an $Fe(acac)_3$ catalysed cross-coupling[122] (**Scheme 3.2b**) based on the reaction conditions previously described by Cahiez[123] for cross-coupling alkyl Grignard reagents and aryl/alkenyl halides. $Fe(acac)_3$ was used without additives, and the reaction mixture was heated under reflux; however, these reaction conditions generally resulted in lower yields of the cross-coupled product compared to the methodology reported by Nakamura.

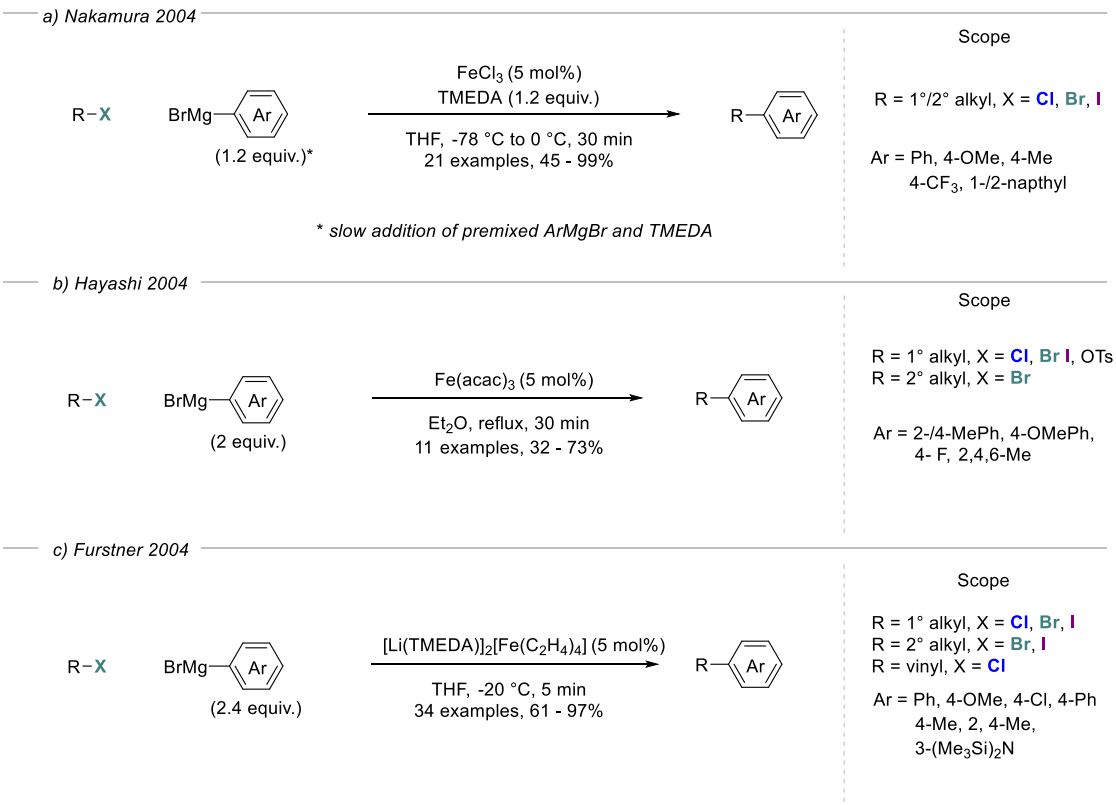

Scheme 3.2 *– Early Kumada cross-couplings between alkyl halides and aryl Grignard reagents.*

Shortly after, a cross-coupling was reported by Furstner using $[Li(TMEDA)]_2[Fe(C_2H_4)_4]$ (**Scheme 3.2c**) which contains a highly reduced Fe(−II) centre.[124] Building on theories

that iron-magnesium clusters of composition $[Fe(MgX)_2]_n$ played an important role in Kumada cross-couplings,[125,126] they selected this iron catalyst due to its highly reduced metal centre with weakly coordinated ethylene ligands and a strong interaction between the lithium cations and ferrate anions. This system proved successful for the cross-coupling of various alkyl and vinyl halides in high yields (61−97%), including with primary alkyl iodides, however tertiary halides did not react under these conditions. The reaction showed good functional group tolerance, including towards ketones, esters and trimethylsilyl groups.

In 2007, Cahiez and co-workers noted the large excess of TMEDA used by Nakamura in the $FeCl_3$/TMEDA catalytic system,[121] and the need to heat Et_2O under reflux in Hayashi's methodology, and sought to improve on this in order to find a set of conditions more suitable for large scale applications (**Scheme 3.3**).[127]

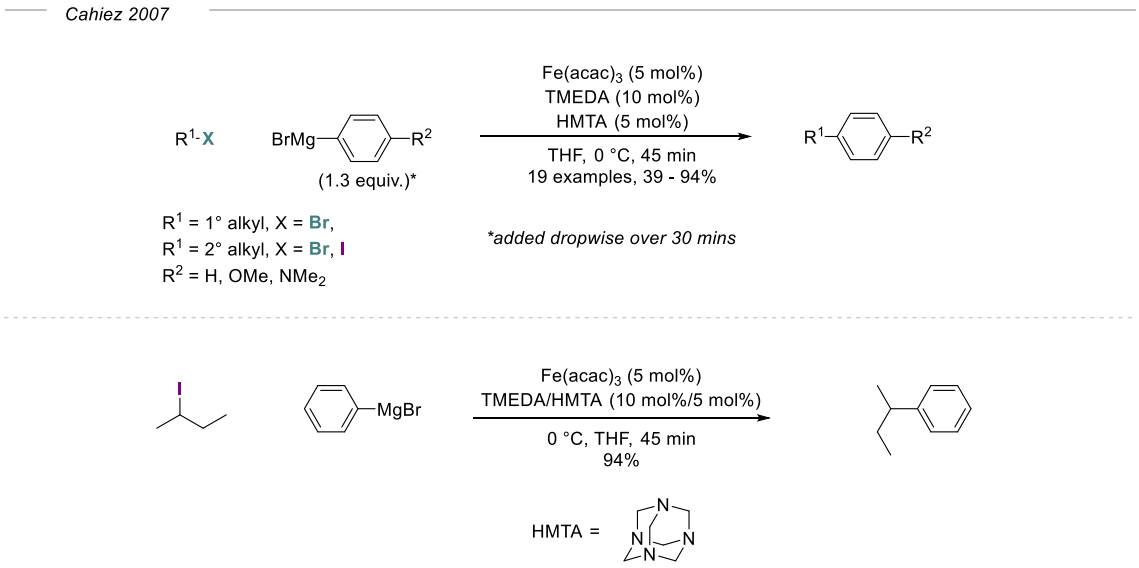

Scheme 3.3 *– Kumada cross-coupling of alkyl halides and aryl Grignard reagents using TMEDA/HMTA additives.*

They favoured the use of $Fe(acac)_3$, as $FeCl_3$ gave irreproducible yields and was not suitable for use on a large scale given its hygroscopicity. In contrast to the results reported

by Nakamura, they found that $Fe(acac)_3$ was a suitable catalyst for the cross-coupling of primary and secondary alkyl halides and aryl Grignard reagents. Similarly to the Nakamura protocol, addition of the Grignard reagent dropwise over 30 mins was beneficial. This method still required the use of 50 mol% of TMEDA to obtain high yields (90%) of the cross-coupled products, and hence the group sought to reduce the loading of this additive. They discovered that a combination of 10 mol% of TMEDA and 5 mol% of HMTA enabled the reaction between 2-iodobutane and phenylmagnesium bromide to proceed in 94% yield.

Bedford *et al.* reported a Kumada cross-coupling of secondary halides with aryl Grignard reagents using an iron(III) salen-type catalyst,[128] building on work form Fürstner and co-workers who had previously used similar iron complexes for the Kumada cross-coupling of aryl halides with alkyl Grignard reagents.[129] The scope reported for this system was limited, however they also conducted a study into the effect of varying ligand structure on yield (**Scheme 3.4a**). Increasing the diamine linker length or replacing it with an aromatic group caused a large decrease or total inhibition of catalytic activity (**94** - **97**). The addition of *t*-butyl groups on the aromatic rings of the ligand (**95**) gave the same yield as the unsubstituted equivalent (**94**), however this also led to a change in the distribution of products – an increase in the homo-coupling of the cyclohexyl bromide to give **93**, but a decrease in the amount of cyclohexane (**92**) formed from reduction of the halide. The use of a ketone-derived Schiff base ligand proved beneficial with a significant increase in yield when using **100** and **101**, giving 72% and 60% yields of the cross-coupled product **91** respectively. The following year, Bedford explored a range of simpler amine ligands in similar Kumada cross-coupling reactions,[130] and found that using NEt_3, TMEDA and DABCO afforded high yields of cross-coupled product **91**, with DABCO being optimal when secondary alkyl iodides were used (**Scheme 3.4b**).

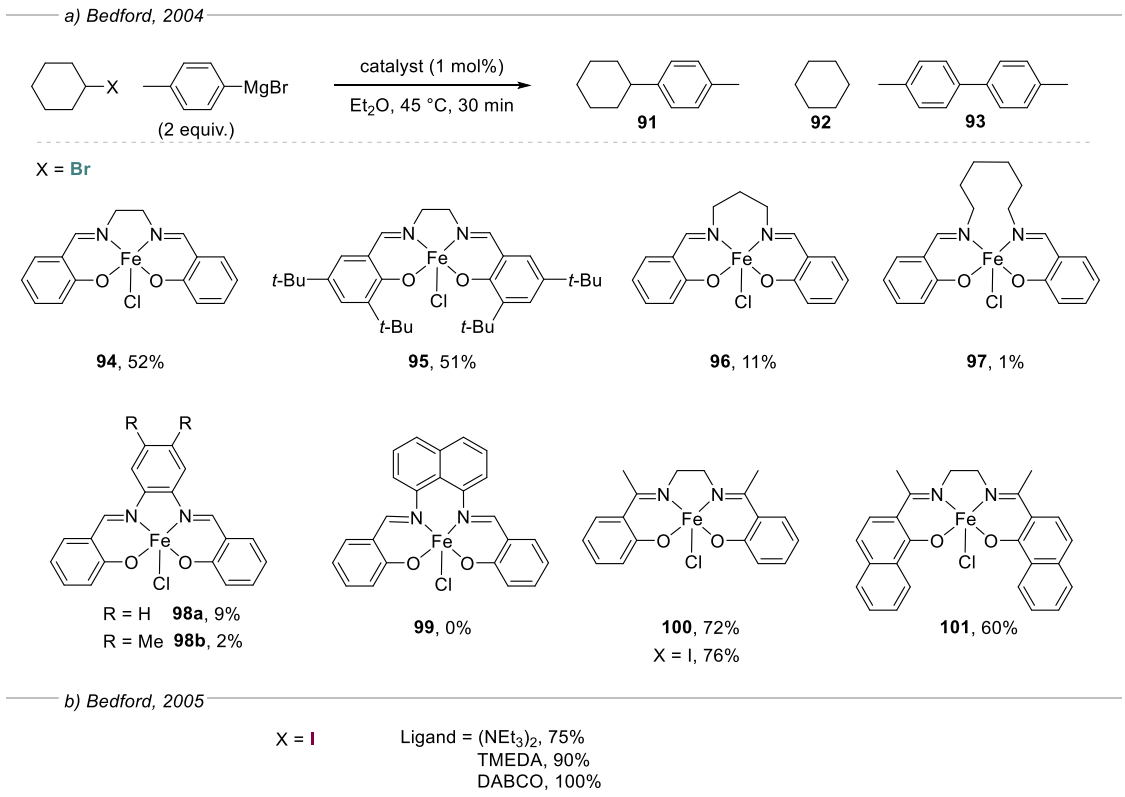

Scheme 3.4 *– Investigation into the effect of a) the diamine ligand linker lengths and b) simple amine ligands on Kumada cross-couplings.*

Following this exploration of amine ligands, Bedford then investigated a range of mono- and bidentate phosphine ligands in the same cross-coupling reaction (**Scheme 3.5**).[131] When comparing monodentate ligands, they found that PCy_3 (87%) was superior to aryl phosphines such as P(*o*-tol)$_3$ (53%) and PPh_3 (72%). After screening a range of monodentate phosphine ligands it was concluded that there were no specific trends between electronic or steric effects of the ligand and reaction yield. Monodentate phosphite ligands also performed well, with the more sterically bulky P(OC_6H_3-2,4-*t*Bu$_2$)$_3$ giving 82% yield, a substantial increase from the 67% yield achieved when using unsubstituted P(OPh)$_3$. This trend was not mirrored when using the alkyl phosphite ligands: P(OMe)$_3$ and P(O*i*-Pr)$_3$ both gave 83% of cross-coupled product **91**, however P(OEt)$_3$ only gave 69% yield.

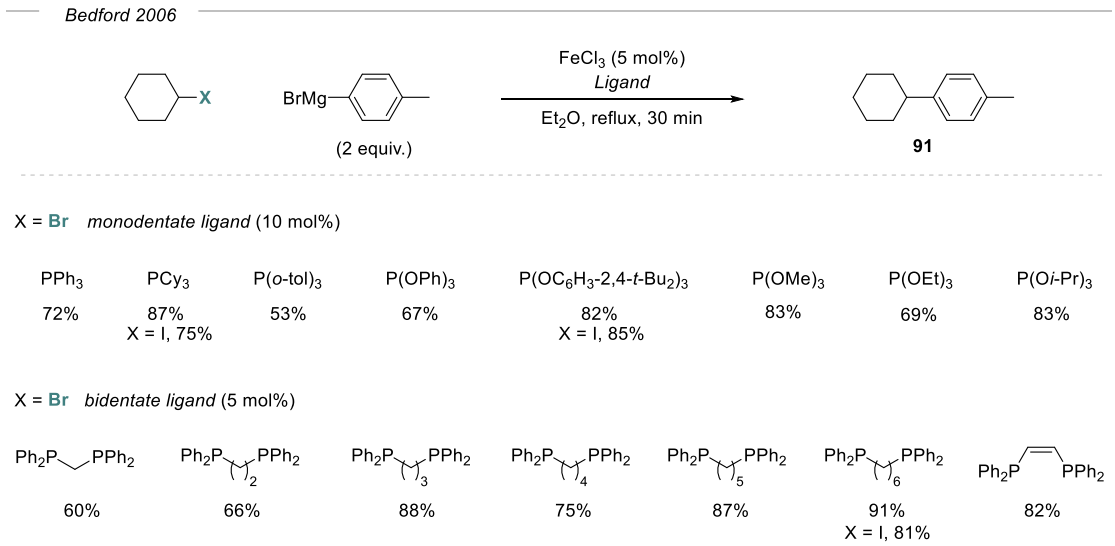

Scheme 3.5 *– Investigation into the effect of a) the substituents on monodentate phosphine ligands and b) the diphosphine ligand linker length on Kumada cross-couplings.*

When examining bidentate phosphine ligands however, a much clearer trend was established. As the chain length increased between the two phosphine groups, the yield increased. The yield increased smoothly from 60% with a chain length of one CH_2 unit, up to 91% with a chain length of six CH_2 units, with the exception of the chain length of three, where a higher yield than expected was observed of 88%. Finally they noted that the more rigid *cis*-$Ph_2P(CH{=}CH)PPh_2$ gave a higher yield (82%) than its saturated equivalent $Ph_2P(CH_2)_2PPh_2$ (66%). While these trends were established when using cyclohexyl bromide as the electrophile coupling partner, three of the best ligands (PCy_3, $P(OC_6H_3\text{-}2,4\text{-}t\text{-}Bu_2)_3$ and $Ph_2P(CH_2)_6PPh_2$) were also tried with the respective iodide, and all gave cross-coupled product **91** in good yields (75%, 85% and 81% respectively).

Noting the hygroscopic nature of $FeCl_3$ and requirement of $Fe(acac)_3$ to be used in conjunction with amine additives, Kozak and co-workers sought to synthesise a non-hygroscopic single component catalyst to carry out Kumada cross-couplings under mild reaction conditions.[132] They were able to synthesise an iron amine-bis(phenolate) complex in good yield, using Mannich condensations to form ligand **L1** (**Scheme 3.6**).

This catalyst efficiently performed Kumada cross-coupling reactions at room temperature between various alkyl halides, including 1-iodopropane and 1-iodocyclohexane, and aryl Grignard reagents in good yields and short reaction times.

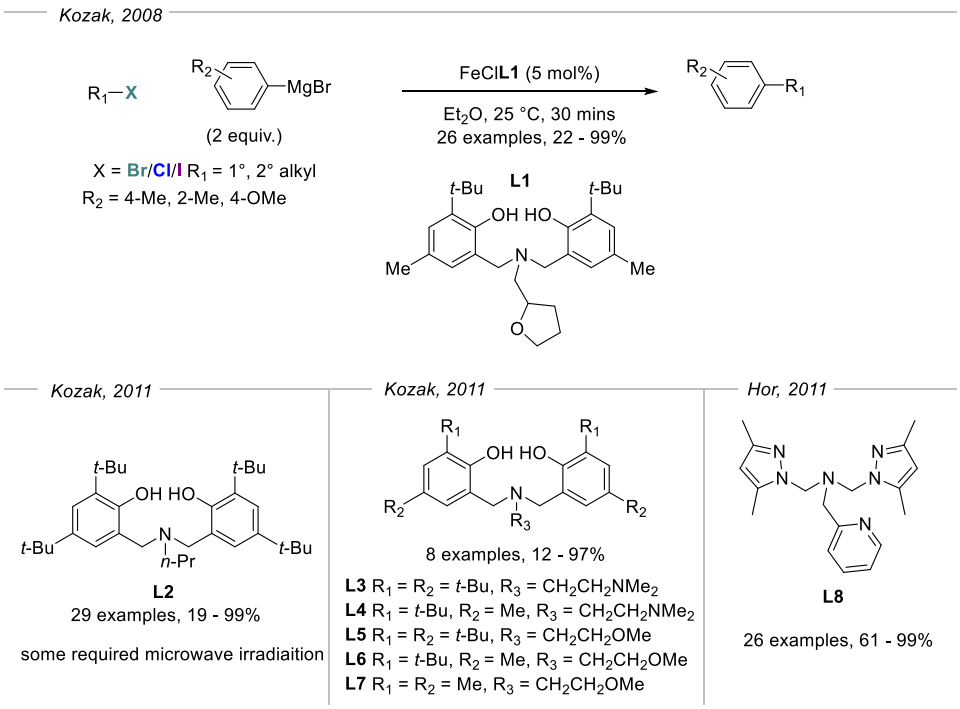

Scheme 3.6 *– Use of amine tripodal ligands Kumada cross-couplings.*

Following this, the group developed a number of similar ligands, varying the substituents on the aryl groups and the identity of the third substituent on the amine (ligands **L2** to **L7**).[133,134] These ligands could be used to perform cross-couplings in good yield (12−99%), although in some specific instances, microwave irradiation was necessary to obtain good conversion. Hor and co-workers also synthesised an amine tripodal ligand **L8** with pyrazolyl groups rather than phenolate.[135] This complex was successful in coupling primary and secondary bromides and iodides with simple aryl Grignard reagents in good yields (61−99%).

3. Iron-catalysed Kumada cross-coupling

A number of studies have been published on the use of $[FeCl_4]^-$ ferrate complexes, often in combination with *N*-heterocyclic carbene (NHC) ligands, for the cross-coupling of aryl Grignard reagents with alkyl halides. First reported by Gaertner and co-workers in 2006 using a relatively simple NHC ligand **L9** (**Scheme 3.7a**),[136] the group were able to cross couple primary and secondary alkyl halides with simple aryl Grignard reagents in just 10 minutes, obtaining good yields (20−89%). This sparked further interest into similar FeX_4-NHC catalysts, with Zhang and co-workers publishing several effective reactions of this type,[137–139] exploring both reactivity and mechanism between 2010–2013 (**Schemes 3.7b** – **3.7d**). More recently, Yamaguchi published a Kumada cross-coupling reaction using a different type of ferrate catalyst with an unusual bis(triphenylphosphoranylidene)ammonium cation (**Scheme 3.7e**).[140] This iron complex is both air- and moisture-stable and successfully catalysed the reaction of secondary and primary alkyl halides with aryl and benzyl Grignard reagents.

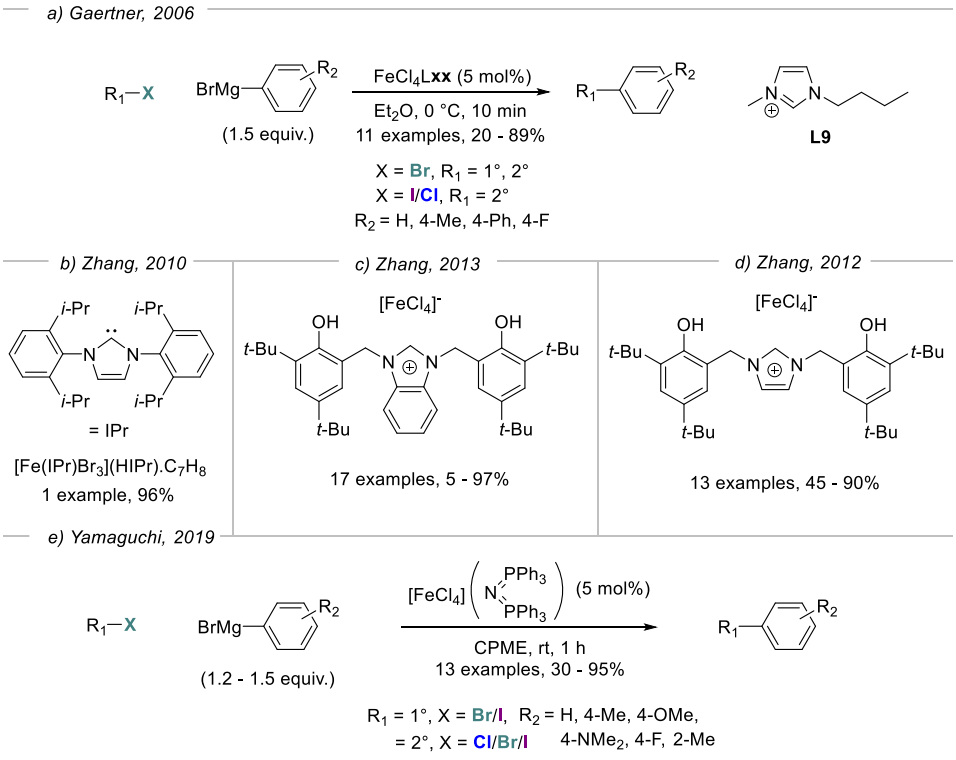

Scheme 3.7 *– Use of iron ferrate complexes in Kumada cross-couplings*

3. Iron-catalysed Kumada cross-coupling

In 2011, Nakamura and co-workers reported a Kumada cross-coupling using an iron(II) complex possessing a bulky biphosphine ligand (**L10**, **Scheme 3.8**).[141] Building on reports by Nagashima that suggested the active iron species adopts a tetrahedral conformation,[142] they developed the bulky ligand to maintain the desired geometry around the iron centre during transmetallation with aryl Grignard reagents. This catalyst system gave cross-coupled products in consistently high yields, and the cross-coupling of octanyl iodide with a mesityl Grignard reagent afforded **102** in an excellent 93% yield. More impressively, the use of this ligand enabled the Kumada cross-coupling of adamantyl bromide with PhMgBr to give **103** in 81% yield, in a rare example of a Kumada cross-coupling using a tertiary halide.

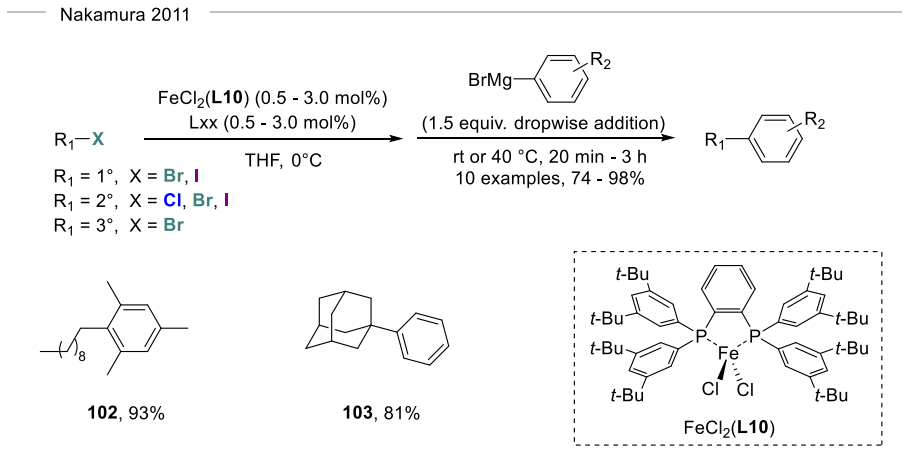

Scheme 3.8 *– Use of a bulky biphosphine ligand by Nakamura and co-workers for the Kumada cross-coupling of 1°, 2°, and 3° alkyl halides with aryl Grignard reagents.*

While most reports of Kumada cross-couplings of alkyl halides with aryl Grignard reagents focused on the exploration of alkyl bromides, in 2014 Cossy and co-workers reported an effective cross-coupling of both protected iodoazetidines and iodopyrrolidines using $FeCl_2$ – an unusual example of an Fe(II) complex being utilised as precatalyst instead of its Fe(III) counterpart – along with (*R*,*R*)-tetramethylcyclohexan-1,2-diamine (**L11**) (**Scheme 3.9a**).[143] A range of electron rich and electron poor aryl

3. Iron-catalysed Kumada cross-coupling

Grignard reagents underwent cross-coupling in good yield, and notably a 3-pyridyl Grignard reagent was also successful in the reaction, cross-coupling with azetidine **104** in an excellent 90% yield, and with the corresponding pyrrolidine in 51% yield. Rueping and co-workers followed this work with a protocol for the $Fe(acac)_3$/TMEDA catalysed cross-coupling of protected iodoazetidines with a range of aryl, heteroaryl, alkyl and vinyl Grignard reagents under mild conditions (**Scheme 3.9b**).[144] The reaction proceeded at −20 °C in 2 h, however, 3 equivalents of the Grignard reagent and TMEDA were required – considerably more than the 1.2 equivalents used by Cossy *et al.*. Nevertheless, this simple catalyst system enabled the cross-coupling of a much larger range of Grignard reagents than its predecessors, in moderate to excellent yields (32–96%) including aryl, heteroaryl, alkyl and vinyl Grignard reagents.

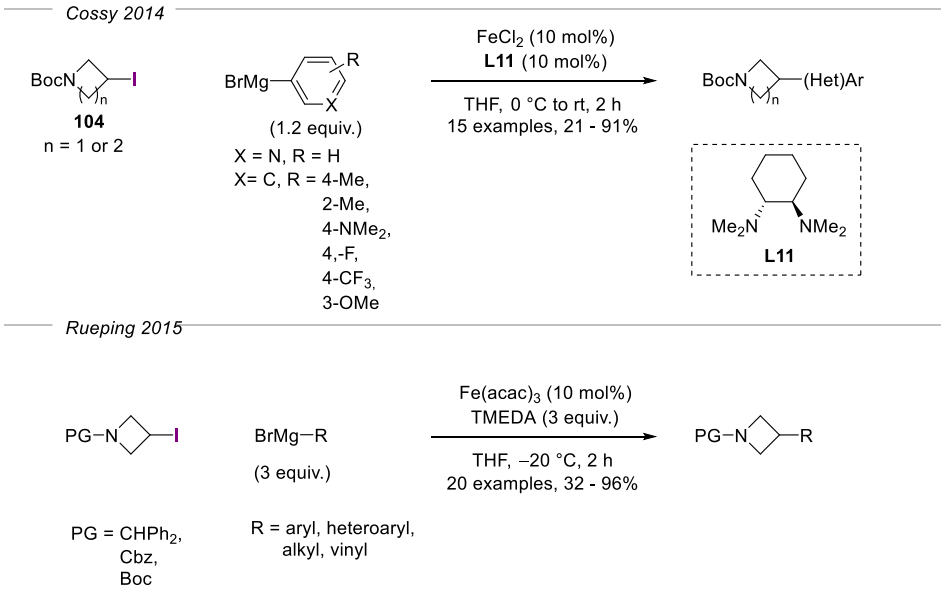

Scheme 3.9 *– Kumada cross-coupling of cyclic alkyl iodides with aryl Grignard reagents.*

3.2 Kumada cross-coupling of tertiary alkyl halides

While the Kumada cross-coupling of primary and secondary alkyl halides has been extensively explored with a plethora of efficient and diverse catalyst/ligand systems, the cross-coupling of tertiary halides remains a challenge. At the time of our investigation, only two reports had been published containing isolated examples. The first was a cross-coupling of adamantyl bromide by $FeCl_2$(SciOPP) ($FeCl_2$**L10**),[141] discussed in the previous section in **Scheme 3.8**. To the best of our knowledge, the only other report on tertiary halides involved the cross-coupling of adamantyl chloride and *t*-butyl chloride with phenylmagnesium bromide, under copper catalysis (**Scheme 3.10**).[145] While adamantyl chloride gave **105** in 78% yield, the *t*-butyl product **106** was only formed in 38% yield and both reactions required heating to 80 °C for 18 h. No Kumada cross-couplings of tertiary iodides were known.

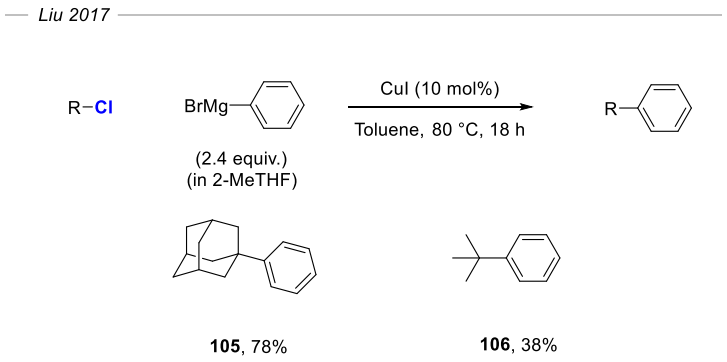

Scheme 3.10 *– Copper-catalysed Kumada cross-coupling of 3° alkyl chlorides with PhMgBr.*

With a large number of BCP iodides in hand *via* photoredox catalysis (**see Chapter 2.4**) or triethylborane-initiation (see **Chapter 2.2.1**), it was hoped that these could be used as substrates in an iron-catalysed cross-coupling with aryl Grignard reagents in order to provide another route to aryl-substituted BCPs.

3.2.1 Cross-coupling of bicyclo[1.1.1]pentanes

Bicyclo[1.1.1]pentanes have previously been demonstrated to undergo cross-coupling with aryl groups, however this has largely involved the use of the BCP compound as the nucleophilic, organometallic component. For example, in 2017 Messner *et al.* demonstrated a Negishi cross-coupling of BCP-zinc reagents with aryl, heteroaryl and vinyl halides (**Scheme 3.11**).[64] Starting from the BCP iodide **107**, *t*-BuLi was used to perform a lithium/halogen exchange followed by transmetallation with $ZnCl_2$, affording **108** as the nucleophilic component in the cross-coupling reaction. Using $PdCl_2$(dppf) as catalyst, Negishi cross-couplings with various sp^2 iodides and bromides were performed to afford 1,3-disubstituted BCPs in moderate to good yields. While a good range of halide coupling partners were tolerated, reaction times were relatively long – 20 h or more – and the use of *t*-BuLi makes this methodology unappealing from a safety perspective, as well as unsuitable for large scale reactions or late-stage functionalisation, and therefore problematic for industrial applications.

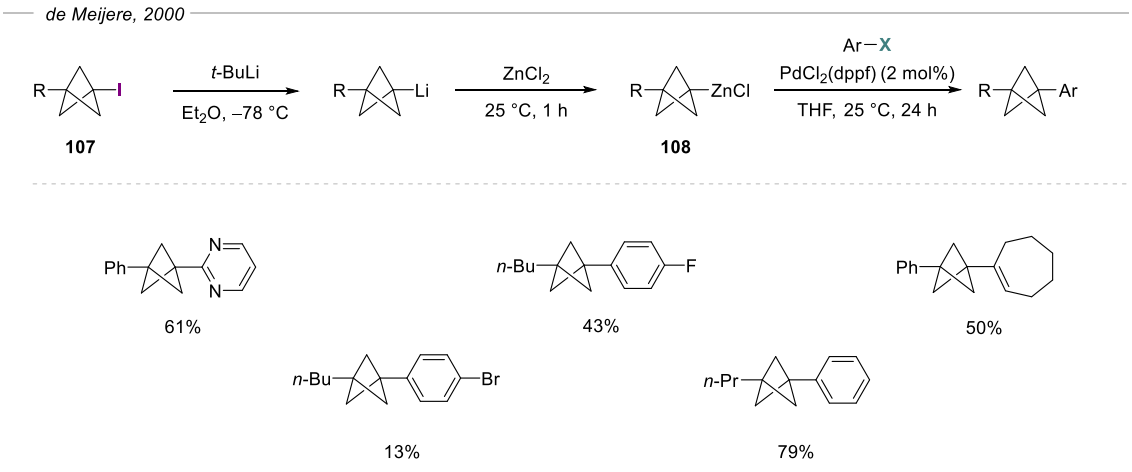

Scheme 3.11 *– Negishi cross-coupling of BCP iodides.*

3. Iron-catalysed Kumada cross-coupling

Knochel and co-workers also developed a Negishi cross-coupling of zincated BCP compounds with aryl Grignard reagents.[65] Their approach began with heating TCP with 2 equivalents of the Grignard reagent in diethyl ether at 100 °C in a sealed tube to afford the BCP-Grignard addition product **35** (**Scheme 3.12**). With this intermediate in hand, transmetallation with $ZnCl_2$ formed the zincated BCP, which could then be submitted to Negishi cross-coupling with aryl halides to afford 1,3-disubstituted BCP products in moderate to good yields. Aryl and heteroaryl halides were well tolerated in the reaction, and although this procedure avoids the use of the pyrophoric *t*-BuLi, the need to heat the Grignard reagents with TCP at elevated temperatures in order to access the organometallic BCP component hinders the applicability of this methodology to large scale industrial processes, and limits the scope of the cross-coupling to aryl BCPs only.

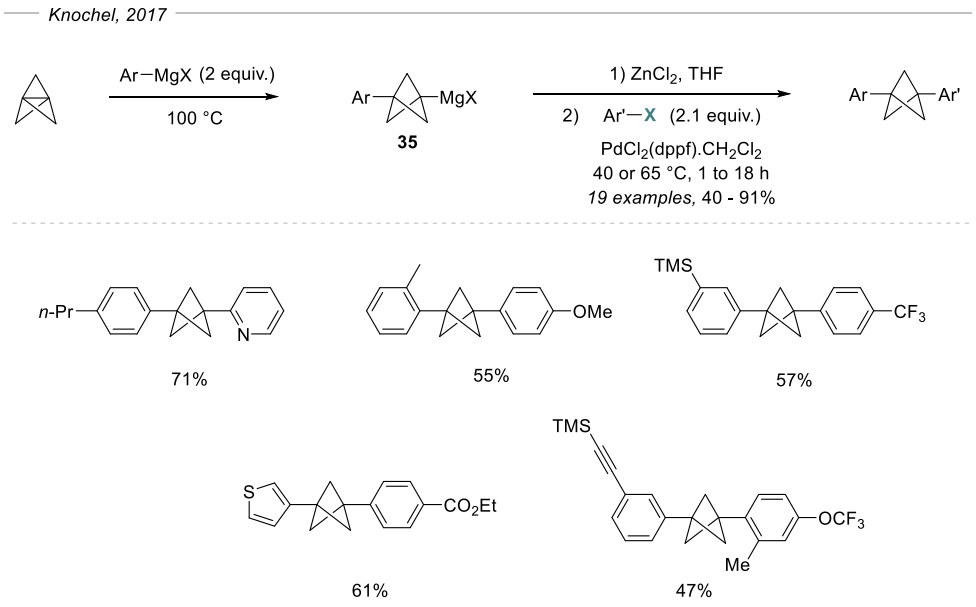

Scheme 3.12 *– Negishi cross-coupling of BCP-Grignard reagents.*

Although there are no generalised methods for the cross-coupling of BCPs where the BCP component acts as the electrophilic partner, two isolated examples did exist. Baran demonstrated that the cross-coupling of redox active esters with diaryl zinc species,

catalysed by $Fe(acac)_3$, was also applicable to BCP **109** to afford aryl-BCP product **110** in 35% yield (**Scheme 3.13**).[146]

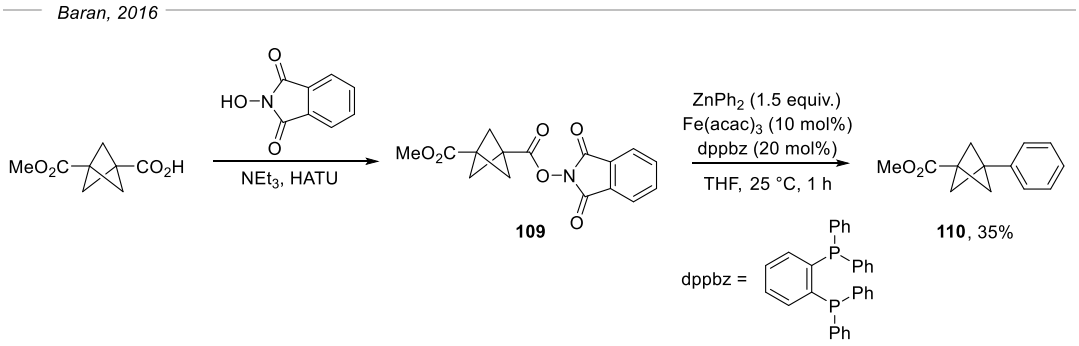

Scheme 3.13 *– Cross-coupling of BCP redox active esters.*

More recently Lalic and co-workers demonstrated the use of a photoinduced copper-catalysed coupling of alkyl iodides with terminal alkynes in good yields (**Scheme 3.14**).[147] They demonstrated the methodology on a range of alkyl iodides including three tertiary iodides; bicyclopentyl, bicyclooctyl, and adamantyl iodides to afford **111**, **112**, and **113** respectively.

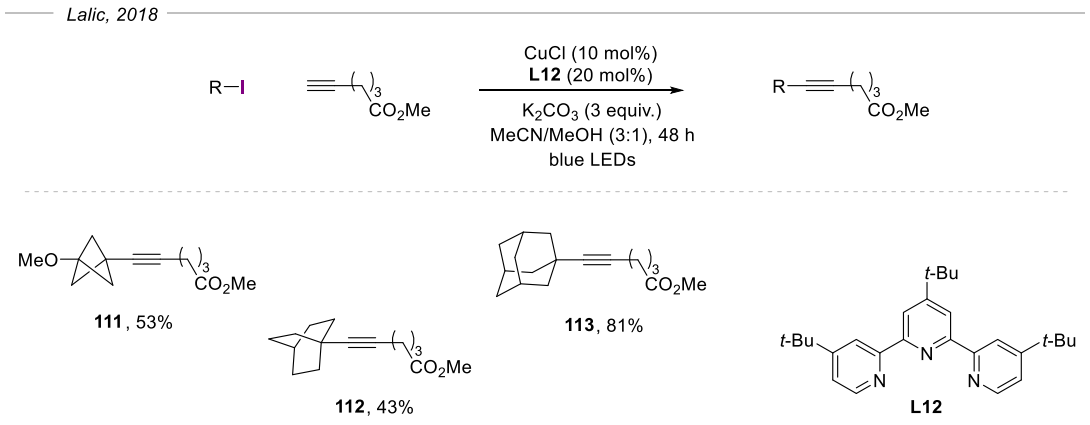

Scheme 3.14 *– Copper catalysed cross-coupling of a BCP iodide with alkynes.*

While **113** was produced in 81% yield, **112** and **111** suffered a drop in yield, giving 43% and 53% respectively. While this methodology provided an isolated example of a BCP iodide acting as the electrophilic component in a cross-coupling reaction, it was only applicable to the use of terminal alkynes.

Given the lack of a generalised cross-coupling methodology using BCP iodides, and the extensive precedent of Kumada cross-couplings with alkyl halides, it was desirable to develop an iron-catalysed cross-coupling of BCP iodides with aryl Grignard reagents.

3.3 Kumada cross-coupling of BCP iodides with (hetero)aryl Grignard reagents

Investigations into the optimisation of an iron-catalysed Kumada cross-coupling reaction using benzyl BCP iodide **114** and 4-MeO-PhMgBr were started by DPhil student Dimitri Caputo, and are described in his DPhil thesis.[148] The key findings from these initial optimisations are summarised in **Tables 3.2** and **3.3**.

Caputo's development of this reaction began using 3 equivalents of the Grignard reagent, 20 mol% of an iron catalyst and 40 mol% of a ligand, with the reaction being carried out in THF at room temperature for 30 minutes. The optimal iron catalyst in the absence of any additives was first explored (**Table 3.2**, entries 1-3). $Fe(acac)_3$ proved to be the best catalyst, giving a 42% yield of cross-coupled product **115**, with 23% of hydrodehalogenated **116** also being formed. Other iron catalysts such as $FeCl_3$ and $FeBr_3$ did not perform as well, forming significantly less **115** and instead favouring the formation of **116**. A wide range of amine and phosphine ligands were then screened under these conditions that had been shown to be successful in other Kumada cross-couplings (see **Chapter 3.2**), however none of these additives improved the yield at all compared

to using the catalyst on its own. Given reports of several Kumada cross-couplings where dropwise addition of the Grignard reagent proved crucial to obtaining good yields,[121,127,141] an updated protocol was used in subsequent experiments, involving addition of the Grignard reagent to the reaction mixture with a syringe pump at 1.8 mL/ h. With dropwise addition of the Grignard reagent but without additional ligands, the yield was significantly worse, forming only 9% of desired product **115** but 45% of **116** (entry 4).

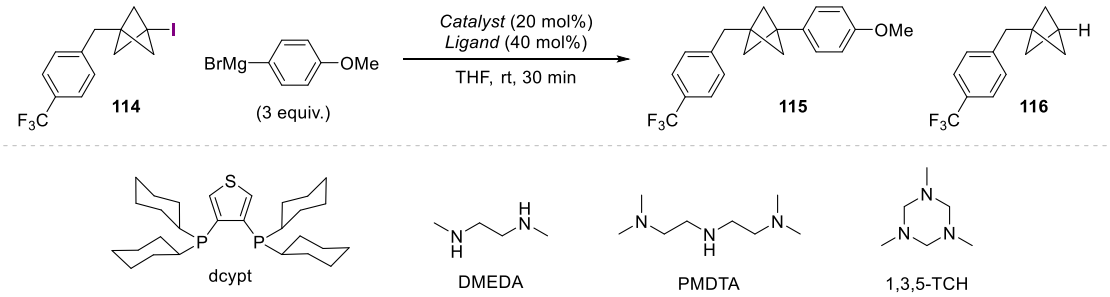

Entry	Catalyst	Ligand	Yield/[b] % **114**:**115**:**116**
1	$Fe(acac)_3$	-	0:42:23
2	$FeCl_3$	-	0:17:35
3	$FeBr_3$	-	0:17:35
4[a]	$Fe(acac)_3$	-	0:9:45
5[a]	$Fe(acac)_3$	dcypt	0:59:22
6[a]	$Fe(acac)_3$	NEt_3	0:12:46
7[a]	$Fe(acac)_3$	DMEDA	0:18:49
8[a]	$Fe(acac)_3$	TMEDA	0:66:9
9[a]	$Fe(acac)_3$	PMDTA	0:17:37
10[a]	$Fe(acac)_3$	1,3,5-	0:12:45

Table 3.2 *– Reactions performed by Dimitri Caputo.* [a] *Grignard added dropwise via syringe pump at 1.8 mL/ h.* [b] *Yields determined by* ^1H *NMR spectroscopy using 1,3,5-trimethoxybenzene as an internal standard.*

A number of bidentate phosphine ligands were then screened and while many did not improve the yield by much, the use of dcypt proved very effective, giving **115** in 59% yield with 22% of **116** (entry 5). Mono-, bi- and tridentate amine ligands were all also

screened, and while monodentate NEt_3 only gave 12% yield of **115** (entry 6), the use of secondary bidentate ligand DMEDA increased the yield slightly to 18% (entry 7), and tertiary bidentate TMEDA caused a dramatic increase in yield to 66% of **115** with only 9% of **116** (entry 8). Stronger chelating ligands PMDTA and 1,3,5-TCH however did not perform well in the reaction giving only 17% and 12% of **115** respectively (entries 9 and 10).

Having identified $Fe(acac)_3$ with TMEDA as the optimal catalyst system, the effects of the solvent, temperature, reaction concentration and Grignard reagent equivalents on the reaction were explored (**Table 3.3**). A number of solvents worked well in the reaction (entries 1-3) with THF giving the best yield. Increasing the temperature did not improve the yield of **115** (entry 4) and cooling the reaction temperature to 0 °C caused a reduction in yield to 58% (entry 5).

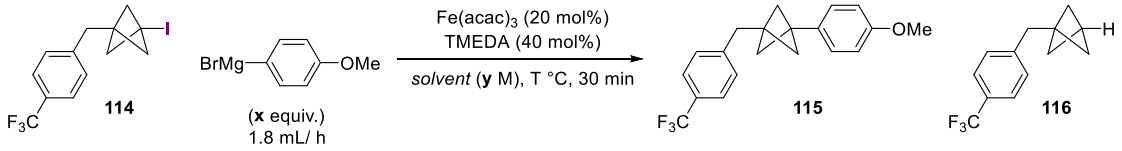

Entry	Solvent	T/ °C	**y**/ M	**x** (equiv.)	Yield/[a] % **114**:**115**:**116**
1	THF	rt	0.2	3	0:66:9
2	Toluene	rt	0.2	3	0:61:5
3	Et_2O	rt	0.2	3	0:57:5
4	THF	45	0.2	3	0:67:3
5	THF	0	0.2	3	0:58:12
6	THF	rt	0.4	3	0:66:3
7	THF	rt	0.8	3	0:73:4
8	THF	rt	1.0	3	0:73:2
9	THF	rt	1.0	1.6	complete
10	THF	rt	1.0	1.4	incomplete

Table 3.3 *- Reactions performed by Dimitri Caputo. [a] Yields determined by ^1H NMR spectroscopy using 1,3,5-trimethoxybenzene as an internal standard.*

A large concentration effect was seen, where increasing the reaction concentration from 0.2 M through to 1.0 M (entries 6 -8) caused an increase in yield to 73% of **115** with only 2% of **116** being formed. Finally, the equivalents of the Grignard reagent were reduced until the reaction no longer reached completion: full reaction conversion was achieved with 1.6 equivalents (entry 9), however lowering this further to 1.4 equivalents led to an incomplete reaction (entry 10).

To begin the investigations in this thesis, the optimisation of the reaction conditions as developed by Caputo for the cross-coupling was revisited. On repeating the previous optimised conditions, but increasing reaction time from 30 minutes to 1 h, an 82% yield of cross-coupled product **115** was obtained (**Table 3.4**, entry 1). The scale of the reactions was then reduced from 0.5 mmol to 0.2 mmol for easier handling, but on doing so a noticeable drop in yield was observed from 82% to 77% (entry 2). Maintaining the same rate of addition of the Grignard reagent (1.8 mL/h) on a smaller reaction scale meant that proportionally more Grignard is added to the reaction per droplet. Therefore, the rate of Grignard addition was slowed down to 0.7 mL/h to compensate for this reduced overall addition time, and the yield of the reaction increased significantly to 86% (entry 3).

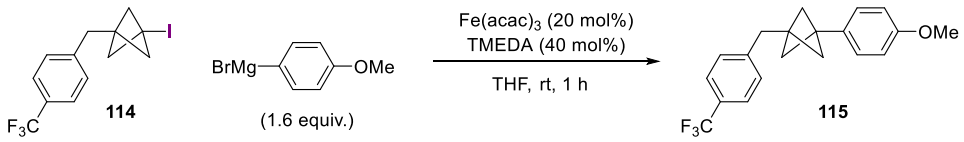

Entry	Reaction scale/ mmol	Rate of Grignard addition/ mL/ h	Yield/ %
1	0.5	1.8	82
2	0.2	1.8	77
3	0.2	0.7	86

Table 3.4 *– Effect of the rate of Grignard reagent addition.*

Given the super-stoichiometric amount of TMEDA used by Nakamura[121] and Rueping,[144] and the benefit observed by Cahiez of using a combination of TMEDA/HMTA,[127] the effect of ligand stoichiometry was next investigated with the cross-coupling of BCP iodides (**Table 3.5**). When using 160 mol% of TMEDA as opposed to 40 mol%, a decrease in yield was seen to 78% (entry 2). Nakamura also noted that premixing TMEDA with the Grignard reagent before addition was beneficial, however when applied to the BCP cross-coupling, only a trace amount of product was observed, with largely unreacted starting material remaining (entry 3). Use of HMTA either on its own or in combination with TMEDA decreased the yield to 68% and 74% respectively (entries 4 and 5).

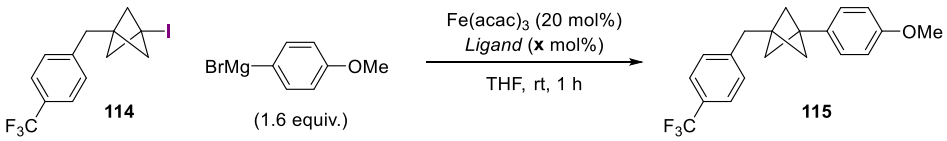

Entry	Additive	**x**/ mol%	Yield/[a] %
1	TMEDA	40	86
2	TMEDA	160	78
3	TMEDA (premixed with Grignard)	160	Trace[b]
4	HMTA	40	68
5	TMEDA/HMTA	40/20	74

Table 3.5 *– Effect of TMEDA/HMTA equivalents. [a] Yields determined by ^{1}H NMR spectroscopy using 1,3,5-trimethoxybenzene as an internal standard. [b] Mostly starting material remaining.*

Although super-stoichiometric TMEDA offered no benefit on the yield of the reaction, it was noted that a high catalyst loading of 20 mol% was still necessary. Reducing the catalyst loading to 10 mol% also caused a significant drop in yield to 62% (**Table 3.6**, entries 1-4). There have been reports of cases of cross-couplings that required high iron catalyst loadings in fact being catalysed by small amounts of copper impurities. To test the possibility that traces of copper could be responsible for this cross-coupling, $Fe(acac)_3$

of 99.9% purity as used in the reaction (entry 5) – higher than the sample used previously which was of 97% purity – to see if this would decrease the yield of the reaction. However, the yield of the reaction was unchanged, still forming 82% of product. Lastly reactions were run with $Fe(acac)_3$ as well as 5 mol% of various copper additives (entries 6-9); interestingly, a significant reduction in yield was observed and in the cases of CuO and Cu_2O, the reaction did not go to completion. None of this evidence suggests copper impurities were responsible for the cross-coupling rather than $Fe(acac)_3$ itself.

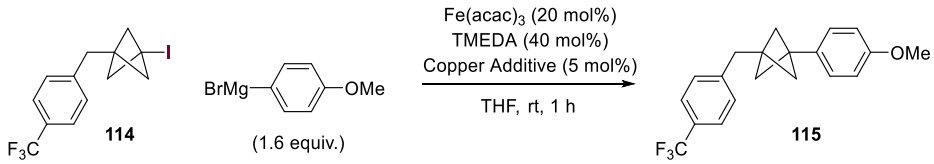

Entry	$Fe(acac)_3$ purity/ %	**x**/ mol%	Grignard addition rate/ mL/ h	Additive	Yield/[a] %
1	97	20	1.8	-	82
2	97	10	1.8	-	69
3	97	20	0.7	-	86
4	97	10	0.7	-	62
5	99.9	20	1.8	-	82
6	97	20	0.7	CuI	65
7	97	20	0.7	$Cu(acac)_2$	58
8	97	20	0.7	CuO	Incomplete reaction
9	97	20	0.7	Cu_2O	Incomplete reaction

Table 3.6 *– Investigations into whether copper impurities were involved in catalysing the cross-coupling.* [a] *Yields determined by* ^1H *NMR spectroscopy using 1,3,5-trimethoxybenzene as an internal standard.*

With these additional results obtained, a range of ligands and solvents were re-screened under the improved protocol (**Table 3.7**). These experiments were performed in collaboration with Dr Jeremy Nugent. Screening secondary bidentate amine DMEDA (entry 1) gave very poor yield, as did tertiary bidentate amine TMCD (entry 2). Tertiary bidentate phosphines 1,2-DPE (entry 3) and dcypt (entry 4) gave moderate yields of 46%

and 55% respectively, however some starting material remained and a small amount of the reduced BCP byproduct **116** was also formed. TMEDA again proved to be the best ligand by a significant margin (entry 5), giving 90% yield (86% isolated yield) of **115** with no starting material remaining and only 2% reduced BCP. 2-MeTHF, MTBE and toluene all gave good yields of **115** (entries 6-8) however THF still proved optimal. Using the LiCl 'turbo' Grignard adduct in the reaction did not improve the yield over a standard Grignard reagent (entry 9), while the use of $Cu(acac)_2$ shut down the reaction entirely (entry 10). Therefore, the conditions in entry 5 were taken as the optimised conditions for this cross-coupling.

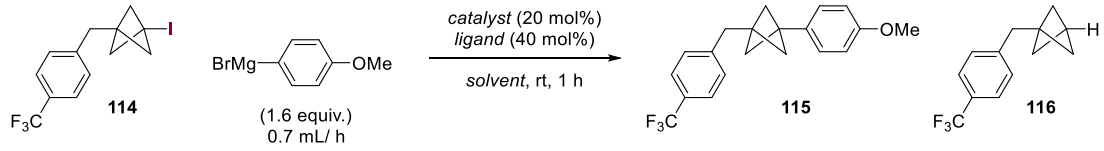

Entry	Catalyst (20 mol%)	Additive (40 mol%)	Solvent	Yield/[a] % **114**:**115**:**116**
1	$Fe(acac)_3$	DMEDA	THF	22:5:9
2	$Fe(acac)_3$	TMCD	THF	76:9:1
3	$Fe(acac)_3$	1,2-DPE	THF	33:46:8
4	$Fe(acac)_3$	dcypt	THF	20:55:11
5	**$Fe(acac)_3$**	**TMEDA**	**THF**	**0:90:2 (86)**
6	$Fe(acac)_3$	TMEDA	2-MeTHF	15:71:2
7	$Fe(acac)_3$	TMEDA	MTBE	16:70:2
8	$Fe(acac)_3$	TMEDA	Toluene	0:79:3
9[b]	$Fe(acac)_3$	TMEDA	THF	0:86:4 (79)
10	$Cu(acac)_2$	TMEDA	THF	100:0:0

Table 3.7 *– Rescreen of conditions [a] Yields determined by ^{1}H NMR spectroscopy using 1,3,5-trimethoxybenzene as an internal standard [b] Reaction performed using 4-MeOPhMgBr.LiCl. Reactions performed by Dr Jeremy Nugent.*

3.4 Scope

With optimised conditions in hand, the scope of the reaction was explored. The range of aryl Grignard reagents were first tested in the reaction (**Figure 3.1**). These experiments were performed in collaboration with Dr Jermey Nugent and Summer student Frank Nightingale, who are credited where appropriate.

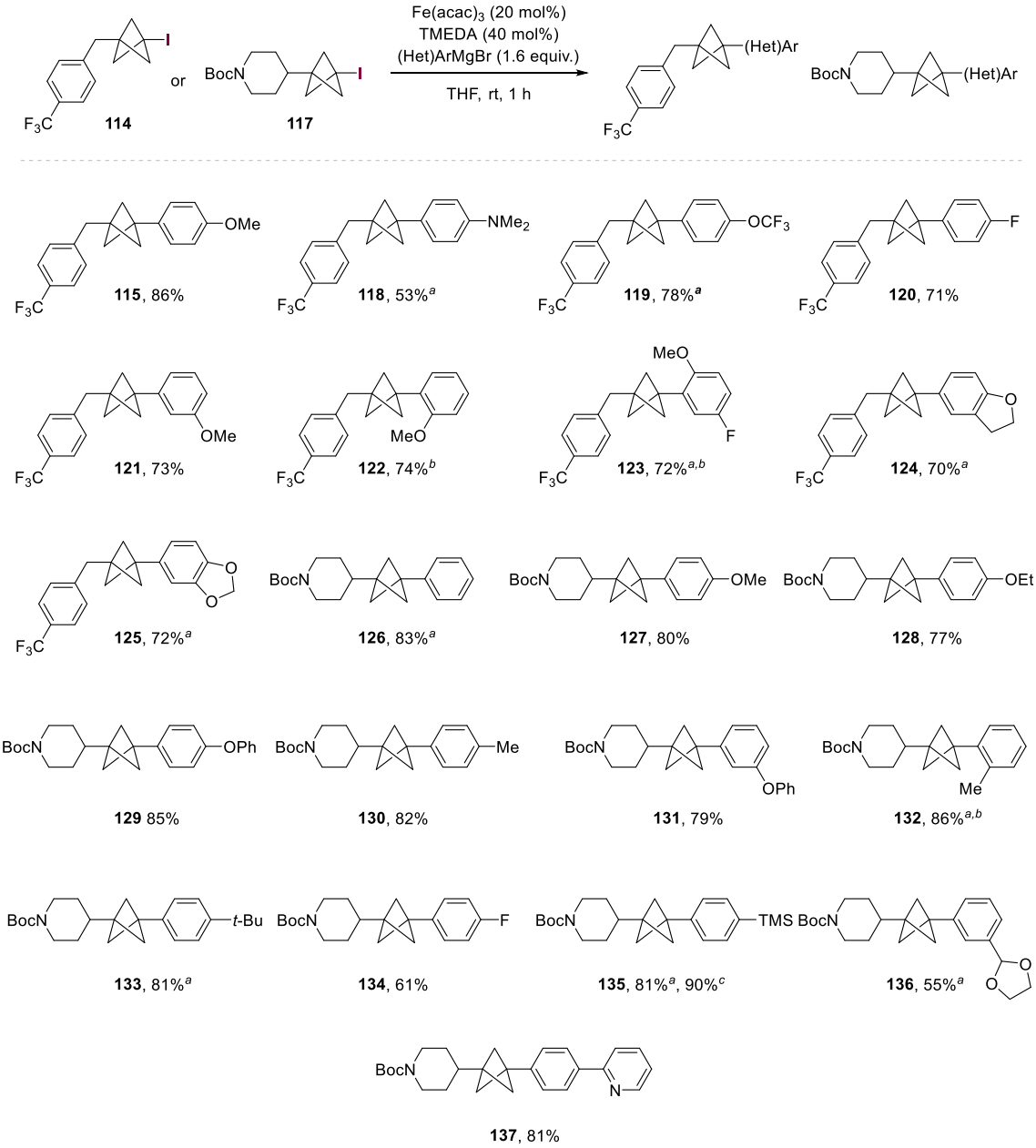

Figure 3.1 *– Scope of aryl Grignard reagents in the Kumada cross-coupling of BCP iodides.* [a] *Reaction performed by Dr Jeremy Nugent.* [b] *Reaction performed at 45 °C.* [c] *Reaction performed on 1 g scale.*

3. Iron-catalysed Kumada cross-coupling

BCP iodides **114** and **117** were cross-coupled with a wide range of aryl Grignard reagents in good to excellent yields. Aryl Grignards bearing electron-rich or neutral para-substituents were well tolerated in the reaction of both **114** and **117**, providing cross-coupled products **115-137** in 53–86% yield. Alkyl and alkoxy substituents all gave good yields of between 77% (**128**) and 86% (**114**, **132**), while NMe_2 substituted aryl BCP **118** was formed in a slightly lower yield of 53%. Mildly electron withdrawing groups could be tolerated, with 4-FPhMgBr giving 71% and 61% of **120** and **134** respectively. More electron-withdrawing substituents were unfortunately not accommodated. Aryl Grignard reagents bearing meta substituents were also tolerated in the reaction giving good yields of cross coupled products **121** and **131** in 73% and 79% yield respectively, while 1,3-dioxolane substituted **136** was formed in a slightly lower yield of 55%. Ortho-substituted Grignards were also successful in this reaction (**122, 123** and **132**), however in these cases, the reaction required gentle warming to 45 °C. 4-TMSPhMgBr cross-coupled efficiently with **117** to give **135** in 81%, and pleasingly when scaling this reaction to 1 g of **117** (2.7 mmol), the yield of the reaction increased to 90%.

Having successfully cross-coupled a wide range of aryl Grignard reagents, the scope of heteroaryl Grignards was investigated (**Figure 3.2**). A number of these substrates were tolerated in the reaction (**138** to **146**), although these generally required warming to 45 °C. 3-pyridyl Grignard was initially submitted to the cross-coupling with **117**, however only 27% of **138** was formed, and the reaction required heating to 60 °C with rapid addition of the Grignard reagent due to its instability. However on substituting the 3-pyridyl Grignard with an electron donating group, the yield increased dramatically, giving 49% and 55% of **139** and **140** respectively. The electron-rich 4-pyridyl Grignard also cross-coupled to give **141** in a slightly lower yield of 35%, however 2-pyridyl Grignards were not successful under the reaction conditions, largely undergoing homo-coupling of the

Grignard instead. It is worth noting that 3 equivalents of the substituted pyridyl Grignard reagent are required to obtain a good yield. The benzofuryl Grignard cross-coupled efficiently in the reaction to give **142** in 67% yield without the need for excess equivalents of Grignard reagent or heating. *N*-heterocyclic products **143** to **146** were also formed in good yield (46%−65%), with the reaction with the indazole Grignard proceeding at room temperature, forming **144** in 46% yield.

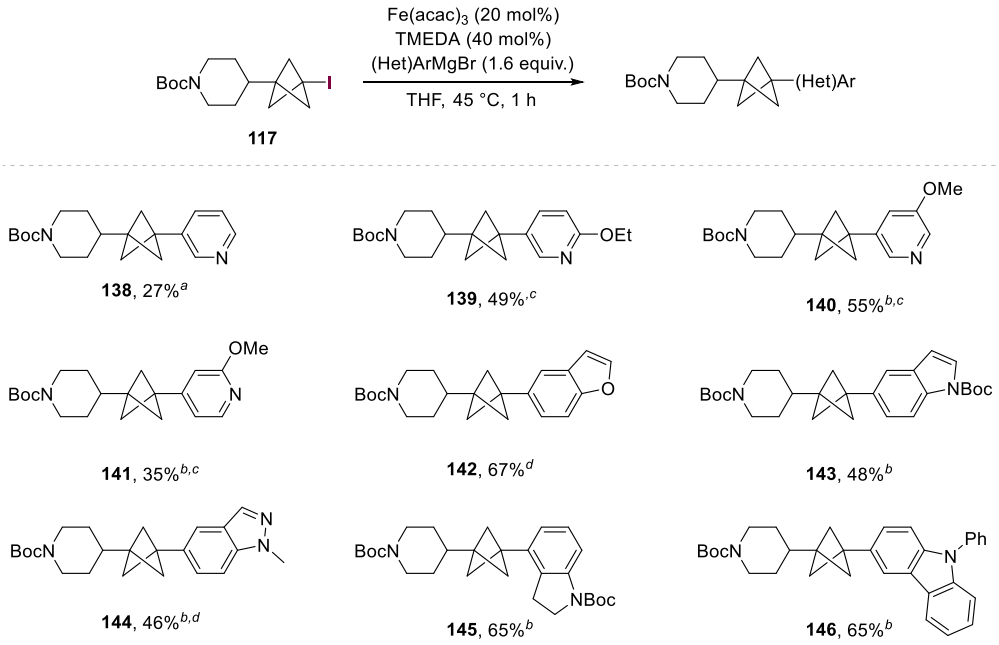

Figure 3.2 *– Scope of heteroaryl Grignard reagents in the Kumada cross-coupling of BCP iodides.* [a] *Reaction performed at 65 °C, rapid addition of Grignard reagent.* [b] *Reaction performed by Dr Jeremy Nugent.* [c] *Reaction performed using 3.0 equivalents of Grignard reagent.* [d] *Reaction performed at room temperature.*

With a wide range of aryl and heteroaryl Grignards successfully cross-coupled, a selection of BCP iodides were submitted to the reaction conditions with 4-MeO-PhMgBr (**Figure 3.3**). Boc-protected azetidine **147** was formed in 73% yield, and sulfone containing **148** was successfully formed in 67% yield. Ethyl ester **149** was formed in an excellent 95% yield, showing no undesirable addition of the Grignard reagent into the ester functionality. However, the more electrophilic ester group in **150** did suffer from

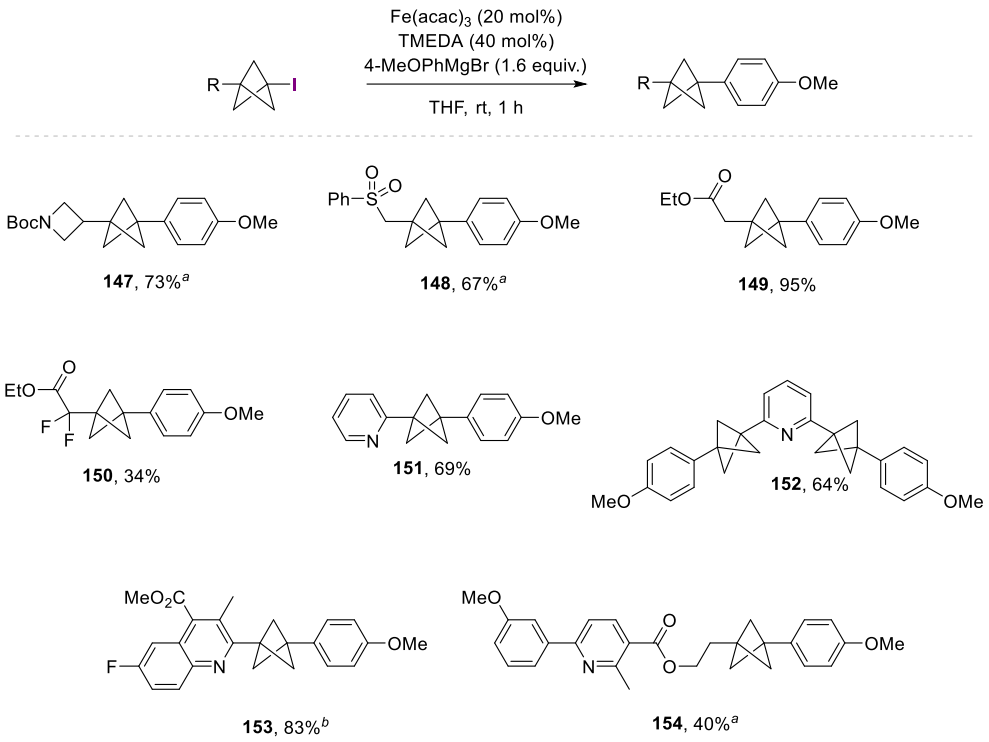

Figure 3.3 *– Scope of BCP iodides in the Kumada cross-coupling with PhMgBr.* [a] *Reaction performed by Dr Jerermy Nugent.* [b] *Reaction performed by Mr Frank Nightingale.*

competing addition of the Grignard reagent, and consequently a large decrease in yield was observed to 34%. 2-Pyridyl substituted BCP iodide cross-coupled in 69% yield to form mixed aryl BCP **151**, and a double cross-coupling of the bis-bicyclopentylated **60** was successfully performed to give 64% of **152**. More complex BCP iodides were also successful under the reaction conditions, giving 83% of the quinoline **153** and 40% of the nicotinic acid derivative **154**.

While a large range of aryl and heteroaryl Grignard reagents were well tolerated in the reaction, there were several classes of Grignard reagents that were not successful (**Figure 3.4**). Whereas *para*-fluorophenyl substituents were tolerated, *para*-CF_3 substituted **155** was too electron-poor to undergo successful cross-coupling. The *ortho*-fluoro substituted Grignard reagent **156** was unsuccessful in the reaction, probably due to instability of the Grignard which can collapse to form a benzyne intermediate.[149,150]

More sterically demanding aryl Grignard reagents such as mesityl **157** were unable to undergo cross-coupling with the BCP iodide, and 5-membered heterocycles such as **158** and **159** also produced no cross-coupled product. As noted, 2-pyridyl Grignard reagents such as **160** were unstable and underwent homo-coupling rather than reacting with the BCP iodide. Disappointingly, vinyl (**161** and **162**) and alkyl (**163** and **164**) Grignard reagents also showed no reactivity in the reaction.

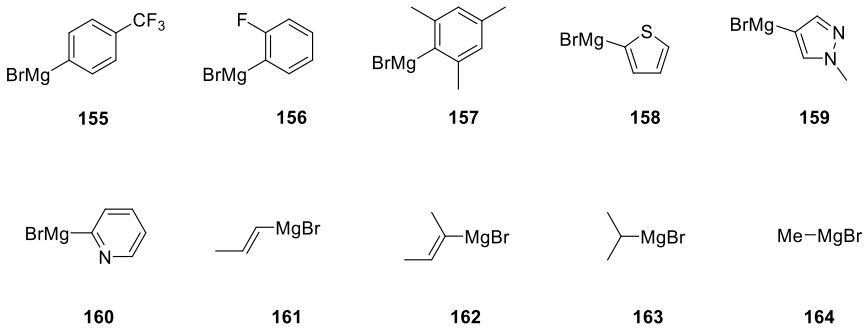

Figure 3.4 *– Unsuccessful Grignard reagents.*

3.5 Applications

This cross-coupling methodology was successfully combined with the atom transfer radical addition chemistry, and applied to the synthesis of two drug analogues

(**Scheme 3.15**). These syntheses were performed by Mr Dimitri Caputo, Dr Jeremy Nugent and Mr Frank Nightingale and will therefore not be discussed in detail; in short, BCP-flurbiprofen **166** was efficiently synthesised in two steps from ethyl 2-iodopropanoate **165**, and a BCP-brequinar analogue **168** could also be synthesised in 2 steps from quinoline **167**.

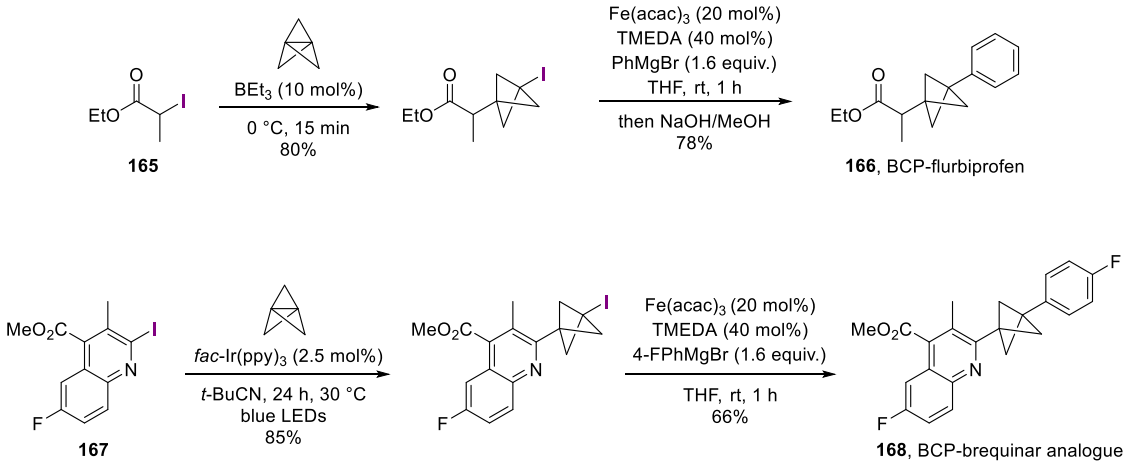

Scheme 3.15 *– Synthesis of BCP-flurbiprofen by Dr Dimitri Caputo and synthesis of BCP-brequinar analogue by Dr Jeremy Nugent and Frank Nightingale.*

TMS substituted **135** could be successfully synthesised on a large scale in high yields (see **Figure 3.1**), enabling further derivatisation through ipso-substitution. As a result, functional groups that were incompatible with the cross-coupling conditions could be accessed (**Scheme 3.16**). Use of KBr and NCS gave bromide **169** in 69% yield, and use of ICl provided the iodide **170** in 64% yield. A Friedel-Crafts acylation could also be employed to form **171** in 67% yield.

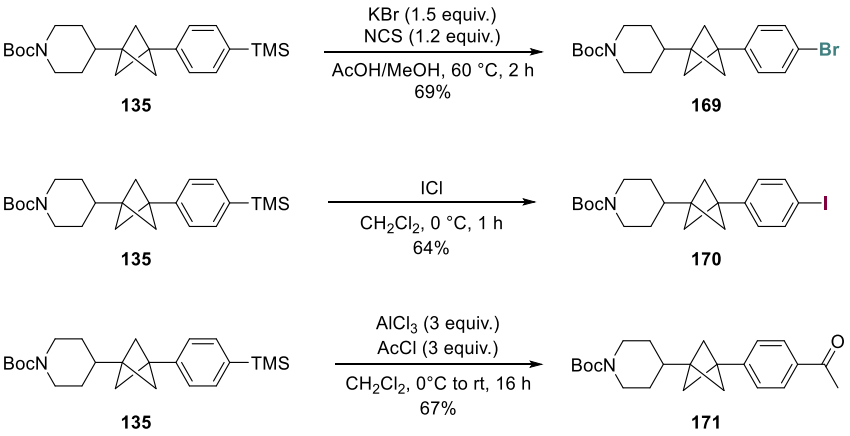

Scheme 3.16 *– Further functionalisations of cross-coupled products.*

3.6 Mechanistic investigations

While many iron-catalysed cross-couplings have been developed, elucidation of the mechanism of these reactions has remained challenging and under-developed. The difficulty in studying these systems is due to several factors. Firstly, organoiron intermediates formed during the reaction can be unstable and sensitive to both air and temperature. Moreover, iron is able to undergo many different redox processes via both one and two electron transfers, forming intermediates with a variety of oxidation states as well as spin states, many of which are paramagnetic and therefore difficult to characterise using NMR spectroscopy.[118] It is also common for multiple reactive iron complexes to form over the course of the reaction, all of which may be able to catalyse the reaction with varying rates, and so identifying the predominant species and/or most effective catalytic complexes can be challenging. Many studies have looked into identifying potential iron intermediates and elucidating the mechanisms of these cross-couplings, but the mechanism is highly dependent on the identity of the electrophile, the Grignard reagent, the ligands, the solvent, and the speed of Grignard addition, and so applying any observations to other systems must be done with caution.[151–154]

Several investigations into the mechanism of iron-catalysed Kumada cross-couplings of aryl Grignard reagents and alkyl halides using TMEDA as an additive have been conducted. Nagashima studied the $FeCl_3$/TMEDA catalysed cross-coupling of a mesityl Grignard reagent with 1-bromooctane which gave 32% yield of the cross-coupled product **172** after 18 h (**Scheme 3.17a**).[142] When $FeCl_3$ and TMEDA were mixed with 3 equivalents of mesityl Grignard, they isolated (TMEDA)Fe(mesityl)$_2$ (**173**), which upon resubmission to reaction conditions with 2 equivalents of 1-bromooctane formed (TMEDA)Fe(mesityl)Br (**174**) (**Scheme 3.17b**). Reaction of **173** with another equivalent

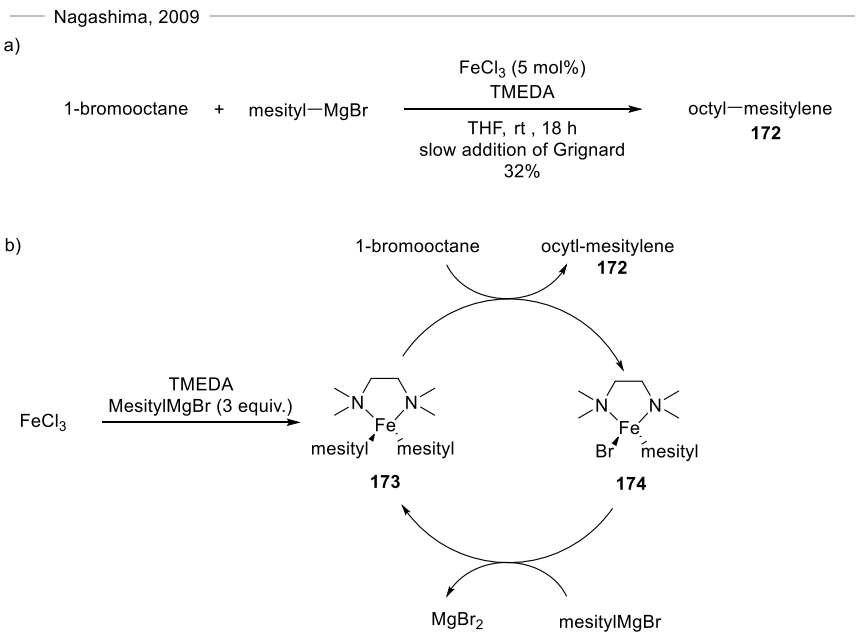

Scheme 3.17 *– Initial proposed mechanism for the $FeCl_3$/TMEDA catalysed Kumada cross-couplings of 1-bromoocatane with mesityl Grignard by Nagashima and co-workers.*

of 1-bromooctane proceeded at a faster rate than that of **174** with 1-bromooctane. **174** also reacted with another equivalent of the Grignard to reform **173**. Radical clock experiments showed 1-bromo-5-hexene treated with **173** gave the cross-coupled product **175** but no cyclised/cross-coupled product **176** (**Scheme 3.18**).

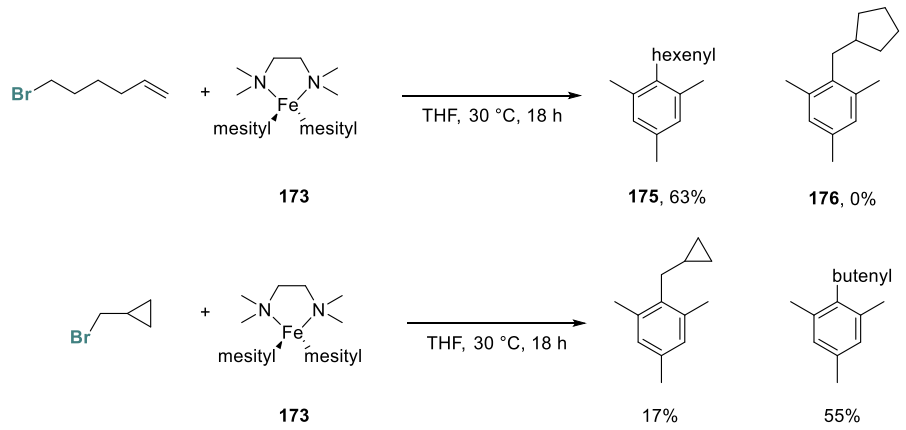

Scheme 3.18 *– Radical clock experiments performed by Nagashima and co-workers.*

However, reaction of bromomethylcyclopropane gave a mixture of cross-coupling products, where most of the cyclopropane motif had ring opened prior to cross-coupling. This suggested the formation of a short-lived radical during the oxidation of Fe(II) to Fe(III).

Bedford looked further into this mechanism and found that on performing the control reaction where TMEDA was left out of the cross-coupling reaction, a slightly improved yield of **172** of 36% was obtained, but a smaller amount of unreacted bromooctane (and more octane and octene side products) were observed.[154] This suggested that TMEDA was not necessary for the cross-coupling mechanism itself but may help prevent other undesirable pathways from proceeding that form these side-products. They also found that while **173** is formed with low Grignard loadings, increasing the equivalents instead forms the homoleptic 'ate' complex **177** (**Scheme 3.19**) until it is the only paramagnetic complex when 8 equivalents of the Grignard (with respect to iron) are used.

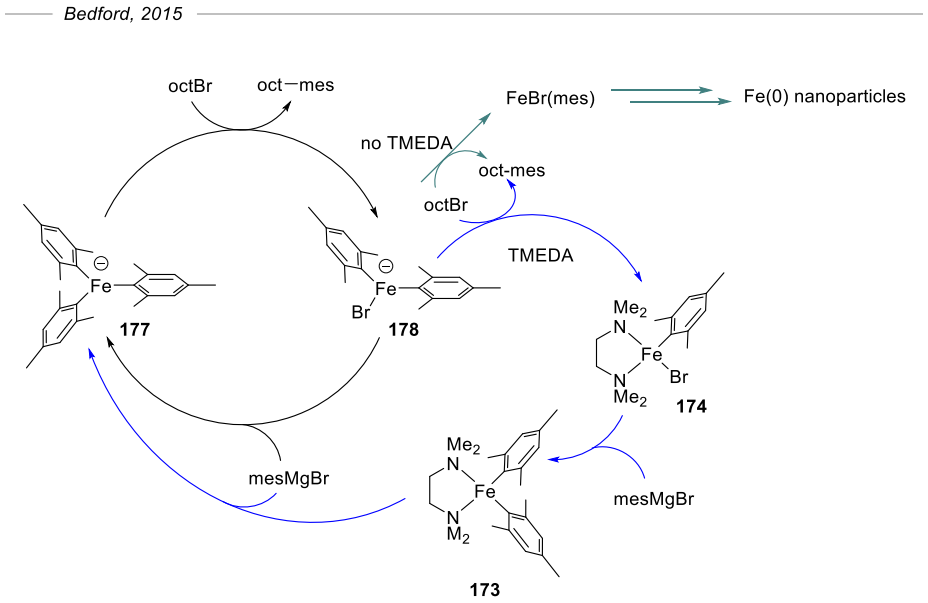

Scheme 3.19 *– Proposed mechanism involving iron 'ate' complex by Bedford and co-workers.*

177 reacts more efficiently with 1-bromooctane to give cross-coupled **172** and a paramagnetic species suggested to be **178**. The group therefore suggested that cross-coupling proceeds via **177** and **178**, and **173** and **174** instead stabilise off-cycle species as TMEDA adducts to prevent other pathways that could lead to side-product formation, for example, through the formation of iron nanoparticles.

The group also noted that reactions using bulky mesityl Grignard reagents are not representative of most aryl Grignard reagents. This difference between bulky and non-bulky aryl Grignards was demonstrated visibly, as the reaction mixture with $FeCl_2$/TMEDA and MesMgBr stays a clear orange colour, whereas with 4-Me-PhMgBr turned an opaque black suggesting the formation of iron nanoparticles, although these may themselves be active pre-catalysts. Bedford later found when investigating other amine ligands that the use of less labile ligands in the presence of excess benzyl Grignard led to a decrease in the catalytic activity of the iron complex.[155] If the ligands were not displaced by the excess benzyl Grignard at all, then very poor activity was seen and the reaction appeared homogenous throughout, whereas the reaction mixture turned black using labile ligands, again suggesting iron nanoparticle formation.

Neidig also found the formation of homoleptic 'ate' complexes when reacting $Fe(acac)_3$ with excess equivalents of Grignard in the absence of additives, and characterised them using SC-XRD (**Scheme 3.20**).[156] They also found distinctive colour changes taking place with each additional equivalent of Grignard added. On reacting $Fe(acac)_3$ with one equivalent of Grignard the reaction turned red, and complex **179** was isolated; on a second equivalent of Grignard, the reaction turned yellow and while this complex could not be isolated, on addition of a third equivalent of Grignard reagent, **180** was formed and was isolated alongside a colour change to orange. The addition of a fourth equivalent of Grignard forms a red solution and the dimeric compound **181** was isolated.

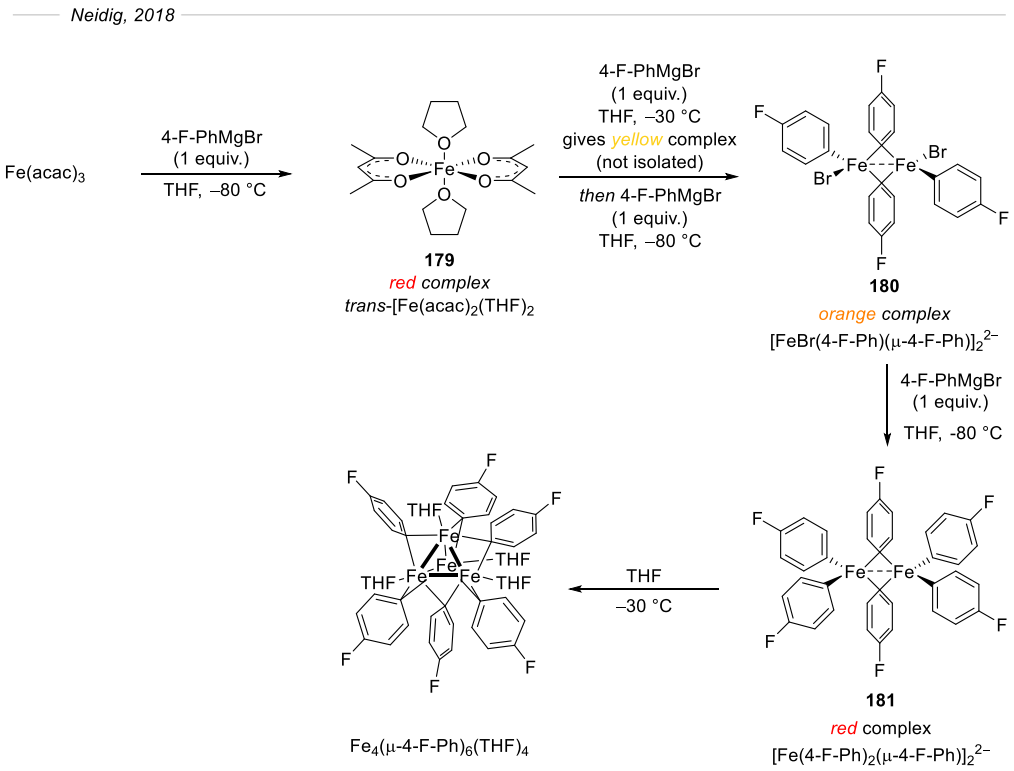

Scheme 3.20 *– Observed and identified iron complexes on reaction on Fe(acac)$_3$ with 4-F-PhMgBr by Neidig and co-workers.*

181 appears similar to a dimeric version of homoleptic complex **177** proposed by Bedford, which was shown to be catalytically active in cross-coupling reactions with alkyl halides. The cross-couplings of BCP iodides with aryl Grignard reagents saw very similar colour changes as the Grignard reagent was added (**Figure 3.5**). 0.2 equivalents of Fe(acac)$_3$ and 1.6 equivalents of Grignard were necessary for the reaction to go to completion which would also align with Neidig's observation that it wasn't until 3 equivalents of Grignard (respective to iron) had been added that **181** started to form.

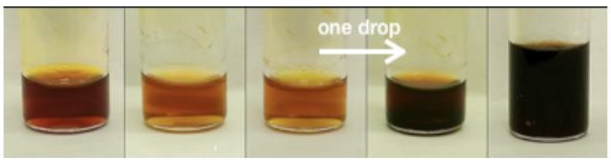

Time (mins)	0	5	10	11	90
Equiv. added	0	0.29	0.58	0.6	1.6

Figure 3.5 *– Observed colour changes on slow addition of 4-MeOPhMgBr to a mixture of BCP iodide **114** and Fe(acac)$_3$/TMEDA in THF at room temperature. Photos taken by Dr Jeremy Nugent.*

After these 3 equivalents with respect to iron had been added, the reaction turned black, suggesting the formation of iron nanoparticles.

Very recently, Neidig and co-workers published a further paper reinvestigating the iron-species formation and mechanism in the $FeBr_2$/TMEDA-catalysed cross-coupling of aryl Grignard reagents with alkyl halides.[157] They noted that the role of TMEDA is still unclear in these reactions, and that most previous studies had made use of the mesityl Grignard reagent which may not be representative or applicable to more general Kumada cross-coupling using smaller nucleophiles. Therefore the 'ate' complex suggested by Bedford might in fact be a part of a less efficient catalytic pathway correlating with the low yield observed for the cross-coupling. They also noted that different iron species had been shown to form with mesityl Grignard reagents compared to phenyl Grignard reagents when bisphosphine ligands were employed.[158,159] Therefore Neidig used a combination of x-ray diffraction, ^{57}Fe Mössbauer spectroscopy, EPR spectroscopy and detailed reaction/kinetic studies to elucidate the structure of active catalytic complexes and the role of TMEDA in the reaction. While the exact role that TMEDA plays, and its precise contribution to the catalytic pathway remained ambiguous, they were able to demonstrate that for less sterically bulky Grignard reagents such as phenylmagnesium bromide, TMEDA-bound iron complexes are involved in the primary catalytic pathway (**Scheme 3.21**), stabilising a monomeric iron species. They found that **174** was involved in the cross-coupling pathway while **173** is a radical initiator that can also lead to homocoupling of the Grignard reagent. They noted that while the formation of any homoleptic iron complexes was not observed, these could contribute to the initiation of the catalysis in addition to **173**. Overall, a mechanism was suggested that involves an Fe(II)/Fe(III)/Fe(I) cycle where catalysis is initiated by reaction of alkyl halide with **173** to give alkyl radical and complex **182**, which can undergo reductive elimination to give

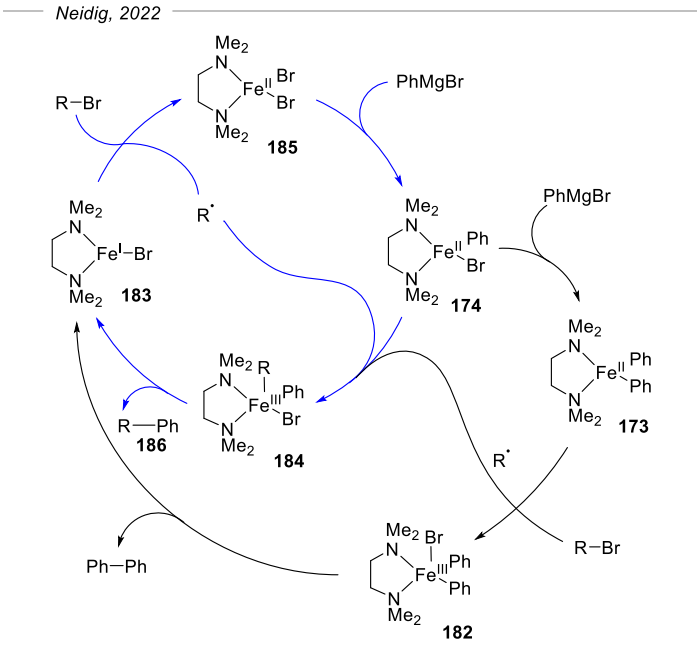

Scheme 3.21 *– Recently proposed mechanism for Kumada cross-coupling of alkyl halides with aryl Grignard reagents using an iron catalyst and TMEDA additive by Neidig and co-workers*

the homocoupled Grignard product and complex **183**. The alkyl radical can recombine with **174** to give complex **184** which can undergo reductive elimination to form the cross-coupled product **186** and complex **183**. This Fe(I) complex is now able to react with another alkyl halide to give the alkyl radical and complex **185** which on reaction with the Grignard reforms complex **174**.

.

This mechanism could reasonably be applied to the cross-coupling of BCP iodides with aryl Grignard reagents under $Fe(acac)_3$/TMEDA catalysis, except it would require an extra equivalent of Grignard with respect to the iron catalyst to initiate the reaction compared to the $FeBr_2$ system studied by Neidig. This fits with the 0.2 equivalents of $Fe(acac)_3$ used and 0.6 equivalents of Grignard reagent needed to be added until the reaction turns a black colour – which could indicate the homoleptic complex **181** having been formed and the reaction being initiated.

3. Iron-catalysed Kumada cross-coupling

To gain more insight into the mechanism of the cross-coupling of BCP iodides and aryl Grignard reagents, a series of competition experiments were carried out. A premixed solution of PhMgBr and 4-XPhMgBr was added at once to a solution of BCP iodide **117**, $Fe(acac)_3$, and TMEDA in THF, and then the ratio of cross-coupled products was measured by NMR spectroscopy using an internal standard. These product ratios were then compared to the Hammett constant for the functional group, X (**Table 3.8**), and plotted on a graph (**Figure 3.6**). Three equivalents of both Grignard reagents were used and were added at once, to ensure there was an excess of both throughout the reaction.

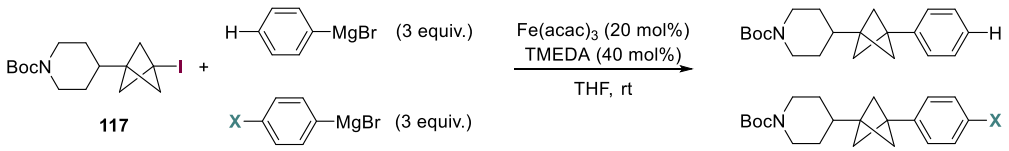

X	σX	Product Ratio: X/H
OMe	−0.27	0.3
OEt	−0.24	0.4
t-Bu	−0.20	0.7
Me	−0.17	0.6
TMS	−0.07	1.0
OPh	−0.03	0.7
F	0.06	0.38
2-Py	0.17	0.7
m-OPh	0.25	0.7
OCF_3	0.35	0.11

Table 3.8 *– Comparison of Hammett substituent constants and product ratios for competition experiments between PhMgBr and XPhMgBr. Product ratios calculated using ^1H NMR spectroscopy in comparison to an internal standard of 1,3,5-trimethoxybenzene. Reported ratios are an average taken from three experiments. Substituents are para- unless indicated otherwise*

Surprisingly, the Hammett plot showed that both electron-rich and electron-poor Grignard reagents reacted at a slower rate than PhMgBr, with only 4-TMSPhMgBr reacting at the same rate. For electron rich Grignard reagents there is a positive correlation

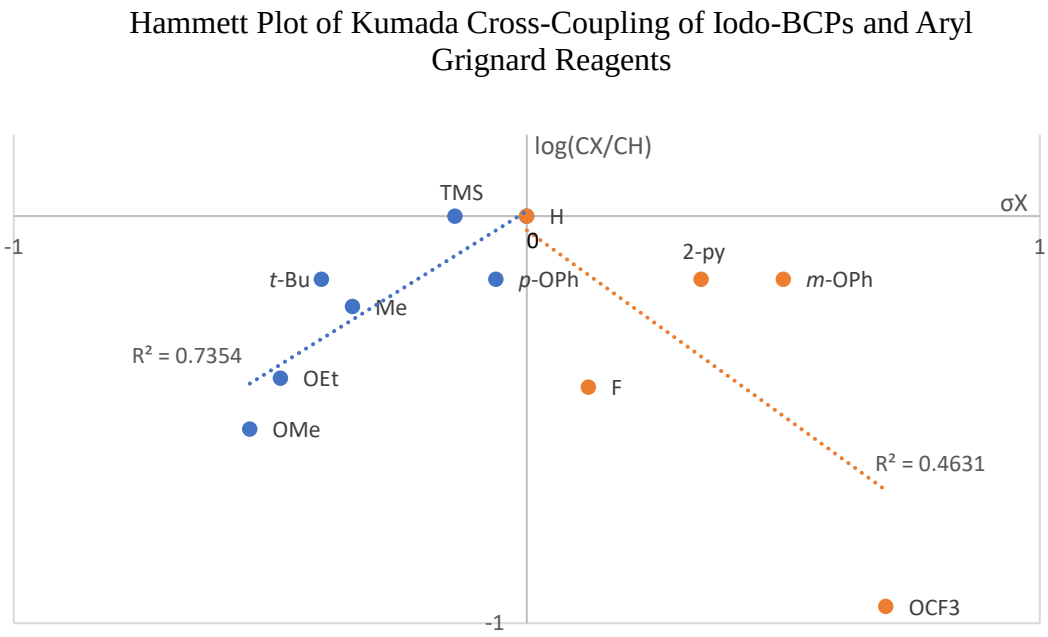

Figure 3.6 *– Hammett plot for the Kumada cross-coupling of* ***117*** *with X-PhMgBr.*

between the Hammett constant and rate of reaction, giving a positive sensitivity (reaction) constant of ρ = 1.57. This correlation is relatively strong, giving an R^2 value of 0.73. The most electron donating group – OMe – gave the slowest rate and being formed in a ratio of 0.3:1 (OMe:H) compared to the reaction with unsubstituted PhMgBr. Notably, this does not correspond to the observed reaction efficiency with 4-OMe-PhMgBr which gave one of the highest yields of 86% (see **Figure 3.1**). For substituents with positive Hammett constants (electron-withdrawing groups) however, the sensitivity constant is negative (ρ = −1.82). These electron-deficient Grignard reagents only give a weak negative correlation however, with an R^2 value of 0.46. Norrby and co-workers also looked at the correlation between substituents and reaction rate in the cross-coupling of aryl Grignard reagents with bromocyclohexane and found a negative correlation for all substituents, however they found that halide substituents gave outlying results.[160] For the cross-coupling of BCP iodides, if 4-F-PhMgBr is also treated as an anomalous result then a far better correlation is seen with an R^2 of 0.83. The inverted V-shape of the graph suggests

that there is a change in mechanism or a change in the rate determining step between electron-donating groups and electron-withdrawing groups. This provides significant insight into the reaction, and suggests there is the potential for further investigation into the precise mechanism in the future.

3.7 Investigations towards tandem ATRA/cross-coupling reactions

Having developed an ATRA reaction of a wide variety of iodides with TCP to form BCP iodides as well as a general methodology for their subsequent cross-coupling, the possibility of combining these two processes into a one-pot reaction was considered.

Kang and co-workers previously showed that $FeCl_2$ could catalyse the tandem cyclisation/Kumada cross-coupling of iodide **187** with 4-MeOPhMgBr to form **188** in 71% yield (**Scheme 3.22**), as well as cyclised products **189** and **190** in 20% and 6% yield respectively.[161]

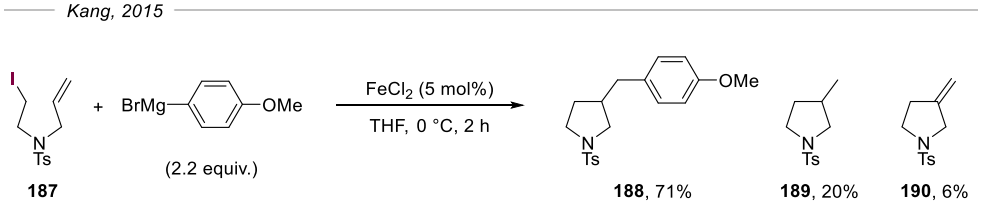

Scheme 3.22 *– Iron-catalysed tandem cyclisation/cross-coupling with aryl Grignard reagents by Kang and co-workers.*

To explore the mechanism of the iron-catalysed cross-coupling, Gutierrez used the tandem radical cyclisation/Kumada cross-coupling of α-chloro ester **191** and PhMgBr using $Fe(acac)_3$ and a chiral phosphine ligand (**Scheme 3.23**) as a radical clock mechanistic probe.[162] After 1 h at 0 °C, a mixture of the direct cross-coupled product

192 (12% yield and 85:15 er), and the racemic tandem cyclised/cross-coupled product **193** (40% yield) was formed.

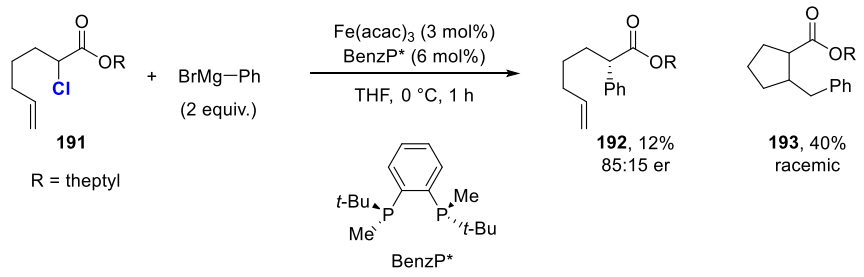

Scheme 3.23 *– Iron-catalysed tandem cyclisation/cross-coupling as a radical clock probe by Gutierrez and co-workers.*

Given the precedence for the formation of radicals using iron catalysis in the above examples, and the efficient capture of radicals by TCP when generated by triethylborane catalysis or photoredox catalysis (see **Chapter 2**), investigations were initiated as to whether iron could catalyse a tandem radical addition of iodides across TCP followed by a Kumada cross-coupling of the resulting BCP radical with aryl Grignard reagents. This would enable the two methodologies developed so far to be combined into a one-step procedure. Iodide **187** was used as an example substrate that has been shown to undergo both a photoredox-catalysed ATRA reaction with TCP to form **194**,[112] and tandem cyclisation/cross-coupling to form **188**.[161] Therefore, the reaction of **187** with TCP and 4-MeOPhMgBr was investigated (**Table 3.9**).

The initial conditions in entry 1 used 5 mol% of $Fe(acac)_3$ with 2.2 equivalents of 4-MeO-PhMgBr added at once to the reaction, and stirred for 1 h at 0 °C. The structures of **195** and **194** were verified through authentic samples of each compound. Pleasingly no starting material remained after this period, however none of the desired product **195** was observed. A very small amount of the BCP iodide ATRA product **194** was formed along with 50% of cyclised/cross-coupled product **188**. Slow addition of the Grignard using a

syringe pump at 0.7 mL/ h (entry 2) gave a large increase in formation of BCP iodide **194** to 30%, and a reduction of **188** to 24%, however, no **195** was observed. The addition of 10 mol% of TMEDA (entry 3) led to a large decrease in conversion with 50% of unreacted starting material **187** remaining and only 13% and 17% of **194** and **188** respectively.

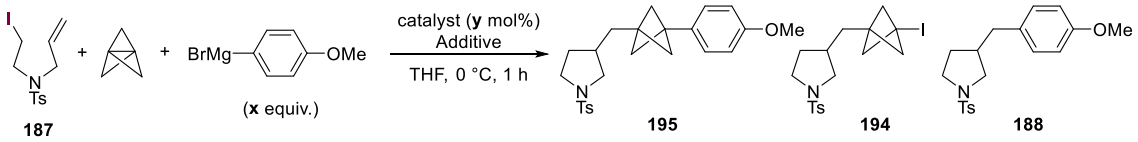

Entry	Catalyst	Additive	**y**/ mol%	**x** (equiv.)	Grignard Addition	Yield/[a] %			
						187	**195**	**194**	**188**
1	$Fe(acac)_3$	-	5	2.2	Rapid	0	0	3	50
2	$Fe(acac)_3$	-	5	2.2	Slow	0	0	30	24
3	$Fe(acac)_3$	TMEDA	5	2.2	Slow	50	0	13	17
4	$Fe(acac)_3$	TMEDA	20	2.2	Slow	0	0	31	85
5	$Fe(acac)_3$	-	20	2.2	Slow	13	0	42	45
6	$FeCl_2$	-	5	2.2	Slow	0	0	100	0
7	$FeCl_2$	TMEDA	5	2.2	Slow	0	0	68	9
8	$FeCl_2$/$Fe(acac)_3$	TMEDA	5/20	2.2	Slow	16	0	5	62
9[b]	$FeCl_2$/$Fe(acac)_3$	TMEDA	5/20	2.2	Slow	17	0	24	47
10[c]	$FeCl_2$	-	5	0.2 × 5	Rapid	12	0	62	22
11[cd]	$FeCl_2$	-	5	0.2 × 5	Rapid	46	0	10	23
12	$FeCl_2$	-	5	2.2	Slow	0	0	82[e]	0

Table 3.9 *– [a] Yield calculated by ^1H NMR spectroscopy using an internal standard of 1,3,5-trimethoxybenzene. [b] 0.2 equivalents of Grignard added at once, the reaction stirred for an hour, then $Fe(acac)_3$ and TMEDA were added and a further 2 equivalents of Grignard added via syringe pump. [c] 0.2 equivalents added at start of reaction then another 0.2 equivalents added every hour for a total of 5 hours. [d] Reaction run at room temperature. [e] Reaction started at 0 °C then allowed to warn to rt. Product appeared to be a mixture of **194** and another BCP containing compound that could not be identified, with total yield equalling 82%, measured by integration of the two BCP peaks.*

Increasing the catalyst loading to 20 mol% increased the combined yield of **194** and **188**, both with and without TMEDA (entries 4 and 5, respectively), the former of which significantly favoured the formation of cross-coupled product (85% yield). Interestingly, on switching the catalyst to $FeCl_2$, 100% conversion of **187** to the BCP iodide product **195** was observed (entry 6), however addition of TMEDA decreased the yield (entry 7).

3. Iron-catalysed Kumada cross-coupling

To promote both the ATRA and cross-coupling reactions, the reaction was performed with both iron salts present (entry 8). At the end of reaction, 16% of unreacted starting material remained, 5% of **194** had formed but the majority had been cross-coupled to form product **188** in 62% yield. To prevent premature cross-coupling of the ATRC product before the capture of TCP, several experiments were performed with portionwise addition of the Grignard reagents both at 0°C and room temperature (entries 9 – 12). In all cases however, no tandem ATRA/cross-coupled was observed.

It appeared that once the BCP iodide **194** was formed, the iodide could not be reactivated by the iron catalyst to undergo a further cross-coupling under the reaction conditions. However, the primary radical formed by cyclisation prior to the capture of TCP appears to be very reactive and can undergo efficient cross-coupling with the Grignard reagent before the BCP can form. The reaction of the bromide equivalent **196** to iodide **187** was therefore subject to the reaction conditions as bromides undergo far less efficient ATRA and therefore, if formed, the BCP-radical may be longer lived and so have more opportunity to subsequently undergo cross-coupling. Unfortunately, formation of the desired product **195** was not observed (**Scheme 3.24**).

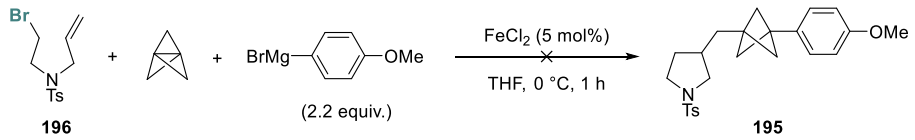

Scheme 3.24 *– Unsuccessful use of alkyl bromide **196** in the tandem cyclisation/cross-coupling reaction with 4-MeO-PhMgBr.*

The tandem reaction was also attempted with iodo-piperidine **197** which has been shown to undergo ATRA reaction with TCP efficiently under triethylborane initiation or photoredox catalysis, and the secondary radical formed on iodide abstraction would be more stable and therefore could reduce premature cross-coupling. The BCP iodide **117**

has also been shown to undergo cross-coupling with aryl Grignard reagents in high yield. Iodo-piperidine **197** was therefore subjected to the reaction with $FeCl_2$ (**Scheme 3.25**) and $Fe(acac)_3$, however only low amounts of the ATRA product was observed in both cases, and no cross-coupling products were formed.

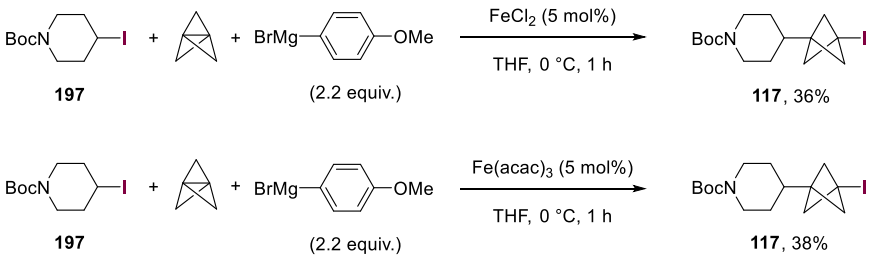

Scheme 3.25 *– Unsuccessful use of **197** in tandem ATRA/cross-coupling reaction with 4-MeOPhMgBr.*

Throughout these experiments none of desired product **195** was ever observed even in trace amounts. While iron salts could be used to perform ATRC/ATRA reactions to form the BCP iodide or ATRC/cross-coupling reaction to form the prematurely cross-coupled product, these two reactions did not occur sequentially under any of the conditions investigated.

3.8 Conclusions

An efficient Kumada cross-coupling of BCP iodides with a large range of aryl and heteroaryl Grignard reagents was developed, giving high yields of the cross-coupled products. The catalytic system used cheap and readily available $Fe(acac)_3$ in combination with TMEDA as an additive, and most reactions proceeded at room temperature within an hour. Aryl Grignard reagents substituted with *ortho*-, *meta*- or *para*-substituents were tolerated as well as other functionalities, including ester and sulfonyl groups. Grignard reagents bearing electron-donating, neutral and mildly withdrawing substituents could be

used as well as a range of heteroaryl Grignard reagents. This methodology performed better on a larger scale and its utility was demonstrated through the synthesis of the BCP analogues of flurbiprofen and brequinar. This is the first general methodology for the cross-coupling of BCPs as the electrophilic component, and the first example of the Kumada cross-coupling of a tertiary iodide. The work presented in this chapter was published in *Angewandte Chemie* in 2020.[163]

Although attempts to combine this methodology with an ATRA reaction of an iodide with TCP to functionalise both bridgeheads of TCP in one pot were unsuccessful, achieving such a tandem reaction could be a valuable focus area for future work, as well as further study of the ability of iron catalysts to promote addition reactions to TCP.

4

Borylation and oxidation of 1-iodo-3-substituted-bicyclo[1.1.1]pentanes

Alkylboronates are valuable compounds as precursors to a wide range of functional groups,[164] and in turn these boronates have been accessed in many ways, including photocatalytic methods, decarboxylative or deaminative borylations, and transition metal assisted borylations.[165] A particularly valuable method is through the catalytic cross-coupling of alkyl halides. In particular copper-catalysed reactions have demonstrated the ability to borylate a wide range of alkyl halides including alkyl iodides and tertiary halides, which is discussed in the following section.

4.1 Copper-catalysed borylation of alkyl halides

One of the first copper-catalysed borylations of unactivated alkyl halides was developed by Liu and co-workers in 2012.[166] Based on previous work developed by Marder *et al.* demonstrating the copper-catalysed borylation of aryl halides,[167] and Liu's cross-coupling of alkyl electrophiles and aryl boronic esters using similar conditions,[168] they used a CuI catalyst along with PPh_3, LiOMe and B_2pin_2 to form alkyl-Bpin species in good yields from primary and secondary alkyl halides (**Scheme 4.1a**).

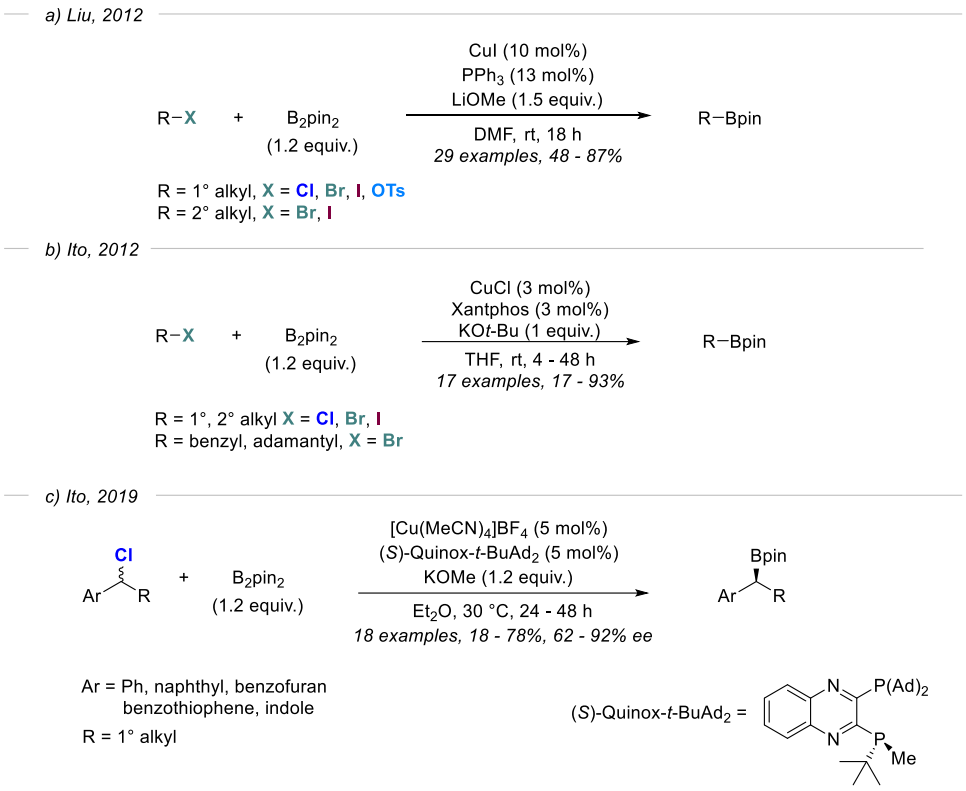

Scheme 4.1 *– Copper(I)-catalysed borylations of alkyl halides.*

Around the same time, Ito *et al.* reported a similar borylation reaction of alkyl halides.[169] They also used a copper(I) catalyst, phosphine ligand and a base to perform the transformation, but were able to use lower catalyst loadings, although extended reaction times were sometimes necessary (**Scheme 4.1b**). Notably, they demonstrated the borylation of a tertiary halide: adamantyl bromide was successfully borylated over 48 h, although only 17% of the product was obtained. Ito later built on this work, using a chiral bisphosphine ligand in order to perform the enantioconvergent borylation of various racemic benzyl chlorides in good yields and high *ee* (**Scheme 4.1c**).[170]

Copper(II) catalysts have also been shown to catalyse the borylation of alkyl halides. In 2015. Deng and co-workers reported the borylation of alkyl halides using $Cu(CF_3SO_3)_2$ and either B_2pin_2 or bis(neopentylglycolato)diboron **198** to form primary and secondary

borylated products in moderate to good yields (**Scheme 4.2a**).[171] They used an amino acid based ligand – dimethylglycine (proline, alanine, phenylalanine and cystine were also successful) – as a cheap and environmentally benign ligand for a 'greener' reaction. In 2016, Marder reported the use of $CuCl_2$ with an NHC ligand to catalyse the borylation of alkyl halides (**Scheme 4.2b**).[172] Notably, the reaction was performed in air and a number of tertiary chlorides and bromides were successfully borylated, although higher catalyst loadings, elevated temperatures and prolonged reaction times were necessary.

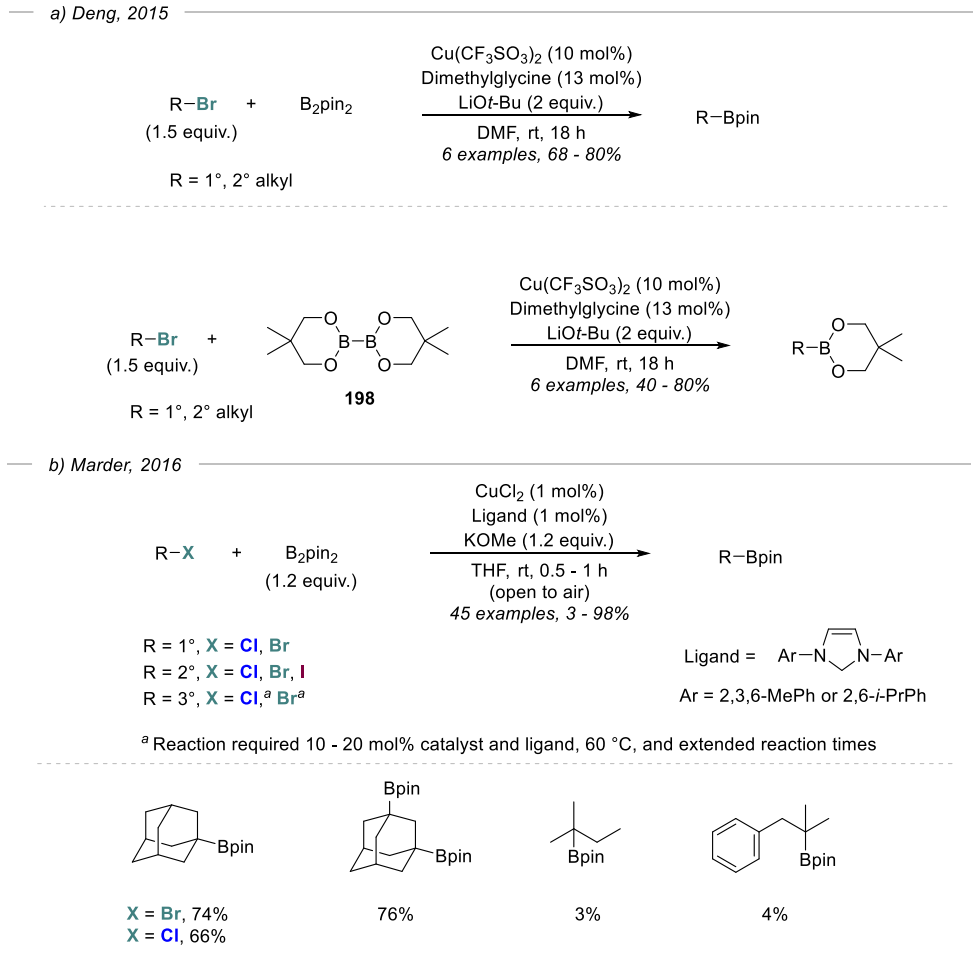

Scheme 4.2 *– Copper(II)-catalysed borylations of alkyl halides.*

4.2 Synthesis of 1-bicyclo[1.1.1]pentyl alcohols

The synthesis of 1-bicyclo[1.1.1]pentyl alcohols is desirable for their use as phenol bioisosteres in the drug discovery process, as phenols are commonly found in biologically active molecules (**Figure 4.1**).[173–175]

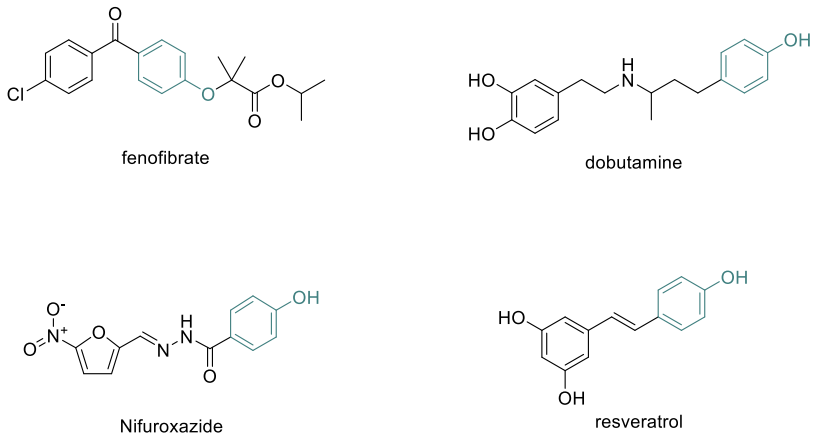

Figure 4.1 *– Phenol-containing drug compounds.*

The synthesis of a hydroxylated BCP as a drug analogue was first demonstrated by Adsool and co-workers in 2017 (**Scheme 4.3**), who synthesised BCP-resveratrol in 11 steps from the commercially available BCP **199**.[176] Five steps were required just to install the hydroxy group on the BCP unit. This began with hydrolysis of the ester group in **200** to give carboxylic acid **201**, followed by the formation of the Weinreb amide and addition of PhMgBr to form the ketone **202**. A Baeyer-Villiger oxidation then converted the ketone **202** to the ester in **203** using *m*-CPBA. After several other transformations, the protected alcohol in **204** could be deprotected using MeLi·LiBr to give BCP-resveratrol with the unprotected alcohol **205** in an overall 8% yield over 11 steps.

While this synthesis benefitted from using the commercially available BCP **199** as the starting material, converting this to the alcohol requires many functional group transformations and changes of oxidation levels. An alternative approach that requires far

fewer steps to install the hydroxyl group at the BCP bridgehead position is to oxidise BCP boronic esters. This is discussed in the next section.

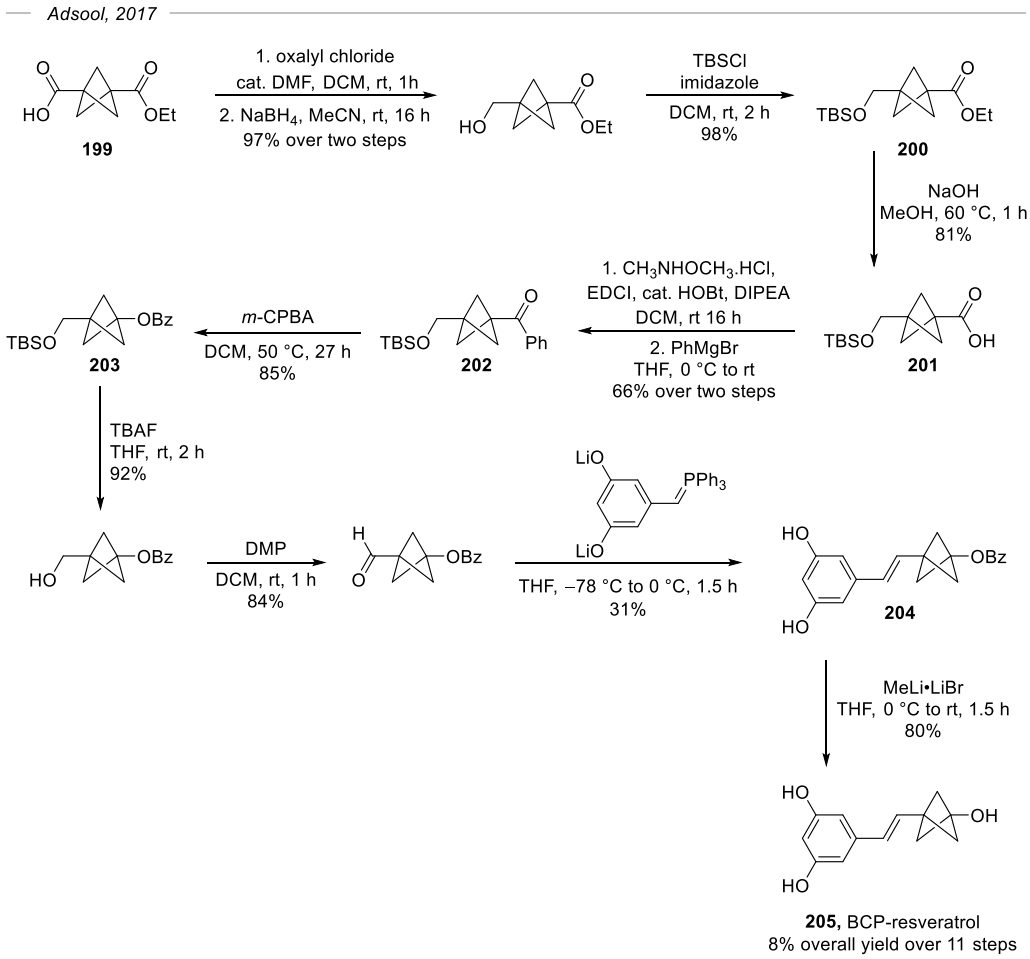

Scheme 4.3 *– Synthesis of BCP-resveratrol by Adsool and co-workers.*

4.2.1 Synthesis and oxidation of pinacolato borane-substituted bicyclo[1.1.1]pentanes

There have been several recent reports of the synthesis of bicyclo[1.1.1]pentanes substituted with pinacolatoboron (Bpin) groups from a variety of starting materials. The subsequent oxidation of these BCP-Bpin compounds to BCP-alcohols is demonstrated in most reports, although typically as an individual exemplary reaction rather than an

optimised procedure. In 2020, Aggarwal and co-workers reported the addition of Grignard reagents across the central bond of TCP followed by the addition of various boronic esters in a 3-component reaction to form BCP-boronate complexes.[177] The main focus of this work was using alkenyl boronic esters to form BCP-boronate complexes which could undergo 1,2-migration and boron elimination upon addition of iodine and sodium methoxide to give alkenyl-BCPs. However, they also demonstrated an example of adding a tolyl Grignard reagent to TCP, followed by addition of HBpin to form the BCP-Bpin intermediate. Following treatment with sodium hydroxide and hydrogen peroxide, they were able to access the BCP-alcohol **206** in 95% yield (**Scheme 4.4**).

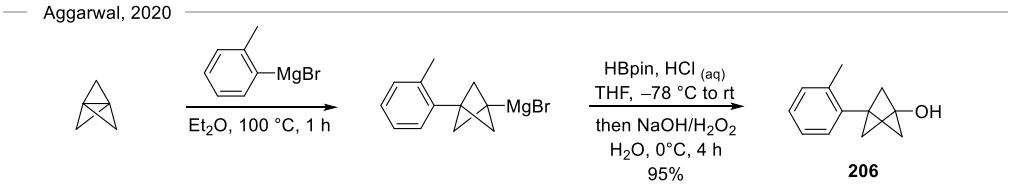

Scheme 4.4 *– Borylation and subsequent oxidation of BCP-Grignard reagents.*

The following year, several more procedures for the synthesis of BCP-Bpin compounds were reported. Building on their previous work on the synthesis of BCP benzylamines (see **Chapter 1.4.3**, **Scheme 1.9**),[178] Walsh described a three-component reaction between 2-azaallyl anions, TCP and a large excess of *i*-PrOBpin to form a range of benzylamine BCP-boronates (**Scheme 4.5**).[179]

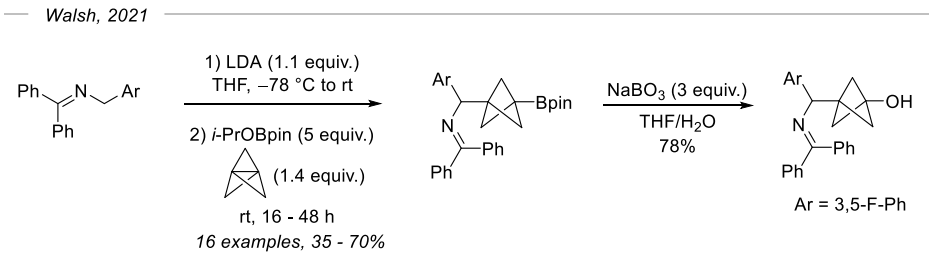

Scheme 4.5 *– Synthesis and oxidation of benzylamine BCP-boronates.*

4. Borylation and oxidation

They demonstrated a range of further functionalisations of the boronate products, including an oxidation using $NaBO_3$ to form the alcohol in 78% yield.

Based on previous work using redox active esters and copper catalysis to form a wide range of alkyl-Bpin compounds,[180] Baran and co-workers demonstrated the ability to use an electrochemical decarboxylative borylation to form a wide variety of alkyl-Bpin products, including a Bpin-substituted BCP in reasonable yield (**Scheme 4.6**).[181] While it offers a fast and scalable route to boronates, 4 equivalents of pinacol were required, and only one BCP example was demonstrated, so its applicability to a wider range of BCP compounds is uncertain.

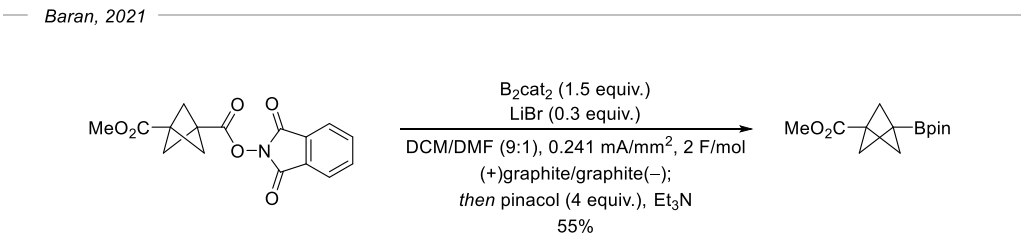

Scheme 4.6 *– Electrochemical decarboxylative borylation of BCP redox active esters.*

Qin and co-workers accessed a diverse range of BCP boronic esters *via* an innovative intramolecular coupling of highly substituted cyclobutanones (**Scheme 4.7**).[182] By initially forming a sulfonyl hydrazone intermediate **208** from the cyclobutanone **207**, they were able to perform a base-promoted intramolecular cyclisation to directly form the BCP-Bpin **209**, which could be substituted both at the bridgehead and the bridge positions, building complex BCPs quickly and in good yields. They demonstrated a number of further functionalisations of the Bpin group including an oxidation using NaOAc and 10 equivalents of H_2O_2 to obtain the alcohol in good yield.

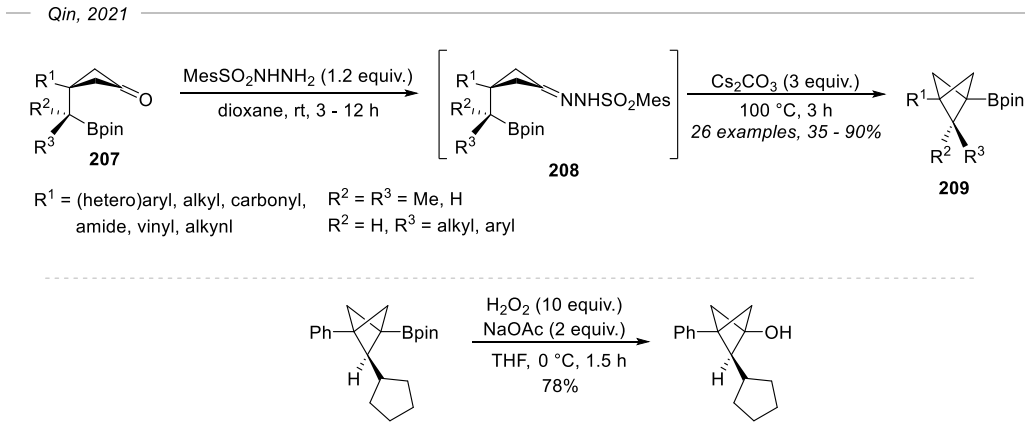

Scheme 4.7 *– Synthesis and oxidation of BCP-boronates via intramolecular coupling of sulfonyl hydrazones.*

4.2.2 Oxidation of iodo-bicyclo[1.1.1]pentanes

Very few methods exist for the synthesis of BCP-alcohols from BCP iodides. In 2017, Auberson and co-workers demonstrated a multi-step synthesis of the amino acid BCP-alcohol **210** from iodide **211** en route to making their desired BCP **214** (**Scheme 4.8**).[15] They employed $SnBu_3H$ as a radical initiator along with biacetyl to form the acetyl BCP **212**. From there, they employed a similar strategy to Adsool and co-workers[183] (see **Chapter 4.2, Scheme 4.3**) in performing a Baeyer-Villiger reaction with *m*-CPBA to form the ester **213**, followed by acid hydrolysis to form the BCP alcohol **210**.

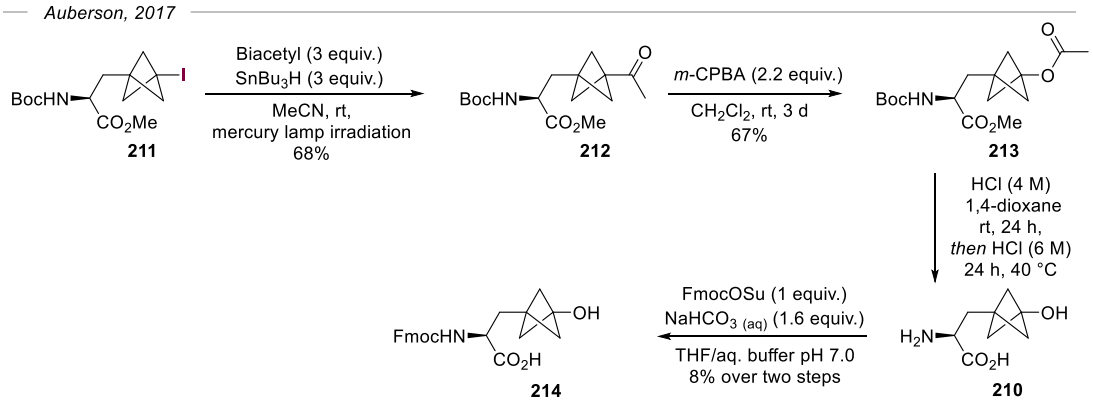

Scheme 4.8 *– Synthesis of a BCP-alcohol from a BCP iodide by Auberson and co-workers.*

The Anderson group previously demonstrated a one-step reaction from BCP iodide **114** to form the corresponding BCP-alcohol **215** in good yield (**Scheme 4.9**).[77] They used *t*-BuLi to perform a lithium/halogen exchange reaction with the iodide followed by quenching with a mixed boronic ester. The borylated intermediate could then be oxidised by sodium perborate to give **215** in 61% yield. While this method provides a fast route to the BCP-alcohol in good yield, the use of *t*-BuLi limits the applicability of this method and its scalability.

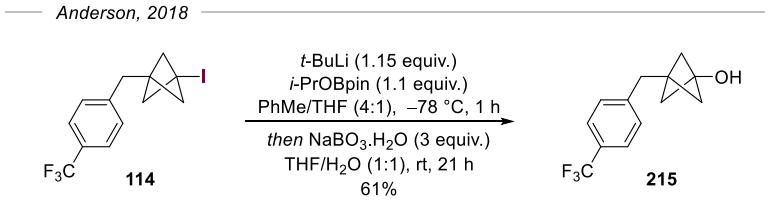

Scheme 4.9 *– Synthesis of a BCP-alcohol through lithiation and borylation of a BCP iodide.*

Given that there is good precedent demonstrating the ability of copper catalysts to borylate alkyl halides, a similar catalytic system could provide a significantly milder and more scalable method for the borylation of BCP iodides. In particular, copper-catalysed borylations have been successfully demonstrated with tertiary halides and therefore could be suitable for the BCP iodide system, which could subsequently be oxidised to afford desirable BCP-alcohols.

4.3 Optimisation of the copper-catalysed borylation and oxidation of iodo-bicyclo[1.1.1]pentanes

Investigations into the optimisation of a copper-catalysed borylation / oxidation of iodo-BCPs was initially started by collaborators at Merck, who provided us with details of their

preliminary studies. Their work is credited in scheme legends where appropriate. They began by investigating the copper-catalysed borylation of the protected amino acid iodo-BCP derivative **211** (**Scheme 4.10**), using conditions based on Marder's copper(II)-catalysed borylation (see **Scheme 4.2b**).[172] Although they tried a variety of copper(II) catalysts, phosphine and NHC ligands, and bases in all possible combinations, only unreacted starting material was observed in all instances.

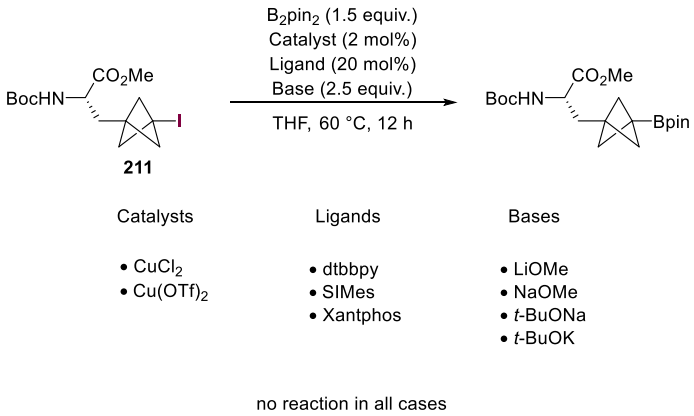

Scheme 4.10 *– Investigations by Merck towards a copper(II)-catalysed borylation of BCP iodides. All combinations of catalyst, ligand and base were screened. No reaction seen in all cases. All reactions performed by Merck.*

Having not seen any success with copper(II) catalysts, they then explored the borylation using CuI as a copper(I) catalyst and using conditions similar to those used by Liu (see **Scheme 4.1a**).[166] They used B_2pin_2 and LiOMe with CuI as a catalyst, and tested a range of phosphine ligands in the reaction in DMF at 45 °C for 12 h (**Table 4.1**). They found that a mixture of products was observed including the desired BCP-Bpin **216**, as well as the boronic acid **217** (although this was suspected to arise from **216** being hydrolysed during analysis of the reaction mixture performed through mass spectroscopy), and the reduced BCP **218**. The highest combined yield observed of **216** and **217** was obtained when either dppf or SPhos were used as ligands (entries 1 and 2, respectively), giving a combined yield of 48%. Almost as successful in the reaction were PPh_3, PCy_3 and

BINAP, which gave 42%, 41% and 39% combined yields respectively (entries 3, 4 and 5, respectively). PPh_3 had given a sufficiently high yield compared to the reaction with dppf and SPhos, but is also significantly cheaper and, therefore, was chosen to investigate a large-scale reaction.

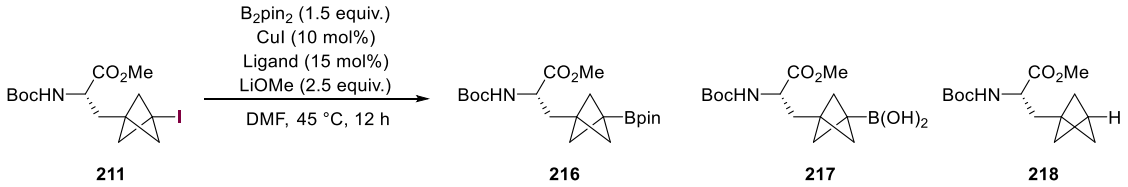

Entry	Ligand	Yield/ %				
		211	**216**	**217**	**216+217**	**218**
1	dppf	0	40	8	48	23
2	SPhos	0	37	11	48	22
3	**PPh_3**	**0**	**32**	**10**	**42**	**21**
4	PCy_3	0	28	13	41	36
5	BINAP	0	30	9	39	33
6	Xantphos	0	36	0	36	17
7	CataxiumA Pd G2	0	26	10	36	12
8	P(*t*-Bu)$_3$	0	17	5	23	16
9	XPhos	0	21	9	30	27
10	$(PdCl_2AmPhos)_2$	0	0	17	17	44

Table 4.1 *– Investigations by Merck towards a copper(I)-catalysed borylation of BCP iodides. All reactions performed by Merck.*

The Cbz-protected BCP iodide **219** was chosen for the large-scale reaction; submitting 40 g (93 mmol) of the starting material to the reaction conditions gave 40 g of the unpurified BCP-Bpin **220** after an aqueous work up (**Scheme 4.11**). This compound was then redissolved in THF and submitted to an oxidation using 1.2 equivalents each of urea hydrogen peroxide (UHP) and NaOAc, similar to the conditions used by Aggarwal and Qin,[177,182] to afford the BCP alcohol **221** in 54% yield (50 mmol) over two steps.

4. Borylation and oxidation

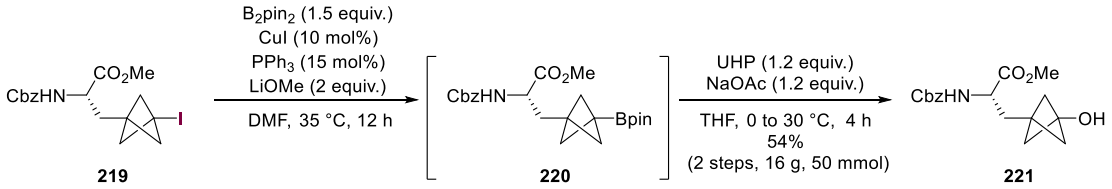

Scheme 4.11 *– Large scale copper-catalysed borylation / oxidation of a BCP iodide by Merck.*

To begin the investigations in this thesis, the reaction of the Cbz-protected BCP iodide **219** was repeated (although both reaction steps were left for 18 h to promote full conversion), and a 54% isolated yield of BCP alcohol **221** was obtained – matching the yield observed by Merck. From here, a number of alternative boronate dimers were first investigated in the reaction, but all produced very low yields of the alcohol **221** compared to B_2pin_2 (**Table 4.2**, entries 1 – 4). Using 2 equivalents of B_2pin_2 instead of 1.5 reduced the yield of **221** to 44% (entry 5), and using 20 mol% of CuI was also detrimental to the yield (entry 6). The four phosphine ligands that had produced the best yields in the experiments performed by Merck were then also investigated in the reaction with **219**. Using dppf produced a significantly lower yield of **221** than PPh_3 (23%, entry 7), whereas the use of BINAP, SPhos and PCy_3 all gave similar good yields of between 50–55% (entries 8 – 10). The use of PPh_3 as a ligand still proved to be optimal for this reaction in our hands.

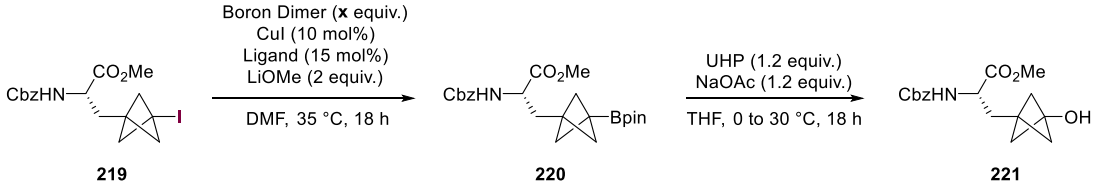

Entry	Boron Dimer	**x** (equiv.)	Ligand	Yield/[a] %
1	B_2pin_2	1.5	PPh_3	64(54)
2	$B_2(cat)_2$	1.5	PPh_3	8
3	$B_2(OH)_4$	1.5	PPh_3	5
4[b]	Bis(neopentyl glycolato)diboron	1.5	PPh_3	7
5	B_2pin_2	2	PPh_3	44
6[b]	B_2pin_2	1.5	PPh_3	34

7	B_2pin_2	1.5	Dppf	23
8	B_2pin_2	1.5	BINAP	50
9	B_2pin_2	1.5	SPhos	55
10	B_2pin_2	1.5	PCy_3	51

Table 4.2 *– Optimisation of boron dimer and ligands. [a] Yields calculated by NMR spectroscopy using 1,3,5-trimethoxybenzene as an internal standard. Yields in parentheses are isolated yields. [b] 20 mol% of CuI was used.*

The effect of the identity of the base on the reaction was next investigated. To avoid transesterification of the methyl ester of the amino acid BCP **219**, piperidine BCP iodide **117** was used instead. The use of LiOMe gave the BCP-alcohol product **222** in 64% yield (**Table 4.3**, entry 1). The use of *tert*-butoxide bases proved to be detrimental, with both the lithium and potassium salts giving 25% yield of **222** (entries 2 and 3). The use of silanolate bases gave increased yields (30–38%, entries 4 and 5) compared to the *tert*-butoxide bases, but these yields were still significantly lower than the reaction with LiOMe.

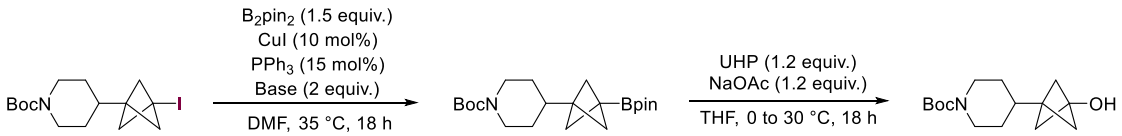

117 **222**

Entry	Base	Yield/[a] %
1	LiOMe	64
2	LiO*t*-Bu	25
3	KO*t*-Bu	25
4	$NaOSiMe_3$	38
5	$KOSiMe_3$	30

Table 4.3 *– Investigations into the effect of the identity of the base in the copper-catalysed borylation of BCP iodides. [a] Yields calculated by NMR spectroscopy using 1,3,5-trimethoxybenzene as an internal standard.*

The effects of the reaction temperature and duration on the borylation of **219** were also investigated. At both 35 °C and 45 °C, the borylation was stopped at a series of time

points over 44 hours, and then submitted to the oxidation (**Figure 4.2**, yields reported are for the BCP-alcohol). At 35 °C, the reaction proceeded rapidly over the first 4 h, before slowing and reaching the maximum yield of 65% at 20 h. Between 20 h and 44 h, the yield of **221** decreased to 44%, suggesting that there may be some competing decomposition of the boronate product over time, although no identifiable decomposition products could be isolated. At 45 °C, the reaction initially proceeded much more quickly, reaching a maximum yield of 56% after 6 h. From 6 h to 44 h, there was a decrease in yield to 46%, similar to that observed at 35 °C. Temperature clearly has a strong effect on the rate of the reaction; the maximum yield obtained significantly decreases at the higher temperature of 45 °C, accompanied by a much sharper switch to product degradation.

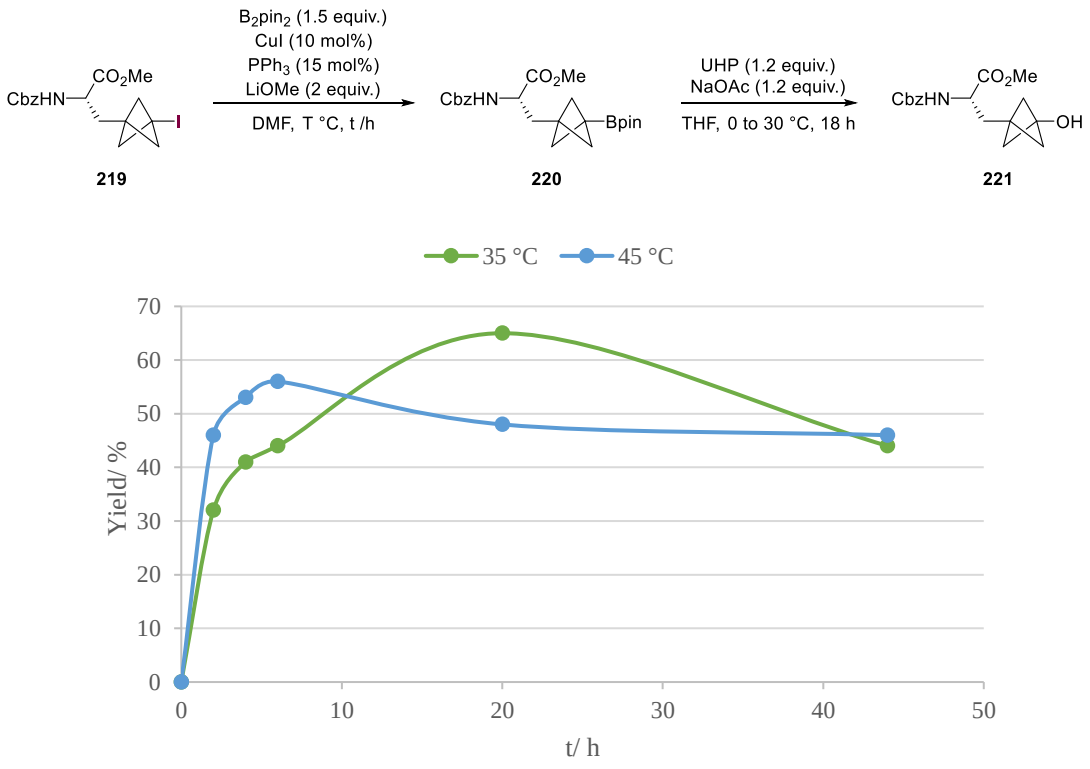

Figure 4.2 *– Investigations into the effects of temperature on the borylation of BCP iodide* ***219*** *over 44 hours.*

4. Borylation and oxidation

As the reaction at 35 °C had formed the maximum yield of **221** at 20 h, the reaction was investigated at a range of temperatures for 20 h (**Figure 4.3**). The highest yield was observed after 20 h for the reaction at 35 °C (64%) , with a decrease in yield at temperatures both above and below this optimal temperature (48 – 63%). The yield decreases more rapidly at higher temperatures (between 35 °C to 45 °C) than at lower temperatures (between rt to 35 °C), which may again reflect the more rapid decomposition of the oxidation product at higher temperatures.

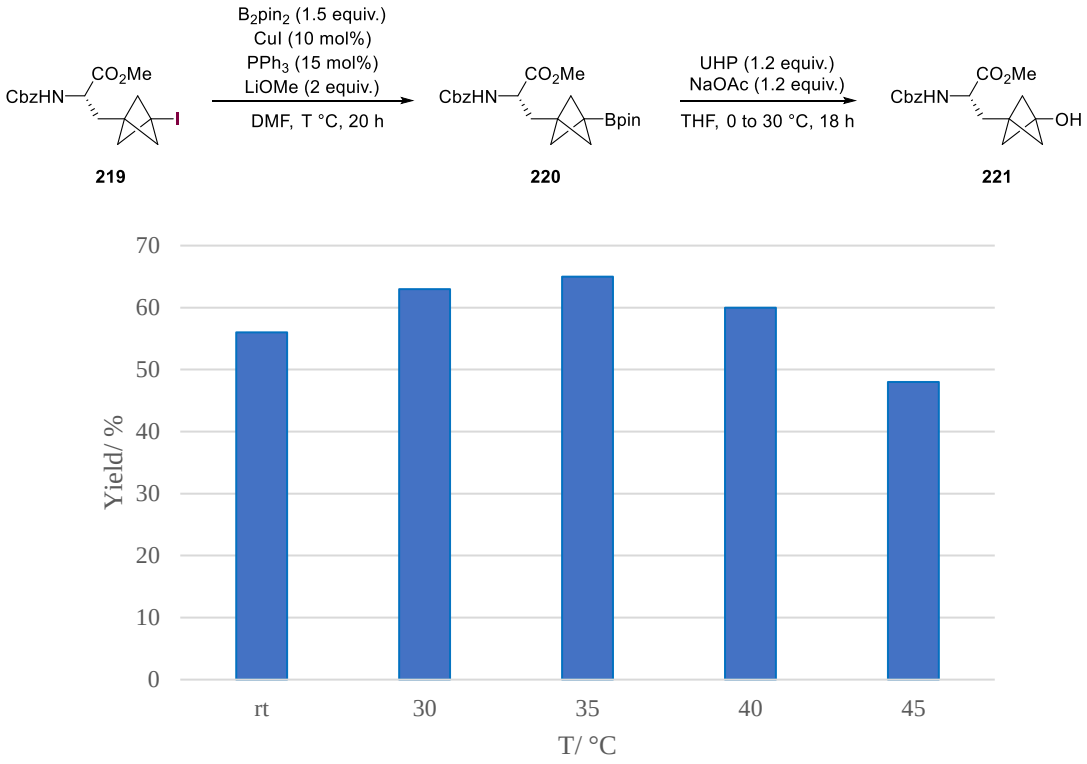

Figure 4.3 *– Effect of temperature on the copper-catalysed borylation of BCP iodides.*

Finally the length of time needed for the oxidation of the BCP-Bpin intermediate was investigated. After the borylation step, intermediate **220** was subjected to the oxidation conditions with 1.2 equivalents of both UHP and NaOAc for increasing lengths of time (**Table 4.4**). The oxidation occurs rapidly within the first two hours, giving 57% of the BCP alcohol. The yield of the reaction increased to 64% over the next two hours, but did

not increase any further between 4 and 20 hours. Therefore 4 hours seems to be sufficient for the oxidation reaction to take place.

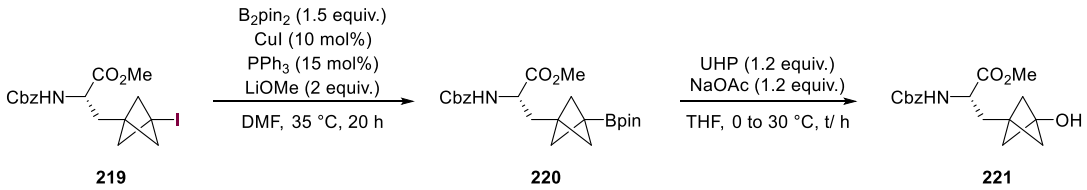

Entry	t/ h	Yield/[a] %
1	2	57
2	4	64
3	20	65

Table 4.4 *– Progression of the oxidation of the BCP boronate ester with time.* [a] *Yields calculated by NMR spectroscopy using 1,3,5-trimethoxybenzene as an internal standard.*

4.4 Scope of the borylation/oxidation of bicyclo[1.1.1]pentyl iodides

With the optimised reaction conditions in hand, investigations began to explore the scope of BCP iodides tolerated in the reaction (**Figure 4.4**). The scope of the reaction was investigated in collaboration with an MRes student, Nils Frank. As discussed in section **4.3**, iodides **219** and **117** could be subjected to the reaction to obtain **221** and **222** in 54% and 64% yield, respectively. Esters **223** and **224** could also be formed in 56% and 45% yield respectively, as well as sulfone **225** which was made in 50% yield. Benzyl BCP-alcohol **226** could be isolated in 41% yield and heteroaryl BCP iodides also successfully underwent borylation and subsequent oxidation to give the pyridyl (**227**) and quinoline (**228**) BCP-alcohol products in 48% and 25% yield respectively.

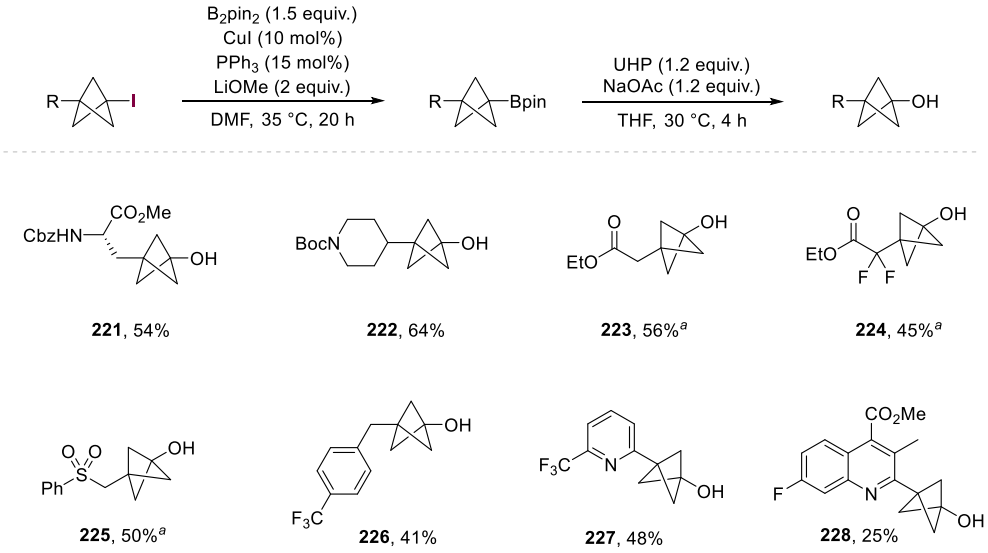

Figure 4.4 *– Investigations into the scope of the copper-catalysed borylation and subsequent oxidation of BCP iodides. [a] Reaction performed by Nils Frank.*

Interestingly, when substrates bearing a BCP unit at the α-carbonyl position of an aryl- or heteroaryl-substituted ketone were used, such as **229** or **230** (**Scheme 4.12**), a rearrangement occurs during the borylation step. Instead of undergoing direct borylation, the BCP group fragments and the tertiary Bpin-substituted exo-methylene cyclobutane **231** was isolated in 39% yield instead (see Section **4.5** for mechanistic discussion).

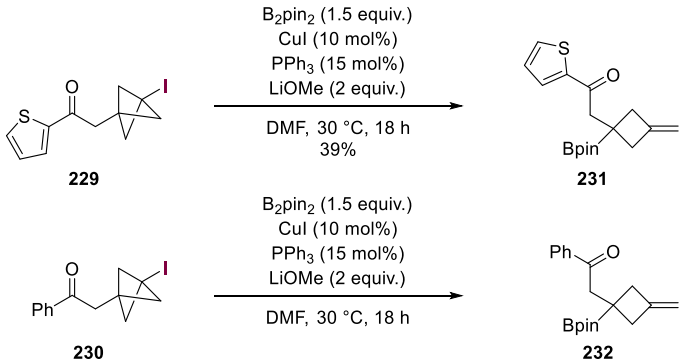

Scheme 4.12 *– Observed fragmentation and subsequent borylation of BCP iodides bearing (hetero)aromatic-substituted ketones under copper(I)-catalysed conditions.*

With the phenyl-substituted ketone substrate **230**, ^{1}H NMR analysis of a sample of the reaction mixture after aqueous work-up showed the characteristic signals associated with

the terminal alkene and cyclobutane protons of the corresponding methylene cyclobutane fragmentation product **232**. However, this product could not be isolated.

While the scope of the reaction was being explored, it was noted that during some of the oxidation steps, large amounts of an impurity that could not be separated from the desired product was observed. This was identified as the oxidised THF compound tetrahydrofuran-2-ol, where the solvent was being oxidised preferentially to the BCP-Bpin intermediate. Two sources of THF solvent had been used for performing these oxidations, one of which contained THF stabilised with butylated hydroxytoluene (BHT) and the other contained non-stabilised THF. When non-stabilised THF was used, oxidation of the solvent was observed. However, if stabilised THF was used, solvent oxidation was almost entirely supressed, suggesting that a radical oxidation of THF was taking place in the absence of BHT. Copper has previously been shown by Kwong and co-workers to catalyse oxidative C–H aminations of THF,[184] and it is therefore possible that THF oxidation could be catalysed by traces of copper remaining from the initial borylation step.

More BCP iodides will be screened using these reaction conditions to further explore the scope of the borylation/oxidation. An exploration of alternative oxidation conditions that do not require THF, in order to eliminate the competitive oxidation of the solvent, is also planned.

4.5 Mechanistic studies of the borylation reaction

The mechanism of the copper-catalysed borylation of alkyl halides is yet to be fully elucidated; however, multiple radical clock experiments have been performed using various reaction conditions that suggest a radical-mediated pathway.[166,169,172]

4. Borylation and oxidation

Further mechanistic investigations were performed by Ito and co-workers while they were exploring an enantioconvergent borylation, and this is now the generally accepted mechanism.[170] They performed the borylation reaction between benzyl chloride **233** and B_2pin_2 in the presence of different amounts of the base KOMe (**Scheme 4.13a**). Using one equivalent of KOMe relative to the copper(I) salt, ligand, and B_2pin_2 afforded poorer reactivity and enantioselectivity (39%, 50% *ee*) than in the optimised reaction conditions using 1.2 equivalents of base (70%, 86% *ee*). When two equivalents of KOMe were used, however, the reactivity and enantioselectivity were much improved (71%, 84% *ee*). This suggests that use of an excess of base is important for the generation of the catalytic species. From these studies, combined with computational studies investigating the origin of the enantioselectivity in the transition state, they proposed the mechanism shown in **Scheme 4.13b**.

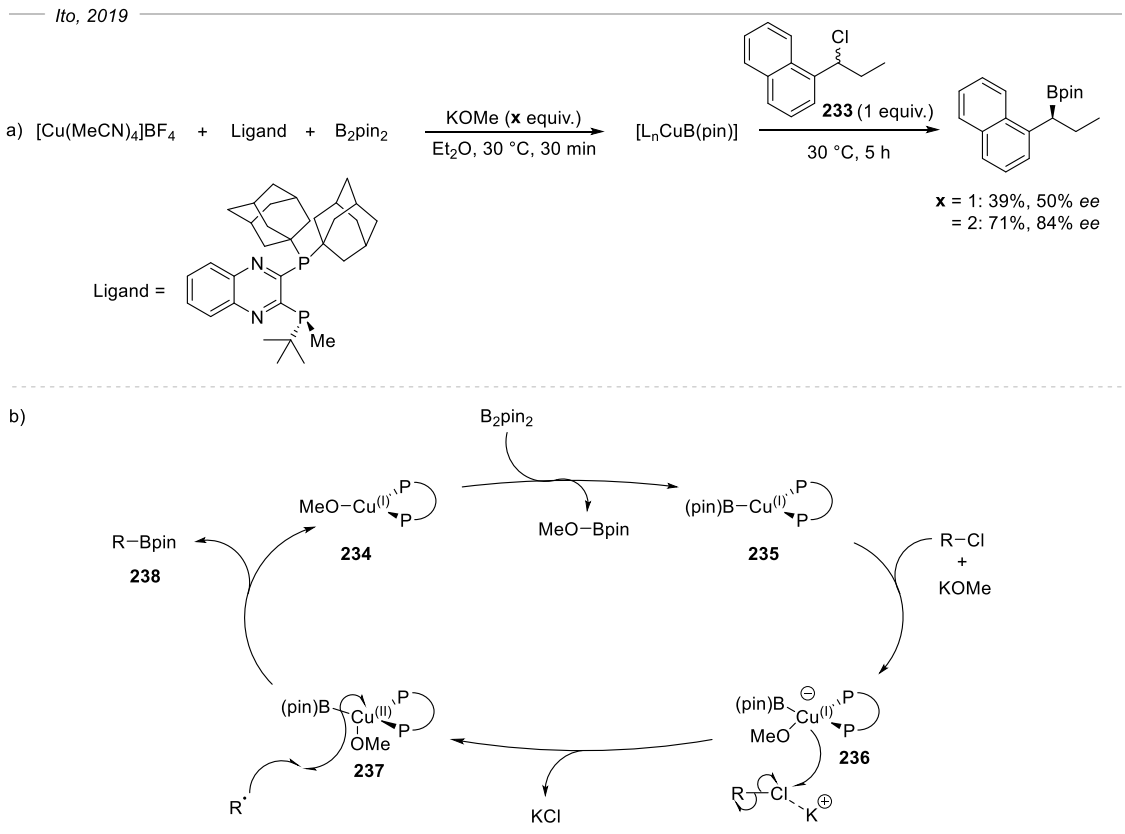

Scheme 4.13 *– Experiments to probe reaction stoichiometry and the proposed mechanism of the enantioconvergent copper-catalysed borylation of benzylic chlorides by Ito and co-workers.*

Firstly, the Cu–OMe species **234** is formed from the initial copper catalyst, the ligand and KOMe base. The subsequent reaction of **234** with B_2pin_2 forms the copper complex **235** which is thought to be inactive, based on the stoichiometry of base required for the reaction. Another molecule of KOMe can then coordinate to **235** to form cuprate **236**, which can then reduce the C–Cl bond in the alkyl halide *via* single electron transfer, forming **237** and the alkyl radical. This alkyl radical can then be borylated by **237** to afford the alkyl-Bpin product **238** and reform the copper species **234**.

It is possible that the borylation of BCP iodides follows a similar mechanism. However, as noted in the previous section, BCP iodides bearing (hetero)aromatic-substituted ketones undergo fragmentation to the Bpin-substituted methylene cyclobutane product (see **Scheme 4.12**). The mechanism of this fragmentation is unclear; however, it is has been demonstrated that such fragmentations occur when the BCP unit bears a partial positive charge at the bridgehead position (see **Chapter 1.4.2**), and this was also observed as a by-product in the photoredox-catalysed ATRA reaction between aryl iodides and TCP (see **Chapter 2.5**, **Scheme 2.8**). Therefore, an analogous process could be occurring in the copper-catalysed borylation of BCP iodides. However, it is not clear why only these specific substrates underwent the fragmentation. Once the positive charge has formed, the BCP unit can fragment to give the tertiary cation **239** (**Scheme 4.14**). The cation can recombine with an iodide anion to give iodide **240**, which can itself undergo copper-catalysed borylation to give the observed product **231**. This is a possible mechanism for the α-carbonyl BCP iodides that formed the methylene cyclobutane products. However, further investigations into the reaction mechanism for the borylation reactions that produced the boron-substituted BCPs would be valuable, as well as the elucidation of the role of the non-halide BCP bridgehead substituent in the reaction.

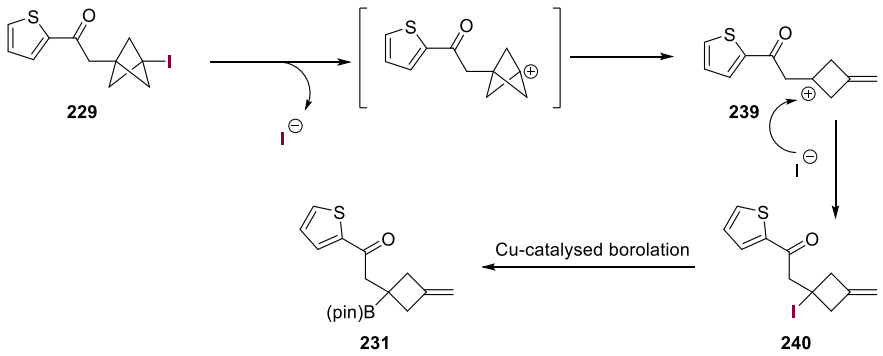

Scheme 4.14 *– Proposed general mechanism for the fragmentation of α-carbonyl BCP iodides bearing (hetero)aryl ketone substituents.*

4.6 Conclusions

The copper-catalysed borylation / oxidation of BCP iodides to form BCP-alcohols has been investigated to develop a milder method for the conversion of BCP iodides to alcohols that circumvents the need for pyrophoric reagents and reaction conditions that are not amenable to large-scale applications. Reaction optimisation identified conditions suitable for the borylation and oxidation of a selection of BCP iodides in moderate yields over two steps. However, due to time constraints, further reaction optimisation and exploration could not be carried out.

While exploring the scope of the reaction, competing oxidation of the non-stabilised THF solvent was observed and the use of stabilised THF reduces this undesired reactivity. The oxidation step can be investigated further to find alternative conditions with different solvents that are not susceptible to undesired side reactions and subsequently, the scope of the reaction can be extended to a wider range of BCP iodides.

Further research into the mechanism of the borylation and oxidation reactions would also be useful and would aid optimisation of the reaction conditions. This can help elucidate the role of the non-halide BCP substituents in the reaction, as it was observed that

rearrangement products are consistently formed with α-aryl-carbonyl-substituted BCP iodides.

After optimising the borylation / oxidation conditions, the reaction could be applied to the synthesis of a bioisosteric BCP-analogue of a phenol-containing drug target such as dobutamine **241**. A proposed retrosynthesis of **242** is shown in **Scheme 4.15**. BCP-dobutamine **242** could be obtained from the reductive amination from commercially available dopamine **243** and the methyl ketone-containing BCP alcohol **244**. This alcohol can be accessed *via* the copper-catalysed borylation and subsequent oxidation of BCP iodide **245** using the methodology described in this chapter. This BCP iodide could be formed from the photoredox-catalysed ATRA reaction between iodide **246** and TCP using the methodology described in **Chapter 2**. Lastly, this iodide could be obtained from the Appel reaction of commercially available alcohol **247**.

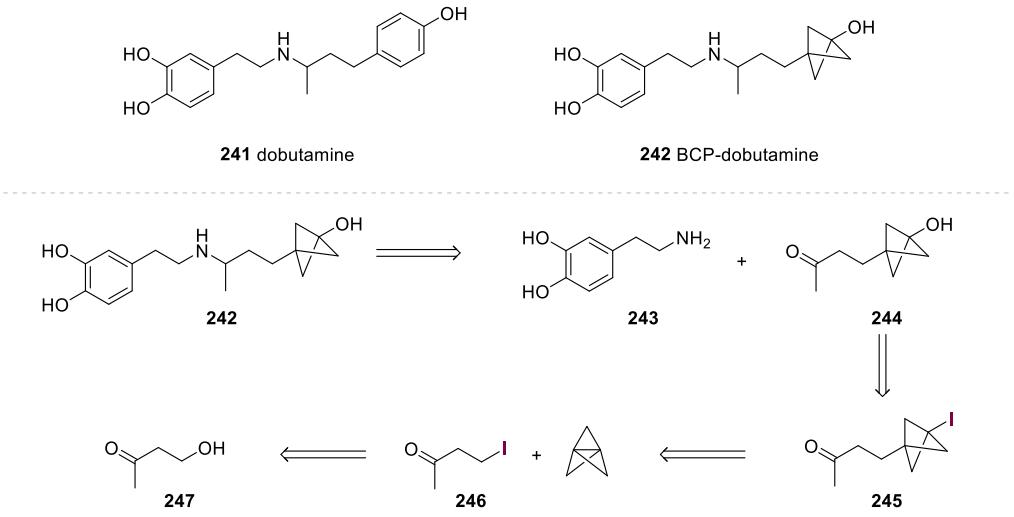

Scheme 4.15 *– Proposed retrosynthetic route for the synthesis of a BCP-dobutamine analogue using the copper-catalysed borylation and subsequent oxidation of BCP iodides.*

5

Conclusions and future work

Bicyclo[1.1.1]pentanes have been the object of increasing interest within the pharmaceutical and agrochemical industries as a result of their demonstrable ability to improve the pharmacokinetic properties of biologically active compounds when used as a bioisostere for 1,4-substituted arenes. Many methodologies for the synthesis of BCPs have been developed, largely focused on the reactions of TCP, the most common precursor to bicyclopentanes. Due to the unusual electronic structure of TCP that involves delocalisation of the inter-bridgehead electron density onto the bridging carbons, TCP possesses omniphilic reactivity, reacting with electrophiles, nucleophiles and radicals. Despite this diverse reactivity, the synthesis of aryl substituted BCPs has remained underdeveloped, with pre-existing methodologies generally relying on harsh organometallics and high temperatures, or low yielding irradiation, making them unsuitable for many industrial applications, which is a particular challenge given that the current applications of BCPs are largely in the commercial sector. Also underdeveloped are methods for the synthesis of BCP alcohols, which to date have relied on either many steps and functional group transformations, or borylations using a limited range of BCPs followed by isolated examples of subsequent oxidations.

This thesis details the investigations towards the development of new catalytic methods for the synthesis of aryl-substituted BCPs and BCP alcohols that use milder conditions more suitable for industrial applications (**Scheme 5.1**).

Building upon previous work by the Anderson group on the triethyl borane-initiated atom transfer radical addition (ATRA) reaction between alkyl halides and TCP, a mild photoredox catalysed ATRA reaction between aryl and heteroaryl iodides was developed (**Chapter 2**). Aryl and heteroaryl-substituted BCP iodides were synthesised in good yields and showed good functional group tolerance and selectivity in the presence of other halides. This reaction enabled the formal synthesis of the BCP analogue of the drug darapladib in half the number of steps and over twice the overall yield, and demonstrated the first activation of sigma bonds using photoredox catalysis.

Given easy access to BCP iodides through ATRA methodologies, an iron-catalysed Kumada cross-coupling of BCP iodides with aryl and heteroaryl Grignard reagents was developed (**Chapter 3**). Electron rich, neutral and mildly electron poor aryl Grignard reagents were successfully cross-coupled in high yields at room temperature or gentle warming, in an hour. The reaction exhibited good functional group tolerance and could be applied to two highly efficient syntheses of BCP drug analogues in combination with the ATRA methodologies. This reaction demonstrated the first general cross-coupling of BCPs where the BCP was the electrophilic partner, as well as the first Kumada cross-coupling of a tertiary iodide.

An additional functionalisation of BCP iodides in the form of a copper catalysed borylation and subsequent oxidation was also investigated (**Chapter 4**). Optimisation provided mild conditions that did not require pyrophoric *t*-BuLi and allowed the synthesis of a number of both alkyl and heteroaryl BCP alcohols in moderate yields over two steps.

While some interesting competing side-reactions have emerged under these conditions, the study has shown excellent potential for a mild oxidation of BCP iodides, and further exploration of this reaction can increase the reliability and scope of the reaction.

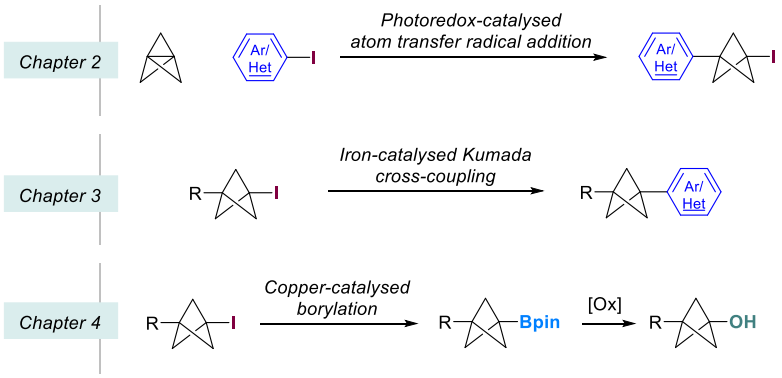

Scheme 5.1 *– Project overview.*

Further work has been planned to investigate the copper-catalysed borylation in order to gain insight into the mechanism and investigate the observed fragmentation of specific substrates. Additionally, an improved oxidation protocol will be explored in order to eliminate any competing solvent oxidation. Furthermore, the Bpin handle could be functionalised in a variety of other ways such as aminations or cross-couplings, thus providing a route to transform BCP iodides into a wider range of both carbon and heteroatom 1,3-substituted BCPs.

The cross-coupling of electron deficient aryl Grignard reagents with BCP iodides would also be a valuable avenue to explore. Mechanistic investigations have suggested a change in mechanism when electron deficient Grignards were used, and so the development of an alternative catalytic system better suited to this alternative pathway could greatly expand the scope of this reaction.

The developed methodologies discussed in this thesis have already begun to be applied to reactions with other propellanes. In investigations currently being carried out within

our group, [3.1.1]propellane has been identified as an excellent precursor to bicyclo[3.1.1]heptanes (BCHs) which have exciting potential as bioisosteres for *meta*-substituted arenes. They are able to undergo photoredox catalysed ATRA reactions with aryl and alkyl iodides, and the BCH iodides formed can undergo iron-catalysed cross-coupling with (hetero)aryl Grignard agents in even higher yields than their BCP iodide counterparts (**Scheme 5.2**). A range of BCH drug analogues are also presently being targeted.

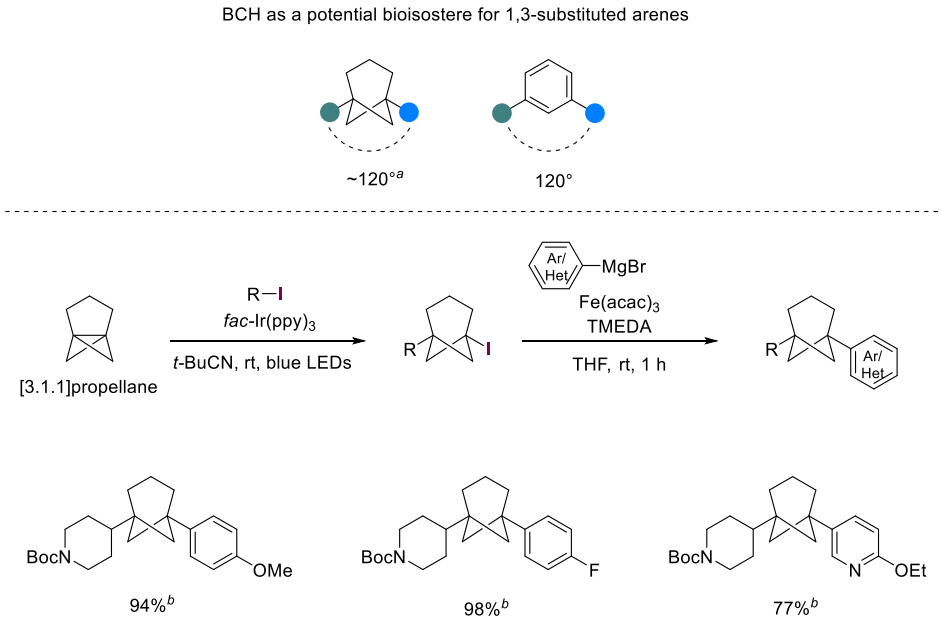

Scheme 5.2 *– Application of photoredox-catalysed ATRA reactions and iron-catalysed cross-coupling to BCH iodides.* [a] *Computationally derived angles calculated by Nils Frank.* [b] *The N-*Boc-piperidine *BCH iodide starting material for the cross-coupling reactions was synthesised by Nils Frank.*

Overall, with an expanded toolkit of reactions to form complex di-substituted BCPs, it would be valuable to synthesise more BCP drug analogues that were previously inaccessible. The synthesis and biological evaluation of a wider range of BCP drug analogues would provide important information regarding the effects of a BCP bioisostere on the pharmacokinetic properties of a drug, and thus offer a more cohesive

blueprint of when bioisosteric replacements can be of benefit in the drug discovery process.

6

References

[1] I. Langmuir, *J. Am. Chem. Soc.* **1919**, *41*, 1543–1559.

[2] I. Langmuir, *J. Am. Chem. Soc.* **1919**, *41*, 868–934.

[3] H. G. Grimm, *Z. Electrochem* **1925**, *31*, 474–480.

[4] H. Erlenmeyer, M. Leo, *Helv. Chim. Acta* **1932**, *15*, 1171–1186.

[5] H. Erlenmeyer, M. Leo, *Helv. Chim. Acta* **1933**, *16*, 1381–1389.

[6] H. Erlenmeyer, E. Berger, M. Leo, *Helv. Chim. Acta* **1933**, *16*, 733–738.

[7] H. L. Friedman, *Influence of Isosteric Replacements upon Biological Activity*, **1951**.

[8] C. W. Thornber, *Chem. Soc. Rev.* **1979**, *8*, 563–580.

[9] A. Burger, *Prog. Drug Res.* **1991**, *37*, 287–371.

[10] G. A. Patani, E. J. LaVoie, *Chem. Rev.* **1996**, *96*, 3147–3176.

[11] N. A. Meanwell, *J. Med. Chem.* **2011**, *54*, 2529–2591.

[12] N. A. Meanwell, *J. Med. Chem.* **2018**, *61*, 5822–5880.

[13] P. Lassalas, K. Oukoloff, V. Makani, M. James, V. Tran, Y. Yao, L. Huang, K. Vijayendran, L. Monti, J. Q. Trojanowski, et al., *ACS Med. Chem. Lett.* **2017**, *8*, 864–868.

[14] P. Mukherjee, M. Pettersson, J. K. Dutra, L. Xie, C. W. am Ende, *ChemMedChem* **2017**, *12*, 1574–1577.

[15] Y. P. Auberson, C. Brocklehurst, M. Furegati, T. C. Fessard, G. Koch, A. Decker, L. La Vecchia, E. Briard, *ChemMedChem* **2017**, *12*, 590–598.

[16] A. A. Kirichok, I. Shton, M. Kliachyna, I. Pishel, P. K. Mykhailiuk, *Angew. Chemie - Int. Ed.* **2017**, *56*, 8865–8869.

[17] B. A. Chalmers, H. Xing, S. Houston, C. Clark, S. Ghassabian, A. Kuo, B. Cao, A. Reitsma, C.-E. P. Murray, J. E. Stok, et al., *Angew. Chemie* **2016**, *128*, 3644–3649.

[18] J. A. Bull, R. A. Croft, O. A. Davis, R. Doran, K. F. Morgan, *Chem. Rev.* **2016**, *116*, 12150–12233.

[19] T. J. Ritchie, S. J. F. Macdonald, *Drug Discov. Today* **2009**, *14*, 1011–1020.

[20] F. Lovering, J. Bikker, C. Humblet, *J. Med. Chem.* **2009**, *52*, 6752–6756.

[21] R. Pellicciari, M. Raimondo, M. Marinozzi, B. Natalini, G. Costantino, C. Thomsen, *J. Med. Chem.* **1996**, *39*, 2874–2876.

[22] A. F. Stepan, C. Subramanyam, I. V. Efremov, J. K. Dutra, T. J. O'Sullivan, K. J. Dirico, W. S. McDonald, A. Won, P. H. Dorff, C. E. Nolan, et al., *J. Med. Chem.* **2012**, *55*, 3414–3424.

[23] N. D. Measom, K. D. Down, D. J. Hirst, C. Jamieson, E. S. Manas, V. K. Patel, D. O. Somers, *ACS Med. Chem. Lett.* **2017**, *8*, 43–48.

[24] K. C. Nicolaou, D. Vourloumis, S. Totokotsopoulos, A. Papakyriakou, H. Karsunky, H. Fernando, J. Gavrilyuk, D. Webb, A. F. Stepan, *ChemMedChem* **2016**, *11*, 31–37.

[25] K. B. Weiberg, D. S. Connor, G. M. Lampman, *Tetrahedron Lett.* **1964**, 531–534.

[26] K. B. Wiberg, D. S. Connor, *J. Org. Chem.* **1966**, *280*, 4437–4441.

[27] K. B. Wiberg, G. M. Lampman, R. P. Ciula, D. S. Connor, P. Schertler, J. Lavanish, *Tetrahedron* **1965**, *21*, 2749–2769.

[28] R. Srinivasan, K. H. Carlough, *J. Am. Chem. Soc.* **1967**, *89*, 4932–4936.

[29] J. Meinwald, W. Szkrybalo, D. R. Dimmel, *Tetrahedron Lett.* **1967**, *8*, 731–733.

[30] M. R. Rifi, *Tetrahedron Lett.* **1969**, *13*, 1043–1046.

[31] X. Ma, L. Nhat Pham, *Asian J. Org. Chem.* **2020**, *9*, 8–22.

[32] J. M. Anderson, N. D. Measom, J. A. Murphy, D. L. Poole, *Angew. Chemie - Int. Ed.* **2021**, *60*, 24754–24769.

[33] J. Altman, E. Babad, J. Itzchaki, D. Ginsburg, *Tetrahedron* **1966**, *22*, 279–304.

[34] A. J. Pihko, A. M. P. Koskinen, *Tetrahedron* **2005**, *61*, 8769–8807.

[35] L. H. Zalkow, R. N. Harris III, D. Van Derveer, *J. Chem. Soc., Chem Commun.* **1978**, 420–421.

[36] F. Schneider, K. Samarin, S. Zanella, T. Gaich, *Science (80-.).* **2020**, *367*, 676–681.

[37] A. M. Dilmaç, T. Wezeman, R. M. Bär, S. Bräse, *Nat. Prod. Rep.* **2020**, *37*, 224–245.

[38] P. Seiler, *Helv. Chim. Acta* **1990**, *73*, 1574–1585.

[39] L. Hedberg, K. Hedberg, *J. Am. Chem. Soc.* **1985**, *107*, 7257–7260.

[40] M. D. Harmony, *J. Chem. Phys.* **1990**, *93*, 7522–7523.

[41] K. B. Wiberg, F. H. Walker, *J. Am. Chem. Soc.* **1982**, *104*, 5239–5240.

[42] E. Honegger, H. Huber, E. Heilbronner, *J. Am. Chem. Soc.* **1985**, *107*, 7172–7174.

[43] M. Messerschmidt, S. Scheins, L. Grubert, M. Pätzel, G. Szeimies, C. Paulmann, P. Luger, *Angew. Chemie - Int. Ed.* **2005**, *44*, 3925–3928.

[44] W. Wu, J. Gu, J. Song, S. Shaik, P. C. Hiberty, *Angew. Chemie - Int. Ed.* **2009**, *48*, 1407–1410.

[45] A. J. Sterling, A. B. Dürr, R. C. Smith, E. A. Anderson, F. Duarte, *Chem. Sci.* **2020**, *11*, 4895–4903.

[46] H. D. Pickford, B. R. Shire, E. A. Anderson, in *Encycl. Reagents Org. Synth.*, **2019**.

[47] M. D. Levin, P. Kaszynski, J. Michl, *Chem. Rev.* **2000**, *100*, 169–234.

[48] K. Semmler, G. Szeimies, J. Belzner, *J. Am. Chem. Soc.* **1985**, *107*, 6410–6411.

[49] R. Gianatassio, J. M. Lopchuk, J. Wang, C. Pan, L. R. Malins, L. Prieto, T. A. Brandt, M. R. Collins, G. M. Gallego, N. W. Sach, et al., *Science (80-.).* **2016**, *351*, 241–246.

[50] M. Werner, D. S. Stephenson, G. Szeimies, *Liebigs Ann.* **1996**, 1705–1715.

[51] X. Ma, Y. Han, D. J. Bennett, *Org. Lett.* **2020**, *22*, 9133–9138.

[52] J. X. Zhao, Y. X. Chang, C. He, B. J. Burke, M. R. Collins, M. Del Bel, J. Elleraas, G. M. Gallego, T. P. Montgomery, J. J. Mousseau, et al., *Proc. Natl. Acad. Sci. U. S. A.* **2021**, *118*, 1–5.

[53] M. Kenndoff, A. Singer, G. Szeimies, *J. fur Prakt. Chemie - Chem. - Zeitung* **1997**, *339*, 217–232.

[54] K. B. Wiberg, S. T. Waddell, *Tetrahedron Lett.* **1988**, *29*, 289–292.

[55] E. W. Della, D. K. Taylor, J. Tsanaktsidis, *Tetrahedron Lett.* **1990**, *31*, 5219–5220.

[56] E. W. Della, D. K. Taylor, *J. Org. Chem.* **1994**, *59*, 2986–2996.

[57] S. J. Hamrock, J. Michl, *J. Org. Chem.* **1992**, *57*, 5027–5031.

[58] K. B. Wiberg, N. McMurdie, *J. Am. Chem. Soc.* **1994**, *116*, 11990–11998.

[59] M. Newton, K. B. Wiberg, W. P. Dailey, F. H. Walker, S. T. Waddell, L. S. Crocker, *J. Am. Chem. Soc.* **1985**, *107*, 7247–7257.

[60] D. Lasányi, G. L. Tolnai, *Org. Lett.* **2019**, *21*, 10057–10062.

[61] S. Yu, A. Noble, R. B. Bedford, V. K. Aggarwal, *J. Am. Chem. Soc.* **2019**, *141*, 20325–20334.

[62] G. Szeimies, in *Meijere, A., Blechert, S. Strain Its Implic. Org. Chem. NATO ASI Ser. Vol 273. Springer, Dordrecht.*, **1989**, pp. 361–381.

[63] J. D. Daniel Rehm, B. Ziemer, G. Szeimies, *European J. Org. Chem.* **1999**, *1999*, 2079–2085.

[64] M. Messner, S. I. Kozhushkov, A. De Meijere, *European J. Org. Chem.* **2000**, 1137–1155.

[65] I. S. Makarov, C. E. Brocklehurst, K. Karaghiosoff, G. Koch, P. Knochel, *Angew. Chemie - Int. Ed.* **2017**, *56*, 12774–12777.

[66] K. Schwärzer, H. Zipse, K. Karaghiosoff, P. Knochel, *Angew. Chemie - Int. Ed.* **2020**, *59*, 20235–20241.

[67] J. M. Lopchuk, K. Fjelbye, Y. Kawamata, L. R. Malins, C. M. Pan, R. Gianatassio, J. Wang, L. Prieto, J. Bradow, T. A. Brandt, et al., *J. Am. Chem. Soc.* **2017**, *139*, 3209–3226.

[68] J. M. E. Hughes, D. A. Scarlata, A. C. Y. Chen, J. D. Burch, J. L. Gleason, *Org. Lett.* **2019**, *21*, 6800–6804.

[69] R. A. Shelp, P. J. Walsh, *Angew. Chemie - Int. Ed.* **2018**, *57*, 15857–15861.

[70] N. Trongsiriwat, Y. Pu, Y. Nieves-Quinones, R. A. Shelp, M. C. Kozlowski, P. J. Walsh, *Angew. Chemie - Int. Ed.* **2019**, *58*, 13416–13420.

[71] K. B. Wiberg, S. T. Waddell, K. Laidig, *Tetrahedron Lett.* **1986**, *27*, 1553–1556.

[72] K. B. Wiberg, S. T. Waddell, *J. Am. Chem. Soc.* **1990**, *112*, 2194–2216.

[73] P. Kaszynski, J. Michl, *J. Org. Chem.* **1988**, *53*, 4593–4594.

[74] V. Ripenko, D. Vysochyn, I. Klymov, S. Zhersh, P. K. Mykhailiuk, *J. Org. Chem.* **2021**, *86*, 14061–14068.

[75] L. D. Elliott, J. P. Knowles, P. J. Koovits, K. G. Maskill, M. J. Ralph, G. Lejeune, L. J. Edwards, R. I. Robinson, I. R. Clemens, B. Cox, et al., *Chem. - A Eur. J.* **2014**, *20*, 15226–15232.

[76] P. Kaszynski, N. D. McMurdie, J. Michl, *J. Org. Chem.* **1991**, *56*, 307–316.

[77] D. F. J. Caputo, C. Arroniz, A. B. Dürr, J. J. Mousseau, A. F. Stepan, S. J. Mansfield, E. A. Anderson, *Chem. Sci.* **2018**, *9*, 5295–5300.

[78] R. M. Bär, S. Kirschner, M. Nieger, S. Bräse, *Chem. - A Eur. J.* **2018**, *24*, 1373–1382.

[79] P. Kaszynski, A. C. Friedli, J. Michl, *J. Am. Chem. Soc.* **1992**, *114*, 601–620.

[80] D. M. Hedstrand, W. H. Kruizinga, R. M. Kellogg, *Tetrahedron Lett.* **1978**, *19*, 1255–1258.

[81] C. Pac, M. Ihama, M. Yasuda, Y. Miyauchi, H. Saurai, *J. Am. Chem. Soc.* **1981**, *103*, 6495–6497.

[82] S. Fukuzumi, S. Mochizuki, T. Tanaka, *J. Phys. Chem.* **1990**, *94*, 722–726.

[83] D. A. Nicewicz, D. W. C. MacMillan, *Science (80-.).* **2008**, *322*, 77–80.

[84] M. A. Ischay, M. E. Anzovino, J. Du, T. P. Yoon, *J. Am. Chem. Soc.* **2008**, *130*, 12886–12887.

[85] J. M. R. Narayanam, J. W. Tucker, C. R. J. Stephenson, *J. Am. Chem. Soc.* **2009**, *131*, 8756–8757.

[86] N. A. Romero, D. A. Nicewicz, *Chem. Rev.* **2016**, *116*, 10075–10166.

[87] J. W. Tucker, C. R. J. Stephenson, *J. Org. Chem.* **2012**, *77*, 1617–1622.

[88] R. C. McAtee, E. J. McClain, C. R. J. Stephenson, *Trends Chem.* **2019**, *1*, 111–125.

[89] L. Marzo, S. K. Pagire, O. Reiser, B. König, *Angew. Chemie - Int. Ed.* **2018**, *57*, 10034–10072.

[90] C. K. Prier, D. A. Rankic, D. W. C. MacMillan, *Chem. Rev.* **2013**, *113*, 5322–5363.

[91] M. S. Kharasch, E. V. Jensen, W. H. Urry, *Science (80-.).* **1945**, *102*, 128–128.

[92] D. H. R. Barton, M. A. Csiba, J. C. Jaszberenyi, *Tetrahedron Lett.* **1994**, *35*, 2869–2872.

[93] J. D. Nguyen, J. W. Tucker, M. D. Konieczynska, C. R. J. Stephenson, *J. Am. Chem. Soc.* **2011**, *133*, 4160–4163.

[94] C. J. Wallentin, J. D. Nguyen, P. Finkbeiner, C. R. J. Stephenson, *J. Am. Chem. Soc.* **2012**, *134*, 8875–8884.

[95] J. W. Tucker, Y. Zhang, T. F. Jamison, C. R. J. Stephenson, *Angew. Chemie - Int. Ed.* **2012**, *51*, 4144–4147.

[96] M. Pirtsch, S. Paria, T. Matsuno, H. Isobe, O. Reiser, *Chem. - A Eur. J.* **2012**, *18*, 7336–7340.

[97] M. Knorn, T. Rawner, R. Czerwieniec, O. Reiser, *ACS Catal.* **2015**, *5*, 5186–5193.

[98] E. Arceo, E. Montroni, P. Melchiorre, *Angew. Chemie - Int. Ed.* **2014**, *53*, 12064–12068.

[99] Y. Shen, J. Cornella, F. Juliá-Hernández, R. Martin, *ACS Catal.* **2017**, *7*, 409–412.

[100] D. P. Curran, T. R. McFadden, *J. Am. Chem. Soc.* **2016**, *138*, 7741–7752.

[101] C. T. Cao, M. Chen, Z. Fang, C. Au, C. Cao, *ACS Omega* **2020**, *5*, 19304–19311.

[102] D. Best, C. Wang, A. C. Weymouth-Wilson, R. A. Clarkson, F. X. Wilson, R. J. Nash, S. Miyauchi, A. Kato, G. W. J. Fleet, *Tetrahedron Asymmetry* **2010**, *21*, 311–319.

[103] P. F. McGarry, J. C. Scaiano, *Can. J. Chem* **1998**, *76*, 1474–1489.

[104] Y. Zhang, J. Xu, H. Guo, *Org. Lett.* **2019**, *21*, 9133–9137.

[105] J. I. Bardagi, I. Ghosh, M. Schmalzbauer, T. Ghosh, B. König, *European J. Org. Chem.* **2018**, *2018*, 34–40.

[106] T. U. Connell, C. L. Fraser, M. L. Czyz, Z. M. Smith, D. J. Hayne, E. H. Doeven, J. Agugiaro, D. J. D. Wilson, J. L. Adcock, A. D. Scully, et al., *J. Am. Chem. Soc.* **2019**, *141*, 17646–17658.

[107] F. O. Hara, D. G. Blackmond, P. S. Baran, *J. Am. Chem. Soc.* **2013**, *135*, 12122–12134.

[108] H. Tan, X. Liu, J. Su, Y. Wang, X. Gu, D. Yang, E. R. Waclawik, H. Zhu, Z. Zheng, *Sci. Rep.* **2019**, 1–7.

[109] C. Lin, B. Hong, W. Chang, G. Lee, *Org. Lett.* **2015**, *17*, 2314–2317.

[110] M. Cheng, L. Gao, M. Tan, C. Wang, *Dalt. Trans.* **2019**, *48*, 9949–9953.

[111] T. Hirao, J. Shiori, N. Okahata, *Bull. Chem. Soc. Jpn.* **2004**, *77*, 1763–1764.

[112] J. Nugent, C. Arroniz, B. R. Shire, A. J. Sterling, H. D. Pickford, M. L. J. Wong, S. J. Mansfield, D. F. J. Caputo, B. Owen, J. J. Mousseau, et al., *ACS Catal.* **2019**, *9*, 9568–9574.

[113] J. J. Devery, J. D. Nguyen, C. Dai, C. R. J. Stephenson, *ACS Catal.* **2016**, *6*, 5962–5967.

[114] C. P. Seath, D. B. Vogt, Z. Xu, A. J. Boyington, N. T. Jui, *J. Am. Chem. Soc.* **2018**, *140*, 15525–15534.

[115] K. S. Egorova, V. P. Ananikov, *Angew. Chemie - Int. Ed.* **2016**, *55*, 12150–12162.

[116] EMA/CHMP/SWP/4446/2000, *Guideline on the Specification Limits for Residues of Metal Catalysts or Metal Reagents. Draft Agreed by the Safety Working Party Adoption ByCHMP*, **2016**.

[117] I. Bauer, H. J. Knölker, *Chem. Rev.* **2015**, *115*, 3170–3387.

[118] A. Fürstner, *ACS Cent. Sci.* **2016**, *2*, 778–789.

[119] P. Dabell, S. P. Thomas, *Synth.* **2020**, *52*, 949–963.

[120] M. Tamura, J. Kochi, *J. Am. Chem. Soc.* **1971**, *93*, 1487–1489.

[121] M. Nakamura, K. Matsuo, S. Ito, E. Nakamura, *J. Am. Chem. Soc.* **2004**, *126*, 3686–3687.

[122] T. Nagano, T. Hayashi, *Org. Lett.* **2004**, *6*, 1297–1299.

[123] G. Cahiez, H. Avedissian, *Synthesis (Stuttg).* **1998**, *8*, 1199–1205.

[124] R. Martin, A. Fürstner, *Angew. Chemie - Int. Ed.* **2004**, *43*, 3955–3957.

[125] B. Bogdanovi, M. Schwickardi, *Angew. Chemie - Int. Ed.* **2000**, *39*, 4610–4612.

[126] B. Scheiper, M. Bonnekessel, H. Krause, A. Fürstner, *J. Org. Chem.* **2004**, *69*, 3943–3949.

[127] G. Cahiez, V. Habiak, C. Duplais, A. Moyeux, *Angew. Chemie - Int. Ed.* **2007**, *46*, 4364–4366.

[128] R. B. Bedford, D. W. Bruce, R. M. Frost, M. Hird, *Chem. Commun.* **2004**, 2822–2823.

[129] A. Fürstner, A. Leitner, M. Méndez, H. Krause, *J. Am. Chem. Soc.* **2002**, *124*, 13856–13863.

[130] R. B. Bedford, D. W. Bruce, R. M. Frost, M. Hird, *Chem. Commun.* **2005**, 4161–4163.

[131] R. B. Bedford, M. Betham, D. W. Bruce, S. A. Davis, R. M. Frost, M. Hird, *J. Med. Chem.* **2006**, *71*, 1104–1110.

[132] R. R. Chowdhury, A. K. Crane, C. Fowler, P. Kwong, C. M. Kozak, *Chem. Commun.* **2008**, 94–96.

[133] X. Qian, L. N. Dawe, C. M. Kozak, *Dalt. Trans.* **2011**, *40*, 933–943.

[134] K. Hasan, L. N. Dawe, C. M. Kozak, *Eur. J. Inorg. Chem.* **2011**, 4610–4621.

[135] F. Xue, J. Zhao, A. Hor, *Dalt. Trans.* **2011**, *40*, 8935–8940.

[136] K. Bica, P. Gaertner, *Org. Lett.* **2006**, *8*, 733–735.

[137] H. H. Gao, C. H. Yan, X. P. Tao, Y. Xia, H. M. Sun, Q. Shen, Y. Zhang, *Organometallics* **2010**, *29*, 4189–4192.

[138] C. L. Xia, C. F. Xie, Y. F. Wu, H. M. Sun, Q. Shen, Y. Zhang, *Org. Biomol. Chem.* **2013**, *11*, 8135–8144.

[139] H. N. Deng, Y. L. Xing, C. L. Xia, H. M. Sun, Q. Shen, Y. Zhang, *Dalt. Trans.* **2012**, *41*, 11597–11607.

[140] T. Hashimoto, T. Maruyama, T. Yamaguchi, Y. Matsubara, Y. Yamaguchi, *Adv. Synth. Catal.* **2019**, *361*, 4232–4236.

[141] T. Hatakeyama, Y. Fujiwara, Y. Okada, T. Itoh, T. Hashimoto, S. Kawamura, K. Ogata, H. Takaya, M. Nakamura, *Chem. Lett.* **2011**, *40*, 1030–1032.

[142] D. Noda, Y. Sunada, T. Hatakeyama, M. Nakamura, H. Nagashima, *J. Am. Chem. Soc.* **2009**, *131*, 6078–6079.

[143] B. Baptiste, L. Gonnard, R. Campagne, S. Reymond, J. Marin, P. Ciapetti, M. Brellier, A. Guérinot, J. Cossy, *Org. Lett.* **2014**, *16*, 6160–6163.

[144] D. Parmar, L. Henkel, J. Dib, M. Rueping, *Chem. Commun.* **2015**, *51*, 2111–2113.

[145] C. Tao, L. Sun, B. Wang, Z. Liu, Y. Zhai, X. Zhang, D. Shi, *Tetrahedron Lett.* **2017**, *58*, 305–308.

[146] F. Toriyama, J. Cornella, L. Wimmer, T. Chen, D. D. Dixon, G. Creech, P. S. Baran, *J. Am. Chem. Soc.* **2016**, *138*, 11132–11135.

[147] A. Hazra, M. T. Lee, J. F. Chiu, G. Lalic, *Angew. Chemie - Int. Ed.* **2018**, *57*, 5492–5496.

[148] D. F. J. Caputo, New Directions Towards the Synthesis of Bicyclo[1.1.1]Pentane Derivatives, University of Oxford, **2018**.

[149] R. Huisgen, R. Knorr, *Tetrahedron Lett.* **1963**, *4*, 1017–1021.

[150] R. W. Hoffmann, *Dehydrobenzene and Cycloalkynes*, Academic Press, **1967**.

[151] T. L. Mako, J. A. Byers, *Inorg. Chem. Front.* **2016**, *3*, 766–790.

[152] A. Hedström, Z. Izakian, I. Vreto, C. J. Wallentin, P. O. Norrby, *Chem. - A Eur. J.* **2015**, *21*, 5946–5953.

[153] M. L. Neidig, S. H. Carpenter, D. J. Curran, J. C. Demuth, V. E. Fleischauer, T. E. Iannuzzi, P. G. N. Neate, J. D. Sears, N. J. Wolford, *Acc. Chem. Res.* **2019**, *52*, 140–150.

[154] R. B. Bedford, *Acc. Chem. Res.* **2015**, *48*, 1485–1493.

[155] R. B. Bedford, P. B. Brenner, D. Elorriaga, J. N. Harvey, J. Nunn, *Dalt. Trans.* **2016**, *45*, 15811–15817.

[156] S. H. Carpenter, T. M. Baker, S. B. Muñoz, W. W. Brennessel, M. L. Neidig, *Chem. Sci.* **2018**, *9*, 7931–7939.

[157] N. J. Bakas, J. D. Sears, W. W. Brennessel, M. L. Neidig, *Angew. Chemie - Int. Ed.* **2022**, *61*, e202114986.

[158] S. L. Daifuku, J. L. Kneebone, B. E. R. Snyder, M. L. Neidig, *J. Am. Chem. Soc.* **2015**, *137*, 11432–11444.

[159] S. L. Daifuku, M. H. Al-afyouni, B. E. R. Snyder, J. L. Kneebone, M. L. Neidig, *J. Am. Chem. Soc.* **2014**, *136*, 9132–9143.

[160] A. Hedström, U. Bollmann, J. Bravidor, P. O. Norrby, *Chem. - A Eur. J.* **2011**, *17*, 11991–11993.

[161] J. G. Kim, Y. H. Son, J. W. Seo, E. J. Kang, *European J. Org. Chem.* **2015**, *2015*, 1781–1789.

[162] L. Liu, W. Lee, J. Zhou, S. Bandyopadhyay, O. Gutierrez, *Tetrahedron* **2019**, *75*, 129–136.

[163] J. Nugent, B. R. Shire, D. F. J. Caputo, H. D. Pickford, F. Nightingale, I. T. T. Houlsby, J. J. Mousseau, E. A. Anderson, *Angew. Chemie - Int. Ed.* **2020**, 1–6.

[164] C. Sandford, V. K. Aggarwal, *Chem. Commun.* **2017**, *53*, 5481–5494.

[165] F. W. Friese, A. Studer, *Chem. Sci.* **2019**, *10*, 8503–8518.

[166] C. T. Yang, Z. Q. Zhang, H. Tajuddin, C. C. Wu, J. Liang, J. H. Liu, Y. Fu, M. Czyzewska, P. G. Steel, T. B. Marder, et al., *Angew. Chemie - Int. Ed.* **2012**, *51*, 528–532.

[167] C. Kleeberg, L. Dang, Z. Lin, T. B. Marder, *Angew. Chemie - Int. Ed.* **2009**, *48*, 5350–5354.

[168] C. T. Yang, Z. Q. Zhang, Y. C. Liu, L. Liu, *Angew. Chemie - Int. Ed.* **2011**, *50*, 3904–3907.

[169] H. Ito, K. Kubota, *Org. Lett.* **2012**, *14*, 890–893.

[170] H. Iwamoto, K. Endo, Y. Ozawa, Y. Watanabe, K. Kubota, T. Imamoto, H. Ito, *Angew. Chemie - Int. Ed.* **2019**, *58*, 11112–11117.

[171] M. Y. Liu, S. Bin Hong, W. Zhang, W. Deng, *Chinese Chem. Lett.* **2015**, *26*, 373–376.

[172] S. K. Bose, S. Brand, H. O. Omoregie, M. Haehnel, J. Maier, G. Bringmann, T. B. Marder, *ACS Catal.* **2016**, *6*, 8332–8335.

[173] B. R. Albuquerque, S. A. 8. Heleno, M. B. P. P. Oliveira, L. Barros, I. C. F. R. Ferreira, *Food Funct.* **2021**, *12*, 14–29.

[174] E. M. Aldred, C. Buck, K. Vall, *Pharmacology* **2009**, 149–166.

[175] J. H. Chávez, P. C. Leal, R. A. Yunes, R. J. Nunes, C. R. M. Barardi, A. R. Pinto, C. M. O. Simões, C. R. Zanetti, *Vet. Microbiol.* **2006**, *116*, 53–59.

[176] Y. L. Goh, Y. T. Cui, V. Pendharkar, V. A. Adsool, *ACS Med. Chem. Lett.* **2017**, *8*, 516–520.

[177] S. Yu, C. Jing, A. Noble, V. K. Aggarwal, *Angew. Chemie - Int. Ed.* **2020**, *59*, 3917–3921.

[178] R. A. Shelp, P. J. Walsh, *Angew. Chemie - Int. Ed.* **2018**, *57*, 15857–15861.

[179] R. A. Shelp, A. Ciro, Y. Pu, R. R. Merchant, J. M. E. Hughes, P. J. Walsh, *Chem. Sci.* **2021**, *12*, 7066–7072.

[180] J. Wang, M. Shang, H. Lundberg, K. S. Feu, S. J. Hecker, T. Qin, D. G. Blackmond, P. S. Baran, *ACS Catal.* **2018**, *8*, 9537–9542.

[181] L. M. Barton, L. Chen, D. G. Blackmond, P. S. Baran, *Proc. Natl. Acad. Sci. U. S. A.* **2021**, *118*, DOI 10.1073/pnas.2109408118.

[182] Y. Yang, J. Tsien, J. M. E. Hughes, B. K. Peters, R. R. Merchant, T. Qin, *Nat. Chem.* **2021**, *13*, 950–955.

[183] Y. L. Goh, Y. T. Cui, V. Pendharkar, V. A. Adsool, *ACS Med. Chem. Lett.* **2017**, *8*, 516–520.

[184] Q. Yang, P. Y. Choy, W. C. Fu, B. Fan, F. Y. Kwong, *J. Org. Chem.* **2015**, *80*, 11193–11199.

7

Supplementary information

Table of contents

7.1 General experimental considerations

NMR Spectroscopy: ^{1}H, ^{13}C and ^{19}F NMR spectra were recorded on Bruker AV400 or Bruker AVII500 spectrometers using TOPSPIN software, with the deuterated solvent acting as the internal deuterium lock. ^{1}H NMR spectra were recorded at 400 or 500 MHz, ^{13}C NMR spectra were recorded at 101 or 126 MHz with ^{1}H decoupling, and ^{19}F NMR spectra were recorded at 376 or 470 MHz. Assignments were determined either on the basis of unambiguous chemical shift / coupling patterns, or from 2D COSY, HMBC and/or HSQC experiments. Peak multiplicities are defined as: s = singlet, d = doublet, t = triplet, q = quartet, quin. = quintet, m = multiplet, br. = broad, app. = apparent; coupling constants (*J*) are reported to the nearest 0.1 Hz.

Infrared Spectroscopy: Infrared spectra were recorded on a Bruker Tensor 27 FT-IR spectrometer with the sample being prepared as a thin film on a diamond ATR module. Absorption maxima (ν_{max}) are quoted in wavenumbers (cm^{-1}).

Mass Spectrometry: Mass Spectrometry: Low resolution mass spectra were recorded on a Micromass LCT Premier Open Access using electrospray ionization (ESI). Accurate mass (HRMS) data was determined under conditions of ESI, EI and CI on a Bruker MicroTOF. High resolution values are calculated to 4 decimal places from the molecular formula, and all values are within a tolerance of 5 ppm.

Melting Points: Melting points were obtained using a Griffin melting point apparatus and are uncorrected.

Chromatography: Column chromatography refers to normal phase column chromatography and was performed on silica gel obtained from Merck (Silica gel Si 60, 0.040-0.063 mm) under a positive pressure of nitrogen, using the stated solvent system. Analytical thin-layer chromatography (TLC) was used to monitor reaction progress and performed on pre-coated aluminium-backed plates (Merck Kieselgel 60 F_{254} plates) with visualisation by ultraviolet light (254 nm) and/or by staining in vanillin, ninhydrin, phosphomolybdic acid and potassium permanganate. Retention factr (R_f) are reported with the solvent system in parentheses.

Reagents, solvents and techniques: All reagents were used directly as supplied. Solvents were either used as commercially supplied, or dried/purified by standard techniques. Anhydrous Et_2O, CH_2Cl_2, DMF, THF and toluene were obtained from solvent dispenser units having been passed through an activated alumina column under argon. Unless otherwise stated, non-aqueous reactions were performed using flame-dried glassware under a nitrogen atmosphere.

7.2 Synthesis of tricyclo[1.1.1.0^{1,3}]pentane

According to the procedure of Baran et al.[1] To a solution of 1,1-dibromo-2,2-bis(chloromethyl)cyclopropane 28 (28.2 g, 95.0 mmol, 1.0 equiv.) in Et_2O (60 mL) at –40 °C under an inert atmosphere was added phenyllithium (1.9 M in dibutyl ether, 100 mL, 190 mmol, 2.0 equiv.) via cannula over 30 min. The resulting mixture was then stirred at 0 °C for 2 h and distilled in a rotary evaporator at room temperature, having both the condenser and collection flask of the rotary evaporator cooled to –78 °C. The title compound was collected as a clear, colorless solution (0.62 M in Et_2O, 85.0 mL, 52.7 mmol, 56%) and used in subsequent reactions as a solution in Et2O. The yield and approximate concentration of the solution was calculated using quantitative NMR with DCE as an internal standard. 0.2 mL of the solution of [1.1.1]propellane 2 in Et_2O was diluted with DCE (50 µL) and $CDCl_3$ (0.5 mL). The ratio of DCE (4H) to [1.1.1]propellane 2 (6H) was determined and used to calculate the approximate concentration of the solution. Two runs were carried out and the average used as the final approximated concentration.

^{1}H NMR (200 MHz, $CDCl_3$) δ 1.94 (6H, s).

Spectroscopic data in agreement with that reported previously.[2]

7.3 Chapter 2: Photoredox catalysed atom transfer radical addition reactions

7.3.1 General Procedures

General Procedure 1: Visible light-promoted atom-transfer radical addition of (hetero)aryl iodides to tricyclo[1.1.1.0^{1,3}]pentane.

To a screw-capped vial equipped with a stirrer bar was added *fac*-Ir(ppy)$_3$ (2.5 mg, 4.0 μmol, 0.025 equiv.), the specified halide (0.15 mmol, 1.0 equiv.), *t*-BuCN (1.5 mL) and tricyclo[1.1.1.0^{1,3}]pentane (2.0 equiv., 0.5–0.7 M solution in Et_2O). The vial was sealed and placed under nitrogen, and the solution was degassed *via* three freeze-pump-thaw cycles (vacuum was only applied while the reaction mixture was frozen due to TCP volatility). The stirred mixture was irradiated with blue LEDs for the indicated time. The reaction mixture was concentrated, and the residue was purified by column chromatography.

7.3.2 Photochemical Equipment and Setup

Two Blue LED lamps were used for this work:

a. Tingkam® Waterproof 5M 5050 SMD RGB Led Strips, fixed to the inside of a crystallization dish (left).
b. Evoluchem™ 455 nm 18W LED, placed in an Evoluchem™ PhotoRedOx box (right).

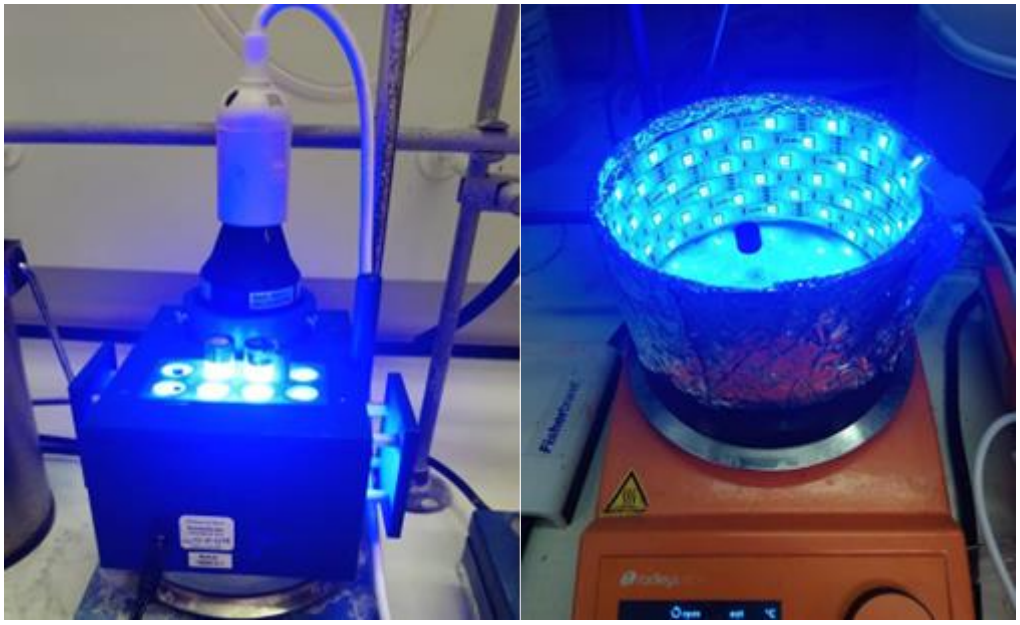

Left: Set up **a**: Tingkam® Waterproof 5M 5050 SMD RGB LED Strips fixed to the inside of a crystallization dish.

Right: Set up **b**: Evoluchem™ 455 nm 18W LED placed in an Evoluchem™ PhotoRedOx box.

7.3.3 Reaction scope

4-(3-Iodobicyclo[1.1.1]pentan-1-yl)benzonitrile, 43

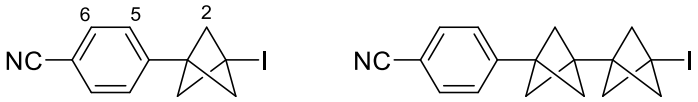

43 **43s**

fac-Ir(ppy)$_3$ (2.5 mg, 4 µmol, 0.025 equiv.), 4-iodobenzonitrile (34 mg, 0.15 mmol, 1.0 equiv.) and TCP (0.33 mL, 0.9 M in Et_2O, 0.30 mmol, 2.0 equiv.) in *t*-BuCN (1.0 mL) were submitted to **General Procedure 1** at room temperature for 16 h. Purification by column chromatography (SiO_2, pentane / Et_2O, 97:3) afforded **43** and **43s** (26 mg, 1:0.12 ratio of **43**:**43s** isolated as an inseparable mixture, 50% yield of **43**, as determined by ^{1}H NMR spectroscopy), as a white solid.

R_f = 0.20 (pentane)

m.p. = 107-109 °C

^{1}H NMR (400 MHz, $CDCl_3$) δ 7.61-7.57 (2H, m, H6), 7.24-7.20 (2H, m, H5), 2.61 (6H, s, H2).

^{13}C NMR (101 MHz, $CDCl_3$) δ 143.5, 132.4, 127.0, 118.8, 111.1, 61.8, 50.2, 5.6.

HRMS (ESI$^+$) Found $[M+Na]^+$ = 317.9750; $C_{12}H_{10}NINa$ requires 317.9750.

IR (film) ν_{max}/cm^{-1} 2360, 2341, 1275, 750, 668, 612.

2-(3-Iodobicyclo[1.1.1]pentan-1-yl)benzonitrile, 44

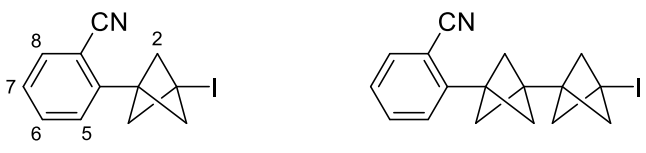

44 **44s**

fac-Ir(ppy)$_3$ (2.5 mg, 4 µmol, 0.025 equiv.), 2-iodobenzonitrile (34 mg, 0.15 mmol, 1.0 equiv.) and TCP (0.33 mL, 0.9 M in Et_2O, 0.30 mmol, 2.0 equiv.) in *t*-BuCN (1.0 mL) were submitted to **General Procedure 1** at room temperature for 16 h. Purification by column chromatography (SiO_2, pentane / Et_2O, 97:3) afforded **44** and **44s** (26 mg, 1:0.06 ratio of **44**:**44s** isolated as an inseparable mixture, 55% yield of **44**, as determined by ^{1}H NMR spectroscopy), as a colourless oil.

R_f = 0.47 (pentane / EtOAc, 9:1)

^{1}H NMR (400 MHz, $CDCl_3$) δ 7.60 (1H, ddd, *J* = 7.7, 1.4, 0.6 Hz, H8), 7.52 (1H, td, *J* = 7.7, 1.4 Hz, H6), 7.34 (1H, td, *J* = 7.7, 1.2 Hz, H7), 7.18 (1H, ddd, *J* = 7.7, 1.2, 0.6 Hz, H5), 2.81 (6H, s, H2).

^{13}C NMR (101 MHz, $CDCl_3$) δ 141.4, 133.7, 132.9, 128.1, 127.8, 118.3, 110.6, 61.5, 49.6, 5.8.

HRMS (ESI$^+$) Found $[M+Na]^+$ = 317.9751; $C_{12}H_{10}NINa$ requires 317.9750 .

IR (film) ν_{max}/cm^{-1} 2980, 2225, 1596, 1483, 1444, 1382, 1198, 1190, 1116, 1068, 954, 846, 778, 757.

1-Iodo-3-(4-(trifluoromethyl)phenyl)bicyclo[1.1.1]pentane, 45

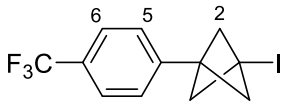

fac-Ir(ppy)$_3$ (2.5 mg, 4 µmol, 0.025 equiv.), 1-iodo-4-(trifluoromethyl)benzene (22 µL, 0.15 mmol, 1.0 equiv.) and TCP (0.33 mL, 0.9 M in Et_2O, 0.30 mmol, 2.0 equiv.) in *t*-BuCN (1.0 mL) were submitted to **General Procedure 1** at room temperature for 16 h. Purification by column chromatography (SiO_2, pentane) afforded **45** (26 mg, 0.08 mmol, 51%) as a white solid.

R_f = 0.50 (pentane)

m.p. = 148-150 °C

^{1}H NMR (400 MHz, $CDCl_3$) δ 7.59-7.54 (2H, m, H6), 7.24 (2H, m, H5), 2.62 (6H, s, H2).

^{13}C NMR (101 MHz, $CDCl_3$) δ 142.2, 129.4 (q, *J* = 32.5 Hz), 126.6, 125.5 (q, *J* = 3.8 Hz), 124.2 (q, *J* = 271.8 Hz) 61.9, 50.1, 6.1.

^{19}F NMR (376 MHz, $CDCl_3$) δ –62.5.

HRMS (ESI^+, CI^+, EI^+): Not found.

IR (film) ν_{max}/cm^{-1} 2918, 2360, 1616, 1327, 1195, 1157, 1114, 1060, 843.

Methyl 4-(3-iodobicyclo[1.1.1]pentan-1-yl)benzoate, 46

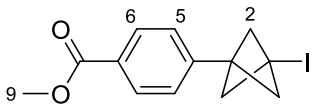

fac-Ir(ppy)$_3$ (2.5 mg, 4 μmol, 0.025 equiv.), methyl 4-iodobenzoate (40 mg, 0.15 mmol, 1.0 equiv.) and TCP (0.33 mL, 0.9 M in Et_2O, 0.30 mmol, 2.0 equiv.) in *t*-BuCN (1.0 mL) were submitted to **General Procedure 1** at room temperature for 16 h. Purification by column chromatography (SiO_2, pentane / Et_2O, 95:5) afforded **46** (20 mg, 0.06 mmol, 40%) as a colourless foam.

R_f = 0.43 (pentane / Et_2O, 9:1)

^{1}H NMR (400 MHz, $CDCl_3$) δ 7.99-7.95 (2H, m, H6), 7.20-7.16 (2H, m, H5), 3.90 (3H, s, H9), 2.62 (6H, s, H2).

^{13}C NMR (101 MHz, $CDCl_3$) δ 166.9, 143.3, 129.9, 129.0, 126.2, 61.9, 52.3, 50.3, 6.5.

HRMS ($APCI^+$) Found $[M+H]^+$ = 329.0030; $C_{13}H_{14}O_2I$ requires 329.0033 .

IR (film) ν_{max}/cm^{-1} 2914, 1719, 1609, 1438, 1406, 1281, 1193, 1110, 1070, 839, 745, 699.

4-(3-Iodobicyclo[1.1.1]pentan-1-yl)-2-(trifluoromethyl)benzonitrile, 47

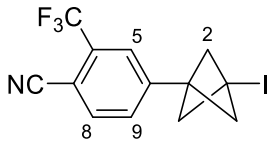

47

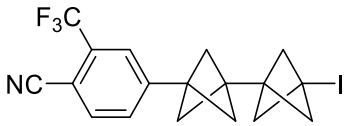

47s

fac-Ir(ppy)$_3$ (2.5 mg, 4 µmol, 0.025 equiv.), 4-iodo-2-(trifluoromethyl)benzonitrile (45 mg, 0.15 mmol, 1.0 equiv.) and TCP (0.33 mL, 0.9 M in Et_2O, 0.30 mmol, 2.0 equiv.) in *t*-BuCN (1.0 mL) were submitted to **General Procedure 1** at room temperature for 16 h. Purification by column chromatography (SiO_2, pentane / Et_2O, 9:1) afforded **47** and **47s** (35 mg, 1:0.04 ratio of **47**:**47s** isolated as an inseparable mixture, 60% yield of **47**, as determined by ^{1}H NMR spectroscopy), as a white solid.

R_f = 0.18 (pentane / Et_2O, 9:1)

m.p. = 107-109 °C

^{1}H NMR (400 MHz, $CDCl_3$) δ 7.78 (1H, dt, *J* = 8.0, 0.7 Hz, H8), 7.52-7.48 (1H, m, H5), 7.42 (1H, ddd, *J* = 8.0, 1.8, 0.7 Hz, H9), 2.65 (6H, s, H2).

^{13}C NMR (101 MHz, $CDCl_3$) δ 144.0, 135.0, 133.2 (q, *J* = 32.8 Hz), 130.0, 124.6 (q, *J* = 4.6 Hz), 122.3 (q, *J* = 274.2 Hz), 115.5, 108.7, 61.6, 49.7, 4.7.

^{19}F NMR (376 MHz, $CDCl_3$) δ –62.2.

HRMS (ESI$^+$) Found $[M+Na]^+$ = 385.9625; $C_{13}H_9NF_3INa$ requires 385.9624 .

IR (film) ν_{max}/cm^{-1} 2917, 2231, 1614, 1425, 1338, 1296, 1177, 1135, 1078, 1054, 851, 671.

2-(3-Iodobicyclo[1.1.1]pentan-1-yl)pyridine, 48

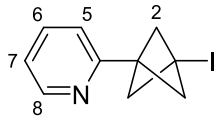

fac-Ir(ppy)$_3$ (2.5 mg, 4 µmol, 0.025 equiv.), 2-iodopyridine (16 µL, 0.15 mmol, 1.0 equiv.) and TCP (0.33 mL, 0.9 M in Et_2O, 0.30 mmol, 2.0 equiv.) in *t*-BuCN (1.0 mL) were submitted to **General Procedure 1** at room temperature for 16 h. Purification by column chromatography (SiO_2, pentane / EtOAc, 7:3) afforded **48** (34 mg, 0.13 mmol, 84%) as a pale yellow foam.

R_f = 0.50 (pentane / EtOAc, 7:3)

^{1}H NMR (400 MHz, $CDCl_3$) δ 8.53 (1H, ddd, *J* = 4.9, 1.9, 1.0 Hz, H8), 7.63 (1H, td, *J* = 7.7, 1.9 Hz, H6), 7.16 (1H, ddd, *J* = 7.7, 4.9, 1.2 Hz, H7), 7.10 (1H, dt, *J* = 7.7, 1.2 Hz, H5), 2.68 (6H, s, H2).

^{13}C NMR (101 MHz, $CDCl_3$) δ 157.0, 149.6, 136.7, 122.3, 120.8, 61.6, 51.2, 7.4.

HRMS (ESI$^+$) Found $[M+H]^+$ = 271.9928; $C_{10}H_{11}NI$ requires 271.9931.

IR (film) ν_{max}/cm^{-1} 2919, 1588, 1567, 1471, 1432, 1192, 1091, 844, 795, 747.

2-(3-Iodobicyclo[1.1.1]pentan-1-yl)-6-methylpyridine, 49

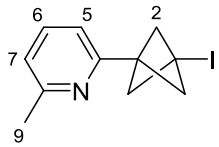

fac-Ir(ppy)$_3$ (2.5 mg, 4.0 µmol, 0.025 equiv.), 2-iodo-6-methylpyridine (33 mg, 0.15 mmol, 1.0 equiv.), TCP (0.25 mL, 0.9 M in Et_2O, 0.23 mmol, 1.5 equiv.) in *t*BuCN (1.5 mL) were submitted to **General Procedure 1** at room temperature for 16 h. Purification

by column chromatography (SiO_2, pentane / Et_2O, 95:5) afforded **49** (37 mg, 0.13 mmol, 87%) as a colourless oil.

R_f = 0.44 (pentane / Et_2O, 9:1)

^{1}H NMR (400 MHz, $CDCl_3$) δ 7.49 (1H, t, *J* = 7.7 Hz, H6), 7.00 (1H, d, *J* = 7.7 Hz, H7), 6.88 (1H, d, *J* = 7.7 Hz, H5), 2.67 (6H, s, H2), 2.52 (3H, s, H9).

^{13}C NMR (100 MHz, $CDCl_3$) δ 158.4, 156.5, 136.6, 121.8, 117.7, 61.8, 51.3, 24.8, 7.9.

HRMS (ESI^+) Found $[M+H]^+$ = 286.0086; $C_{11}H_{13}NI$ requires 286.0087.

IR (film) ν_{max}/cm^{-1} 2922, 1576, 1548, 1115, 773.

Reaction and characterisation by Dr Jeremy Nugent.

2-(3-Iodobicyclo[1.1.1]pentan-1-yl)-6-(trifluoromethyl)pyridine, 50

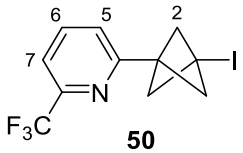

50

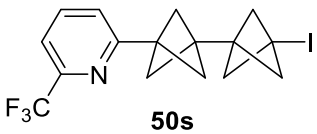

50s

fac-Ir(ppy)$_3$ (2.5 mg, 4 μmol, 0.025 equiv.), 2-iodo-6-(trifluoromethyl)pyridine (40 mg, 0.15 mmol, 1.0 equiv.) and TCP (0.45 mL, 0.67 M in Et_2O, 0.23 mmol, 1.5 equiv.) in *t*-BuCN (1.0 mL) were submitted to **General Procedure 1** at room temperature for 18 h. Purification by column chromatography (SiO_2, pentane / Et_2O, 1:0→95:5) afforded **50** and **50s** (43 mg, 1:0.03 ratio of **50**:**50s** isolated as an inseparable mixture, 81% yield of **50**, as determined by ^{1}H NMR spectroscopy), as a white solid.

R_f = 0.46 (pentane / Et_2O, 85:15)

m.p. = 56 °C

^{1}H NMR (400 MHz, $CDCl_3$) δ 7.79 (1H, td, *J* = 7.8, 0.7 Hz, H6), 7.54 (1H, dd, *J* = 7.8, 1.0 Hz, H7), 7.28 (1H, d, *J* = 7.8 Hz, H5), 2.70 (6H, s, H2).

^{13}C NMR (101 MHz, $CDCl_3$) δ 157.7, 148.2 (q, *J* = 34.3 Hz), 137.8, 123.4, 121.5 (q, *J* = 274.2 Hz), 118.8 (q, *J* = 2.8 Hz), 61.7, 50.9, 6.8.

^{19}F NMR (376 MHz, $CDCl_3$) δ –68.0.

HRMS (ESI^+, CI^+, EI^+): Not found.

IR (film) ν_{max}/cm^{-1} 2921, 1599, 1511, 1355, 1199, 1142, 1094, 852.

3-Chloro-2-(3-iodobicyclo[1.1.1]pentan-1-yl)pyridine, 51

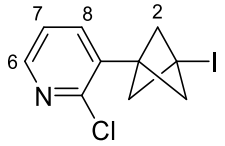

51

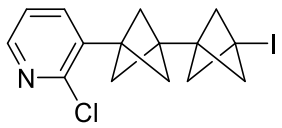

51s

fac-$Ir(ppy)_3$ (2.5 mg, 4 μmol, 0.025 equiv.), 2-chloro-3-iodopyridine (36 mg, 0.15 mmol, 1.0 equiv.) and TCP (0.45 mL, 0.67 M in Et_2O, 0.30 mmol, 2.0 equiv.) in *t*-BuCN (1.0 mL) were submitted to **General Procedure 1** at room temperature for 18 h. Purification by column chromatography (SiO_2, pentane / Et_2O, 9:1→4:1) gave **51** and **51s** (20 mg, 1:0.05 ratio of **51**:**51s**, isolated as an inseparable mixture, 40% yield of **51** as determined by ^{1}H NMR spectroscopy) as a clear oil.

R_f = 0.42 (pentane / Et_2O, 4:1)

^{1}H NMR (500 MHz, $CDCl_3$) δ 8.28 (1H, dd, *J* = 4.8, 2.0 Hz, H6), 7.40 (1H, dd, *J* = 7.5, 2.0 Hz, H8), 7.19 (1H, dd, *J* = 7.5, 4.8 Hz, H7), 2.75 (6H, s, H2)

^{13}C NMR (126 MHz, $CDCl_3$) δ 150.2, 148.4, 137.9, 132.2, 122.6, 61.1, 49.1, 6.5.

HRMS (ESI^+) Found $[M+H]^+$ = 305.9541; $C_{10}H_{10}NClI$ requires 305.9543.

IR (film) ν_{max}/cm^{-1} 2971, 2915, 1559, 1397, 1191, 843.

Reaction and characterisation by Dr James Mousseau.

4-(3-Iodobicyclo[1.1.1]pentan-1-yl)pyridine, 52

and 4-(1-(3-iodobicyclo[1.1.1]pentan-1-yl)-3-methylenecyclobutyl)pyridine, 71

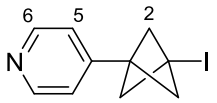

52

52s

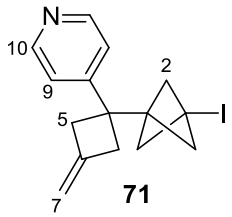

71

fac-Ir(ppy)$_3$ (2.5 mg, 4 µmol, 0.025 equiv.), 4-iodopyridine (31 mg, 0.15 mmol, 1.0 equiv.) and TCP (0.33 mL, 0.9 M in Et_2O, 0.30 mmol, 2.0 equiv.) in *t*-BuCN (1.0 mL) were submitted to **General Procedure 1** at room temperature for 16 h. Purification by column chromatography (SiO_2, pentane / EtOAc, 85:15) afforded **52** and **52s** (26 mg, 1:0.04 ratio of **52**:**52s** isolated as an inseparable mixture, 49% yield of **52**, as determined by ^{1}H NMR spectroscopy), as a white solid and **71** (4-6% isolated yield) as a white solid.

Data for **52**

R_f = 0.14 (pentane / EtOAc, 7:3)

m.p. = 126-128 °C

^{1}H NMR (400 MHz, $CDCl_3$) δ 8.51-8.44 (2H, m, H6), 7.00-6.95 (2H, m, H5), 2.55 (6H, s, H2).

^{13}C NMR (101 MHz, $CDCl_3$) δ 149.9, 146.8, 121.3, 61.5, 51.6, 5.8.

HRMS (EI^+) Found $[M+H]^+$ = 271.9931; $C_{10}H_{11}NI$ requires 271.9931 .

IR (film) ν_{max}/cm^{-1} 2990, 2911, 2871, 1597, 1551, 1443, 1409, 1200, 1088, 829, 673.

Data for **71**

R_f = 0.33 (pentane / EtOAc, 3:2)

m.p. = 101-103°C

^{1}H NMR (400 MHz, $CDCl_3$) δ 8.54 (2H, d, *J* = 4.3 Hz, H10), 7.02-6.90 (2H, m, H9), 4.86 (2H, app. quin. *J* = 2.4 Hz, H7), 2.97-2.93 (4H, m, H5), 2.10 (6H, s, H2).

^{13}C NMR (100 MHz, $CDCl_3$) δ 154.0, 149.8, 141.9, 121.5, 108.0, 57.3, 53.6, 43.3, 40.0, 7.5.

HRMS (ESI^+) Found $[M+H]^+$ = 338.0397; $C_{15}H_{17}NI$ requires 338.0400.

IR (film) ν_{max}/cm^{-1} 2989,2876, 1681, 1597, 1189, 840.

3-Bromo-2-(3-iodobicyclo[1.1.1]pentan-1-yl)quinolone, 53

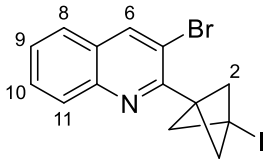

fac-$Ir(ppy)_3$ (2.5 mg, 4 μmol, 0.025 equiv.), 3-bromo-2-iodoquinoline (50 mg, 0.15 mmol, 1.0 equiv.) and TCP (0.33 mL, 0.9 M in Et_2O, 0.30 mmol, 2.0 equiv.) in *t*-BuCN (1.0 mL) were submitted to **General Procedure 1** at room temperature for 16 h. Purification by column chromatography (SiO_2, pentane / EtOAc, 95:5) afforded **53** (45 mg, 0.11 mmol, 75%) as a white solid.

R_f = 0.45 (pentane / Et_2O, 95:5)

m.p. = 87-89 °C

^{1}H NMR (400 MHz, $CDCl_3$) δ 8.29 (1H, d, *J* = 1.0 Hz, H6), 8.02 (1H, ddd, *J* = 8.6, 1.9, 1.0 Hz, H11), 7.73-7.67 (2H, m, H8, H10), 7.56-7.50 (1H, m, H9), 2.95 (6H, s, H2).

^{13}C NMR (101 MHz, $CDCl_3$) δ 153.5, 146.3, 139.8, 130.1, 129.5, 128.4, 127.6, 126.5, 116.3, 62.0, 53.3, 8.6.

HRMS (EI^+) Found $[M+H]^+$ = 399.9189; $C_{14}H_{12}NBrI$ requires 399.9192.

IR (film) ν_{max}/cm^{-1} 3004, 1580, 1485, 1403, 1300, 1190, 1146, 987, 864, 836, 749.

1-(3-Iodobicyclo[1.1.1]pentan-1-yl)isoquinoline, 54

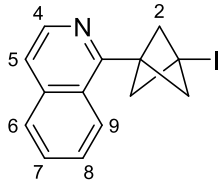

fac-Ir(ppy)$_3$ (2.5 mg, 4 µmol, 0.025 equiv.), 1-iodoisoquinoline (38 mg, 0.15 mmol, 1.0 equiv.) and TCP (0.33 mL, 0.9 M in Et_2O, 0.30 mmol, 2.0 equiv.) in *t*-BuCN (1.0 mL) were submitted to **General Procedure 1** at room temperature for 16 h. Purification by column chromatography (SiO_2, pentane / EtOAc, 9:1) afforded **54** (32 mg, 0.10 mmol, 66%) as a white solid.

R_f = 0.33 (pentane / EtOAc, 9:1)

m.p. = 123-125 °C

^{1}H NMR (400 MHz, $CDCl_3$) δ 8.44 (1H, d, *J* = 5.7 Hz, H4), 8.28 (1H, dt, *J* = 8.4, 1.1 Hz, ArH), 7.83 (1H, dt, *J* = 8.4, 1.1 Hz, ArH), 7.68 (1H, ddd, *J* = 8.4, 6.8, 1.1 Hz, ArH), 7.62-7.55 (2H, m, ArH), 2.98 (6H, s, H2).

^{13}C NMR (101 MHz, $CDCl_3$) δ 155.7, 142.0, 136.6, 130.1, 127.7, 127.3, 127.0, 125.5, 120.7, 63.1, 52.3, 8.3.

HRMS ($APCI^+$) Found $[M+H]^+$ = 329.0030; $C_{13}H_{14}O_2I$ requires 329.0033.

IR (film) ν_{max}/cm^{-1} 2998, 2919, 2362, 1583, 1392, 1194, 1171, 847, 823, 741, 666.

3-Chloro-2-(3-iodobicyclo[1.1.1]pentan-1-yl)pyridine, 55

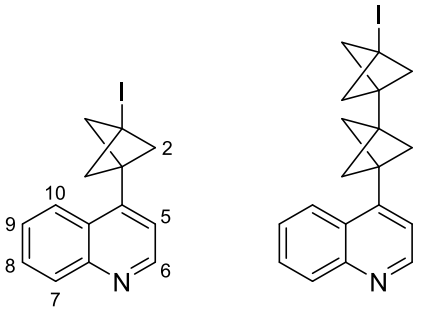

55 **55s**

fac-Ir(ppy)$_3$ (7 mg, 0.011 mmol, 0.025 equiv.), 4-iodoquinoline (109 mg, 0.43 mmol, 1.0 equiv.) and TCP (1.0 mL, 0.9 M in Et_2O, 0.86 mmol, 2.0 equiv.) in *t*-BuCN (2.9 mL) were submitted to **General Procedure 1** at room temperature for 18 h. Purification by column chromatography (SiO_2, pentane / Et_2O, 9:1→4:1) gave **55** and **55s** (72 mg, 1:0.05 ratio of **55**:**55s** isolated as an inseparable mixture, 49% yield of **55**, as determined by ^{1}H NMR spectroscopy), as a clear oil.

^{1}H NMR (500 MHz, $CDCl_3$) δ 8.83 (1H, d, *J* = 4.4 Hz, H5), 8.17-8.09 (2H, m, H7, H10), 7.72 (1H, ddd, *J* = 8.4, 6.9, 1.4 Hz, ArH), 7.57 (1H, ddd, *J* = 8.4, 6.9, 1.4 Hz, ArH), 7.06 (1H, d, *J* = 4.4 Hz, H4), 2.90 (6H, s, H2).

^{13}C NMR (101 MHz, $CDCl_3$) δ 150.2, 148.7, 143.2, 130.6, 129.4, 127.0, 126.7, 124.5, 120.3, 62.6, 50.4, 6.4.

HRMS (ESI$^+$) Found $[M+H]^+$ = 322.0079; $C_{14}H_{13}NI$ requires 322.0087.

IR (film) ν_{max}/cm^{-1} 2993, 2913, 1584, 1508, 1205, 845.

Reaction and characterisation by Dr James Mousseau.

7-Chloro-4-(3-iodobicyclo[1.1.1]pentan-1-yl)quinolone, 56

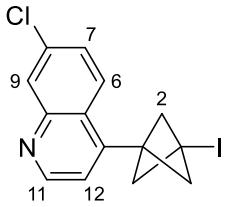

56

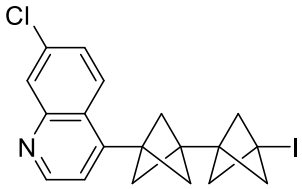

56s

fac-Ir(ppy)$_3$ (2.5 mg, 4 µmol, 0.025 equiv.), 7-chloro-4-iodoquinoline (43 mg, 0.15 mmol, 1.0 equiv.) and TCP (0.33 mL, 0.9 M in Et_2O, 0.30 mmol, 2.0 equiv.) in *t*-BuCN (1.0 mL) were submitted to **General Procedure 1** at room temperature for 16 h. Purification by column chromatography (SiO_2, pentane / EtOAc, 9:1) afforded **56** and **56s** (22 mg, 1:0.11 ratio of **56**:**56s** isolated as an inseparable mixture, 36% yield of **56**, as determined by ^{1}H NMR spectroscopy), as a white solid.

R_f = 0.34 (pentane / EtOAc, 4:1)

m.p. = 123-125 °C

^{1}H NMR (400 MHz, $CDCl_3$) δ 8.82 (1H, d, *J* = 4.4 Hz, H11), 8.11 (1H, d, *J* = 2.2 Hz, H9), 8.07 (1H, d, *J* = 9.0 Hz, H6), 7.51 (1H, dd, *J* = 9.0, 2.2 Hz, H7), 7.05 (1H, d, *J* = 4.4 Hz, H12), 2.88 (6H, s, H2).

^{13}C NMR (101 MHz, $CDCl_3$) δ 151.3, 149.2, 143.3, 135.2, 129.5, 127.7, 125.8, 125.3, 120.4, 62.5, 53.0, 6.1.

HRMS (ESI^+) Found $[M+H]^+$ = 355.9709; $C_{14}H_{12}NClI$ requires 355.9698.

IR (film) ν_{max}/cm^{-1} 2992, 2915, 2359, 1605, 1583, 1498, 1419, 1206, 1145, 1073, 872, 640.

Methyl 4-hydroxy-8-(3-iodobicyclo[1.1.1]pentan-1-yl)quinoline-3-carboxylate, 57

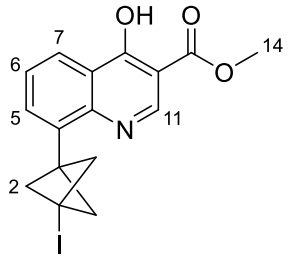

fac-Ir(ppy)$_3$ (2.5 mg, 4 µmol, 0.025 equiv.), methyl 4-hydroxy-8-iodoquinoline-3-carboxylate (50 mg, 0.15 mmol, 1.0 equiv.) and TCP (0.33 mL, 0.9 M in Et_2O, 0.30 mmol, 2.0 equiv.) in *t*-BuCN (1.0 mL) were submitted to **General Procedure 1** at room temperature for 16 h. Purification by column chromatography (SiO_2, pentane / EtOAc, 4:1) afforded **57** (32 mg, 0.08 mmol, 53%) as a white solid.

R_f = 0.50 (pentane / EtOAc, 7:3)

m.p. = 96-98 °C (decomp.)

^{1}H NMR (400 MHz, $CDCl_3$) δ 11.66 (1H, s, OH), 9.20 (1H, d, *J* = 0.9 Hz, H11), 8.34 (1H, dt, *J* = 8.4, 1.2 Hz, H7), 7.69 (1H, dd, *J* = 8.4, 7.2 Hz, H6), 7.41 (1H, dd, *J* = 7.2, 1.2 Hz, H5), 4.10 (3H, s, H14), 2.87 (6H, s, H2).

^{13}C NMR (101 MHz, $CDCl_3$) δ 171.0, 156.8, 140.8, 135.4, 130.3, 130.1, 129.8, 128.4, 122.9, 120.7, 63.1, 53.2, 50.5, 6.4.

HRMS (ESI$^+$) Found $[M+H]^+$ = 396.0091; $C_{16}H_{15}O_3NI$ requires 396.0091.

IR (film) ν_{max}/cm^{-1} 2923, 1661, 1578, 1458, 1386, 1352, 1273, 1212, 1195, 1161, 844, 796, 627.

4-Chloro-6-(3-iodobicyclo[1.1.1]pentan-1-yl)quinazoline, 58

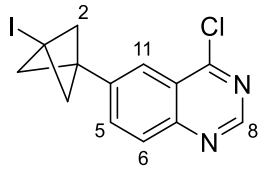

fac-Ir(ppy)$_3$ (2.5 mg, 4 µmol, 0.025 equiv.), 4-chloro-6-iodoquinazoline (44 mg, 0.15 mmol, 1.0 equiv.) and TCP (0.33 mL, 0.9 M in Et_2O, 0.30 mmol, 2.0 equiv.) in *t*-BuCN (1.0 mL) were submitted to **General Procedure 1** at room temperature for 16 h. Purification by column chromatography (SiO_2, pentane / EtOAc, 95:5) afforded **58** (16 mg, 0.04 mmol, 29%) as a pale yellow oil.

R_f = 0.15 (pentane / EtOAc, 95:5)

^{1}H NMR (400 MHz, $CDCl_3$) δ 9.03 (1H, s, H8), 8.03 (1H, d, *J* = 8.6 Hz, H6), 7.92 (1H, dd, *J* = 1.9, 0.6 Hz, H11), 7.76 (1H, dd, *J* = 8.6, 1.9 Hz, H5), 2.73 (6H, s H2).

^{13}C NMR (101 MHz, $CDCl_3$) δ 162.3, 153.8, 150.4, 139.8, 133.5, 129.3, 124.0, 122.5, 61.9, 50.3, 5.6.

HRMS (EI$^+$) Found $[M+H]^+$ = 356.9651; $C_{13}H_{11}N_2ClI$ requires 356.9650.

IR (film) ν_{max}/cm^{-1} 2360, 2342, 1564, 1193, 846.

5-Iodo-2-(3-iodobicyclo[1.1.1]pentan-1-yl)pyridine, 59

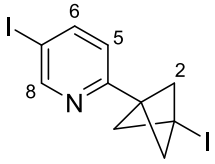

fac-Ir(ppy)$_3$ (2.5 mg, 4 µmol, 0.025 equiv.), 2,5-diiodopyridine (50 mg, 0.15 mmol, 1.0 equiv.) and TCP (0.33 mL, 0.9 M in Et_2O, 0.30 mmol, 2.0 equiv.) in *t*-BuCN (1.0 mL) were submitted to **General Procedure 1** at room temperature for 16 h. Purification by

column chromatography (SiO_2, pentane / Et_2O, 98:2) afforded **59** (37 mg, 0.09 mmol, 62%) as a white solid.

R_f = 0.40 (pentane / Et_2O, 95:5)

m.p. = 123-125 °C (decomp).

^{1}H NMR (400 MHz, $CDCl_3$) δ 8.72 (1H, dd, *J* = 2.2, 0.8 Hz, H8), 7.93 (1H, dd, *J* = 8.2, 2.2 Hz, H6), 6.90 (1H, dd, *J* = 8.2, 0.8 Hz, H5), 2.65 (6H, s, H2).

^{13}C NMR (101 MHz, $CDCl_3$) δ 155.9, 155.6, 144.8, 122.7, 91.6, 61.5, 50.7, 6.8.

HRMS (ESI^+) Found $[M+H]^+$ = 397.8900; $C_{10}H_{10}NI_2$ requires 397.8897.

IR (film) ν_{max}/cm^{-1} 2920, 2359, 2340, 1567, 1508, 1460, 1359, 1193, 1069, 999, 833, 668.

2,6-Bis(3-iodobicyclo[1.1.1]pentan-1-yl)pyridine, 60

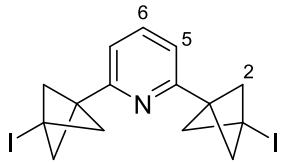

fac-$Ir(ppy)_3$ (2.5 mg, 4 µmol, 0.025 equiv.), 2,6-diiodopyridine (50 mg, 0.15 mmol, 1.0 equiv.) and TCP (0.66 mL, 0.9 M in Et_2O, 0.30 mmol, 4.0 equiv.) in *t*-BuCN (1.0 mL) were submitted to **General Procedure 1** at room temperature for 16 h. Purification by column chromatography (SiO_2, pentane / Et_2O, 95:5) afforded **60** (39 mg, 0.08 mmol, 56%) as a white solid.

R_f = 0.42 (pentane / Et_2O, 95:5).

m.p. = 84-86 °C (decomp.)

^{1}H NMR (400 MHz, $CDCl_3$) 7.53 (1H, t, *J* = 7.7 Hz, H6), 6.93 (2H, d, *J* = 7.7 Hz, H5), 2.63 (12H, s, H2).

^{13}C NMR (101 MHz, $CDCl_3$) δ 156.7, 136.7, 118.8, 61.7, 51.3, 7.9.

HRMS (ESI^+) Found $[M+H]^+$ = 463.9367; $C_{15}H_{16}NI_2$ requires 463.9367.

IR (film) ν_{max}/cm^{-1} 3000, 2916, 2360, 2341, 1587, 1565, 1455, 1196, 843, 667.

7.3.4 Formal synthesis of BCP-darapladib

3-(4-(Trifluoromethyl)phenyl)bicyclo[1.1.1]pentane-1-carboxylic acid, 78

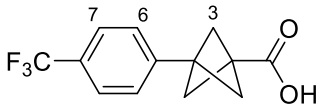

To a solution of **45** (60 mg, 0.18 mmol, 1.0 equiv.) in Et_2O (1.5 ml) cooled to –78 °C, was added *t*-BuLi (0.27 ml, 1.6 M in pentane, 0.36 mmol, 2.5 equiv.). After stirring for 30 min, $CO_{2\,(g)}$ was bubbled through the solution for 30 min. The resulting solution was warmed to room temperature and quenched with NH_4Cl (5 mL, sat. aq.). The mixture was then acidified to pH 1 with HCl (1 M, aq.) and extracted with EtOAc (3 × 10 ml), and the combined organic layers concentrated *in vacuo*. Purification by column chromatography (SiO_2, CH_2Cl_2 / MeOH, 95:5) afforded **78** (34 mg, 0.13 mmol, 73%) as a white solid.

^{1}H NMR (400 MHz, DMSO-d_6) δ 7.67 (2H, d, *J* = 8.0 Hz, H7), 7.45 (2H, d, *J* = 8.0 Hz, H6), 2.26 (6H, s, H3).

^{13}C NMR (101 MHz, DMSO-d_6) δ 171.1, 144.3, 127.6 (q, *J* = 31.8 Hz), 127.0, 125.2 (q, *J* = 3.9 Hz), 124.4 (q, *J* = 271.9 Hz), 52.6, 40.7, 36.9.

Spectroscopic data in agreement with that reported previously.

7.3.5 TCP Degradation experiments

To two screw-capped vials was added to a solution of TCP (0.33 mL, 0.9 M in Et_2O, 0.30 mmol) in *t*-BuCN (1.0 mL). To one of the vials was also added *fac*-Ir(ppy)$_3$ (2.5 mg, 4 µmol, 0.01 equiv.). Both vials were then sealed and placed under nitrogen, and the solution was degassed *via* three freeze-pump-thaw cycles (vacuum was only applied while the reaction mixture was frozen due to TCP volatility). The stirred mixtures were irradiated with blue LEDs and at the specified times, a 200 µL aliquot was removed using a microsyringe and added to an NMR tube containing dichloroethane (50 µL) of and $CDCl_3$ (0.4 mL). The concentration of the TCP was the determined by ^{1}H NMR spectroscopy using the DCE as an internal standard.

Time/ h	Concentration of TCP/ M	
	Without *fac*-Ir(ppy)$_3$	With *fac*-Ir(ppy)$_3$
0	0.58	0.58
0.5	0.58	0.58
1	0.57	0.56
2	0.58	0.53
4	0.51	0.50
6	0.52	0.43
24	0.34	0.16

Table 7.1 *– TCP degradation experiments with/without catalyst present.*

7.3.6 Light on/off experiment

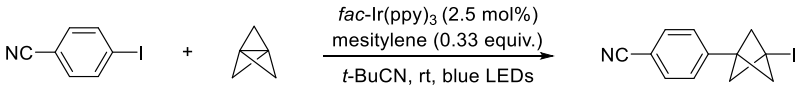

To a screw capped vial was added *fac*-Ir(ppy)$_3$ (2.5 mg, 4 µmol, 0.025 equiv.), 4-iodobenzonitrile (34 mg, 0.15 mmol, 1.0 equiv.), mesitylene (6.0 mg, 0.05mmol, 0.33 equiv.) and TCP (0.33 mL, 0.9 M in Et_2O, 0.30 mmol, 2.0 equiv.) in *t*-BuCN (1.0 mL).

The mixture was stirred under blue LED light irradiation for 1 hour, at which point an aliquot (100 μL) was taken of the reaction mixture, concentrated *in vacuo* and then diluted with $CDCl_3$ and analysed by ^1H NMR spectroscopy. The light was then switched off and the reaction stirred for 0.5 h, at which point an aliquot (100 μL) was taken of the reaction mixture, concentrated *in vacuo* and then diluted with $CDCl_3$ and analysed by ^1H NMR spectroscopy. The light was then switched on again and the reaction stirred for 1.5 h, at which point an aliquot (100 μL) was taken of the reaction mixture, concentrated *in vacuo* and then diluted with $CDCl_3$ and analysed by ^1H NMR spectroscopy. The light was then switched off and the reaction stirred for 0.5 h, at which point an aliquot (100 μL) was taken of the reaction mixture, concentrated *in vacuo* and then diluted with $CDCl_3$ and analysed by ^1H NMR spectroscopy. The light was then switched on again and the reaction stirred for 1 h, at which point an aliquot (100 μL) was taken of the reaction mixture, concentrated *in vacuo* and then diluted with $CDCl_3$ and analysed by ^1H NMR spectroscopy. The light was then switched off again and the reaction stirred for 0.5 h, at which point an aliquot (100 μL) was taken of the reaction mixture, concentrated *in vacuo* and then diluted with $CDCl_3$ and analysed by ^1H NMR spectroscopy. The light was then switched on again and the reaction stirred for 1 h, at which point an aliquot (100 μL) was taken of the reaction mixture, concentrated *in vacuo* and then diluted with $CDCl_3$ and analysed by ^1H NMR spectroscopy.

t/ h	conversion/ %
0	0
1	8
1.5	8
3	41
3.5	42
4.5	56
5	56
6	60

Table 7.2 *– Light on/off experiment*

7.3.7 Investigations towards the ATRA reaction of aryl bromides

1-(4-(3-Iodobicyclo[1.1.1]pentan-1-yl)phenyl)ethan-1-one, S1

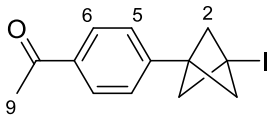

To a screw capped vial was added 1-(4-iodophenyl)ethan-1-one (243 mg, 1.0 mmol, 1.0 equiv.), *fac*-Ir(ppy)$_3$ (18 mg, 0.025 mmol, 0.025 equiv.), and TCP (0.9 mL, 0.7 M in Et_2O, 2.0 mmol, 2.0 equiv.) in *t*-BuCN (9 mL). The vial was then sealed and placed under nitrogen, and the solution was degassed *via* three freeze-pump-thaw cycles (vacuum was only applied while the reaction mixture was frozen due to TCP volatility). The stirred mixture was then irradiated with blue LEDs for 24 h and the reaction mixture concentrated *in vacuo*. Purification by column chromatography (SiO_2, pentane / Et_2O, 95:5) afforded **S1** (109 mg, 0.35 mmol, 35%) as a colourless tacky solid.

R_f = 0.26 (pentane / EtOAc, 95:5)

^{1}H NMR (400 MHz, $CDCl_3$) δ 7.92 – 7.88 (2H, m, ArH), 7.22 – 7.19 (2H, m, ArH), 2.62 (6H, s, H2), 2.58 (3H, s, H9)

^{13}C NMR (101 MHz, $CDCl_3$) δ 197.6, 143.5, 136.0, 128.7, 126.4, 61.9, 50.3, 29.8, 26.8, 6.3

HRMS (ESI$^+$) $[M+H]^+$ = 313.0085; $C_{13}H_{14}OI$ requires 313.0084.

IR (film) ν_{max}/cm^{-1} 2995, 2360, 1685, 1605, 1403, 1292, 1271, 1194.

1-(4-(Bicyclo[1.1.1]pentan-1-yl)phenyl)ethan-1-one, 84

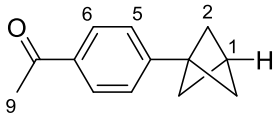

To a solution of **S1** (40 mg, 0.13 mmol, 1.0 equiv.) in MeOH (0.32 mL) and THF (0.15 mL), was added TTMSS (48 μL, 0.15 mmol, 1.2 equiv.). BEt_3 (13 μL, 0.1 M in hexanes, 0.013 mmol, 0.1 equiv.) was then added via syringe (needle tip in the solution), and the reaction was then stirred for 6 h. The reaction mixture was then concentrated *in vacuo* and purified by column chromatography (SiO_2, pentane → pentane / Et_2O, 95:5) to afford **84** (11.3 mg, 0.061 mmol, 47%) as a colourless oil.

R_f = 0.43 (pentane / EtOAc, 95:5)

^{1}H NMR (400 MHz, $CDCl_3$) δ 7.91 – 7.87 (2H, m, ArH), 7.30-7.25 (2H, m, ArH), 2.58 (3H, s, H9), 2.58 (1H, s, H1), 2.11 (6H, s, H2).

^{13}C NMR (101 MHz, $CDCl_3$) δ 198.0, 147.1, 135.5, 128.5, 126.3, 52.4, 47.1, 27.1, 26.8.

HRMS (ESI$^+$) $[M+H]^+$ = 187.1118; $C_{13}H_{15}O$ requires 187.1117.

IR (film) ν_{max}/cm^{-1} 2969, 2909, 2871, 2361, 1681, 1607, 1427, 1270, 1210.

7.4 Chapter 3: Kumada cross-coupling of BCP iodides

7.4.1 General Procedures

General Procedure 1: BEt_3-initiated bicyclopentylation of alkyl iodides

To a vial containing the specified halide (1.0 equiv.) was added [1.1.1]propellane (1.12.0 equiv., 0.5-0.7 M solution in Et_2O). BEt_3 (10 mol%, 1 M in hexane) was added to the solution via syringe (needle tip in the solution). After the indicated time the reaction was concentrated *in vacuo* and purified by column chromatography.

General Procedure 2: Formation of Grignard reagents

Mg turnings (88 mg, 3.6 mmol, 1.2 equiv.) were added to a flask which was then heated (heat gun) under vacuum for 2 minutes with stirring. To the cooled flask was added anhydrous THF (2.5 mL) and I_2 (1 crystal) before dropwise addition of the aryl halide (3 mmol, 1 equiv.). The mixture was then heated at reflux for 2 h (unless specified otherwise). The concentration of the resulting Grignard reagent was determined *via* iodometric titration.

General Procedure 3: Formation of Turbo Grignard reagents

Mg turnings (146 mg, 2.0 equiv., 6 mmol) and LiCl (140 mg, 1.1 equiv., 3.3 mmol) were added to a flask which was then heated (heat gun) under vacuum for 2 minutes with stirring. To the cooled flask was added anhydrous THF (3 mL) and DIBALH (0.15 mL, 1 M in hexanes or toluene, 0.05 equiv., 0.15 mmol). After 5 mins at room temperature, the halide (1 equiv., 3 mmol) was added at the specified temperature and stirred for the specified time. The concentration of the resulting Turbo Grignard reagent was determined *via* iodometric titration.

General Procedure 4: Kumada cross coupling of iodo-BCPs

To a flame-dried vial was added iodo-BCP (0.2 mmol, 1 equiv.) and $Fe(acac)_3$ (14 mg, 20 mol%, 0.04 mmol). The vial was then evacuated and refilled with $N_{2\ (g)}$ three times. To this was added THF (0.2 mL) and TMEDA (12 µL, 40 mol%, 0.08 mmol), and the resulting mixture was stirred for 5 min. The Grignard reagent (1.6 equiv., 0.32 mmol) was then added via syringe pump at a rate of 0.7 mL/h (over approximately 45 mins) at the specified temperature. The reaction was stirred for a further 1 h, then quenched by addition of aqueous HCl (5 mL, 1 M) or aqueous NH_4Cl (5 mL, saturated). The layers were separated, and the aqueous layer was extracted with Et_2O (3 × 10 mL). The combined organic layers were washed with brine, dried over $MgSO_4$ and concentrated *in vacuo*. The crude product was purified by column chromatography.

7.4.2 Synthesis of starting materials

1-Iodo-3-(4-(trifluoromethyl)benzyl)bicyclo[1.1.1]pentane, 114

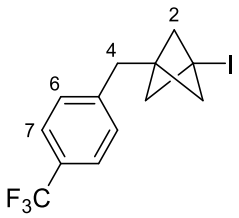

fac-$Ir(ppy)_3$ (2.5 mg, 4 µmol, 0.025 equiv.), 1-(iodomethyl)-4-(trifluoromethyl)benzene (43 mg, 0.15 mmol, 1.0 equiv.) and TCP (0.33 mL, 0.9 M in Et_2O, 0.30 mmol, 2.0 equiv.) in *t*-BuCN (1.5 mL) were submitted to General Procedure **1** at room temperature for 16 h. Purification by column chromatography (SiO_2, pentane) afforded **114** (45 mg, 0.13 mmol, 85%) as white solid.

$\mathbf{R_f}$ = 0.48 (pentane)

^{1}H NMR (400 MHz, CDCl3) δ 7.55 (2H, d, J = 8.0 Hz, H7), 7.17 (2H, d, J = 8.0 Hz, H6), 2.87 (2H, s, H4), 2.16 (6H, s, H2).

^{13}C NMR (101 MHz, CDCl3) δ 142.4, 129.2, 129.0 (q, J = 33.3 Hz), 125.5 (q, J = 3.8 Hz), 124.4 (q, J = 271.8 Hz), 60.3, 47.9, 39.1, 7.6.

Spectroscopic data in agreement with that reported previously.[3]

tert-Butyl 4-(3-iodobicyclo[1.1.1]pentan-1-yl)piperidine-1-carboxylate, 117

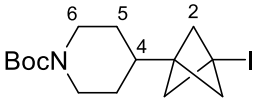

tert-Butyl 4-iodopiperidine-1-carboxylate (156 mg, 0.50 mmol, 1.0 equiv.), [1.1.1]propellane (1.7 mL, 0.54 M in Et_2O, 0.90 mmol, 1.8 equiv.) and BEt_3 (50 µL, 1.0 M in Et_2O, 0.05 mmol, 0.1 equiv.) were subjected to **General Procedure 1** at room temperature for 2 h. Purification by column chromatography (SiO_2, pentane / EtOAc, 100:0 to 95:5) afforded **117** (155 mg, 0.31 mmol, 61%) as a white solid.

R_f 0.43 (pentane / EtOAc, 95:5)

m.p. 50-52 °C

^{1}H NMR (400 MHz, $CDCl_3$) δ 4.16-4.06 (2H, m, H6), 2.61 (2H, app t, *J* = 12.7 Hz, H6), 2.16 (6H, s, H2), 1.63-1.49 (3H, m, H4, H5), 1.44 (9H, s, *t*-Bu) 1.06 (2H, app qd, *J* = 12.7, 4.4 Hz, H5).

^{13}C NMR (101 MHz, $CDCl_3$) δ 154.9, 79.6, 58.6, 51.6, 43.6, 37.9, 28.8, 28.6, 7.9.

HRMS [ESI^+, EI^+, CI^+] Not found.

IR (film) ν_{max}/cm^{-1} 2974, 2929, 2852, 1691, 1421, 1171, 769.

Additional BCP iodides

The following BCP iodides were also used in the Kumada cross-coupling reaction (see **Chapter 3.4**, **Figure 3.17**). Iodides **S3** and **S5** had been previously synthesised by Dimitri Caputo and were available in the lab.[3] Iodides **S4** and **S7** had been previously synthesised by Dr Jeremy Nugent and were available in the lab.[4] Iodides **S1** and **S6** were new and were synthesised by Dr Jeremy Nugent.

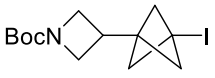

S2

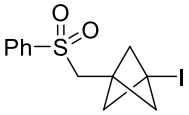

S3

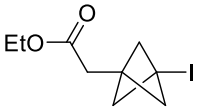

S4

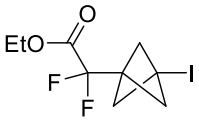

S5

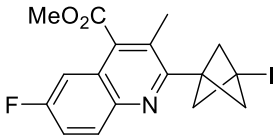

S6

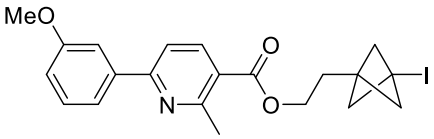

S7

7.4.3 Reaction Scope

1-(4-Methoxyphenyl)-3-(4-(trifluoromethyl)benzyl)bicyclo[1.1.1]pentane, 115

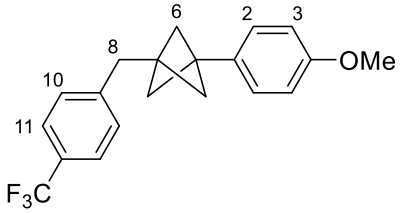

114 (70 mg, 0.20 mmol, 1.0 equiv.), $Fe(acac)_3$ (14 mg, 0.04 mmol, 20 mol%), TMEDA (12 µL, 0.08 mmol, 40 mol%) and 4-methoxyphenylmagnesium bromide (0.44 mL, 0.9 M in THF, 0.32 mmol, 1.6 equiv.) were submitted to **General Procedure 4** at room temperature. The reaction was quenched with aqueous HCl (5 mL, 1 M). Purification by

column chromatography (SiO_2, pentane / Et_2O, 1:0 to 98:2) afforded **115** (57 mg, 0.17 mmol, 86%) as a colourless oil.

R_f 0.12 (pentane)

^{1}H NMR (500 MHz, $CDCl_3$) δ 7.56 (2H, d, *J* = 7.9 Hz, ArH), 7.27-7.22 (2H, d, *J* = 7.9, ArH), 7.11–7.06 (2H, m, ArH), 6.84-6.78 (2H, m, ArH), 3.78 (3H, s, OMe), 2.90 (2H, s, H8), 1.84 (6H, s, H6).

^{13}C NMR (126 MHz, $CDCl_3$) δ 158.4, 143.9, 133.5, 129.4, 128.4 (q, *J* = 32.3 Hz), 127.2, 125.3 (q, *J* = 3.8 Hz), 124.6 (q, *J* = 271.7 Hz), 113.7, 55.4, 52.3, 42.2, 39.1, 38.7.

^{19}F NMR (471 MHz, $CDCl_3$) δ –62.2.

HRMS (CI^+) Found $[M+H]^+$ = 333.1463; $C_{20}H_{20}OF_3$ requires 333.1461.

IR (film) ν_{max}/cm^{-1} 2965, 2867, 2871, 1615, 1517, 1317, 1244, 1161, 1115, 1062, 1040.

***N,N*-Dimethyl-4-(3-(4-(trifluoromethyl)benzyl)bicyclo[1.1.1]pentan-1-yl)aniline, 118**

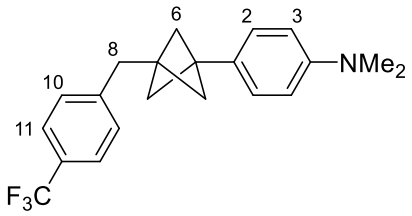

4-(*N,N*-Dimethyl)aniline magnesium bromide: 4-Bromo-*N,N*-dimethylaniline (600 mg, 3.0 mmol, 1.0 equiv.), and Mg turnings (88 mg, 3.6 mmol, 1.2 equiv.) were submitted to **General Procedure 2** to give 4-(*N,N*-dimethyl)aniline magnesium bromide as a 1.0 M solution in THF.

114 (70 mg, 0.20 mmol, 1.0 equiv.), $Fe(acac)_3$ (14 mg, 0.04 mmol, 20 mol%), TMEDA (12 μL, 0.08 mmol, 40 mol%) and 4-(*N,N*-dimethyl)aniline magnesium bromide (0.32 mL, 1.0 M in THF, 0.32 mmol, 1.6 equiv.) were submitted to **General Procedure 4** at

room temperature. The reaction was quenched with aqueous HCl (5 mL, 1 M). Purification by column chromatography (SiO_2, pentane / Et_2O, 98:2) afforded **118** (37 mg, 0.11 mmol, 53%) as a white solid.

R_f 0.47 (pentane / Et_2O, 96:4)

m.p. 100-102 °C

^{1}H NMR (400 MHz, $CDCl_3$) δ 7.58 (2H, d, *J* = 8.0 Hz, H11), 7.29-7.23 (2H, d, *J* = 8.0 Hz, H10), 7.12-7.04 (2H, m, H2), 6.75-6.67 (2H, m, H3), 2.92 (6H, s, NMe_2), 2.91 (2H, s, H8), 1.85 (6H, s, H6).

^{13}C NMR (101 MHz, $CDCl_3$) δ 149.6, 144.0, 129.5, 129.4, 128.3 (q, *J* = 31.6 Hz), 126.8, 125.3 (q, *J* = 3.9 Hz), 124.6 (q, *J* = 271.6 Hz), 112.7, 52.2, 42.2, 41.0, 39.2, 38.7.

^{19}F NMR (376 MHz, $CDCl_3$), δ –62.2.

HRMS (ESI^+) Found $[M+H]^+$ = 346.1774; $C_{21}H_{23}NF_3$ requires 346.1777.

IR (film) ν_{max}/cm^{-1} 2969, 2906, 2869, 1614, 1525, 1323, 1157, 1114, 1066.

Reaction and characterisation performed by Dr Jeremy Nugent.

1-(4-(Trifluoromethoxy)phenyl)-3-(4(trifluoromethyl)benzyl)bicyclo[1.1.1]pentane, 119

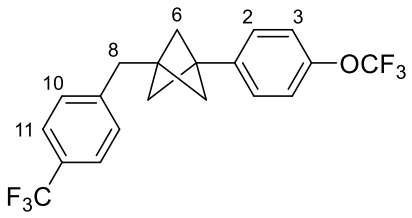

4-Trifluoromethoxyphenylmagnesium bromide: 1-Bromo-4-(trifluoromethoxy)benzene (0.45 mL, 3.0 mmol, 1.0 equiv.), and Mg turnings (88 mg, 3.6 mmol, 1.2 equiv.) were submitted to **General Procedure 2** to give 4-trifluoromethoxyphenylmagnesium bromide as a 1.0 M solution in THF.

114 (70 mg, 0.20 mmol, 1.0 equiv.), $Fe(acac)_3$ (14 mg, 0.04 mmol, 20 mol%), TMEDA (12 μL, 0.08 mmol, 40 mol%) and 4-trifluoromethoxyphenylmagnesium bromide (0.32 mL, 1.0 M in THF, 0.32 mmol, 1.6 equiv.) were submitted to **General Procedure 4** at room temperature. The reaction was quenched with aqueous HCl (5 mL, 1 M). Purification by column chromatography (SiO_2, pentane / Et_2O, 98:2) afforded **119** (60 mg, 0.16 mmol, 78%) as a white solid.

R_f 0.32 (pentane)

m.p. 59-60 °C

^{1}H NMR (400 MHz, CD_3OD) δ 7.60-7.56 (2H, d, *J* = 8.1 Hz, H11), 7.35-7.30 (2H, d, *J* = 8.1 Hz, H10), 7.24-7.19 (2H, m, H2), 7.12 (2H, m, H3), 2.93 (2H, s, H8), 1.86 (6H, s, H6).

^{13}C NMR (101 MHz, CD_3OD) δ 149.1 (q, *J* = 1.6 Hz), 145.3, 141.6, 130.6, 129.4 (q, *J* = 32.1 Hz), 128.6, 126.2 (q, *J* = 3.6 Hz), 125.9 (q, *J* = 270.8 Hz), 121.9 (q, *J* = 253.2), 121.7, 53.0, 42.8, 39.8, 39.5.

^{19}F NMR (376 MHz, CD_3OD) δ –55.6, –59.8.

HRMS (CI^+) Found $[M+H]^+$ = 387.1175; $C_{20}H_{17}OF_6$ requires 387.1178.

IR (film) ν_{max}/cm^{-1} 2967, 2871, 1326, 1261, 1224, 1162, 1124, 1067, 1020.

Reaction and characterisation performed by Dr Jeremy Nugent.

1-(4-Fluorophenyl)-3-(4-(trifluoromethyl)benzyl)bicyclo[1.1.1]pentane, 120

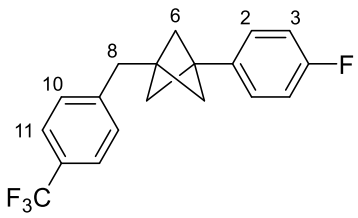

4-Fluorophenylmagnesium bromide: 4-Bromo-fluorobenzene (0.33 mL, 3.0 mmol, 1.0 equiv.) and Mg turnings (88 mg, 3.6 mmol, 1.2 equiv.) were submitted to **General Procedure 2** at room temperature for 1 h to give 4-fluorophenylmagnesium bromide as a 0.7 M solution in THF.

114 (70 mg, 0.20 mmol, 1.0 equiv.), $Fe(acac)_3$ (14 mg, 0.04 mmol, 20 mol%), TMEDA (12 μL, 0.08 mmol, 40 mol%) and 4-fluorophenylmagnesium bromide (0.45 mL, 0.7 M in THF, 0.32 mmol, 1.6 equiv.,) were submitted to **General Procedure 4** at room temperature. The reaction was quenched with aqueous HCl (5 mL, 1 M). Purification by column chromatography (SiO_2, pentane) afforded **120** (45 mg, 0.14 mmol, 71%) as a white solid.

R_f 0.57 (pentane)

m.p. 58-60 °C

^{1}H NMR (400 MHz, $CDCl_3$) δ 7.58 (2H, d, *J* = 7.9 Hz, H11), 7.26 (2H, d, *J* = 7.9 Hz, H10), 7.16-7.09 (2H, m, H2), 7.00-6.92 (2H, m, H3), 2.92 (2H, s, H8), 1.88 (6H, s, H6).

^{13}C NMR (101 MHz, $CDCl_3$) δ 161.8 (d, *J* = 244.2 Hz), 143.7, 137.0 (d, *J* = 3.2 Hz), 129.4, 128.5 (q, *J* = 32.2 Hz), 127.7 (d, *J* = 8.0 Hz), 125.4 (q, *J* = 3.7 Hz), 124.6 (q, *J* = 271.3 Hz), 115.0 (d, *J* = 21.6 Hz), 52.3, 42.1, 39.0, 38.8.

^{19}F NMR (376 MHz, CDCl3) δ –62.2, –116.6.

HRMS (CI^+) Found $[M+H]^+$ = 321.1265; $C_{19}H_{17}F_4$ requires 321.1261.

IR (film) ν_{max}/cm^{-1} 2969, 2908, 2869, 1519, 1503, 1325, 1162, 1124.

1-(3-Methoxyphenyl)-3-(4-(trifluoromethyl)benzyl)bicyclo[1.1.1]pentane, 121

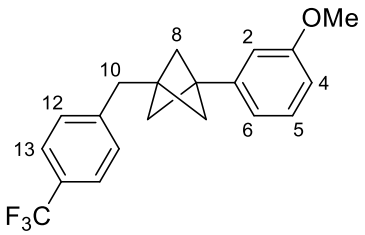

114 (70 mg, 0.20 mmol, 1.0 equiv.), $Fe(acac)_3$ (14 mg, 0.04 mmol, 20 mol%), TMEDA (12 μL, 0.08 mmol, 40 mol%) and 3-methoxyphenylmagnesium bromide (0.32 mL, 1 M in THF, 0.32 mmol, 1.6 equiv.) were submitted to **General Procedure 4** at room temperature. The reaction was quenched with aqueous HCl (5 mL, 1 M). Purification by column chromatography (SiO_2, pentane / Et_2O, 1:0 to 98:2) afforded **121** (48 mg, 0.15 mmol, 73%) as a colourless oil.

R_f 0.14 (pentane / Et_2O, 98:2).

^{1}H NMR (400 MHz, $CDCl_3$) δ 7.58 (2H, d, *J* = 8.5 Hz, H13), 7.27 (2H, d, *J* = 8.5 Hz, H12), 7.21 (1H, app t, *J* = 7.8 Hz, ArH), 6.80-6.73 (3H, m, ArH), 3.80 (3H, s, OMe), 2.93 (2H, s, H10), 1.89 (6H, s, H8).

^{13}C NMR (101 MHz, $CDCl_3$) δ 159.7, 143.8, 142.8, 129.4, 129.3, 128.4 (q, *J* = 32.9 Hz), 125.3 (q, *J* = 3.7 Hz), 122.6 (q, *J* = 272.3 Hz), 118.5, 111.9, 111.8, 55.3, 52.2, 42.6, 39.0, 38.8.

^{19}F NMR (376 MHz, $CDCl_3$) δ –62.2.

HRMS (CI^+) Found $[M+H]^+$ = 333.1462; $C_{20}H_{20}OF_3$ requires 333.1461.

IR (film) ν_{max}/cm^{-1} 2962, 1603, 1582, 1434, 1322, 1160, 1066, 696.

1-(2-Methoxyphenyl)-3-(4-(trifluoromethyl)benzyl)bicyclo[1.1.1]pentane, 122

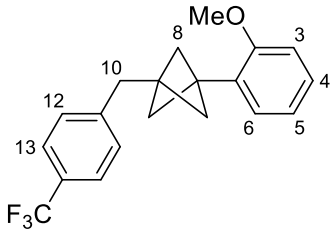

2-Methoxyphenylmagnesium bromide: 2-Bromoanisole (0.37 mL, 3 mmol, 1.0 equiv.), and Mg turnings (88 mg, 3.6 mmol, 1.2 equiv.) were submitted to **General Procedure 2** to give 2-methoxyphenylmagnesium bromide as a 0.7 M solution in THF.

114 (70 mg, 0.20 mmol, 1.0 equiv.), $Fe(acac)_3$ (14 mg, 0.04 mmol, 20 mol%), TMEDA (12 mL, 0.08 mmol, 40 mol%) and 2-methoxyphenylmagnesium bromide (0.45 mL, 0.7 M in THF, 0.32 mmol, 1.6 equiv.) were submitted to **General Procedure 4** at 45 °C. The reaction was quenched with aqueous HCl (5 mL, 1 M). Purification by column chromatography (SiO_2, pentane) afforded **122** (49 mg, 0.15 mmol, 74%) as a white solid.

R_f = 0.21 (pentane / Et_2O, 98:2)

m.p. 81-83 °C

^{1}H NMR (400 MHz, $CDCl_3$) δ 7.62-7.57 (2H, m, H13), 7.31-7.26 (2H, m, H12), 7.21 (1H, ddd, *J* = 8.2, 7.4, 1.8 Hz, ArH), 7.06 (1H, dd, *J* = 7.4, 1.8 Hz, ArH), 6.89 (1H, app td, *J* = 7.4, 1.1 Hz, ArH), 6.83 (1H, dd, *J* = 8.3, 1.1 Hz, ArH), 3.81 (3H, s, OMe), 2.93 (2H, s, H10), 1.97 (6H, s, H8).

^{13}C NMR (101 MHz, $CDCl_3$) δ 158.9, 144.1, 129.4, 128.8, 128.4, 128.2 (q, *J* = 32.2 Hz), 128.0, 125.3 (q, *J* = 3.7 Hz), 123.3 (q, *J* = 271.9 Hz), 120.2, 110.5, 55.2, 52.2, 41.1, 40.3, 39.2.

^{19}F NMR (376 MHz, $CDCl_3$) δ –62.2.

HRMS (CI^+) Found $[M+H]^+$ = 333.1463; $C_{20}H_{20}OF_3$ requires 333.1461.

IR (film) ν_{max}/cm^{-1} 2970, 2870, 1492, 1324, 1162, 1116, 752.

1-(5-Fluoro-2-methoxyphenyl)-3-(4-(trifluoromethyl)benzyl)bicyclo[1.1.1]pentane, 123

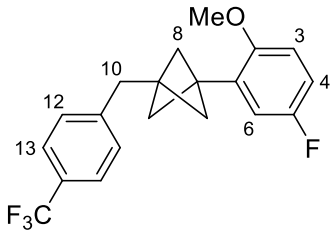

2-Methoxy-5-fluorophenylmagnesium bromide: 2-Bromo-4-fluoro-1-methoxybenzene (0.33 mL, 3.0 mmol, 1.0 equiv.) and Mg turnings (88 mg, 3.6 mmol, 1.2 equiv.) were submitted to **General Procedure 2** to give 2-methoxy-5-fluorophenylmagnesium bromide as a 1.0 M solution in THF.

114 (70 mg, 0.20 mmol, 1.0 equiv.), $Fe(acac)_3$ (14 mg, 0.04 mmol, 20 mol%), TMEDA (12 μL, 0.08 mmol, 40 mol%) and 2-methoxy-5-fluorophenylmagnesium bromide (0.32 mL, 1.0 M in THF, 0.32 mmol, 1.6 equiv.) were submitted to **General Procedure 4** at 45 °C. The reaction was quenched with aqueous HCl (5 mL, 1 M). Purification by column chromatography (SiO_2, pentane / Et_2O, 98:2) afforded **123** (50 mg, 0.143 mmol, 72%) as a white solid.

R_f 0.45 (pentane / Et_2O, 98:2)

m.p. 86-88 °C

^{1}H NMR (400 MHz, $CDCl_3$) δ 7.59-7.54 (2H, d, *J* = 7.9 Hz, H13), 7.27-7.23 (2H, d, *J* = 7.9 Hz, H12), 6.84 (1H, ddd, *J* = 8.8, 8.0, 3.2 Hz, ArH), 6.75-6.68 (2H, m, ArH), 3.75 (3H, s, OMe), 2.90 (2H, s, H10), 1.93 (6H, s, H8).

^{13}C NMR (101 MHz, $CDCl_3$) δ 157.0 (d, *J* = 238.6 Hz), 155.0 (d, *J* = 2.17), 143.9, 130.7 (d, *J* = 6.6 Hz), 129.4, 128.4 (q, *J* = 32.1 Hz), 125.3 (q, *J* = 3.8 Hz), 124.6 (q, *J* = 271.3 Hz), 115.3 (d, *J* = 22.2 Hz), 113.5 (d, *J* = 22.2 Hz), 111.4 (d, *J* = 6.7 Hz), 55.9, 52.2, 40.8, 40.3, 39.1.

^{19}F NMR (376 MHz, $CDCl_3$) δ −62.2, −124.8.

HRMS [ESI^+, EI^+, CI^+] Not found.

IR (film) ν_{max}/cm^{-1} 2966, 2906, 2866, 1615, 1330, 1110

Reaction and characterisation performed by Dr Jeremy Nugent.

5-(3-(4-(Trifluoromethyl)benzyl)bicyclo[1.1.1]pentan-1-yl)-2,3-dihydrobenzofuran, 124

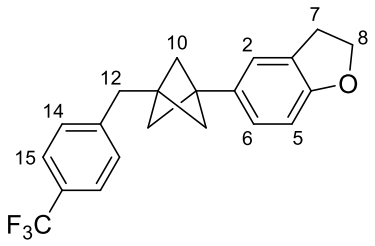

(2,3-Dihydrobenzofuran-5-yl)magnesium bromide: 5-Bromo-2,3-dihydrobenzofuran (597 mg, 3.0 mmol, 1.0 equiv.) and Mg turnings (88 mg, 3.6 mmol, 1.2 equiv.) were submitted to **General Procedure 2** to give (2,3-dihydrobenzofuran-5-yl)magnesium bromide as a 0.9 M solution in THF.

114 (70 mg, 0.20 mmol, 1.0 equiv.), $Fe(acac)_3$ (14 mg, 0.04 mmol, 20 mol%), TMEDA (12 μL, 0.08 mmol, 40 mol%) and (2,3-dihydrobenzofuran-5-yl)magnesium bromide (0.35 mL, 0.9 M in THF, 0.32 mmol, 1.6 equiv.) were submitted to **General Procedure 4** at room temperature. The reaction was quenched with aqueous HCl (5 mL, 1 M). Purification by column chromatography (SiO_2, pentane / Et_2O, 98:2) afforded **124** (48 mg, 0.14 mmol, 70%) as a white solid.

R_f 0.42 (pentane / Et_2O, 98:2)

m.p. 65-67 °C

^{1}H NMR (400 MHz, $CDCl_3$) δ 7.56 (2H, d, *J* = 8.0 Hz, H15), 7.25 (2H, d, *J* = 8.0 Hz, H14), 7.02 (1H, d, *J* = 1.4 Hz, H2), 6.92-6.89 (1H, m, H6), 6.69 (1H, d, *J* = 8.1 Hz, H5), 4.53 (2H, t, *J* = 8.7 Hz, H8), 3.16 (2H, t, *J* = 8.7 Hz, H7), 2.90 (2H, s, H12), 1.84 (6H, s, H10).

^{13}C NMR (101 MHz, $CDCl_3$) δ 158.9, 143.9, 133.5, 129.4, 128.4 (q, *J* = 32.6 Hz), 127.0, 125.7, 125.3 (q, *J* = 3.8 Hz), 124.6 (q, *J* = 270.3), 122.8, 108.9, 71.3, 52.3, 42.4, 39.1, 38.6, 29.8.

^{19}F NMR (376 MHz, $CDCl_3$) δ –62.2.

HRMS (ESI^+) Found $[M+H]^+$ = 345.1461; $C_{21}H_{20}OF_3$ requires 345.1461.

IR (film) ν_{max}/cm^{-1} 2962, 2905, 2866, 1492, 1323, 1162, 1117, 822.

Reaction and characterisation performed by Dr Jeremy Nugent.

5-(3-(4-(Trifluoromethyl)benzyl)bicyclo[1.1.1]pentan-1-yl)benzo[d][1,3]dioxole, 125

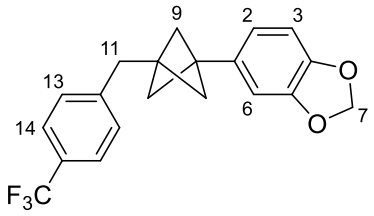

Benzo[*d*][1,3]dioxol-5-ylmagnesium bromide: 5-Bromo-1,3-benzodioxole (0.36 mL, 3.0 mmol, 1.0 equiv.) and Mg turnings (88 mg, 3.6 mmol, 1.2 equiv.) were submitted to **General Procedure 2** to give benzo[*d*][1,3]dioxol-5-ylmagnesium bromide as a 1.1 M solution in THF.

114 (70 mg, 0.20 mmol, 1.0 equiv.), $Fe(acac)_3$ (14 mg, 0.04 mmol, 20 mol%), TMEDA (12 μL, 0.08 mmol, 40 mol%) and benzo[*d*][1,3]dioxol-5-ylmagnesium bromide (0.30 mL, 1.1 M in THF, 0.32 mmol, 1.6 equiv.) were submitted to **General Procedure 4** at room temperature. The reaction was quenched with aqueous HCl (5 mL, 1 M). Purification by column chromatography (SiO_2, pentane / Et_2O, 98:2) afforded **125** (50 mg, 0.14 mmol, 72%) as a white solid.

R_f 0.22 (pentane)

m.p. 64-66 °C

^{1}H NMR (400 MHz, $CDCl_3$) δ 7.57 (2H, d, *J* = 8.1 Hz, H14), 7.25 (2H, d, *J* = 8.1 Hz, H13), 6.72 (1H, d, *J* = 7.9 Hz, H3), 6.66 (1H, d, *J* = 1.6 Hz, H6), 6.61 (1H, dd, *J* = 7.9, 1.6 Hz, H2), 5.90 (2H, s, H7), 2.90 (2H, s, H11), 1.83 (6H, s, H9).

^{13}C NMR (101 MHz, $CDCl_3$) δ 147.6, 146.3, 143.8, 135.3, 129.3, 128.4 (q, *J* = 32.6 Hz), 125.3 (q, *J* = 3.8 Hz), 124.6 (q, *J* = 271.1 Hz), 119.1, 108.1, 106.8, 101.0, 52.3, 42.5, 39.0, 38.6.

^{19}F NMR (376 MHz, $CDCl_3$) δ –62.2.

HRMS (ESI) Found $[M+H]^+$ = 347.1255; $C_{20}H_{18}O_2F_3$ requires 347.1253.

IR (film) ν_{max}/cm^{-1} 2964, 2906, 1489, 1439, 1323, 1117

Reaction and characterisation performed by Dr Jeremy Nugent.

tert-Butyl 4-(3-phenylbicyclo[1.1.1]pentan-1-yl)piperidine-1-carboxylate, 126

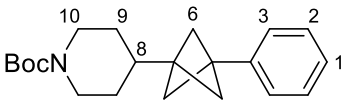

117 (76 mg, 0.20 mmol, 1.0 equiv.), $Fe(acac)_3$ (14 mg, 0.04 mmol, 20 mol%), TMEDA (12 μL, 0.08 mmol, 40 mol%) and phenylmagnesium bromide (0.32 mL, 1.0 M in THF,

0.32 mmol, 1.6 equiv.) were submitted to **General Procedure 4** at room temperature. The reaction was quenched with aqueous NH_4Cl (5 mL, saturated). Purification by column chromatography (SiO_2, pentane / Et_2O, 90:10) afforded **126** (54 mg, 0.17 mmol, 83%) as a white solid.

R_f 0.25 (pentane / Et_2O, 90:10)

m.p. 100-102 °C

^{1}H NMR (400 MHz, $CDCl_3$) δ 7.35-7.28 (2H, m, ArH), 7.26-7.20 (3H, m, ArH), 4.23-4.09 (2H, m, H10), 2.70 (2H, app t, *J* = 12.9 Hz, H10), 1.88 (6H, s, H6), 1.74-1.52 (3H, m, H8, H9), 1.50 (9H, s, *t*-Bu), 1.24-1.08 (2H, m, H9).

^{13}C NMR (101 MHz, $CDCl_3$) δ 155.0, 141.5, 128.2, 126.4, 126.1, 79.4, 50.0, 43.9, 41.9, 41.0, 36.6, 28.62, 28.57.

HRMS (ESI$^+$) Found $[M+H]^+$ = 328.2273; $C_{21}H_{30}O_2N$ requires 328.2271.

IR (film) ν_{max}/cm^{-1} 2964, 2865, 1691, 1423, 1235, 1161, 698.

Reaction and characterisation performed by Dr Jeremy Nugent.

tert-Butyl 4-(3-(4-methoxyphenyl)bicyclo[1.1.1]pentan-1-yl)piperidine-1-carboxylate, xx

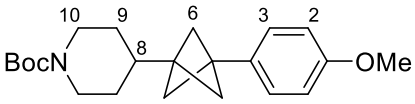

117 (83 mg, 0.22 mmol, 1.0 equiv.), $Fe(acac)_3$ (16 mg, 0.04 mmol, 20 mol%), TMEDA (13 μL, 0.09 mmol, 40 mol%) and 4-methoxyphenylmagnesium bromide (0.44 mL, 0.8 M in THF, 0.35 mmol, 1.6 equiv.) were submitted to **General Procedure 4** at room temperature. The reaction was quenched with aqueous NH_4Cl (5 mL, saturated).

Purification by column chromatography (SiO_2, pentane / EtOAc, 95:5) afforded **127** (63 mg, 0.18 mmol, 80%) as a white solid.

R_f 0.43 (pentane / EtOAc, 95:5)

m.p. 103-105 °C

^{1}H NMR (400 MHz, CD_3OD) δ 7.12-7.08 (2H, m, H3), 6.83-6.79 (2H, m, H2), 4.11 (2H, m, H10), 3.75 (3H, s, OMe), 2.71 (2H, m, H10), 1.81 (6H, s, H6), 1.67-1.53 (3H, m, H8, H9), 1.46 (9H, s, *t*-Bu), 1.16-1.01 (2H, m, H9).

^{13}C NMR (101 MHz, CD_3OD) δ 159.8, 156.5, 134.9, 128.0, 114.5, 80.9, 55.6, 50.8, 44.9, 42.5, 41.5, 37.7, 29.6, 28.7.

HRMS (ESI^+) Found $[M+Na]^+$ = 380.2196 ; $C_{22}H_{31}O_3NNa$ requires 380.2196.

IR (film) ν_{max}/cm^{-1} 2957, 2864, 2342, 1692, 1422, 1246, 1161

***tert*-Butyl 4-(3-(4-ethoxyphenyl)bicyclo[1.1.1]pentan-1-yl)piperidine-1-carboxylate, 128**

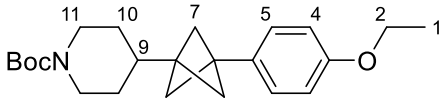

117 (76 mg, 0.20 mmol, 1.0 equiv.), $Fe(acac)_3$ (14 mg, 0.04 mmol, 20 mol%), TMEDA (12 μL, 0.08 mmol, 40 mol%) and 4-ethoxyphenylmagnesium bromide (0.32 mL, 1.0 M in THF, 0.32 mmol, 1.6 equiv.) were submitted to **General Procedure 4** at room temperature. The reaction was quenched with aqueous NH_4Cl (5 mL, saturated). Purification by column chromatography (SiO_2, pentane / EtOAc, 95:5) afforded **128** (57 mg, 0.15 mmol, 77%) as a colourless foam.

R_f 0.48 (pentane / EtOAc, 90:10)

^{1}H NMR (400 MHz, $CDCl_3$) δ 7.12 (2H, d, *J* = 8.7 Hz, ArH), 6.82 (2H, d, *J* = 8.7 Hz, ArH), 4.15 (2H, app d, *J* = 13.0 Hz, H11), 4.01 (2H, q, *J* = 7.0 Hz, H2), 2.66 (2H, td, *J* = 13.0, 2.6 Hz, H11), 1.81 (6H, s, H7), 1.66-1.48 (3H, m, H9, H10), 1.46 (9H, s, *t*Bu), 1.39 (3H, t, *J* = 7.0 Hz, H1) 1.19-1.06 (2H, m, H10).

^{13}C NMR (101 MHz, $CDCl_3$) δ 157.7, 155.0, 133.7, 127.2, 114.3, 79.4, 63.6, 50.1, 43.9, 41.7, 40.6, 36.6, 28.6, 28.6, 15.0.

HRMS (ESI^+) Found $[M+Na]^+$ = 394.2352; $C_{23}H_{33}O_3NNa$ requires 394.2352.

IR (film) ν_{max}/cm^{-1} 2960, 2857, 2332, 1691, 1425.

***tert*-Butyl 4-(3-(4-phenoxyphenyl)bicyclo[1.1.1]pentan-1-yl)piperidine-1-carboxylate, 129**

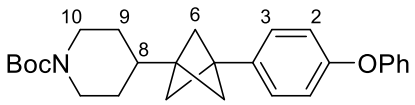

117 (76 mg, 0.20 mmol, 1.0 equiv.), $Fe(acac)_3$ (14 mg, 0.04 mmol, 20 mol%), TMEDA (12 μL, 0.08 mmol, 40 mol%) and 4-phenoxyphenylmagnesium bromide (0.36 mL, 0.9 M in THF, 0.32 mmol, 1.6 equiv.) were submitted to **General Procedure 4** at room temperature. The reaction was quenched with aqueous NH_4Cl (5 mL, saturated). Purification by column chromatography (SiO_2, pentane / EtOAc, 95:5) afforded **129** (71 mg, 0.15 mmol, 85%) as a white solid.

R_f 0.52 (pentane / EtOAc, 90:10)

m.p. 68-70 °C

^{1}H NMR (400 MHz, $CDCl_3$) δ 7.36-7.27 (2H, m, ArH), 7.22-7.14 (2H, m, ArH), 7.12-7.03 (1H, m, ArH), 7.03-6.95 (2H, m, ArH), 6.97-6.91 (2H, m, ArH), , 4.16 (2H, app d, J

= 13.1 Hz, H10), 2.67 (2H, td, J = 13.0, 2.6 Hz, H10), 1.85 (6H, s, H6), 1.70-1.51 (3H, m, H8, H9), 1.47 (9H, s, *t*Bu), 1.24-1.06 (2H, m, H9).

^{13}C NMR (101 MHz, $CDCl_3$) δ 157.7, 155.7, 155.0, 136.6, 129.8, 127.5, 123.1, 118.9, 118.7, 79.4, 50.1, 43.9, 41.8, 40.6, 36.6, 28.6, 28.6.

HRMS (ESI^+) Found $[M+Na]^+$ = 442.2353; $C_{27}H_{33}O_3NNa$ requires 442.2353.

IR (film) ν_{max}/cm^{-1} 2955, 2862, 2341, 1685, 1161.

tert-Butyl 4-(3-(_p_-tolyl)bicyclo[1.1.1]pentan-1-yl)piperidine-1-carboxylate, 130

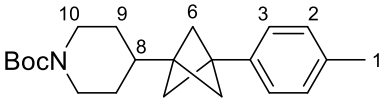

117 (76 mg, 0.20 mmol, 1.0 equiv.), $Fe(acac)_3$ (14 mg, 0.04 mmol, 20 mol%), TMEDA (12 μL, 0.08 mmol, 40 mol%) and 4-methylphenylmagnesium bromide (0.54 mL, 0.6 M in THF, 0.32 mmol, 1.6 equiv.) were submitted to **General Procedure 4** at room temperature. The reaction was quenched with aqueous NH_4Cl (5 mL, saturated). Purification by column chromatography (SiO_2, pentane / Et_2O, 90:10) afforded **130** (56 mg, 0.16 mmol, 82%) as a white solid.

R_f 0.27 (pentane / Et_2O, 90:10)

m.p. 109-111 °C

^{1}H NMR (400 MHz, $CDCl_3$) δ 7.15-7.07 (4H, m, ArH), 4.15 (2H, m, H10), 2.66 (2H, app t, *J* = 12.7 Hz, H10), 2.32 (3H, s, H1), 1.83 (6H, s, H6), 1.64-1.49 (3H, m, H8, H9), 1.47 (9H, s, tBu), 1.13 (2H, app qd, *J* = 12.7, 4.7 Hz, H9).

^{13}C NMR (101 MHz, $CDCl_3$) δ 155.0, 138.6, 136.0, 128.9, 126.1, 79.4, 50.1, 43.9, 41.8, 40.8, 36.6, 28.6, 28.6, 21.2.

HRMS (ESI^+) Found $[M+Na]^+$ = 364.2247; $C_{22}H_{31}O_2NNa$ requires 364.2247.

IR (film) ν_{max}/cm^{-1} 2963, 2925, 2853, 1696, 1160.

***tert*-Butyl 4-(3-(3-phenoxyphenyl)bicyclo[1.1.1]pentan-1-yl)piperidine-1-carboxylate, 131**

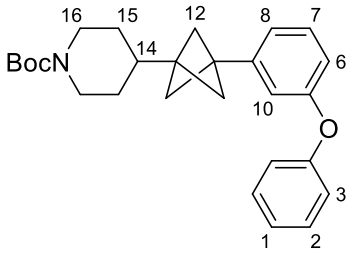

(3-Phenoxyphenyl)magnesium bromide: 1-bromo-3-phenoxybenzene (0.55 mL, 3.0 mmol, 1.0 equiv.), and Mg turnings (88 mg, 3.6 mmol, 1.2 equiv.) were submitted to **General Procedure 2** to give (3-phenoxyphenyl)magnesium bromide as a 1.1 M solution in THF.

117 (76 mg, 0.20 mmol, 1.0 equiv.), $Fe(acac)_3$ (14 mg, 0.04 mmol, 20 mol%), TMEDA (12 µL, 0.08 mmol, 40 mol%) and (3-phenoxyphenyl)magnesium bromide (0.31 mL, 1.1 M in THF, 0.32 mmol, 1.6 equiv.) were submitted to **General Procedure 4** at room temperature. The reaction was quenched with aqueous NH_4Cl (5 mL, saturated). Purification by column chromatography (SiO_2, pentane / Et_2O, 90:10) afforded **131** (66 mg, 0.16 mmol, 78%) as a white solid.

R_f 0.24 (pentane / Et_2O, 90:10)

m.p. 60-62 °C

^{1}H NMR (400 MHz, $CDCl_3$) δ 7.36-7.31 (2H, m, ArH), 7.27-7.22 (1H, m, ArH), 7.13-7.07 (1H, m, ArH), 7.04-6.99 (2H, m, ArH), 6.96 (1H, ddd, *J* = 7.6, 1.6, 1.0 Hz, ArH), 6.90 (1H, dd, *J* = 2.5, 1.5 Hz, ArH), 6.82 (1H, ddd, *J* = 8.1, 2.5, 1.0 Hz, ArH), 4.16 (2H,

app s, H16), 2.73-2.61 (2H, m, H16), 1.84 (6H, s, H12), 1.65-1.56 (2H, m, H15), 1.53 (1H, dt, *J* = 11.7, 3.6 Hz, H14), 1.47 (9H, s, *t*-Bu), 1.19-1.06 (2H, m, H15).

^{13}C NMR (101 MHz, $CDCl_3$) δ 157.4, 157.2, 155.0, 143.7, 129.8, 129.5, 123.2, 121.1, 118.8, 116.9, 116.8, 79.4, 50.1, 43.9, 41.9, 40.8, 36.5, 28.6, 28.5.

HRMS (ESI^+) Found $[M+Na]^+$ = 442.2350; $C_{27}H_{33}O_3NNa$ requires 442.2350.

IR (film) ν_{max}/cm^{-1} 2962, 2929, 2865, 1691, 1489, 1424, 1233, 1151

***tert*-Butyl 4-(3-(o-tolyl)bicyclo[1.1.1]pentan-1-yl)piperidine-1-carboxylate, 132**

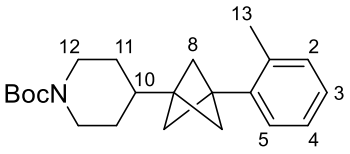

***o*-Tolylmagnesium bromide:** 2-Methylbromobenzene (360 µL, 3.0 mmol, 1.0 equiv.) and Mg turnings (88 mg, 3.6 mmol, 1.2 equiv.) were submitted to **General Procedure 2** to give *o*-tolylmagnesium bromide as a 0.8 M solution in THF.

117 (76 mg, 0.20 mmol, 1.0 equiv.), $Fe(acac)_3$ (14 mg, 0.04 mmol, 20 mol%), TMEDA (12 µL, 0.08 mmol, 40 mol%) and *o*-tolylmagnesium bromide (0.40 mL, 0.8 M in THF, 0.32 mmol, 1.6 equiv.) were submitted to **General Procedure 4** at 45 °C. The reaction was quenched with aqueous NH_4Cl (5 mL, saturated). Purification by column chromatography (SiO_2, pentane / Et_2O, 95:5) afforded **132** (59 mg, 0.17 mmol, 86%) as a clear oil.

R_f 0.28 (pentane / Et_2O, 90:10)

^{1}H NMR (400 MHz, $CDCl_3$) δ 7.15-7.05 (4H, m, ArH), 4.24-4.01 (2H, m, H12), 2.67 (2H, app t, *J* = 13.2 Hz, H12), 2.39 (3H, s, H13), 1.96 (6H, s, H8), 1.68-1.50 (3H, m, H10, H11), 1.47 (9H, s, *t*-Bu), 1.24-1.05 (2H, m, H11).

^{13}C NMR (101 MHz, $CDCl_3$) δ 155.0, 138.7, 137.0, 130.6, 127.9, 126.9, 125.8, 79.4, 50.1, 43.9, 43.1, 42.1, 36.6, 28.6, 28.6, 20.8.

HRMS (ESI$^+$) Found $[M+Na]^+ = 364.2249$; $C_{22}H_{31}O_2NNa$ requires 364.2247.

IR (film) ν_{max}/cm^{-1} 2981, 1692, 1612, 1392, 1155.

Reaction and characterisation performed by Dr Jeremy Nugent.

tert-Butyl 4-(3-(4-(_tert_-butyl)phenyl)bicyclo[1.1.1]pentan-1-yl)piperidine-1-carboxylate, 133

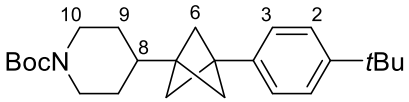

4-_tert_-Butylphenylmagnesium bromide: 1-Bromo-4-(*tert*-butyl)benzene (0.52 mL, 3.0 mmol, 1.0 equiv.) and Mg turnings (88 mg, 3.6 mmol, 1.2 equiv.) were submitted to **General Procedure 2** to give 4-*tert*-butylphenylmagnesium bromide as a 1.0 M solution in THF.

117 (76 mg, 0.20 mmol, 1.0 equiv.), $Fe(acac)_3$ (14 mg, 0.04 mmol, 20 mol%), TMEDA (12 μL, 0.08 mmol, 40 mol%) and 4-*tert*-butylphenylmagnesium bromide (0.32 mL, 1.0 M in THF, 0.32 mmol, 1.6 equiv.) were submitted to **General Procedure 4** at room temperature. The reaction was quenched with aqueous NH_4Cl (5 mL, saturated). Purification by column chromatography (SiO_2, pentane / Et_2O, 90:10) afforded **133** (62 mg, 0.16 mmol, 81%) as a colourless oil.

R_f 0.29 (pentane / Et_2O, 90:10)

^{1}H NMR (400 MHz, $CDCl_3$) δ 7.36-7.32 (2H, m, ArH), 7.20-7.15 (2H, m, ArH), 4.24-4.08 (2H, m, H10), 2.67 (2H, app t, *J* = 12.7 Hz, H10), 1.85 (6H, s, H6), 1.71-1.50 (3H, m, H8, H9), 1.47 (9H, s, *t*-Bu), 1.32 (9H, s, *t*-Bu), 1.21-1.07 (2H, m, H9).

^{13}C NMR (101 MHz, $CDCl_3$) δ 155.0, 149.3, 138.5, 125.9, 125.1, 79.3, 50.1, 43.9, 41.9, 40.7, 36.6, 34.6, 31.5, 28.62, 28.61.

HRMS (ESI^+) Found $[M+Na]^+$ = 406.2718; $C_{25}H_{37}O_2NNa$ requires 406.2717.

IR (film) ν_{max}/cm^{-1} 2960, 2864, 1361, 1693, 1421, 1234, 1161, 841

Reaction and characterisation performed by Dr Jeremy Nugent.

***tert*-Butyl 4-(3-(4-fluorophenyl)bicyclo[1.1.1]pentan-1-yl)piperidine-1-carboxylate, 134**

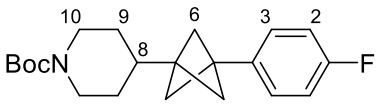

4-Fluorophenylmagnesium bromide: 4-Bromo-fluorobenzene (0.33 mL, 3.0 mmol, 1.0 equiv.) and Mg turnings (88 mg, 3.6 mmol, 1.2 equiv.) were submitted to **General Procedure 2** at room temperature for 1 h to give 4-fluorophenylmagnesium bromide as a 0.9 M solution in THF.

117 (76 mg, 0.20 mmol, 1.0 equiv.), $Fe(acac)_3$ (14 mg, 0.04 mmol, 20 mol%), TMEDA (12 μL, 0.08 mmol, 40 mol%) and 4-fluorophenylmagniesium bromide (0.38 mL, 0.9 M in THF, 0.32 mmol, 1.6 equiv.) were submitted to **General Procedure 4** at room temperature. The reaction was quenched with aqueous NH_4Cl (5 mL, saturated). Purification by column chromatography (SiO_2, pentane / Et_2O, 90:10) afforded **134** (42 mg, 0.12 mmol, 61%) as a white solid.

R_f 0.58 (pentane / Et_2O, 70:30)

m.p. 53-55 °C

^{1}H NMR (400 MHz, $CDCl_3$) δ ^{1}H NMR (400 MHz, $CDCl_3$) δ 7.19-7.11 (2H, m, H3), 7.00-6.92 (2H, m, H2), 4.23-4.08 (2H, m, H10), 2.66 (2H, app t, *J* = 12.9 Hz, H10), 1.83 (6H, s, H6), 1.68-1.49 (3H, m, H8, H9), 1.46 (9H, s, *t*-Bu), 1.18-1.05 (2H, m, H9).

^{13}C NMR (101 MHz, $CDCl_3$) δ 161.8 (d, *J* = 243.5 Hz) 155.0, 137.3 (d, *J* = 3.4 Hz), 127.7 (d, *J* = 8.1 Hz), 115.0 (d, *J* = 21.4 Hz), 79.4, 50.1, 43.9, 41.8, 40.5, 36.5, 28.6, 28.6.

^{19}F NMR (376 MHz, $CDCl_3$) δ -116.8.

HRMS : Found $[M+Na]^+$ = 368.1997; $C_{21}H_{28}O_2NF^{23}Na$ requires 368.1996

IR (film) ν_{max}/cm^{-1} 2961, 2929, 2866, 1689, 1446, 1234, 1154, 842

***tert*-Butyl 4-(3-(4-(trimethylsilyl)phenyl)bicyclo[1.1.1]pentan-1-yl)piperidine-1-carboxylate, 135**

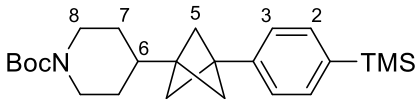

(4-(Trimethylsilyl)phenyl)magnesium bromide: (4-Bromophenyl)trimethylsilane (586 µL, 3.0 mmol, 1.0 equiv.) and Mg turnings (88 mg, 3.6 mmol, 1.2 equiv.) were submitted to **General Procedure 2** to give (4-(trimethylsilyl)phenyl)magnesium bromide as a 0.8 M solution in THF.

117 (76 mg, 0.20 mmol, 1.0 equiv.), $Fe(acac)_3$ (14 mg, 0.04 mmol, 20 mol%), TMEDA (12 µL, 0.08 mmol, 40 mol%) and (4-(trimethylsilyl)phenyl)magnesium bromide (0.4 mL, 0.8 M in THF, 0.32 mmol, 1.6 equiv.) were submitted to **General Procedure 4** at room temperature. The reaction was quenched with aqueous NH_4Cl (5 mL, saturated). Purification by column chromatography (SiO_2, pentane / Et_2O, 90:10) afforded **135** (65 mg, 0.16 mmol, 81%) as a clear foam.

Gram scale:

To a vial was added **117** (1.00 g, 2.70 mmol, 1.0 equiv.), and $Fe(acac)_3$ (186 mg, 0.53 mmol, 20 mol%). The vial was then evacuated and refilled with $N_{2\,(g)}$ three times. To this was added TMEDA (0.16 mL, 1.10 mmol, 40 mol%) and THF (2.7 mL), the resultant

mixture was then stirred for 5 minutes. (4-(Trimethylsilyl)phenyl)magnesium bromide (4.2 mL, 1.0 M in THF, 4.2 mmol, 1.6 equiv.) was then added via syringe pump at a rate of 5.6 mL/h (over approximately 45 min) at room temperature. The reaction was stirred for a further 1 hour then quenched with aqueous NH_4Cl (20 mL, saturated). The layers were separated, and the aqueous layer was extracted with Et_2O (3 × 50 mL). The combined organic layers were washed with brine, dried over $MgSO_4$ and concentrated *in vacuo*. Purification by column chromatography (SiO_2, pentane / Et_2O, 90:10) afforded **135** (0.96 g, 2.4 mmol, 90%) as a clear foam.

R_f 0.36 (pentane / Et_2O, 90:10)

^{1}H NMR (400 MHz, $CDCl_3$) δ 7.47 (2H, d, *J* = 7.0 Hz, ArH), 7.22 (2H, d, *J* = 7.0 Hz, ArH), 4.21-4.07 (2H, m, H8), 2.67 (2H, app t, *J* = 13.0 Hz, H8), 1.85 (6H, s, H5), 1.65-1.50 (3H, m, H6, H7), 1.47 (9H, s, *t*-Bu), 1.13 (2H, app qd, *J* = 12.5, 4.5 Hz, H7), 0.25 (9H, s, TMS).

^{13}C NMR (101 MHz, $CDCl_3$) δ 155.0, 142.0, 138.2, 133.3, 125.6, 79.4, 50.0, 43.9, 42.0, 41.0, 36.6, 28.6, 28.6, -1.0.

HRMS (ESI^+) Found $[M+Na]^+$ = 422.2487; $C_{24}H_{37}O_2NNaSi$ requires 422.2486.

IR (film) ν_{max}/cm^{-1} 2956, 2866, 1696, 1422, 841.

Reaction on 0.2 mmol scale performed by Dr Jeremy Nugent.

tert-Butyl 4-(3-(3-(1,3-dioxolan-2-yl)phenyl)bicyclo[1.1.1]pentan-1-yl)piperidine-1-carboxylate, 136

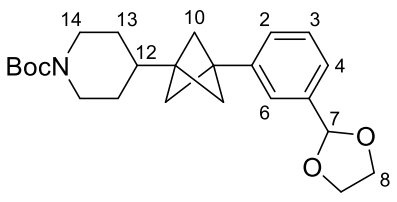

(3-(1,3-Dioxolan-2-yl)phenyl)magnesium bromide: 2-(3-Bromophenyl)-1,3-dioxolane (0.46 mL, 3.0 mmol, 1.0 equiv.), and Mg turnings (88 mg, 3.6 mmol, 1.2 equiv.) were submitted to **General Procedure 2** to give (3-(1,3-dioxolan-2-yl)phenyl)magnesium bromide as a 0.6 M solution in THF.

117 (76 mg, 0.20 mmol, 1.0 equiv.), $Fe(acac)_3$ (14 mg, 0.04 mmol, 20 mol%), TMEDA (12 μL, 0.08 mmol, 40 mol%) and (3-(1,3-dioxolan-2-yl)phenyl)magnesium bromide (0.53 mL, 0.6 M in THF, 0.32 mmol, 1.6 equiv.) were submitted to **General Procedure 4** at room temperature. The reaction was quenched with aqueous NH_4Cl (5 mL, saturated). Purification by column chromatography (SiO_2, pentane / Et_2O, 60:40) afforded **136** (44 mg, 0.11 mmol, 55%) as a colourless oil.

R_f 0.24 (pentane / Et_2O, 70:30)

^{1}H NMR (400 MHz, $CDCl_3$) δ 7.34-7.27 (3H, m, ArH), 7.24-7.19 (1H, m, ArH), 5.79 (1H, s, H7), 4.29-3.84 (6H, m, H8, H14), 2.66 (2H, app t, *J* = 12.8 Hz, H14), 1.85 (6H, s, H14), 1.56 (3H, m, H12, H13), 1.46 (9H, s, *t*-Bu), 1.12 (2H, app qd, *J* = 12.6, 4.4 Hz, H13).

^{13}C NMR (101 MHz, $CDCl_3$) δ 155.0, 141.7, 137.8, 128.3, 127.1, 124.5, 124.1, 103.9, 79.4, 65.4, 50.1, 44.0, 41.9, 41.0, 36.6, 28.6, 28.6.

HRMS (ESI^+) Found $[M+Na]^+$ = 422.2300; $C_{24}H_{33}O_4NNa$ requires 422.2302.

IR (film) ν_{max}/cm^{-1} 2963, 2929, 2865, 1688, 1445, 1235, 1156, 1097.

Reaction and characterisation performed by Dr Jeremy Nugent.

***tert*-Butyl 4-(3-(4-(pyridin-2-yl)phenyl)bicyclo[1.1.1]pentan-1-yl)piperidine-1-carboxylate, 137**

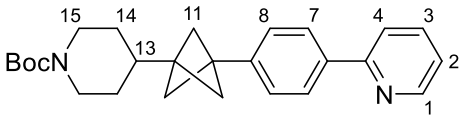

(4-(Pyridin-2-yl)phenyl)magnesium bromide: 2-(4-bromophenyl)pyridine (702 mg, 3.0 mmol, 1.0 equiv.), and Mg turnings (88 mg, 3.6 mmol, 1.2 equiv.) were submitted to **General Procedure 2** for 1 h at 45 °C to give (4-(pyridin-2-yl)phenyl)magnesium bromide as a 0.7 M solution in THF.

117 (76 mg, 0.20 mmol, 1.0 equiv.), $Fe(acac)_3$ (14 mg, 0.04 mmol, 20 mol%), TMEDA (12 µL, 0.08 mmol, 40 mol%) and (4-(pyridin-2-yl)phenyl)magnesium bromide (0.43 mL, 0.7 M in THF, 0.32 mmol, 1.6 equiv.) were submitted to **General Procedure 4** at room temperature. The reaction was quenched with aqueous NH_4Cl (5 mL, saturated). Purification by column chromatography (SiO_2, pentane / Et_2O, 70:30) afforded **137** (66 mg, 0.16 mmol, 81%) as a white solid.

R_f = 0.18 (pentane / Et_2O, 70:30)

m.p. = 152-154 °C

^{1}H NMR (400 MHz, $CDCl_3$) δ 8.71-8.63 (1H, m, H1), 7.96-7.90 (2H, m, H7), 7.75-7.67 (2H, m, ArH), 7.34-7.28 (2H, m, ArH), 7.19 (1H, ddd, *J* = 6.7, 4.8, 2.0 Hz, ArH), 4.27-4.05 (2H, m, H15), 2.74-2.60 (2H, m, H15), 1.89 (6H, s, H11), 1.58 (3H, m, H13, H14), 1.47 (9H, s, *t*-Bu), 1.21-1.07 (2H, m, H14).

^{13}C NMR (101 MHz, $CDCl_3$) δ 157.5, 155.0, 149.7, 142.3, 137.6, 136.8, 126.8, 126.6, 122.0, 120.4, 79.3, 50.1, 43.9, 42.0, 40.9, 36.6, 29.8, 28.6.

HRMS: Found $[M+H]^+$ = 405.2543; $C_{26}H_{33}O_2N_2$ requires 405.2537

IR (film) ν_{max}/cm^{-1} 2962, 2928, 2866, 1680, 1425, 1236, 1162, 777.

***tert*-Butyl 4-(3-(pyridin-3-yl)bicyclo[1.1.1]pentan-1-yl)piperidine-1-carboxylate, 138**

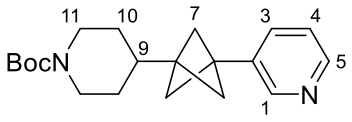

Pyridin-3-ylmagnesium bromide lithium chloride complex: 3-Bromopyridine (0.48 mL, 5.0 mmol, 1.0 equiv.), Mg turnings (365 mg, 15.0 mmol, 3.0 equiv.) and LiCl (318 mg, 7.5 mmol, 1.5 equiv.) were submitted to **General Procedure 3** at 0 °C for 2 h to give pyridin-3-ylmagnesium bromide lithium chloride complex as a 0.6 M solution in THF.

To a vial was added **117** (76 mg, 0.2 mmol, 1.0 equiv.) and $Fe(acac)_3$ (14 mg, 20 mol%, 0.04 mmol). The vial was then evacuated and refilled with $N_{2\,(g)}$ three times. To this was added TMEDA (12 µL, 40 mol%, 0.08 mmol) and THF (0.2 mL), the resultant mixture was then stirred for 5 minutes at 65 °C. Pyridin-3-ylmagnesium bromide lithium chloride complex (1.10 mL, 0.6 M in THF, 0.60 mmol, 3.0 equiv.) was added and resulting mixture was stirred for 1 hour then quenched with aqueous NH_4Cl (5 mL, saturated). The layers were separated, and the aqueous layer was extracted with EtOAc (3 × 10 mL). The combined organic layers were washed with brine, dried over $MgSO_4$ and concentrated *in vacuo*. Purification by column chromatography (SiO_2, pentane / Et_2O, 75:25 to 50:50) afforded **138** (17 mg, 0.05 mmol, 27%) as a yellow solid.

R_f 0.45 (pentane / EtOAc, 50:50)

m.p. 58-60 °C

^{1}H NMR (400 MHz, $CDCl_3$) δ 8.45 (2H, m, H1 + H5), 7.49 (1H, ddd, *J* = 7.7, 2.2, 1.7 Hz, H3), 7.19 (1H, ddd, *J* = 7.8, 4.8, 0.9 Hz, H4), 4.15 (2H, br app s, H11), 2.66 (2H, app t, *J* = 12.8 Hz, H11), 1.90 (6H, s, H7), 1.65-1.51 (3H, m, H10 + H9), 1.46 (9H, s, *t*-Bu), 1.23-1.05 (2H, m, H10).

^{13}C NMR (101 MHz, $CDCl_3$) δ 155.0, 148.1, 147.8, 136.5, 133.8, 123.1, 79.4, 50.1, 44.0, 42.6, 39.1, 36.5, 28.6, 28.5.

HRMS (ESI^+) Found $[M+H]^+$ = 329.2222; $C_{20}H_{29}O_2N_2$ requires 329.2224.

IR (film) ν_{max}/cm^{-1} 2962, 2925, 2865, 1692, 1421, 1236, 1164

***tert*-Butyl 4-(3-(6-ethoxypyridin-3-yl)bicyclo[1.1.1]pentan-1-yl)piperidine-1-carboxylate, 139**

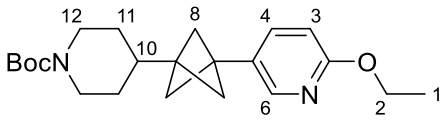

(6-ethoxypyridin-3-yl)magnesium bromide lithium chloride complex: 5-bromo-2-ethoxypyridine (606 mg, 3.0 mmol, 1.0 equiv.), Mg turnings (146 mg, 6.0 mmol, 2.0 equiv.) and LiCl (153 mg, 3.6 mmol, 1.2 equiv.) were submitted to **General Procedure 3** at 60 °C for 2 h to give (6-ethoxypyridin-3-yl)magnesium bromide lithium chloride complex as a 0.6 M solution in THF.

117 (76 mg, 0.20 mmol, 1.0 equiv.), $Fe(acac)_3$ (14 mg, 0.04 mmol, 20 mol%), TMEDA (12 µL, 0.08 mmol, 40 mol%) and (6-ethoxypyridin-3-yl)magnesium bromide lithium chloride complex (1.1 mL, 0.6 M in THF, 0.60 mmol, 3.0 equiv.) were submitted to **General Procedure 4** at 45 °C. The reaction was quenched with aqueous NH_4Cl (5 mL, saturated). Purification by column chromatography (SiO_2, pentane / Et_2O, 85:15) afforded **139** (37 mg, 0.09 mmol, 49%) as a colourless oil.

R_f 0.24 (pentane / Et_2O, 75:25)

^{1}H NMR (400 MHz, $CDCl_3$) δ 7.97 (1H, d, *J* = 2.4 Hz, H6), 7.43 (1H, dd, *J* = 8.5, 2.4 Hz, H4), 6.66 (1H, d, *J* = 8.5 Hz, H3), 4.34 (2H, q, *J* = 7.1 Hz, H2), 4.15 (2H, app s, H12), 2.65 (2H, app t, *J* = 13.0 Hz, H12), 1.84 (6H, s, H8), 1.64 – 1.56 (2H, m, H11), 1.56 –

1.49 (1H, m, H10), 1.45 (9H, s, *t*-Bu), 1.38 (3H, t, *J* = 7.1 Hz, H1), 1.17 – 1.04 (2H, m, H11).

^{13}C NMR (126 MHz, $CDCl_3$) δ 162.6, 155.0, 144.1, 137.4, 129.5, 110.6, 79.4, 62.2, 50.1, 44.0, 42.5, 38.6, 36.5, 28.6, 28.5, 14.8.

HRMS (ESI^+) Found $[M+H]^+$ = 373.2497; $C_{22}H_{33}O_3N_2$ requires 373.2486.

IR (film) ν_{max}/cm^{-1} 3016, 2928, 2866, 2366, 1693, 1607, 1568, 1283, 1164.

***tert*-Butyl 4-(3-(5-methoxypyridin-3-yl)bicyclo[1.1.1]pentan-1-yl)piperidine-1-carboxylate, 140**

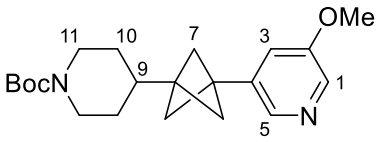

(5-Methoxypyridin-3-yl)magnesium bromide lithium chloride complex: (3-Bromo-5-methoxypyridine (564 mg, 3.0 mmol, 1.0 equiv.), Mg turnings (146 mg, 6.0 mmol, 2.0 equiv.) and LiCl (140 mg, 3.3 mmol, 1.1 equiv.) were submitted to **General Procedure 3** at 0 °C for 2 h to give (5-methoxypyridin-3-yl)magnesium bromide lithium chloride complex as a 0.7 M solution in THF.

140 (76 mg, 0.20 mmol, 1.0 equiv.), $Fe(acac)_3$ (14 mg, 0.04 mmol, 20 mol%), TMEDA (12 μL, 0.08 mmol, 40 mol%) and (5-methoxypyridin-3-yl)magnesium bromide lithium chloride complex (0.86 mL, 0.7 M in THF, 0.60 mmol, 3.0 equiv.) were submitted to **General Procedure 4** at 45 °C. The reaction was quenched with aqueous NH_4Cl (5 mL, saturated). Purification by column chromatography (SiO_2, pentane / EtOAc, 70:30) afforded **140** (39 mg, 0.12 mmol, 55%) as a colourless oil.

R_f = 0.55 (pentane / EtOAc, 50:50)

^{1}H NMR (400 MHz, $CDCl_3$) δ 8.13 (1H, d, *J* = 2.9 Hz, H1), 8.06 (1H, d, *J* = 1.7 Hz, H5), 6.97 (1H, dd, *J* = 2.9, 1.7 Hz, H3), 4.26-4.03 (2H, m, H11), 3.83 (3H, s, OMe), 2.80-2.53

(2H, m, H11), 1.87 (6H, s, H7), 1.67-1.48 (3H, m, H9, H10), 1.44 (9H, s, *t*-Bu), 1.18-1.06 (2H, m, H10).

^{13}C NMR (101 MHz, $CDCl_3$) δ 155.5, 155.0, 140.4, 137.2, 135.5, 118.4, 79.4, 55.6, 50.1, 43.8, 42.6, 38.9, 36.5, 28.6, 28.5.

HRMS (ESI^+) Found $[M+H]^+$ = 359.2337; $C_{21}H_{31}O_3N_2$ requires 359.2340.

IR (film) ν_{max}/cm^{-1} 2965, 2930, 2866, 1687, 1419, 1234, 1152, 873

Reaction and characterisation performed by Dr Jeremy Nugent.

tert-Butyl 4-(3-(2-methoxypyridin-4-yl)bicyclo[1.1.1]pentan-1-yl)piperidine-1-carboxylate, 141

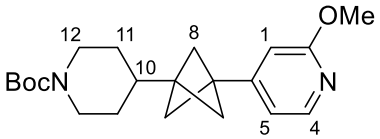

(2-Methoxypyridin-4-yl)magnesium bromide lithium chloride complex: 4-Bromo-2-methoxypyridine (564 mg, 2.0 mmol, 1.0 equiv.), Mg turnings (146 mg, 6.0 mmol, 2.0 equiv.) and LiCl (140 mg, 3.3 mmol, 1.1 equiv.) were submitted to **General Procedure 3** at room temperature for 2 h to give (2-methoxypyridin-4-yl)magnesium bromide lithium chloride complex as a 0.5 M solution in THF.

117 (76 mg, 0.20 mmol, 1.0 equiv.), $Fe(acac)_3$ (14 mg, 0.04 mmol, 20 mol%), TMEDA (12 μL, 0.08 mmol, 40 mol%) and (2-methoxypyridin-4-yl)magnesium bromide lithium chloride complex (1.2 mL, 0.5 M in THF, 0.32 mmol, 3.0 equiv.) were submitted to **General Procedure 4** at 45 °C. The reaction was quenched with aqueous NH_4Cl (5 mL, saturated). Purification by column chromatography (SiO_2, pentane / Et_2O, 80:20) afforded **141** (25 mg, 0.07 mmol, 35%) as a clear oil.

R_f 0.42 (pentane / Et_2O, 4:1)

m.p. 79-80 °C

^{1}H NMR (400 MHz, $CDCl_3$) δ 8.05 (1H, dd, *J* = 5.2, 0.8 Hz, H4), 6.71 (1H, dd, *J* = 5.2, 1.4 Hz, H5), 6.53 (1H, dd, *J* = 1.4, 0.8 Hz, H1), 4.17-4.13 (2H, m, H12), 3.91 (3H, s, OMe), 2.65 (2H, app t, *J* = 13.0 Hz, H12), 1.83 (6H, s, H8), 1.64-1.48 (3H, m, H10, H11), 1.24-1.03 (2H, m, H11).

^{13}C NMR (101 MHz, $CDCl_3$) δ 164.6, 155.0, 152.7, 146.7, 115.0, 108.2, 79.4, 53.5, 49.9, 43.9, 42.4, 40.1, 36.5, 28.6, 28.5.

HRMS (ESI^+) Found $[M+H]^+ = 359.2330$; $C_{21}H_{31}O_3N_2$ requires 359.2329.

IR (film) ν_{max}/cm^{-1} 2980, 1692, 1612, 1392, 1155.

Reaction and characterisation performed by Dr Jeremy Nugent.

tert-Butyl 4-(3-(benzofuran-5-yl)bicyclo[1.1.1]pentan-1-yl)piperidine-1-carboxylate, 142

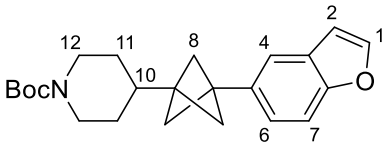

Benzofuran-5-ylmagnesium bromide lithium chloride complex: 5-bromobenzofuran (0.38 mL, 3.00 mmol, 1.0 equiv.), Mg turnings (146.0 mg, 6.00 mmol, 2.0 equiv.) and LiCl (153 mg, 3.60 mmol, 1.2 equiv.) were submitted to **General Procedure 3** at 60 °C for 2 h to give benzofuran-5-ylmagnesium bromide lithium chloride complex as a 1.0 M solution in THF.

117 (76 mg, 0.20 mmol, 1.0 equiv.), $Fe(acac)_3$ (14 mg, 0.04 mmol, 20 mol%), TMEDA (12 μL, 0.08 mmol, 40 mol%) and benzofuran-5-ylmagnesium bromide lithium chloride complex (0.32 mL, 1.0 M in THF, 0.320 mmol, 1.6 equiv.) were submitted to **General Procedure 4** at room temperature. The reaction was quenched with aqueous NH_4Cl (5

mL, saturated). Purification by column chromatography (SiO_2, pentane / Et_2O, 90:10) afforded **142** (49 mg, 0.13 mmol, 67%) as a white solid.

R_f 0.17 (pentane / Et_2O, 90:10)

m.p. 103-105 °C

^{1}H NMR (400 MHz, $CDCl_3$) δ 7.59 (1H, d, *J* = 2.2 Hz, ArH), 7.44-7.40 (2H, m, ArH), 7.16 (1H, dd, *J* = 8.5, 1.7 Hz, ArH), 6.72 (1H, dd, *J* = 2.2, 0.9 Hz, ArH), 4.16 (2H, br app s, H12), 2.68 (2H, app t, *J* = 13.0 Hz, H12), 1.88 (6H, s, H8), 1.68-1.52 (3H, m, H11 + H10), 1.47 (9H, s, *t*-Bu), 1.21-1.08 (2H, m, H11).

^{13}C NMR (101 MHz, $CDCl_3$) δ 155.0, 154.0, 145.4, 136.2, 127.4, 122.6, 118.5, 111.0, 106.6, 79.4, 50.3, 44.0, 41.7, 41.1, 36.6, 28.6, 28.6.

HRMS (ESI^+) Found $[M+Na]^+$ = 390.2042; $C_{23}H_{29}O_3NNa$ requires 390.2040.

IR (film) ν_{max}/cm^{-1} 3656, 2980, 2865, 2361, 2341, 1691, 1236, 1173, 1150.

***tert*-Butyl 5-(3-(1-(tert-butoxycarbonyl)piperidin-4-yl)bicyclo[1.1.1]pentan-1-yl)-1*H*-indole-1-carboxylate, 143**

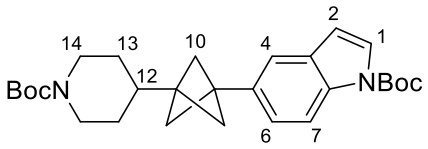

(1-(*tert*-Butoxycarbonyl)-1*H*-indol-5-yl)magnesium bromide lithium chloride complex: (*tert*-Butyl 5-bromo-1*H*-indole-1-carboxylate (564 mg, 3.0 mmol, 1.0 equiv.), Mg turnings (146 mg, 3.2 mmol, 2.0 equiv.) and LiCl (140 mg, 3.30 mmol, 1.1 equiv.) were submitted to **General Procedure 3** at room temperature for 3 h to give (1-(*tert*-butoxycarbonyl)-1*H*-indol-5-yl)magnesium bromide lithium chloride complex as a 0.7 M solution in THF.

117 (76 mg, 0.20 mmol, 1.0 equiv.), $Fe(acac)_3$ (14 mg, 0.04 mmol, 20 mol%), TMEDA (12 μL, 0.08 mmol, 40 mol%) and (1-(*tert*-butoxycarbonyl)-1*H*-indol-5-yl)magnesium bromide lithium chloride complex (0.46 mL, 0.7 M in THF, 0.60 mmol, 1.6 equiv.) were submitted to **General Procedure 4** at 45 °C. The reaction was quenched with aqueous NH_4Cl (5 mL, saturated). Purification by column chromatography (SiO_2, pentane / Et_2O, 90:10) afforded **143** (45 mg, 0.10 mmol, 48%) as a clear oil.

R_f 0.43 (pentane / Et_2O, 80:20)

^{1}H NMR (400 MHz, $CDCl_3$) δ 8.05 (1H, app d, *J* = 8.5 Hz, H7), 7.57 (1H, d, *J* = 3.8 Hz, H1), 7.38 (1H, dd, *J* = 1.7, 0.8 Hz, H4), 7.18 (1H, dd, *J* = 8.5, 1.7 Hz, H6), 6.52 (1H, dd, *J* = 3.8, 0.8 Hz, H2), 4.18-4.14 (2H, m, H14), 2.68 (2H, app t, *J* = 12.8 Hz, H14), 1.88 (6H, s, H10), 1.66 (9H, s, *t*-Bu), 1.64-1.50 (3H, m, H12, H13), 1.47 (9H, s, *t*-Bu), 1.15 (2H, app qd, *J* = 12.8, 4.4 Hz, H13).

^{13}C NMR (101 MHz, $CDCl_3$) δ 155.0, 149.9, 136.0, 134.0, 130.7, 126.3, 122.6, 118.3, 114.9, 107.3, 83.7, 79.4, 50.2, 44.0, 41.8, 41.2, 36.6, 28.6, 28.6, 28.3.

HRMS (ESI^+) Found $[M+Na]^+$ = 489.2723; $C_{28}H_{38}O_4N_2Na$ requires 489.2724.

IR (film) ν_{max}/cm^{-1} 2980, 2889, 1734, 1693, 1380, 1151.

Reaction and characterisation performed by Dr Jeremy Nugent.

***tert*-Butyl 4-(3-(1-methyl-1H-indazol-5-yl)bicyclo[1.1.1]pentan-1-yl)piperidine-1-carboxylate, 144**

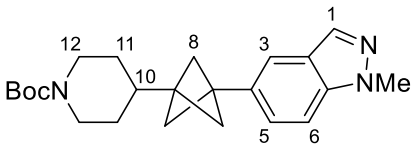

(3-Methyl-3*H*-indazol-6-yl)magnesium bromide lithium chloride complex: 6-Bromo-3-methyl-3*H*-indazole (422 mg, 2.0 mmol, 1.0 equiv.), Mg turnings (71 mg, 3.0 mmol, 1.5 equiv.) and LiCl (93 mg, 2.2 mmol, 1.1 equiv.) were submitted to **General**

Procedure 3 at room temperature for 2 h to give (3-methyl-3*H*-indazol-6-yl)magnesium bromide lithium chloride complex as a 0.7 M solution in THF.

117 (76 mg, 0.20 mmol, 1.0 equiv.), $Fe(acac)_3$ (14 mg, 0.04 mmol, 20 mol%), TMEDA (12 μL, 0.08 mmol, 40 mol%) and (3-methyl-3*H*-indazol-6-yl)magnesium bromide lithium chloride complex (0.5 mL, 0.7 M in THF, 0.32 mmol, 1.6 equiv.) were submitted to **General Procedure 4** at room temperature. The reaction was quenched with aqueous NH_4Cl (5 mL, saturated). Purification by column chromatography (SiO_2, pentane / Et_2O, 70:30) afforded **144** (35 mg, 0.09 mmol, 46%) as a white solid.

R_f 0.11 (pentane / Et_2O, 70:30)

m.p. 146-148 °C

^{1}H NMR (400 MHz, $CDCl_3$) δ 7.91 (1H, d, *J* = 0.8 Hz, H1), 7.51 (1H, app t, *J* = 1.2 Hz, H3), 7.36-7.27 (2H, m, H5, H6), 4.23-4.10 (2H, m, H12), 4.05 (3H, s, Me), 2.68 (2H, app t, *J* = 12.7 Hz, H12), 1.89 (6H, s, H8), 1.69-1.51 (3H, m, H10, H11), 1.47 (9H, s, *t*-Bu), 1.22-1.08 (2H, m, H11).

^{13}C NMR (101 MHz, $CDCl_3$) δ 155.1, 139.1, 134.0, 132.6, 125.2, 124.2, 117.8, 108.7, 79.4, 50.2, 43.7, 41.9, 41.2, 36.6, 35.7, 28.6, 28.6.

HRMS (ESI^+) Found $[M+H]^+$ = 382.2489; $C_{23}H_{32}O_2N_3$ requires 382.2489.

IR (film) ν_{max}/cm^{-1} 2961, 2864, 1689, 1423, 1236, 1174, 1150

Reaction and characterisation performed by Dr Jeremy Nugent.

tert-Butyl 4-(3-(4-(trifluoromethyl)benzyl)bicyclo[1.1.1]pentan-1-yl)indoline-1-carboxylate, 145

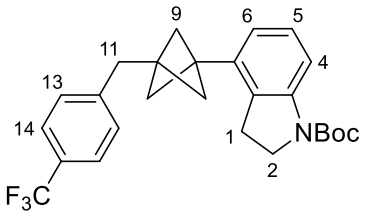

(1-(_tert_-Butoxycarbonyl)indolin-4-yl)magnesium bromide lithium chloride complex: *tert*-Butyl 4-bromoindoline-1-carboxylate (596 mg, 2.0 mmol, 1.0 equiv.), Mg turnings (97 mg, 4.0 mmol, 1.5 equiv.) and LiCl (93 mg, 2.2 mmol, 1.1 equiv.) were submitted to **General Procedure 3** at room temperature for 3 h to give (1-(*tert*-butoxycarbonyl)indolin-4-yl)magnesium bromide lithium chloride complex as a 0.7 M solution in THF.

117 (70 mg, 0.20 mmol, 1.0 equiv.), $Fe(acac)_3$ (14 mg, 0.04 mmol, 20 mol%), TMEDA (12 µL, 0.08 mmol, 40 mol%) and (1-(*tert*-butoxycarbonyl)indolin-4-yl)magnesium bromide lithium chloride complex (0.5 mL, 0.7 M in THF, 0.32 mmol, 1.6 equiv.) were submitted to **General Procedure 4** at 45 °C. The reaction was quenched with aqueous NH_4Cl (5 mL, saturated). Purification by column chromatography (SiO_2, pentane / Et_2O, 90:10) afforded **145** (57 mg, 0.13 mmol, 65%) as a clear oil.

R_f 0.43 (pentane / Et_2O, 70:30)

m.p. 122-123 °C

^{1}H NMR (400 MHz, $CDCl_3$) δ 7.75 (1H, m, H4), 7.57 (2H, d, *J* = 8.0 Hz, H14), 7.28-7.21 (2H, d, *J* = 8.0 Hz, H13), 7.09 (1H, app t, *J* = 7.7 Hz, H5), 6.70 (1H, dd, *J* = 7.7, 1.1 Hz, H6), 3.95 (2H, t, *J* = 8.7 Hz, H2), 3.06 (2H, t, *J* = 8.7 Hz, H1), 2.91 (2H, s, H11), 1.93 (6H, s, H9), 1.56 (9H, s, *t*Bu).

^{13}C NMR {^{19}F} (125 MHz, $CDCl_3$) δ 152.7, 143.6, 142.9, 136.4, 129.3, 128.4, 127.5, 125.3, 124.5, 120.9, 113.3, 81.0, 52.0, 47.7, 42.3, 40.1, 39.0, 28.6, 26.6. *(one aromatic signal overlapping).*

HRMS (ESI^+) Found $[M+Na]^+$ = 466.1967; $C_{26}H_{28}O_2NF_3Na$ requires 466.1964.

IR (film) ν_{max}/cm^{-1} 2981, 2883, 1763, 1247, 1157.

Reaction and characterisation performed by Dr Jeremy Nugent.

***tert*-Butyl 4-(3-(9-phenyl-9*H*-carbazol-3-yl)bicyclo[1.1.1]pentan-1-yl)piperidine-1-carboxylate**, **146**

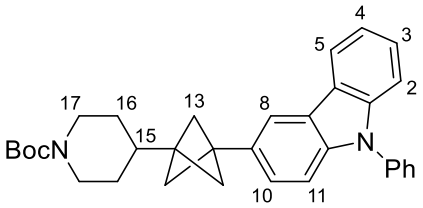

(9-Phenyl-9*H*-carbazol-3-yl)magnesium bromide: 3-bromo-9-phenyl-9*H*-carbazole (967 mg, 3.0 mmol, 1.0 equiv.), and Mg turnings (88 mg, 3.6 mmol, 1.2 equiv.) were submitted to **General Procedure 2** for 3 h at reflux to give (9-phenyl-9*H*-carbazol-3-yl)magnesium bromide as a 1.0 M solution in THF.

117 (76 mg, 0.20 mmol, 1.0 equiv.), $Fe(acac)_3$ (14 mg, 0.04 mmol, 20 mol%), TMEDA (12 μL, 0.08 mmol, 40 mol%) and (9-phenyl-9*H*-carbazol-3-yl)magnesium bromide (0.46 mL, 1.0 M in THF, 0.32 mmol, 1.6 equiv.) were submitted to **General Procedure 4** at 45 °C. The reaction was quenched with aqueous NH_4Cl (5 mL, saturated). Purification by column chromatography (SiO_2, pentane / Et_2O, 90:10) afforded **146** (64 mg, 0.13 mmol, 65%) as a clear oil.

R_f = 0.43 (pentane / Et_2O, 80:20)

^{1}H NMR (400 MHz, $CDCl_3$) δ 8.14 (1H, dt, *J* = 7.8, 1.0 Hz, ArH), 7.96 (1H, dd, *J* = 1.6, 0.7 Hz, ArH), 7.63-7.52 (4H, m, ArH), 7.49-7.43 (1H, m, ArH), 7.41-7.38 (2H, m, ArH), 7.35-7.26 (3H, m, ArH), 4.29-4.11 (2H, m, H17), 2.77-2.65 (2H, m, H17), 1.96 (6H, s, H13), 1.71-1.54 (3H, m, H15, H16), 1.48 (9H, s, *t*-Bu), 1.20 (2 H, app qd, *J* = 13.3, 12.2, 9.2 Hz, H16).

^{13}C NMR (101 MHz, $CDCl_3$) δ 155.1, 141.3, 139.9, 138.0, 133.4, 130.0, 127.5, 127.2, 126.0, 124.3, 123.42, 123.39, 120.4, 119.9, 117.7, 109.9, 109.5, 79.4, 50.4, 43.9, 41.8, 41.4, 36.7, 28.7, 28.6.

HRMS (ESI^+) Found $[M+H]^+ = 493.2849$; $C_{33}H_{37}O_2N_2$ requires 493.2850.

IR (film) ν_{max}/cm^{-1} 2980, 2865, 1688, 1234, 1154.

Reaction and characterisation performed by Dr Jeremy Nugent.

tert-Butyl 3-(3-(4-methoxyphenyl)bicyclo[1.1.1]pentan-1-yl)azetidine-1-carboxylate, 147

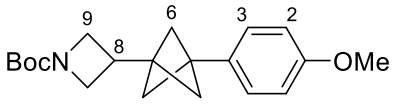

S2 (70 mg, 0.20 mmol, 1.0 equiv.), $Fe(acac)_3$ (14 mg, 0.04 mmol, 20 mol%), TMEDA (12 μL, 0.08 mmol, 40 mol%) and 4-methoxyphenylmagnesium bromide (0.4 mL, 0.9 M in THF, 0.32 mmol, 1.6 equiv.) were submitted to **General Procedure 4** at room temperature. The reaction was quenched with aqueous NH_4Cl (5 mL, saturated). Purification by column chromatography (SiO_2, pentane / Et_2O, 95:5) afforded **147** (48 mg, 0.12 mmol, 73%) as a white solid.

R_f 0.35 (pentane / Et_2O, 95:5)

^{1}H NMR (400 MHz, $CDCl_3$) δ 7.14 (2H, m, H3), 6.88-6.79 (2H, m, H2), 3.94 (2H, app t, *J* = 8.4 Hz, H9), 3.79 (3H, s, OMe), 3.67 (2H, dd, *J* = 8.4, 5.4 Hz, H9), 2.66 (1H, app tt, *J* = 8.4, 5.4 Hz, H8), 1.92 (6H, s, H6), 1.45 (9H, s, *t*-Bu).

^{13}C NMR (101 MHz, $CDCl_3$) δ 158.5, 156.7, 133.3, 127.2, 113.7, 79.4, 55.4, 51.2, 50.2, 41.6, 39.5, 29.4, 28.6.

HRMS (ESI^+) Found $[M+Na]^+$ = 352.1883; $C_{20}H_{27}O_3NNa$ requires 352.1883.

IR (film) ν_{max}/cm^{-1} 2960, 2867, 1699, 1401, 1365, 1245, 1135.

Reaction and characterisation performed by Dr Jeremy Nugent.

1-(4-Methoxyphenyl)-3-((phenylsulfonyl)methyl)bicyclo[1.1.1]pentane, 148

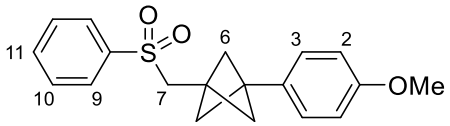

1-Iodo-3-((phenylsulfonyl)methyl)bicyclo[1.1.1]pentane **S3** (70 mg, 0.20 mmol, 1.0 equiv.), $Fe(acac)_3$ (14 mg, 0.04 mmol, 20 mol%), TMEDA (12 μL, 0.08 mmol, 40 mol%) and 4-methoxyphenylmagnesium bromide (0.4 mL, 0.83 M in THF, 0.32 mmol, 1.6 equiv.) were submitted to **General Procedure 4** at room temperature. The reaction was quenched with aqueous HCl (5 mL, 1 M). Purification by column chromatography (SiO_2, pentane / EtOAc, 80:20) afforded **148** (44 mg, 0.13 mmol, 67%) as a white solid.

R_f 0.35 (pentane / EtOAc, 80:20)

m.p. 107-109 °C

^{1}H NMR (400 MHz, $CDCl_3$) δ 7.97-7.90 (2H, m, H9), 7.66 (1H, m, H11), 7.61-7.54 (2H, m, H10), 7.09-7.04 (2H, m, H3), 6.84-6.78 (2H, m, H2), 3.77 (3H, s, OMe), 3.43 (2H, s, H7), 2.04 (6H, s, H6).

^{13}C NMR (101 MHz, $CDCl_3$) δ 158.6, 140.5, 133.8, 132.4, 129.4, 128.0, 127.2, 113.7, 57.6, 55.4, 53.9, 43.2, 32.0.

HRMS (ESI$^+$) Found $[M+Na]^+$ = 351.1026; $C_{19}H_{20}O_3NaS$ requires 351.1025.

IR (film) ν_{max}/cm^{-1} 2971, 2910, 2873, 1521, 1307, 1247, 1147, 1086, 746.

Reaction and characterisation performed by Dr Jeremy Nugent.

Ethyl 2-(3-(4-methoxyphenyl)bicyclo[1.1.1]pentan-1-yl)acetate, 149

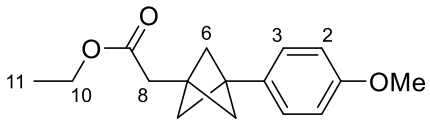

Ethyl 2-(3-iodobicyclo[1.1.1]pentan-1-yl)acetate **S4** (58 mg, 0.21 mmol, 1.0 equiv.), $Fe(acac)_3$ (14 mg, 0.04 mmol, 20 mol%), TMEDA (12 μL, 0.08 mmol, 40 mol%) and 4-methoxyphenylmagnesium bromide (0.4 mL, 0.8 M in THF, 0.32 mmol, 1.6 equiv.) were submitted to **General Procedure 4** at room temperature. The reaction was quenched with aqueous $NH_4Cl_{(sat.)}$ (5 mL). Purification by column chromatography (SiO_2, pentane / Et_2O, 98:2 to 96:4) afforded **149** (51 mg, 0.20 mmol, 95%) as a colourless liquid.

R_f 0.19 (pentane / Et_2O, 95:5)

^{1}H NMR (400 MHz, $CDCl_3$) δ 7.17-7.10 (2H, m, H2), 6.88-6.80 (2H, m, H3), 4.16 (2H, q, *J* = 7.1 Hz, H10), 3.79 (3H, s, OMe), 2.58 (2H, s, H8), 2.01 (6H, s, H6), 1.28 (3H, t, *J* = 7.1 Hz, H11).

^{13}C NMR (101 MHz, $CDCl_3$) δ 171.7, 158.4, 133.3, 127.2, 113.7, 60.4, 55.4, 53.2, 41.9, 37.7, 35.0, 14.5.

HRMS [ESI$^+$, EI$^+$, CI$^+$] Not found.

IR (film) ν_{max}/cm^{-1} 3657, 2980, 2906, 2360, 1735, 1247.

Ethyl 2,2-difluoro-2-(3-(4-methoxyphenyl)bicyclo[1.1.1]pentan-1-yl)acetate, 150

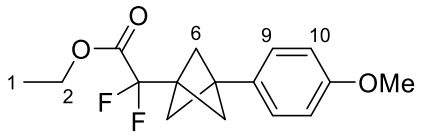

Ethyl 2,2-difluoro-2-(3-iodobicyclo[1.1.1]pentan-1-yl)acetate **S5** (63 mg, 0.20 mmol, 1.0 equiv.), $Fe(acac)_3$ (14 mg, 0.04 mmol, 20 mol%), TMEDA (12 μL, 0.08 mmol, 40 mol%) and 4-methoxyphenylmagnesium bromide (0.4 mL, 0.8 M in THF, 0.32 mmol, 1.6 equiv.) were submitted to **General Procedure 4** at room temperature. The reaction was quenched with aqueous HCl (5 mL, 1 M). Purification by column chromatography (SiO_2, pentane / Et_2O 98:2) afforded **150** (20 mg, 0.07 mmol, 34%) as a colourless oil.

R_f 0.17 (pentane / Et_2O 98:2)

^{1}H NMR (400 MHz, $CDCl_3$) δ 7.13 (2H, d, *J* = 8.7 Hz, H9), 6.85 (2H, d, *J* = 8.7 Hz, H10), 4.36 (2H, q, *J* = 7.1 Hz, H2), 3.80 (3H, s, OMe), 2.16 (6H, s, H6), 1.37 (3H, t, *J* = 7.1 Hz, H1).

^{13}C NMR (101 MHz, $CDCl_3$) δ 163.5, 158.9, 131.7, 127.3, 113.9, 112.5 (t, *J* = 249.8 Hz), 62.8, 55.5 (t, *J* = 3.2 Hz), 50.7, 41.2, 37.7 (t, *J* = 31.5 Hz), 14.3.

^{19}F NMR (376 MHz, $CDCl_3$) δ –111.31.

HRMS (ESI^+) Found $[M+H]^+$ = 297.1298; $C_{16}H_{19}O_3F_2$ requires 297.1297.

IR (film) ν_{max}/cm^{-1} 2980, 2884, 1736, 1247, 1157.

2-(3-(4-Methoxyphenyl)bicyclo[1.1.1]pentan-1-yl)pyridine, 151

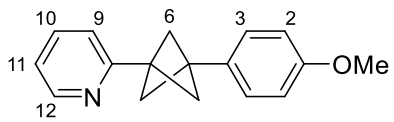

48 (55 mg, 0.20 mmol, 1.0 equiv.), $Fe(acac)_3$ (14 mg, 0.04 mmol, 20 mol%), TMEDA (12 μL, 0.08 mmol, 40 mol%) and 4-methoxyphenylmagnesium bromide (0.4 mL, 0.9 M

in THF, 0.32 mmol, 1.6 equiv.) were submitted to **General Procedure 4** at room temperature. The reaction was quenched with aqueous HCl (5 mL, 1 M). Purification by column chromatography (SiO_2, pentane / Et_2O, 80:20) afforded **151** (35 mg, 0.14 mmol, 69%) as a white solid.

R_f 0.16 (pentane / Et_2O, 70:30)

m.p. 81-83 °C

^{1}H NMR (400 MHz, $CDCl_3$) δ 8.59 (1H, ddd, *J* = 4.9, 1.9, 1.0 Hz, H12), 7.64 (1H, td, *J* = 7.6, 1.9 Hz, H10), 7.30-7.21 (3H, m, H3, H11), 7.15 (1H, ddd, *J* = 7.6, 4.9, 1.2 Hz, H9), 6.94-6.86 (2H, m, H2), 3.81 (3H, s, OMe), 2.40 (6H, s, H6).

^{13}C NMR (101 MHz, $CDCl_3$) δ 159.9, 158.6, 149.5, 136.3, 133.2, 127.4, 121.6, 120.8, 113.8, 55.4, 53.9, 41.6, 40.8.

HRMS (ESI) Found $[M+H]^+$ = 252.1382; $C_{17}H_{18}ON$ requires 252.1383.

IR (film) ν_{max}/cm^{-1} 2973, 2909, 2971, 1587, 1505, 1246, 802.

2,6-*bis*(3-(4-Methoxyphenyl)bicyclo[1.1.1]pentan-1-yl)pyridine, 152

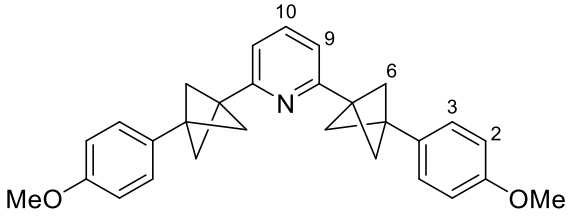

60 (93 mg, 0.20 mmol, 1.0 equiv.), $Fe(acac)_3$ (28 mg, 0.08 mmol, 40 mol%), TMEDA (24 µL, 0.16 mmol, 80 mol%) and 4-methoxyphenylmagnesium bromide (0.91 mL, 0.7 M in THF, 0.636 mmol, 3.2 equiv.) were submitted to **General Procedure 4** at room temperature. The reaction was quenched with aqueous NH_4Cl (5 mL, saturated). Purification by column chromatography (SiO_2, pentane / Et_2O, 95:5) afforded **152** (54 mg, 0.13 mmol, 64%) as a white solid.

R_f 0.55 (pentane / Et_2O, 70:30)

m.p. 198-200 °C

^{1}H NMR (400 MHz, $CDCl_3$) δ 7.56 (1H, t, *J* = 7.7 Hz, H10), 7.26 − 7.23 (4H, m, H3), 7.08 (2H, d, *J* = 7.7, Hz, H9), 6.89-6.85 (4H, m, H2), 3.82 (6H, s, OMe), 2.38 (12H, s, H6).

^{13}C NMR (101 MHz, $CDCl_3$) δ 159.4, 158.5, 136.0, 133.7, 127.4, 118.3, 113.8, 55.5, 54.0, 41.9, 40.8.

HRMS (ESI) Found $[M+H]^+$ = 424.2269; $C_{29}H_{30}O_2N$ requires 424.2271.

IR (film) ν_{max}/cm^{-1} 2978, 1505, 1246, 1030, 804.

Methyl 6-fluoro-2-(3-(4-methoxyphenyl)bicyclo[1.1.1]pentan-1-yl)-3-methylquinoline-4-carboxylate, 153

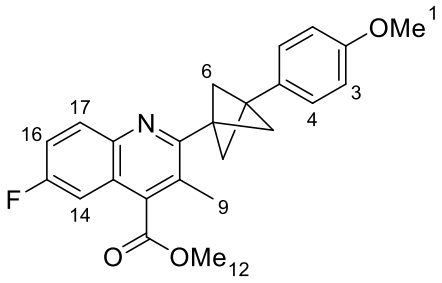

S6 (83 mg, 0.20 mmol, 1.0 equiv.), $Fe(acac)_3$ (14 mg, 0.04 mmol, 20 mol%), TMEDA (12 μL, 0.08 mmol, 40 mol%) and 4-methoxyphenylmagnesium bromide (0.4 mL, 0.8 M in THF, 0.32 mmol, 1.6 equiv.) were submitted to **General Procedure 4**. The reaction was quenched with aqueous NH_4Cl (5 mL, saturated). Purification by column chromatography (SiO_2, pentane / Et_2O, 9:1) afforded **153** (65 mg, 0.17 mmol, 83%) as a white solid.

R_f 0.21 (pentane / Et_2O, 9:1)

m.p. 148−150 °C

^{1}H NMR (400 MHz, $CDCl_3$) δ 8.07 (1H, dd, *J* = 9.2, 5.5 Hz, H14), 7.42 (1H, ddd, *J* = 9.2, 8.4, 2.8 Hz, H16), 7.32-7.21 (3H, m, H4, H17), 6.92-6.86 (2H, m, H3), 4.08 (3H, s, OMe), 3.82 (3H, s, OMe), 2.58 (6H, s, H6), 2.58 (3H, s, H9).

^{13}C NMR (101 MHz, $CDCl_3$) δ 168.4, 161.0 (d, *J* = 248.1 Hz), 158.7, 157.9 (d, *J* = 2.8 Hz), 143.5, 138.1 (d, *J* = 5.4 Hz), 133.1, 132.3 (d, *J* = 9.3 Hz), 127.8, 127.4, 124.2 (d, *J* = 10.2 Hz), 119.1 (d, *J* = 25.6 Hz), 113.9, 107.9 (d, *J* = 23.4 Hz), 55.5, 54.6, 52.8, 43.4, 42.3, 17.4.

^{19}F NMR (377 MHz, $CDCl_3$) δ −112.25 (ddd, *J* = 5.5, 8.4, 9.9 Hz).

HRMS (ESI^+) $[M+H]^+$ = 392.1655; $C_{24}H_{23}O_3NF$ requires 392.1657.

IR (film) ν_{max}/cm^{-1} 2970, 1732, 1498, 1386, 1298, 1246.17, 1208, 1172, 833.

Reaction and characterisation performed by Frank Nightingale.

2-(3-(4-Methoxyphenyl)bicyclo[1.1.1]pentan-1-yl)ethyl 6-(3-methoxyphenyl)-2-methylnicotinate, 154

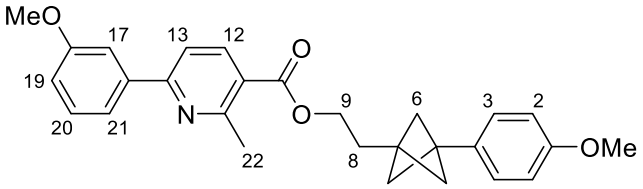

S7 (93 mg, 0.20 mmol, 1.0 equiv.), $Fe(acac)_3$ (14 mg, 0.04 mmol, 20 mol%), TMEDA (12 μL, 0.08 mmol, 40 mol%) and 4-methoxyphenylmagnesium bromide (0.4 mL, 0.9 M in THF, 0.32 mmol, 1.6 equiv.) were submitted to **General Procedure 4** at room temperature. The reaction was quenched with aqueous NH_4Cl (5 mL, saturated). Purification by column chromatography (SiO_2, pentane / Et_2O, 95:5) afforded **154** (35 mg, 0.08 mmol, 40%) as a white solid.

R_f 0.33 (pentane / Et_2O, 90:10)

m.p. 110-112 °C

^{1}H NMR (400 MHz, $CDCl_3$) δ 8.27 (1H, d, *J* = 8.1 Hz, H12), 7.66 (1H, dd, *J* = 2.6, 1.6 Hz, H17), 7.65-7.58 (2H, m, ArH), 7.39 (1H, app t, *J* = 8.1 Hz, H20), 7.18-7.09 (2H, m, H3), 7.00 (1H, ddd, *J* = 8.1, 2.6, 1.0 Hz, ArH), 6.89-6.79 (2H, m, H2), 4.41 (2H, t, *J* = 6.6 Hz, H9), 3.90 (3H, s, OMe), 3.78 (3H, s, OMe), 2.94 (3H, s, H22), 2.04 (2H, t, *J* = 6.6 Hz, H8), 1.99 (6H, s, H6).

^{13}C NMR (101 MHz, *d*6-acetone) δ 166.8, 161.2, 160.2, 159.4, 159.1, 140.5, 140.1, 134.1, 130.6, 127.8, 124.7, 120.3, 118.3, 116.3, 114.3, 113.4, 64.0, 55.7, 55.5, 53.3, 42.4, 37.2, 31.3, 25.4.

HRMS (ESI^+) Found $[M+H]^+ = 444.2168$; $C_{28}H_{30}O_4N$ requires 444.2169.

IR (film) ν_{max}/cm^{-1} 2904, 1719, 1584, 1246, 1083.

Reaction and characterisation performed by Dr Jeremy Nugent.

7.4.4 Further functionalisations

TMS *ipso*-substitution reactions

***tert*-Butyl 4-(3-(4-bromophenyl)bicyclo[1.1.1]pentan-1-yl)piperidine-1-carboxylate, 169**

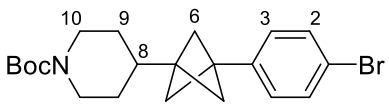

To a vial containing MeOH (0.15 mL) at 60 °C was added a mixture of **135** (80 mg, 0.20 mmol) and KBr (36 mg, 1.5 equiv., 0.30 mmol) in AcOH (1.4 mL). The reaction was stirred for 20 mins. NCS (32 mg, 1.2 equiv., 0.24 mmol) was then added and the reaction was stirred at 60 °C for a further 2 h. The reaction was then cooled to room temperature and poured into ice water. The aqueous solution was extracted with CH_2Cl_2 (3 × 20 mL)

and the combined organic layers washed with NaOH (3 M, 20 mL) and water (20 mL), before drying over $MgSO_4$ and concentrating *in vacuo*. Purification by column chromatography (SiO_2, pentane / Et_2O, 95:5) afforded **169** (56 mg, 0.14 mmol, 69%) as a white solid.

R_f = 0.24 (pentane / Et_2O, 90:10)

m.p. = 83-85 °C

^{1}H NMR (400 MHz, $CDCl_3$) δ 7.39 (2H, d, *J* = 8.3 Hz, ArH), 7.07 (2H, d, *J* = 8.4 Hz, ArH), 4.15 (2H, br app s, H10), 2.66 (2H, app t, *J* = 12.9 Hz, H10), 1.83 (6H, s, H6), 1.64-1.49 (3H, m, H9 + H8), 1.46 (9H, s, *t*-Bu), 1.11 (2H, m , H9).

^{13}C NMR (101 MHz, $CDCl_3$) δ 155.0, 140.4, 131.2, 128.0, 120.3, 79.4, 50.0, 43.9, 41.9, 40.6, 36.5, 28.6, 28.5.

HRMS (ESI^+) Found $[M+Na]^+$ = 428.1196; $C_{21}H_{28}O_2N^{79}Br^{23}Na$ requires 428.1196.

IR (film) ν_{max}/cm^{-1} 2964, 2929, 2866, 1692, 1422, 1236, 1161

***tert*-Butyl 4-(3-(4-iodophenyl)bicyclo[1.1.1]pentan-1-yl)piperidine-1-carboxylate, 170**

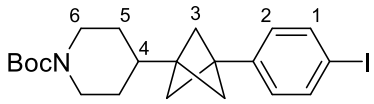

135 (40 mg, 0.10 mmol, 1.0 equiv.) in anhydrous CH_2Cl_2 (1 mL) was cooled to 0 °C and treated with ICl (0.2 mL of a 1 M solution in CH_2Cl_2, 0.2 M). The reaction was maintained at this temperature for 1 h then quenched with $Na_2S_2O_3$ (5 ml of a sat. aq. solution) and $NaHCO_3$ (5 ml of a sat. aq. solution). The phases were separated, and the aqueous phase was extracted with CH_2Cl_2 (3 × 5 mL). The combined organic layers were washed with

brine, dried ($MgSO_4$), and concentrated. Purification by column chromatography (SiO_2, pentane / EtOAc, 9:1) afforded **170** (29 mg, 0.64 mmol, 64%) as a pale yellow solid.

R_f 0.54 (pentane / EtOAc, 80:20)

m.p. 78-80 °C

^{1}H NMR (400 MHz, $CDCl_3$) δ 7.64-7.56 (2H, m, ArH), 7.00-6.91 (2H, m, ArH), 4.22-4.07 (2H, m, H6), 2.66 (2H, app t, *J* = 12.2 Hz, H6), 1.82 (6H, s, H3), 1.63-1.49 (3H, m, H4, H5), 1.46 (9H, s, tBu), 1.19-1.04 (2H, m, H5).

^{13}C NMR (101 MHz, $CDCl_3$) δ 155.0, 141.1, 137.2, 128.3, 91.7, 79.4, 50.0, 43.9, 42.0, 40.7, 36.5, 28.6, 28.5.

HRMS (ESI^+) $[M+H]^+$ = 476.1057; $C_{21}H_{28}O_2NINa$ requires 476.1057.

IR (film) ν_{max}/cm^{-1} 2964, 2928, 2865, 1691, 1422, 1160.

***tert*-Butyl 4-(3-(4-acetylphenyl)bicyclo[1.1.1]pentan-1-yl)piperidine-1-carboxylate, 171**

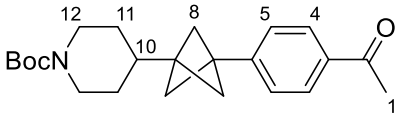

To a flame dried vial under argon was added $AlCl_3$ (40 mg, 0.3 mmol, 3 equiv.) and CH_2Cl_2 (0.5 mL). The mixture was cooled to 0 °C, then AcCl (20 µL, 3 equiv., 0.3 mmol) was added and the mixture stirred for 15 mins. A solution of **135** (40 mg, 0.1 mmol, 1.0 equiv) in CH_2Cl_2 (0.25 mL) was added before warming to room temperature and stirring for 16 h. The reaction was quenched with cold aqueous NH_4Cl (sat., 5 mL), the layers separated, and the aqueous layer extracted with CH_2Cl_2 (2 × 15 mL). The combined organic phases were dried over $MgSO_4$ and concentrated. The crude product was dissolved in CH_2Cl_2 (0.5 mL) and cooled to 0 °C before adding Boc_2O (33 mg, 1.5 equiv.,

0.15 mmol). NEt_3 (40 µL, 3 equiv., 0.3 mmol) was then added dropwise to reaction mixture and the resultant mixture stirred at room temperature for 16 h. Once complete by TLC, water was added to the reaction (10 mL), the layers were separated, and the aqueous layer extracted with CH_2Cl_2 (3 × 20 mL). the combined organic layers were dried over $MgSO_4$, concentrated *in vacuo* and purified by column chromatography (SiO_2, pentane / Et_2O, 90:10 to 80:20), affording **171** (25 mg, 0.07 mmol, 67%) as a white solid.

R_f = 0.21 (pentane / EtOAc, 80:20)

^{1}H NMR (400 MHz, $CDCl_3$) δ 7.91-7.85 (2H, m, H4), 7.31-7.27 (2H, m, H5), 4.14 (2H, br app s, H12), 2.68 (2H, m, H12), 2.57 (3H, s, H1), 1.88 (6H, s, H8), 1.65-1.52 (3H, m, H11 + H10), 1.46 (9H, s, *t*-Bu), 1.19-1.07 (2H, m, H11).

^{13}C NMR (101 MHz, $CDCl_3$) δ 197.9, 155.0, 146.9, 135.5, 128.5, 126.4, 79.4, 50.2, 43.8, 42.2, 41.0, 36.5, 28.6, 28.5, 26.7.

HRMS (ESI^+) $[M+Na]^+$ = 392.2194; $C_{23}H_{31}O_3NNa$ requires 392.2196.

IR (film) ν_{max}/cm^{-1} 3657, 2980, 2927, 2867, 2361, 1686, 1607, 1422, 1162.

7.4.5 Competition Experiments

Procedure: To a flame dried vial under argon was added **117** (76 mg, 0.20 mmol, 1.0 equiv.), $Fe(acac)_3$ (14 mg, 0.04 mmol, 20 mol%), TMEDA (12 µL, 0.08 mmol, 40 mol%) and anhydrous THF (0.2 mL), and the mixture was stirred for 5 minutes. To this mixture was rapidly added a 1:1 mixture of PhMgBr (0.6 mmol, 3 equiv.) and XArMgBr (0.6 mmol, 3 equiv.) as a solution in THF. The reaction mixture was stirred for 5 min then quenched by the dropwise addition of aqueous NH_4Cl (5 mL, saturated). The phases were separated, and the aqueous phase was extracted with Et_2O (3 × 10 mL). The combined

organic phases were washed with brine (10 mL), dried over $MgSO_4$ and concentrated *in vacuo*. The crude mixture was then filtered through a plug of silica, concentrated *in vacuo*, and the ratio of products determined by ^1H NMR spectroscopy.

Calculated ratios are an average taken from three experiments.

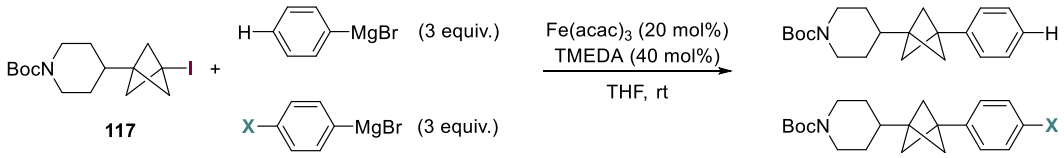

X	σX	Product Ratio: X/H
OMe	−0.27	0.3
OEt	−0.24	0.4
t-Bu	−0.20	0.7
Me	−0.17	0.6
TMS	−0.07	1.0
OPh	−0.03	0.7
F	0.06	0.38
2-Py	0.17	0.7
m-OPh	0.25	0.7
OCF_3	0.35	0.11

*Table **7.3** – Comparison of Hammett substituent constants and product ratios for competition experiments between PhMgBr and XPhMgBr. Reported ratios are an average taken from three experiments. Substituents are para- unless indicated otherwise.*

7.4.6 Investigations towards a tandem ATRA/cross-coupling

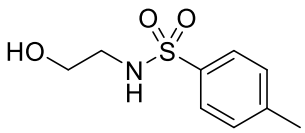

S8

S8 had been previously synthesised and was available in the lab.

***N*-Allyl-*N*-(2-hydroxyethyl)-4-methylbenzenesulfonamide, S9**

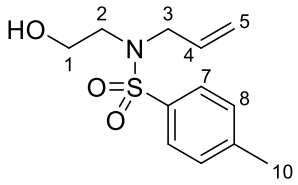

To a flame dried flask was added **S8** (2.26 g, 10.5 mmol, 1.0 equiv.) in acetone (100 mL). To this mixture was then added K_2CO_3 (2.90 g, 21.0 mmol, 2.0 equiv.) and allyl bromide (1.82 mL, 21.0 mmol, 2.0 equiv.) and the resultant mixture heated to reflux and stirred for 15 h. The mixture was then allowed to cool to room temperature and quenched with $NaHCO_3$ (50 mL, saturated), and the organic layer was then separated, dried over $MgSO_4$ and concentrated *in vacuo*. Purification by column chromatography (SiO_2, pentane / EtOAc, 66:33) afforded **S9** (1.71 g, 6.7 mmol, 64%) as a colourless oil.

R_f = 0.14 (pentane / EtOAc, 66:33)

^{1}H NMR (400 MHz, $CDCl_3$) δ 7.75 – 7.68 (m, 2H), 7.32 (d, *J* = 8.1 Hz, 2H), 5.68 (ddt, *J* = 16.7, 10.0, 6.4 Hz, 1H), 5.23 – 5.11 (m, 2H), 3.85 (dt, *J* = 6.4, 1.4 Hz, 2H), 3.73 (q, *J* = 5.4 Hz, 2H), 3.23 (t, *J* = 5.4 Hz, 2H), 2.43 (s, 3H), 2.27 (t, *J* = 5.8 Hz, 1H).

^{13}C NMR (101 MHz, $CDCl_3$) δ 143.8, 136.3, 133.2, 130.0, 127.4, 119.5, 61.2, 52.4, 49.9, 21.7.

Spectroscopic data in agreement with that reported previously.[4]

_N_-Allyl-_N_-(2-iodoethyl)-4-methylbenzenesulfonamide, 187

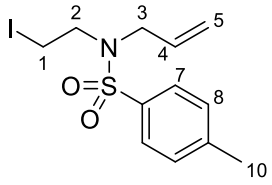

To a flame dried flask was added PPh_3 (5.27 g, 20.1 mmol, 3.0 equiv.), imidazole (1.55 g, 22.8 mmol, 3.4 equiv.), I_2 (5.10 g, 20.1 mmol, 3.0 equiv.) in a mixture of MeCN (13 mL) and Et_2O (42 mL). The mixture was then cooled to 0 °C and stirred for 30 mins. **S9** (1.71 g, 6.7 mmol, 1.0 equiv.) was then added and the resultant mixture stirred for 2 h. The reaction was quenched with NH_4Cl (20 mL, saturated), the aqueous phase extracted with CH_2Cl_2 and the organic fraction then washed with $Na_2S_2O_3$ and concentrated *in vacuo*. Purification by column chromatography (SiO_2, pentane / EtOAc, 66:33) afforded **187** (2.22 g, 6.1 mmol, 91%) as a yellow oil.

R_f = 0.6 (pentane / EtOAc, 80:20)

^{1}H NMR (400 MHz, $CDCl_3$) δ 7.74 – 7.66 (2H, m, ArH), 7.36 – 7.28 (2H, m, ArH), 5.77 – 5.59 (1H, m, H4), 5.20 (1H, m, H5), 5.17 (1H, m, H5), 3.79 (2H, dt, *J* = 6.5, 1.3 Hz, H3), 3.41 (2H, m, H2), 3.30 – 3.15 (2H, m, H1), 2.43 (3H, s, H10).

^{13}C NMR (101 MHz, $CDCl_3$) δ 143.8, 136.5, 133.0, 130.0, 127.3, 119.8, 51.8, 50.3, 21.7, 2.1.

Spectroscopic data in agreement with that reported previously.[4]

3-((3-Iodobicyclo[1.1.1]pentan-1-yl)methyl)-1-tosylpyrrolidine, 194

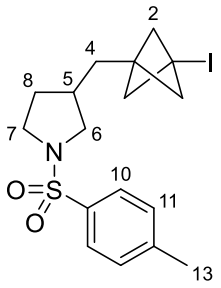

To a screw-capped vial equipped with a stirrer bar was added *fac*-Ir(ppy)$_3$ (10 mg, 0.1 mmol, 0.025 equiv.), **187** (219 mg, 0.6 mmol, 1.0 equiv.), *t*-BuCN (6.0 mL) and TCP (1.13 mL, 1.5 equiv., 0.78 M solution in Et_2O). The vial was sealed and placed under nitrogen, and the solution was degassed *via* three freeze-pump-thaw cycles (vacuum was only applied while the reaction mixture was frozen due to TCP volatility). The stirred mixture was irradiated with blue LEDs for 18 h and then concentrated *in vacuo.* Purification by column chromatography (SiO_2, pentane / EtOAc, 95:5 → 90:10) afforded **194** (194 mg, 0.45 mmol, 75%) as a white solid

R_f = 0.34 (pentane / Et_2O, 70:30)

^{1}H NMR (400 MHz, $CDCl_3$) δ 7.74 – 7.67 (2H, m, ArH), 7.38 – 7.29 (2H, m, ArH), 3.43 – 3.36 (1H, m, H6), 3.31 (1H, ddd, *J* = 9.7, 8.2, 3.4 Hz, H7), 3.15 (1H, ddd, *J* = 9.8, 8.6, 7.0 Hz, H7), 2.78 – 2.68 (1H, m, H6), 2.44 (3H, s, H13), 2.15 (6H, s, H2), 2.01 – 1.88 (2H, m, H8), 1.53 – 1.42 (2H, m, H4), 1.35 (1H, td, *J* = 8.3, 3.4 Hz, H8).

Spectroscopic data in agreement with that reported previously.[4]

3-((3-(4-Methoxyphenyl)bicyclo[1.1.1]pentan-1-yl)methyl)-1-tosylpyrrolidine, 195

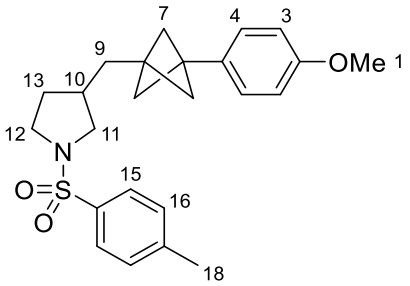

194 (147 mg, 0.34 mmol, 1.0 equiv.), $Fe(acac)_3$ (24 mg, 0.28 mmol, 20 mol%), TMEDA (21 µL, 0.14 mmol, 40 mol%) and 4-methoxyphenylmagnesium bromide (0.59 mL, 0.9 M in THF, 0.56 mmol, 1.6 equiv.) in THF (0.35 mL) were submitted to **General Procedure 4** at room temperature. The reaction was quenched with aqueous NH_4Cl (15 mL, saturated). Purification by column chromatography (SiO_2, pentane / EtOAc, 95:5 → 90:10) afforded **195** (96.2mg, 0.23 mmol, 69%) as a colourless oil.

R_f = 0.35 (EtOAc / pentane, 4:1)

^{1}H NMR (400 MHz, $CDCl_3$) δ 7.72 (2H, d, *J* = 7.9 Hz, ArH), 7.33 (2H, d, *J* = 7.9 Hz, ArH), 7.10 (2H, d, *J* = 8.2 Hz, ArH), 6.83 (2H, d, *J* = 8.2 Hz, ArH), 3.78 (3H, s, OMe), 3.50 (1H, dd, *J* = 9.7, 7.3 Hz, H11), 3.33 (1H, td, *J* = 8.9, 3.5 Hz, H12), 3.24 – 3.14 (1H, m, H12), 2.79 (1H, dd, *J* = 9.8, 8.0 Hz, H11), 2.44 (3H, s, H18), 2.10 – 1.94 (2H, m, H13), 1.88 (6H, s, H7), 1.54 – 1.36 (3H, m, H10 + H9).

^{13}C NMR (101 MHz, $CDCl_3$) δ 158.4, 143.4, 134.1, 133.5, 129.8, 127.7, 127.2, 113.7, 55.5, 53.6, 52.9, 47.6, 41.7, 37.9, 37.1, 35.6, 32.2, 21.7.

HRMS (ESI^+) $[M+H]^+$ = 412.1947; $C_{24}H_{30}O_3N_1S_1$ requires 412.1941.

IR (film) ν_{max}/cm^{-1} 2980, 2917, 1697, 1418, 1324, 1163, 1122, 1067

7.5 Chapter 4: Copper-catalysed borylation/oxidation

7.5.1 General Procedures

General Procedure 1 – Borylation of BCP iodides

To a flame dried vial was added BCP iodide (1 equiv.) and anhydrous DMF (1.5 mL). B_2pin_2 (1.5 equiv.), LiOMe (2.0 equiv) and PPh_3 (0.15 equiv.) were then added sequentially to the vial. The vial was then evacuated and refilled with N_2 three times. CuI (0.1 equiv.) was then added, and the vial evacuated and refilled with nitrogen three more times. The reaction mixture was then stirred at 35 °C for 20 h. The resulting mixture was then diluted with water and extracted with EtOAc (3 × 20 mL), the organic fractions combined, and washed with brine (3 × 20 mL). These combined organic layers were then concentrated *in vacuo* and the crude product material used in the oxidation without further purification.

General Procedure 2 – Oxiation of BCP boronates

To a flame dried vial was added the crude BCP boronate in stabilised THF (1.5 mL). NaOAc (1.2 equiv. based on crude yield) and UHP (1.2 equiv. based on crude yield) were then added to the vial at 0 °C. The reaction mixture was then stirred at 30 °C for 4 h. The resultant mixture was then filtered under reduced pressure, the filter cake washed with THF (3 × 10 mL), and the filtrate concentrated *in vacuo*. The crude product was purified by column chromatography.

7.5.2 Synthesis of starting materials

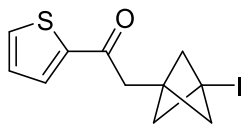

S10

S10 had been previously synthesised by Dimitri Caputo and was available in the lab.

Methyl ((benzyloxy)carbonyl)serinate, S11

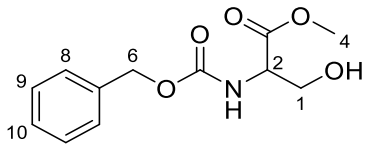

To a flask was added L-serine methyl ester hydrochloride (4.0 g, 25.7 mmol, 1.0 equiv.), $NaHCO_3$ (11g dissolved in 50 mL H_2O) and CH_2Cl_2 (70 mL) and the mixture cooled to 0 °C. CbzCl (3.85 mL, 27 mmol, 1.1 equiv.) was then added, the mixture warmed to room temperature, and stirred for 6 h. The reaction mixture was then cooled to 0 °C and quenched with HCl (1M). The organic layer was then separated and washed with H_2O (50 mL) and brine (50 mL), before drying over $MgSO_4$ and concentrating *in vacuo*. Purification by column chromatography (SiO_2, pentane / EtOAc, 50:50) afforded **S11** (6.51 g, 25.7 mmol, quant.).

$\mathbf{R_f}$ = 0.11 (pentane / EtOAc, 70:30)

^{1}H NMR (400 MHz, $CDCl_3$) δ 7.43 – 7.23 (5H, m, ArH), 6.01 (d, *J* = 8.2 Hz, NH), 5.11 (2H, s, H6), 4.44 (1H, dt, *J* = 7.8, 3.6 Hz, H2), 3.92 (2H, m, H1), 3.75 (3H, s, H4), 3.19 (1H, s, OH).

^{13}C NMR (101 MHz, $CDCl_3$) δ 171.2, 156.4, 136.1, 128.6, 128.3, 128.1, 67.2, 63.0, 56.1, 52.7.

Spectroscopic data in agreement with that reported previously.[5]

Methyl 2-(((benzyloxy)carbonyl)amino)-3-iodopropanoate, S12

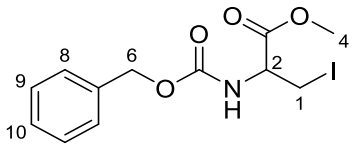

To a flame dried flask containing imidazole (0.54 g, 7.9 mmol, 2.0 equiv.), I_2 (2.0 g, 7.9 mmol, 2.0 equiv.) and CH_2Cl_2 (10 mL) was added PPh_3 (2.1 g, 7.9 mmol, 2.0 equiv.) portion wise. The mixture was then cooled to 0 °C and stirred for 30 mins then room temperature for 1 h. To this mixture was then added **S11** (1.0 g, 4.0 mmol, 1.0 equiv.) in CH_2Cl_2 (2 mL), dropwise, and the resultant mixture stirred for 5 h at room temperature. The reaction mixture was then filtered through celite, and the filtrate washed with H_2O (20 mL × 3) and brine (20 mL × 3). The organic fraction then dried over $MgSO_4$ and concentrated *in vacuo*. Purification by column chromatography (SiO_2, pentane / EtOAc, 100:0 → 90:10) afforded **S12** (0.894 g, 2.5 mmol, 62%) as a cream solid.

$\mathbf{R_f}$ = 0.53 (pentane / EtOAc, 70:30)

^{1}H NMR (400 MHz, $CDCl_3$) δ 7.46 – 7.30 (5H, m, ArH), 5.65 (1H, d, *J* = 7.6 Hz, NH), 5.16 – 5.10 (2H, m, H6), 4.59 (1H, dt, *J* = 7.6, 3.8 Hz, H2), 3.82 (3H, s, H4), 3.65 – 3.53 (2H, m, H1).

^{13}C NMR (101 MHz, $CDCl_3$) δ 169.8, 155.5, 136.1, 128.7, 128.4, 128.3, 67.4, 54.2, 53.3, 7.5.

Spectroscopic data in agreement with that reported previously.[6]

Methyl 2-(((benzyloxy)carbonyl)amino)-3-(3-iodobicyclo[1.1.1]pentan-1-yl)propanoate, 219

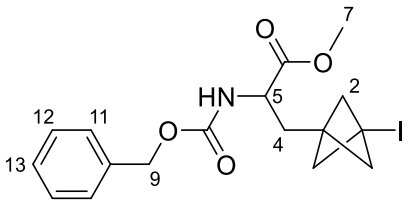

To a flame dried flask was added **S12** (890 mg, 2.45 mmol, 1 equiv.) and TCP (5.4 mL, 0.69 M in Et_2O, 3.7 mmol, 1.5 equiv.) and the mixture cooled to 0 °C. To this, BEt_3 (0.25 mL, 1 M in hexanes, 0.25 mmol, 0.1 equiv.) was added (with needle tip in solution), the reaction stirred for 2 h at room temperature and the resulting mixture was then concentrated *in vacuo*. Purification by column chromatography (SiO_2, pentane / EtOAc, 90:10) afforded **219** (813 mg, 1.9 mmol, 77%) as a dark yellow oil.

R_f = 0.14 (pentane / EtOAc, 90:10)

^{1}H NMR (400 MHz, $CDCl_3$) δ 7.41 – 7.29 (5H, m, ArH), 5.30 (1H, d, *J* = 8.2 Hz, NH), 5.15 – 5.06 (2H, m, H9), 4.36 (1H, td, *J* = 7.8, 4.5 Hz, H5), 3.73 (3H, s, H7), 2.29 – 2.10 (7H, m, H2 + H4), 1.90 (1H, dd, *J* = 14.7, 7.5 Hz, H4).

^{13}C NMR (101 MHz, $CDCl_3$) δ 172.4, 155.7, 136.2, 128.7, 128.4, 128.3, 67.2, 60.9, 52.7, 52.4, 45.4, 34.4, 6.2.

HRMS (ESI^+) $[M+H]^+$ = 430.0512, $C_{17}H_{21}O_4NI$ requires 430.0510.

IR (film) ν_{max}/cm^{-1} 3333(br), 2952, 1721 (br), 1525, 1436, 1212, 1179, 1050

7.5.3 Reaction Scope

Methyl 2-(((benzyloxy)carbonyl)amino)-3-(3-hydroxybicyclo[1.1.1]pentan-1-yl)propanoate, 221

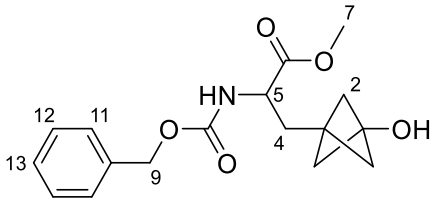

219 (86.0 mg, 0.20 mmol, 1.0 equiv.), B_2pin_2 (76.2 mg, 0.30 mmol, 1.5 equiv.), PPh_3 (7.9 mg, 0.03 mmol, 0.15 equiv.), LiOMe (15.2 mg, 0.40 mmol, 2.0 equiv.) and CuI (3.8 mg, 0.02 mmol, 0.1 equiv.) in DMF (1.5 mL) were subjected to **General Procedure 1** for 20 h to give the crude BCP boronate.

The crude BCP boronate, NaOAc (19.7 mg, 0.24 mmol, 1.2 equiv.), and UHP (22.6 mg, 0.24 mmol, 1.2 equiv.) in THF (1.5 mL) were subjected to **General Procedure 2** for 4 h. Purification by column chromatography (SiO_2, pentane / EtOAc, 95:5) afforded **221** (34.4 mg, 0.11 mmol, 54%) as a yellow oil.

R_f = 0.08 (pentane /EtOAc, 70:30)

^{1}H NMR (400 MHz, $CDCl_3$) δ 7.43 – 7.30 (5H, m, ArH), 5.24 (1H, d, *J* = 8.4 Hz, NH), 5.14 (2H, m, H9), 4.41 (1H, td, *J* = 7.7, 4.5 Hz, H5), 3.76 (3H, s, H7), 2.39 (1H, s, OH), 2.21 (dd, *J* = 14.7, 4.6 Hz, H4), 2.00 (1H, dd, *J* = 14.7, 7.3 Hz, H4), 1.84 (6H, s, H2).

^{13}C NMR (101 MHz, $CDCl_3$) δ 172.6, 155.6, 136.2, 128.6, 128.2, 128.1, 67.1, 62.5, 54.5, 53.0, 52.4, 31.7, 28.2.

HRMS (ESI$^+$) $[M+Na]^+$ = 342.1313, $C_{17}H_{21}O_5NNa$ requires 342.1312

IR (film) ν_{max}/cm^{-1} 3334 (br), 2923, 2854, 2360, 2341, 1719, 1534, 1456, 1256, 1501

***tert*-Butyl 4-(3-hydroxybicyclo[1.1.1]pentan-1-yl)piperidine-1-carboxylate, 222**

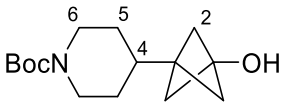

117 (75.0 mg, 0.20 mmol, 1.0 equiv.), B_2pin_2 (76.2 mg, 0.30 mmol, 1.5 equiv.), PPh_3 (7.9 mg, 0.03 mmol, 0.15 equiv.), LiOMe (15.2 mg, 0.40 mmol, 2.0 equiv.) and CuI (3.8 mg, 0.02 mmol, 0.1 equiv.) in DMF (1.5 mL) were subjected to **General Procedure 1** for 20 h to give the crude BCP boronate.

The crude BCP boronate, NaOAc (19.7 mg, 0.24 mmol, 1.2 equiv.), and UHP (22.6 mg, 0.24 mmol, 1.2 equiv.) in THF (1.5 mL) were subjected to **General Procedure 2** for 4 h. Purification by column chromatography (SiO_2, pentane / EtOAc, 90:10 → 70:30) afforded **222** (40 mg, 0.13 mmol, 64%) as a colourless oil.

R_f = 0.33 (pentane / EtOAc, 7:3)

^{1}H NMR (400 MHz, $CDCl_3$) δ 4.21 – 4.00 (4H, m, H6), 2.63 (4H, qpp. t, *J* = 12.2 Hz, H5), 2.50 (1H, s, OH), 1.72 (6H, s, H2), 1.65 – 1.51 (3H, m, H5 + H4), 1.44 (9H, s, *t*Bu), 1.06 (2H, qd, *J* = 12.7, 4.3 Hz, H5).

^{13}C NMR (101 MHz, $CDCl_3$) δ 155.0, 79.5, 62.7, 51.7, 44.1 (br), 34.7, 34.0, 29.3, 28.6.

HRMS (ESI^+) $[M+Na]^+$ =290.1726; requires 290.1727

IR (film) ν_{max}/cm^{-1} 3378 (br), 2970, 1692, 1669, 1292, 1173

Characterisation performed in part by Nils Frank.

Ethyl 2-(3-hydroxybicyclo[1.1.1]pentan-1-yl)acetate, 223

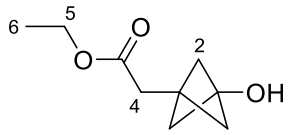

S4 (56.0 mg, 0.20 mmol, 1.0 equiv.), B_2pin_2 (76.2 mg, 0.30 mmol, 1.5 equiv.), PPh_3 (7.9 mg, 0.03 mmol, 0.15 equiv.), LiOMe (15.2 mg, 0.40 mmol, 2.0 equiv.) and CuI (3.8 mg, 0.02 mmol, 0.1 equiv.) in DMF (1.5 mL) were subjected to **General Procedure 1** for 20 h to give the crude BCP boronate.

The crude BCP boronate, NaOAc (35.0 mg, 0.43 mmol, 1.2 equiv.), and UHP (40.6 mg, 0.43 mmol, 1.2 equiv.) in THF (1.5 mL) were subjected to **General Procedure 2** for 4 h. Purification by column chromatography (SiO_2, pentane / EtOAc, 70:30) afforded **223** (19.0 mg, 0.11 mmol, 56%) as a colourless oil.

R_f = 0.36 (pentane / EtOAc, 7:3)

^{1}H NMR (400 MHz, $CDCl_3$) δ 4.13 (2H, q, *J* = 7.1 Hz, H5), 2.58 (2H, s, H4), 1.91 (6H, s, H2), 1.26 (3H, t, *J* = 7.1 Hz, H6).

^{13}C NMR (101 MHz, $CDCl_3$) δ 171.6, 62.8, 60.5, 54.8, 35.0, 27.5, 14.4.

HRMS (ESI^+) $[M+Na]^+$ = 193.0836; $C_9H_{14}O_3Na$ requires 193.0835

IR (film) ν_{max}/cm^{-1} 3359 (br), 1735, 1309, 1250, 1200

Reaction and characterisation performed by Nils Frank.

Ethyl 2,2-difluoro-2-(3-hydroxybicyclo[1.1.1]pentan-1-yl)acetate, 224

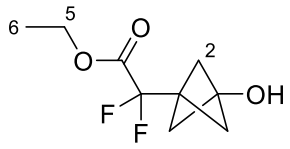

S5 (47.0 mg, 0.15 mmol, 1.0 equiv.), B_2pin_2 (51.0 mg, 0.23 mmol, 1.5 equiv.), PPh_3 (5.3 mg, 0.02 mmol, 0.15 equiv.), LiOMe (10.0 mg, 0.27 mmol, 2.0 equiv.) and CuI (2.5 mg, 0.013 mmol, 0.1 equiv.) in DMF (1.5 mL) were subjected to **General Procedure 1** for 20 h to give the crude BCP boronate.

The crude BCP boronate, NaOAc (26.0 mg, 0.32 mmol, 1.2 equiv.), and UHP (30.0 mg, 0.32 mmol, 1.2 equiv.) in THF (1.5 mL) were subjected to **General Procedure 2** for 4 h. Purification by column chromatography (SiO_2, pentane / EtOAc, 70:30) afforded **224** (14.0 mg, 0.068 mmol, 45%) as a colourless oil.

R_f = 0.36 (pentane / EtOAc, 7:3)

^{1}H NMR (400 MHz, $CDCl_3$) δ 4.33 (2H, q, *J* = 7.1 Hz, H5), 2.09 (6H, s, H2), 1.35 (3H, t, *J* = 7.1 Hz, H6).

^{13}C NMR (101 MHz, $CDCl_3$) δ 163.3 (t, *J* = 33.4 Hz), 113.1 (t, *J* = 249.3 Hz), 63.0, 62.7 (t, *J* = 2.7 Hz), 52.9 (t, *J* = 2.6 Hz), 31.3 (t, *J* = 32.0 Hz), 14.2

^{19}F NMR (375 MHz, $CDCl_3$) δ −108.5

HRMS (ESI/APCI) not found.

IR (film) ν_{max}/cm^{-1} 3295 (br), 1766, 1350, 1308, 1266, 1165, 1096.

Reaction and characterisation performed by Nils Frank.

3-((Phenylsulfonyl)methyl)bicyclo[1.1.1]pentan-1-ol, 225

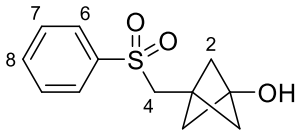

S3 (35.0 mg, 0.10 mmol, 1.0 equiv.), B_2pin_2 (38.0 mg, 0.15 mmol, 1.5 equiv.), PPh_3 (4.0 mg, 0.015 mmol, 0.15 equiv.), LiOMe (7.6 mg, 0.20 mmol, 2.0 equiv.) and CuI (1.9 mg, 0.01 mmol, 0.1 equiv.) in DMF (1.5 mL) were subjected to **General Procedure 1** for 20 h to give the crude BCP boronate.

The crude BCP boronate, NaOAc (9.8mg, 0.12 mmol, 1.2 equiv.), and UHP (11.3 mg, 0.12 mmol, 1.2 equiv.) in THF (1.5 mL) were subjected to **General Procedure 2** for 4 h. Purification by column chromatography (SiO_2, pentane / EtOAc, 90:10 → 80:20) afforded **225** (12.0 mg, 0.050 mmol, 50%) as a colourless oil.

R_f = 0.25 (pentane / EtOAc, 80:20)

^{1}H NMR (500 MHz, $CDCl_3$) δ 7.97 – 7.86 (2H, m, ArH), 7.72 – 7.63 (1H, m, H8), 7.61 – 7.54 (2H, m, ArH), 3.34 (2H, s, H4), 2.32 (6H, s, H2), 1.82 (1H, s, OH).

^{13}C NMR (126 MHz, $CDCl_3$) δ 139.8, 134.1, 129.6, 128.0, 61.3, 57.2, 52.0, 40.7.

HRMS (ESI) not found

IR (film) ν_{max} / cm^{-1} 3000 (br), 2974, 1308, 1184, 1149, 853, 745.

Reaction and characterisation performed by Nils Frank.

3-(4-(Trifluoromethyl)benzyl)bicyclo[1.1.1]pentan-1-ol, 226

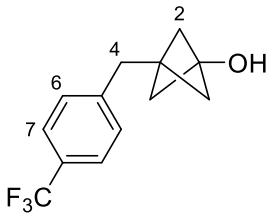

114 (70.0 mg, 0.20 mmol, 1.0 equiv.), B_2pin_2 (76.2 mg, 0.30 mmol, 1.5 equiv.), PPh_3 (7.9 mg, 0.03 mmol, 0.15 equiv.), LiOMe (15.2 mg, 0.40 mmol, 2.0 equiv.) and CuI (3.8 mg, 0.02 mmol, 0.1 equiv.) in DMF (1.5 mL) were subjected to **General Procedure 1** for 20 h to give the crude BCP boronate.

The crude BCP boronate, NaOAc (19.7 mg, 0.24 mmol, 1.2 equiv.), and UHP (22.6 mg, 0.24 mmol, 1.2 equiv.) in THF (1.5 mL) were subjected to **General Procedure 2** for 4 h. Purification by column chromatography (SiO_2, pentane / EtOAc, 80:20) afforded **226** (15.0 mg, 0.062 mmol, 31%) as a colourless oil.

R_f = 0.29 (pentane / EtOAc, 80:20)

^{1}H NMR (500 MHz, $CDCl_3$) δ 7.53 (2H, d, *J* = 8.0 Hz, ArH), 7.20 (2H, d, *J* = 8.0 Hz, ArH), 2.91 (2H, s, H4), 2.25 (1H, s, OH), 1.74 (6H, s, H2).

^{13}C NMR (101 MHz, $CDCl_3$) δ 143.85, 129.26, 128.56 (q, *J* = 32.3 Hz), 125.37 (q, *J* = 4.1 Hz), 124.49 (q, *J* = 271.7 Hz), 63.61, 53.83, 36.37, 31.32.

^{19}F NMR (471 MHz, $CDCl_3$) δ −62.3

HRMS $(APCI)^+$ $[M+H]^+$ = 243.0990, $C_{13}H_{14}F_3O$ requires 243.0991

IR (film) ν_{max}/cm^{-1} 3266, 2974, 2911, 1324, 1249, 1164, 1116, 1066

Characterisation performed by Nils Frank.

3-(6-(Trifluoromethyl)pyridin-2-yl)bicyclo[1.1.1]pentan-1-ol, 227

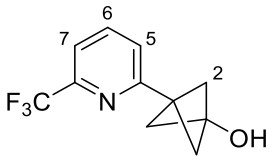

xx (68.0 mg, 0.20 mmol, 1.0 equiv.), B_2pin_2 (76.2 mg, 0.30 mmol, 1.5 equiv.), PPh_3 (7.9 mg, 0.03 mmol, 0.15 equiv.), LiOMe (15.2 mg, 0.40 mmol, 2.0 equiv.) and CuI (3.8 mg, 0.02 mmol, 0.1 equiv.) in DMF (1.5 mL) were subjected to **General Procedure 1** for 20 h to give the crude BCP boronate.

The crude BCP boronate, NaOAc (19.7 mg, 0.24 mmol, 1.2 equiv.), and UHP (22.6 mg, 0.24 mmol, 1.2 equiv.) in THF (1.5 mL) were subjected to **General Procedure 2** for 4 h. Purification by column chromatography (SiO_2, pentane / EtOAc, 80:20), followed by acid-base extraction (pentane / 6M $HCl_{(aq)}$ (5 ×), after basification 6M $NaOH_{(aq)}$: back-extraction with EtOAc (5 ×)) followed by column chromatography (pentane / EtOAc, 90:10 → 80:20) afforded **227** (22.0 mg, 0.096 mmol, 48%) as a colourless oil.

R_f = 0.29 (pentane / EtOAc, 7:3)

^{1}H NMR (400 MHz, $CDCl_3$) δ 7.76 (1H, t, *J* = 7.8 Hz, H6), 7.51 (1H, d, *J* = 7.6 Hz, ArH), 7.37 (1H, d, *J* = 7.8 Hz, ArH), 2.44 (1H, s, OH), 2.34 (6H, s, H2).

^{13}C NMR (101 MHz, $CDCl_3$) δ 159.2, 148.0 (q, *J* = 34.5 Hz), 137.4, 124.1, 121.7 (q, *J* = 274.7 Hz), 118.3 (q, *J* = 2.8 Hz), 62.9, 56.1, 34.6.

^{19}F NMR (471 MHz, $CDCl_3$) δ −68.0

HRMS (ESI/APCI) not found

IR (film) ν_{max}/cm^{-1} 3297 (br), 2360, 1742, 1654, 1267, 1194, 1140

Purification and characterisation performed by Nils Frank.

Methyl 6-fluoro-2-(3-hydroxybicyclo[1.1.1]pentan-1-yl)-3-methylquinoline-4-carboxylate, 228

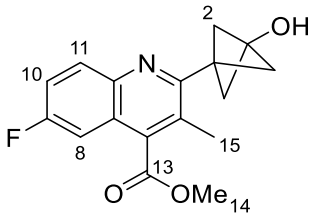

S6 (60.0 mg, 0.15 mmol, 1.0 equiv.), B_2pin_2 (55.6 mg, 0.22 mmol, 1.5 equiv.), PPh_3 (5.7 mg, 0.02 mmol, 0.15 equiv.), LiOMe (11.1 mg, 0.29 mmol, 2.0 equiv.) and CuI (2.8 mg, 0.015 mmol, 0.1 equiv.) in DMF (1.3 mL) were subjected to **General Procedure 1** for 20 h to give the crude BCP boronate.

The crude BCP boronate, NaOAc (23.0 mg, 0.28 mmol, 1.2 equiv.), and UHP (26.4 mg, 0.28 mmol, 1.2 equiv.) in THF (1.5 mL) were subjected to **General Procedure 2** for 4 h. Purification by column chromatography (pentane / EtOAc, 90:10 → 70:30) afforded **228** (11.2 mg, 0.037 mmol, 25%) as a white solid.

R_f = 0.11 (pentane / EtOAc, 7:3)

m.p. 180 °C (decomposition)

^{1}H NMR (400 MHz, $CDCl_3$) δ 8.04 (1H, dd, *J* = 9.2, 5.5 Hz, H10), 7.41 (1H, ddd, *J* = 9.3, 8.1, 2.8 Hz, H11), 7.28 – 7.23 (1H, m, H8), 4.06 (3H, s, H14), 2.91 (1H, s, OH), 2.47 (6H, s, H2), 2.47 (3H, s, H15).

^{13}C NMR (101 MHz, $CDCl_3$) δ 168.31, 161.0 (d, *J* = 248.0 Hz), 156.6 (d, *J* = 2.6 Hz), 143.4, 138.2 (d, *J* = 5.6 Hz), 132.1 (d, *J* = 9.3 Hz), 128.0, 124.1 (d, *J* = 10.1 Hz), 119.3 (d, *J* = 25.6 Hz), 107.9 (d, *J* = 23.4 Hz), 63.73, 56.29, 52.88, 36.32, 17.52.

^{19}F NMR (471 MHz, $CDCl_3$) δ −112.

HRMS (ESI^+) $[M+H]^+$ = 302.1186, $C_{17}H_{17}O_3NF$ requires 302.1187.

IR (film) ν_{max}/cm^{-1} 3347 (br), 2986, 1733, 1628, 1499, 1273,1223, 1206.

7.5.4 Fragmentation of the BCP iodide

2-(3-Methylene-1-(4,4,5,5-tetramethyl-1,3,2-dioxaborolan-2-yl)cyclobutyl)-1-(thiophen-2-yl)ethan-1-one, 231

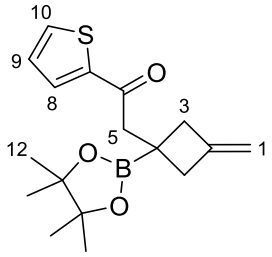

S10 (63.6mg, 0.20 mmol, 1.0 equiv.), B_2pin_2 (76.2 mg, 0.30 mmol, 1.5 equiv.), PPh_3 (7.9 mg, 0.03 mmol, 0.15 equiv.), LiOMe (15.2 mg, 0.40 mmol, 2.0 equiv.) and CuI (3.8 mg, 0.02 mmol, 0.1 equiv.) in DMF (1.5 mL) were subjected to **General Procedure 1** for 20 h. Purification by column chromatography (SiO_2, pentane → pentane / EtOAc, 75:25) afforded **231** (25.0 mg, 0.079 mmol, 39%) as a colourless solid.

m.p. 85 – 87 °C

R_f = 0.33 (pentane / EtOAC, 95:5)

^{1}H NMR (400 MHz, $CDCl_3$) δ 7.73 (1H, dd, *J* = 3.8, 1.2 Hz, ArH), 7.60 (1H, dd, *J* = 5.0, 1.1 Hz, ArH), 7.11 (1H, dd, *J* = 5.0, 3.8 Hz, H9), 4.77 (2H, quin., *J* = 2.4 Hz, H1), 3.33 (2H, s, H5), 3.04 – 2.96 (2H, m, H3), 2.38 – 2.30 (2H, m, H3), 1.25 (12H, s, H12).

^{13}C NMR (101 MHz, $CDCl_3$) δ 192.69, 146.95, 144.30, 133.27, 131.95, 128.09, 107.03, 83.43, 48.82, 39.21, 24.72.

HRMS (ESI^+) $[M+H]^+$ = 319.1536; $C_{17}H_{24}O_3BS$ requires 319.1534.

IR (film) ν_{max}/cm^{-1} 2968, 2907, 2870, 1682, 1607, 1270, 1210

7.6 References

[1] R. Gianatassio, J. M. Lopchuk, J. Wang, C. Pan, L. R. Malins, L. Prieto, T. A. Brandt, M. R. Collins, G. M. Gallego, N. W. Sach, et al., *Science (80-.).* **2016**, *351*, 241–246.

[2] K. D. Bunker, N. W. Sach, Q. Huang, P. F. Richardson, *Org. Lett.* **2011**, *13*, 4746–4748.

[3] D. F. J. Caputo, C. Arroniz, A. B. Dürr, J. J. Mousseau, A. F. Stepan, S. J. Mansfield, E. A. Anderson, *Chem. Sci.* **2018**, *9*, 5295–5300.

[4] J. Nugent, C. Arroniz, B. R. Shire, A. J. Sterling, H. D. Pickford, M. L. J. Wong, S. J. Mansfield, D. F. J. Caputo, B. Owen, J. J. Mousseau, et al., *ACS Catal.* **2019**, *9*, 9568–9574.

[5] Y. Zheng, Y. Zhao, S. Tao, X. Li, X. Cheng, G. Jiang, X. Wan, *European J. Org. Chem.* **2021**, *2021*, 2713–2718.

[6] P. M. E. Hawkins, A. M. Giltrap, G. Nagalingam, W. J. Britton, R. J. Payne, *Org. Lett.* **2018**, *20*, 1019–1022.